

University of Alberta

Effect of fluctuating temperature and propagule flow on invasibility of
global marine habitats and species distribution

by

Harshana Rajakaruna

A thesis submitted to the Faculty of Graduate Studies and Research
in partial fulfillment of the requirements for the degree of

Doctor of Philosophy

in

Ecology

Department of Biological Sciences

© Harshana Rajakaruna
Fall 2013
Edmonton, Alberta

Permission is hereby granted to the University of Alberta Libraries to reproduce single copies of this thesis and to lend or sell such copies for private, scholarly or scientific research purposes only. Where the thesis is converted to, or otherwise made available in digital form, the University of Alberta will advise potential users of the thesis of these terms.

The author reserves all other publication and other rights in association with the copyright in the thesis and, except as herein before provided, neither the thesis nor any substantial portion thereof may be printed or otherwise reproduced in any material form whatsoever without the author's prior written permission.

ABSTRACT

Invasive colonizers propagated through human-mediated vectors are bio-homogenizing the world's oceans and impacting the ecological structures and functions. Where do they come from, and where do they go? What bio-physical mechanisms drive them to do what they do? Can we control the human-mediated spread? In this thesis I focus on how seasonal fluctuation of habitat temperature impacts persistence, range expansion and distribution of invasive marine species by developing simple biologically meaningful metrics and producing results consistent with advanced mathematical methods. First, I show how the ambient temperature impacts the net reproductive rate of invasive marine calanoid copepod *Pseudodiaptomous marinus*, thereby, the invasibility of habitats to *P. marinus*. I extend this approach to include periodic fluctuations of habitat temperature by defining a new weighted net reproductive rate, which is a measure of the cross-periodic growth of a population. I use this and other metrics I developed to understand the bio-geographical structure of invasion dynamics of *P. marinus*. In general, the trend for marine invasives is to progress from ecoregions with high-amplitude periodic temperature (APT) to ecoregions with low APT within a range of optimal mean temperatures. This optimal immigration may increase their cross-periodic fitness suggesting an existence of a *conveyor belt* of invasive marine species generation driven by large gradients of temperature-amplitudes across global ecoregions. For further understanding of marine processes, I investigate the Metabolic Theory of Ecology (MTE) models that

describe species (taxonomic) richness, and show that such models perform better for marine taxa, calanoid copepods, copepods and tunicates when periodic fluctuations of temperature are taken into account. The major conclusion in this thesis is that annual temperature cycles and their amplitude-gradients across ecoregions may drive species invasion dynamics and diversity distribution. A large potential of the conveyor belt together with the escalated human-mediated propagule flow may suggest that there would be high-degree invasions in the future across the world's ecoregions. Finally, I show how stochasticity in propagule flow of species introduced to variable environments can be managed cost-effectively through stochastic control methods to reduce the probability of invasions.

ACKNOWLEDGEMENTS

Ecology is full of colour, texture, tone and shape far more than, possibly, the numbers can capture. Modeling in ecology is like carving a piece out of it with a perspective and scientific rationale. Late Prof. Art(thur) Winfree, the theoretical biologist, who believed himself to be an artist in science, would not disagree, it is truly a fascinating laboratory to work in. Either there are multiple truths in ecology or there is none. I would go for the former for my convenience.

I am deeply indebted and grateful to Prof. Mark Lewis, my supervisor, for giving me this wonderful opportunity to enjoy work in his mathematical laboratory (Mathlab). His great insights, knowledge, meticulous questioning and checking my work helped me immensely through this process, and finally producing this thesis. I believe this work will contribute to the present scientific knowledge in invasion ecology. If not for Mark, and his never-said-no funding (through CAISN, NSERC, etc.), ever flowing intellectual criticism and guidance for the major part of my work, my life would have been extremely difficult.

Dr. Alex Potapov, my mentor, is a brilliant mathematician, intellectual, thoughtful person and friend. His mathematical insights, meticulous checking and intellectual sarcasm always helped me in streamlining my work. I also must thank Dr. Carly Strasser for her guidance in ecology in some of my work.

I extend my thanks to Cecelia and Kim for their great great help in all the official matters, Marie for painfully helping me out with my comprehensive exam, Chris, Justin, Jim, Uli, Mariya, Bogdan and their clans for beer, coffee, music and dancing that kept me going, which also often helped me coming back to an earthly life from my philosophical adventures. And I am so grateful to all of them for all that.

Also, I am indebted to all the scientists, probably many a thousands, who have contributed to the Ocean Bio-geographic Information Systems, and NOAA-

ESRL Physical Sciences Division, Boulder Colorado, USA, DFO Canada and many other free information sources on the internet, where I got all the data from. If not for their free services, this work would have been impossible.

I also wish to thank the Department of Biological Sciences, University of Alberta, for giving me teaching assistantships to support my studies. I had a great time working with Prof. Erin Bayne in teaching laboratories for the last 5 years. And I am again so grateful to all of them for all that.

I dedicate this thesis to Rupika, Mevan, my two sisters and Amma, whom I love, and all the scientists who have spent lifetimes collecting the data that I used in a click of a mouse, and for sharing them freely on the internet.

TABLE OF CONTENTS

CHAPTER 1

General introduction

1.1. Invasive marine species.....	1
1.2. How and why species invade.....	3
1.3. Propagule pressure.....	4
1.4. Ecological impact of marine invasives (copepods and tunicates).....	5
1.5. Fluctuating environments and persistence of small populations.....	7
1.6. Species response to ambient temperature.....	10
1.7. Research questions and objectives.....	13
1.8. Thesis organization.....	14
1.9. References.....	17

CHAPTER 2

Identifying potentially invisable habitats for marine copepods using temperature-dependent R_0

2.1. Introduction.....	29
2.2. Model and Methods.....	31
2.2.1. R_0 as a function of temperature	32
2.2.2. Modeling fecundity rates $\beta(T)$	33
2.2.3. Modeling maturation rates $\gamma_i(T)$	34
2.2.3.1. General solution for $n_a(t)$	34
2.2.3.2. Analysis of the case with constant mortality amongst stages.....	35
2.2.3.3. A simple model for maturation rates $\gamma_i(T)$	37
2.2.3.4. An advanced model for maturation rates $\gamma_i(T)$	38
2.2.4. Modeling mortality rates $\mu(T)$	39

2.2.5.	R_0 as a function of temperature given k sub-stages.....	40
2.2.6.	Application and validation.....	41
2.3.	Results.....	41
2.3.1.	Life-history parameters $\beta(T)$ $\gamma_i(T)$ and $\mu(T)$	41
2.3.2.	Net reproductive rate $R_0(T)$	42
2.4.	Discussion.....	43
2.5.	References.....	53

CHAPTER 3

Are invasive copepods generated in habitats in high-amplitude periodic temperatures? The case specific to *Pseudodiaptomous marinus*

3.1.	Introduction.....	58
3.2.	Model.....	61
3.2.1.	Net reproductive rate in constant temperature environment.....	64
3.2.2.	Explicit functional relationship between R_0 and intrinsic growth rate (λ).....	67
3.2.3.	Approximate condition for persistence in habitats with periodically fluctuating temperatures.....	70
3.2.4.	The persistence condition as a function of net reproductive rate and generation times of populations in periodically fluctuating temperatures.....	73
3.3.	Methods.....	76
3.4.	Results.....	79
3.5.	Discussion.....	82
3.6.	References.....	102

CHAPTER 4

High-amplitude periodic temperatures cause a reduction in species taxonomic richness

4.1.	Introduction.....	109
------	-------------------	-----

4.2. Model.....	110
4.3. Methods.....	114
4.4. Results and Discussion.....	118
4.5. Conclusion.....	122
4.6. References.....	128

CHAPTER 5

On controlling stochastic immigration of colonizing and declining populations

5.1. Introduction.....	131
5.2. Model.....	136
5.2.1. Deterministic population model.....	138
5.2.2. Stochastic population model.....	140
5.2.3. Diffusion approximation for EBE probabilities	141
5.2.4. The point of changing the direction of impact of immigration stochasticity on EBE probability.....	142
5.2.5. First passage time.....	143
5.3. Results.....	144
5.4. Discussion.....	145
5.5. References.....	157

CHAPTER 6

Summary, conclusion, and further extensions.....

6.1. References.....	182
----------------------	-----

APPENDICES

Appendix 1.1. Biology of species.....	187
1.1.1. Marine copepods (Subclass Copepoda).....	187

1.1.2. Marine calanoid copepods (Order Calanoida; Subclass Copepoda).....	188
1.1.3. Genus <i>Pseudodiaptomous</i> (Family Pseudodiaptomidae; Order Calanoida).....	189
1.1.4. Marine-estuary copepod <i>Pseudodiaptomous marinus</i> (Family Pseudodiaptomidae; Order Calanoida).....	190
1.1.5. Marine tunicates (Subphylum Tunicata; Phylum Urochordata).....	191
Appendix 2.1. Deriving R_0 from graph theoretic method.....	192
Appendix 2.2. Fitting Eq. (2.6) to data using multiple sub-stages.....	195
Appendix 4.1. Marine ecoregions and the global invasive species diversity distribution.....	196
Appendix 5.1. EBE probabilities.....	197
5.1.1. Special case: EBE probabilities of population in the presence of demographic and immigration stochasticity.....	197
5.1.2. Special case: EBE probabilities of population in the presence of immigration stochasticity.....	199
Appendix 5.2. Moment generating function of passage times of the population first hitting an upper boundary before a lower boundary.....	200
Appendix 6.1. Marine invasive species generation driven by high-amplitude gradients of global ocean temperature cycles.....	202

LIST OF TABLES

	Description	Page
Table 2-1	Model comparisons for cases $k=1, 2$ and 3 of stage maturation rates	46
Table 2-2	Stage maturation rate, stage duration, and development times at 20°C , and coefficient α_a calculated for each stage a for $k=1$.	47
Table 2-3	Estimation of ϕ and χ in $S_v = \exp(-\phi\alpha^{\chi})$ at different temperatures	48
Table 3-1	The parameter values specific to models $\mu(T), \beta(T)$ and $\gamma(T)$ used to compute $A[T(t)]$. Temperature is measured in $^{\circ}\text{C}$.	90
Table 3-2	Critical mean temperatures and cross-periodic intrinsic growth rate of <i>P. marinus</i> at localities where it is introduced in large densities via ship ballast-water discharge.	91
Table 4-1	Regression results of <i>Model 1</i> and <i>Model 2</i> based on the RMA regression (fixed gradient = -1).	123
Table 4-2	Regression results of <i>Model 1</i> and <i>Model 2</i> based on RMA regression estimating an additional gradient for the linear models without fixing it at -1. This is to evaluate the deviations of gradients from -1.	123

Table 6-1 Percentages of exotic marine and estuary species native 177
at least an ecoregion with high-amplitude periodic
temperatures based on published data.

LIST OF FIGURES

	Description	Page
Figure 2-1	Rate of fecundity of adult females at different temperatures comparing sigmoidal model with linear model by Uye et al. (1983). Dashed lines indicate 95% confidence intervals.	48
Figure 2-2	Proportion of individuals in the population not yet past a given stage a obtained by fitting Eq. (2.6) to data from Uye et al. (1983). Solid lines are the fits for $k=1$, dashed lines are the fits for $k=3$.	49
Figure 2-3	Proportion survived at the end of each stage in different temperature regimes fitted to $S_v = \exp(-\phi a^z)$ calculated based on data from Liang and Uye (1997a)	50
Figure 2-4	Quadratic model of daily mortality rates as a function of temperature estimated from pooled stage-based data. Parameter values for mortality rate model are $\kappa_2=0.0022$ /day, $\kappa_1=-0.0563$ / $^{\circ}\text{C}$ day, $\kappa_0=0.4211$ / $^{\circ}\text{C}^2$ day.	51
Figure 2-5	Net reproductive rate R_0 plotted as a function of temperature (T) for the cases where $k=1$ (exponentially distributed stage duration times), and $k=3$ (gamma distributed stage duration times)	51
Figure 2-6	Range of potentially invisable habitats (11 $^{\circ}\text{C}$ to 23 $^{\circ}\text{C}$) for <i>P. marinus</i> as predicted by the model Eq. (2.10) based on $R_0(T)>1$ for sea surface temperature (T) data averaged	52

from year 1971-2000 through NOAA interactive database. Dots are the habitats where *P. marinus* was detected or has established.

Figure 3-1	Net reproductive rate R_0 as a function of mean habitat temperature (T) considering autonomous (non-fluctuating) system dynamics (reconstructed following methods in Rajakaruna et al. (2012) after incorporating all the temperature-dependent mortality data from Uye et al. (1983), including the ones at 27 ⁰ C).	93
Figure 3-2	Cross-periodic fitness (Λ and R_p) with respect to mean habitat temperatures at given amplitudes.	94
Figure 3-3	Invasible habitat range given the cross-periodic reproductive rate R_p .	96
Figure 3-4	The effect of the increased amplitude of temperature on the cross-periodic fitness λ_p .	97
Figure 3-5	Piecewise temperatures, leading eigenvalues, and population density over time.	99
Figure 3-6	A demonstration of how the effect of increased temperature amplitude, keeping the maximum or minimum temperature the same, on the dynamics of <i>P. marinus</i> population introduced with one fertilized female, based on the given temperature profiles in two localities; one having high, and the other having low mean temperatures.	100
Figure 3-7	Yearly mean SST at Race Rocks, B.C. indicating how mean temperature rise change the habitat invasibility.	101

Figure 4-1	Generation times of marine copepods and tunicates modelled with respect to mean ambient temperature.	124
Figure 4-2	Species richness of calanoid copepods, copepods and tunicates of northern temperate marine ecoregions with respect to peak-to-peak amplitude of habitat temperatures, and $\text{Log}_{10}(G)$ (<i>Model 2</i>).	125
Figure 4-3	Ratio of marine copepod species richness between paired ecoregions with respect to ratio of their mean and amplitude of temperatures.	126
Figure 4-4	Copepod taxonomic richness (data reconstructed from Rombouts et al., 2009) (a) by mean habitat temperatures, (b) by latitude, predicted by <i>Mode 3</i> (c) Yearly mean and (d) amplitude of SST by latitudes.	127
Figure 5-1	Population models $\frac{dx}{dt} = f(x)$, and, $\frac{dx}{dt} = f(x) + p$, with dashed lines for the cases linearized at $\frac{dx}{dt} = 0$.	151
Figure 5-2	Dynamics of deterministic population model $\frac{1}{x} \frac{dx}{dt} = r + \frac{j}{x}$ when net-flow rates (j) and intrinsic growth rates (r) are positive and negative. Here, $j=p-a$.	152
Figure 5-3	Probability of a population <i>establishing before going extinct</i> , $G(x_0)$, with respect to increasing (a) environmental stochasticity, and (b) demographic stochasticity, and in favourable and unfavourable habitats.	153
Figure 5-4	Probability of a population <i>establishing before going extinct</i> , $G(x_0)$, with respect to increasing initial population size at x_0 , in favourable and unfavourable habitats.	154

Figure 5-5	Probability of a population <i>establishing before going extinct</i> , $G(x_0)$, with respect to increasing initial population size, and intrinsic growth rate.	155
Figure 5-6	The parametric combination of intrinsic growth rate (r) and net propagule flow rate (j) at which the direction of the impact of stochasticity in propagule flow on EBE probability changes sign.	156
Figure 5-7	Mean time for population <i>establishing before going extinct</i> , $T_n(x_d, x_0)$, with respect to increasing environmental stochasticity, and in favourable and unfavourable habitats.	157
Figure 6-1	Invasive species taxonomic richness linearly regressed with respect to peak-to-peak amplitude of the northern temperate ecoregion (NTE) temperatures	179
Figure 6-2	Peak-to-peak amplitudes and mean of annual sea surface temperature cycles	180
Figure 6-3	Ecoregion means and amplitudes of annual temperature cycles, and invasive species taxonomic richness.	181

ABBREVIATIONS

Abbreviation	Description
AIC	Akaike information criterion
APT	Amplitude periodic temperature
CAISN	Canadian Aquatic Invasive Species Network
CMT-F	Critical mean temperature-fluctuations (or the mean temperature at stability threshold, $R_p = 1$, in the non-autonomous case of fluctuating temperatures).
CMT-S	Critical mean of temperature-steady (or the temperature at stability threshold, $R_0 = 1$, in the autonomous case of steady temperatures).
EBE	Probability of a population <i>first</i> becoming a nuisance species (or establishing) <i>before</i> going extinct.
ENM	Environmental niche modeling
ESA	Endangered Species Act
FPE	Fokker-Planck equations
MTE	Metabolic theory of ecology
NEA, NWA, SEA, SWA, NEP, NWP, SEP, SWP	A-Atlantic, P-Pacific, N-North, S-South, E-East, W-West
NH	Northern hemisphere
NTE	Northern temperate ecoregions
RMA	Reduced Major Axis regression method

RSS	Residual sum of squares
SDE	Stochastic differential equations
SH	Southern hemisphere
SST	Sea surface temperature
STE	Southern temperate ecoregions

MATHEMATICAL NOTATIONS

Notation	Description
Chapter 2 & 3	
$\mathbf{n}(t)$	Stage-composition of the population at time t .
n_1	Number of eggs.
$n_2 \dots n_6$	Number of individuals in the five naupliar stages (II-VI).
$n_7 \dots n_{12}$	Number of individuals in the six copepodid stages, n_{12} being the adult stage.
T	Temperature.
$\mathbf{A}(T)$	Lefkovitch matrix given a parameter space of maturation rates $\gamma_i(T)$, mortality rates $\mu_i(T)$, and fecundity rates $\beta(T)$ that depend on the ambient temperature (T) (stages $i=1..12$), such that $\frac{d\mathbf{n}}{dt} = \mathbf{A}(T)\mathbf{n}$, where n are vectors of stage classes.
$\beta(T)$	Fecundity rate (rate of egg production) in adult females modeled as a function of temperature T : $\beta(T) = f_m f_l e^{w(T-b)} / [f_m + f_l (e^{w(T-b)} - 1)].$
f_m	Maximum rate of fecundity.
f_l	Fecundity at the lowest temperature.
w	Shape parameter that accounts for the depression in fecundity rate at low temperatures.
b	Lag parameter to relax the assumption that fecundity rate curve otherwise intercepts y-axis at the origin.

q	Average proportion of ovigerous females in the adult population: assumed to be a constant at 0.61 for <i>P. marinus</i> .
$\mu_i(T)$	Rate of mortality in stage i as a function of temperature T . Average is given by $\mu(T) = \kappa_2 T^2 + \kappa_1 T + \kappa_0$. Here, κ are parameters.
$\gamma_i(T)$	Rate of maturation of individuals surviving to stage i as a function of temperature T : $\gamma_a(T) = (T-1)^{1.8} / (\alpha_a - \alpha_{a-1})$ for each stage a at temperatures (T). Here, α_a are temperature-independent constants that varies with stage a , with $\alpha_0 = 0$.
α_a	Temperature-independent constants that vary with stage a in the maturation rate function $\gamma_a(T) = (T-1)^{1.8} / (\alpha_a - \alpha_{a-1})$, with $\alpha_0 = 0$, which is derived from the Belehradek's function.
F	Fecundity matrix given by partitioning of matrix as A into two subcomponents as F-V .
V	Transition (including mortality) matrix given by partitioning of matrix as A into two subcomponents as F-V .
ρ	Spectral radius of the matrix $[\mathbf{FV}^{-1}]$, that is, $\rho[\mathbf{FV}^{-1}] = \max_{1 \leq i \leq n} R_{0i} $, where $R_{01}, R_{02} \dots R_{0n}$ are the eigenvalues of the square matrix $[\mathbf{FV}^{-1}]$.
s	Last stage in matrix A .
k	Shape parameter in the Gamma distribution of stage-duration times (or the number of virtual sub-stages in each stage in matrix A).
$R_0 = \rho[\mathbf{FV}^{-1}]$	The net reproductive rate, which yields $R_0(T) = \frac{q\beta_s(T)}{\mu_s(T)} \prod_{i=1}^{s-1} \left(\frac{\gamma_i(T)}{\gamma_i(T) + \mu_i(T)} \right)^k, \quad \text{at}$ constant temperature T .
$\sigma_i = \gamma_i + \mu_i$	Overall transition rate in stages i . Here, $\gamma_i > 0$

and $\mu_i > 0$ for any stage i .

$z_a(t)$

Proportion of each stage a that remains at time t

given by
$$\sum_{i=1}^a z_i(t) = 1 - \sum_{i=1}^a \left[\prod_{\substack{j=1 \\ j \neq i}}^a \frac{\gamma_j}{\gamma_j - \gamma_i} (1 - e^{-\gamma_i t}) \right]$$

d_a

Stage duration time random variable (of stage a).

\bar{d}_a

Mean stage duration time, $\bar{d}_a = \frac{1}{\gamma_a}$ of stage a .

D_a

Stage development time distribution of stage a

given by
$$D_a = \sum_{i=1}^a d_i.$$

\bar{D}_a

Mean stage development time of stage a , also given by $\bar{D}_a = \alpha_a (T-1)^{-1.8}$ (Belehradek's function).

$S_v = \exp(-\phi \alpha^\chi)$

Proportion surviving from eggs to stage a .

ϕ

Scale parameter in $S_v = \exp(-\phi \alpha^\chi)$.

χ

Shape parameter in $S_v = \exp(-\phi \alpha^\chi)$.

$l=ks$

Total number of sub-stages in matrix \mathbf{A} (the dimensions) after incorporating virtual sub-stages for each stage).

λ

The dominant eigenvalue of the matrix $\mathbf{A}=[\mathbf{F}-\mathbf{V}]$ yielded by solving the condition, $\det[(\mathbf{F}-\mathbf{V})-\mathbf{I}\lambda]=0$. Here, \mathbf{I} is the identity matrix.

$g_i = 1/\sigma_i$

Mean sub-stage maturation time within stages i (for $i=1..s$) (s.t., $\sigma_i = \gamma_i + \mu_i$ is the overall transition rate in a sub-stage in stage i , and

	$\sigma_s = \mu_s$ is the transition rate in the last sub-stage of stage $i=s$.
$l = k(s-1) + 1$	Dimensions of matrix \mathbf{A} (after the reduction).
g	Mean sub-stage maturation time.
$d_i = g_i - g$	Deviations from the mean sub-stage maturation time.
$\xi(d)$	Error correction term in the non-linear functional relationship between R_0 and λ , which is a function of d_i .
t_p	Period.
$(\lambda_j, \mathbf{v}_j)$	Dominant eigenpair of \mathbf{A}_i , where each eigenvector is normalized so that $(\mathbf{v}_j, \mathbf{v}_j) = 1$.
$\bar{\lambda} = \frac{1}{t_p} \sum_{j=1}^m \lambda_j (t_j - t_{j-1})$	Time-average of the piecewise intrinsic growth rates over a period (year).
$V = \frac{1}{t_p} \sum_{j=1}^m \log(\mathbf{v}_{j-1}, \mathbf{v}_j) \leq 0$	A measure of the time-averaged variation in stage-structure throughout the period (year).
$\Lambda = \bar{\lambda} + V$	Cross-periodic intrinsic growth rate of the population, or a cross-periodic fitness parameter of the population in periodically fluctuating environment.
$\bar{\Psi} = e^{\Lambda_p}$	Geometrically averaged piecewise growth rates cross a period (year) (piecewise finite growth rates given by $\psi_j = (\mathbf{v}_{j-1}, \mathbf{v}_j) e^{\lambda_j}$ for each time step $j=1:m$).

$$G = \sum_{j=1}^m \left(\frac{t_j - t_{j-1}}{g_j} \right)$$

Total number of generations within the period (year).

$$P_i = \frac{\left(\frac{t_j - t_{j-1}}{g_j} \right)}{\sum_{j=1}^m \left(\frac{t_j - t_{j-1}}{g_j} \right)}$$

Proportion of the number of generations within the interval $(t_j - t_{j-1})$ at temperature T_j to the total number of generations within the period.

$$g_p = (t_p / G)$$

Average generation time of the population within the period.

$$R_p$$

Cross-periodic (weighted net) reproductive rate of the population $R_p = \left(\sum_{j=1}^m P_j R_{0,j} \left(\frac{1}{l} \right) + g_p V \right)^l$.

$$\Lambda_p = \frac{1}{g_p} \left(R_p^{\frac{1}{l}} - 1 \right)$$

Cross-periodic intrinsic growth rate of the population. Here, $\lambda_p = \frac{1}{g_p} \left(R_p^{\frac{1}{l}} - 1 \right)$ where $V=0$.

$$h_j = \left(\frac{t_j - t_{j-1}}{g_j} \right)$$

Number of generations that last in season j .

$$\bar{T}$$

Periodic average temperature of annual habitat temperature cycles given by $T(t) = \bar{T} + \alpha \sin(\omega t + \varphi)$.

$$\alpha$$

Amplitude of the annual habitat temperature cycles.

$$\omega = 2\pi / t_p$$

Frequency of the annual habitat temperature cycles.

$$\varphi$$

Phase of the annual habitat temperature cycles.

Chapter 4

A	Habitat area
S	Taxonomic richness of species.
N_j	Population density of species j per unit area, $j=1..S$.
$J = \sum_{j=1}^S N_j A$	Total number of individuals across all species.
B_j	Metabolic rate (Jules s^{-1}) of an average individual of species j varying with body-size M_j , and the ambient temperature T , such that $B_j = b_0 M_j^{3/4} e^{-E/k_b[T+273.2]}$.
b_0	A normalization constant independent of body size and temperature ($b_0 \sim 2.65 \times 10^{10} \text{ W g}^{-3/4}$).
$e^{-E/k_b(T+273.2)}$	Boltzmann factor that describes the temperature dependence of the metabolic rate.
E	Activation energy of metabolism ($\sim 0.78 \text{ eV}$).
k_b	Boltzmann constant ($8.62 \times 10^{-5} \text{ eV K}^{-1}$).
T	Temperature in centigrade.
\overline{M}	Average body size of an individual.
$\overline{B_T} = \overline{BN}$	Average energy flux of a population (a species) in the community, which is considered as a temperature-independent constant.

$\bar{N} = \frac{1}{S} \sum_{j=1}^S N_j$	Density of a population averaged over the number of species.
$\bar{g} = \eta \bar{M}^{1/4} \exp^{E/k_b [T+273.2]}$	Average generation time per species for individuals of the populations having average body size, \bar{M} . Here, η is the proportionality constant.
$G = \left(\frac{1}{T_0} \int_t^{t+T_0} \bar{g} dt \right)$	Average generation time per species over the period T_0 .
T_0	Period (year).
α	Peak-to-peak amplitude of annual ecoregion temperature cycles.
$R_{Adj}^2 = 1 - \frac{(n-1)}{(n-p)} (1 - R^2)$	Adjusted R^2 . Here p is the sample size, and n is the number of parameters.
w	Scaling parameter.

Chapter 5

λ	Intrinsic growth rate term in the stochastic differential equation (SDE) (r_m in Fagan et al., 2010).
p	Propagule flow rate.
a	Rate of virtual loss of population due to individuals that cannot, on average, replace themselves resulting from the demographic Allee effect (the simplest Allee form described

in Gregory, 2010).

$$j = p - a$$

Net propagule flow rate into a habitat.

$$\alpha(x) = \lambda x + j$$

Infinitesimal mean of the process (x -population size).

$$\beta(x) = \sqrt{\sigma_e^2 x^2 + \sigma_d^2 x + \sigma_p^2}$$

$\sigma_e^2 x^2$, $\sigma_d^2 x$ and σ_p^2 are infinitesimal variances in the population fluctuations corresponding to the environment (see Ricciardi, 1986), demography (see Feller, 1951), and immigration.

$$P(x_0, t)$$

Transition probability density for a population at *initial* position (x_0) and time ($-t$), given that the final position and time are *fixed*.

$$A(x) = \alpha(x)$$

Drift coefficient.

$$B(x) = 2(\beta_e x^2 + \beta_d x + \beta_p)$$

Diffusion coefficient, where $2\beta_e = \sigma_e^2$, $2\beta_d = \sigma_d^2$ and $2\beta_p = \sigma_p^2$ are the spectral densities of the zero average Gaussian processes corresponding to environmental, demographic, and immigration stochasticity.

$$G(x_0)$$

The *probability of a population first hitting an arbitrary upper threshold (x_d) before first hitting an arbitrary lower threshold (x_e)* assuming initial position $x_d > x_0 > x_e$. Here, x_d and x_e can be interpreted as the establishment and the extinction boundaries in ecology, and thus, $G(x_0)$ can be defined as the EBE probability (i.e., the probability of population

establishment before extinction).

$$E(x_i) = (bx_i + c)^k {}_1F_1\left(k, k+1; \frac{-\lambda}{b^2}(bx_i + c)\right) \quad \text{That corresponds to } G(x_0) = \frac{E(x_0) - E(x_e)}{E(x_d) - E(x_e)},$$

$$\text{where } b \equiv \sigma_d^2/2, \quad c \equiv \sigma_p^2/2, \quad k = \left(\frac{\lambda c}{b^2} - \frac{j}{b}\right) + 1,$$

and x_i denotes x_0 , x_e , and x_d . Here, ${}_1F_1$ is the Kummer confluent hypergeometric function of the first kind

$$E(x_i) = \text{Erf}_z\left(\frac{j + \lambda x_i}{\sigma_p \sqrt{\lambda}}\right)$$

$$\text{The term in equation } G(x_0) = \frac{E(x_0) - E(x_e)}{E(x_d) - E(x_e)},$$

which is the solution $G(x_0)$ for case of immigration stochasticity alone present. Here, x_i takes subscript values $i=0, e, d$.

$$T_n(x_d, x_0)$$

The n^{th} moment of the first passage time, given that the population first hits an arbitrary upper threshold, x_d , before an arbitrary lower threshold, x_e . As before, x_d and x_e can be interpreted as establishment and extinction boundaries in ecology, thus $T_n(x_d, x_0)$ can be defined as the n^{th} moment of first passage time for EBE assuming the initial position of the population size is at $x_d > x_0 > x_e$

Chapter 6

\bar{T}	Mean of annual ecoregion temperature cycles.
A	Peak-to-peak amplitude of annual ecoregion temperature cycles.

CHAPTER 1

General Introduction

Every level of biological and ecological organization from cells, organisms, populations, and communities to ecosystems and also world's marine ecoregions at large, are subjected to, or driven by external forces. These forces are most often periodic, trended, and stochastic. At organism level, which is collectively reflected at population level, the temporal and spatial transition of these forces affects the life-history traits (parameters) of populations, mainly fecundity, mortality, and maturation rates. Thus, persistence and the growth of a population are determined by how a population responds to these in time and space, and evolutionarily over generations. The spatial variability of temporal profiles of external forces, therefore, may determine the persistence, immigration, and distribution of populations in native and introduced environments. In this thesis, I investigate how habitat temperature profiles; the variability of temperature over time and space; impact population dynamics of ectothermic invasive marine calanoid copepod *Pseudodiaptomous marinus*, and taxa, calanoid copepods, copepods (in general), and tunicates, and also marine invasive species in general. I also investigate how stochastic propagule flow and the resulting population establishment in novel environments could be managed through stochastic control methods.

1.1. Invasive marine species

Among ecologists, there is much debate regarding what is an invasive species. It is fundamentally based upon epistemic and linguistic uncertainties (McGeoch et al., 2012). Ricciardi (2013) defines invasives as “non-native species with conspicuously high colonization rates” and “have the potential to spread over long distances”. He further claims that “the term invasive is also used (often by

policy makers) to describe colonizing species that cause undesirable ecological or economic impacts”.

Heger et al. (2013) are of the view that biological invasions are a matter of perspective. While some argue that only the impact factor of invasives should be considered regardless of their origin (Davis et al., 2011), others argue that the origin of invasives matters because they benefit from the functional traits that are brought with them (Knapp and Kühn, 2012). Ricciardi et al. (2013) propose a theoretical framework for defining and predicting the impact of non-native species.

However, a major practical implication of Ricciardi's (2013) definition, or any other for that matter, is the ambiguity or the fuzziness surrounding the terms such as “conspicuously high” colonization rates, and spread over “long distance”. The quantitative (measures of these definitions are hard to be made, thus, mostly based upon the consensus among ecologists. We cannot clearly delineate a slow colonizer from a rapid colonizer by the degree of their colonization rate (either range or population expansion in a novel range). In invasion ecology, quantitative (mathematical) definitions are hard to find. Therefore, we stick to the definition, whereby, we call a species an “invasive” in conformity with the popular agreement amongst the ecologists based on published work. Thus, our definition does not necessarily involve the degree of impact of a species in a novel environment. In this sense, *P. marinus* is an invasive species, as it expands its range widely and rapidly around the world regardless of the measurable impacts.

There is much ambiguity also surrounding native and non-native ranges of species (for e.g., Carlton, 1996; Pysek, 2003; Richardson et al., 2000). There are often cases where the origins (the native range) of invasives are misidentified (Stefaniak et al., 2012). McGeoch et al. (2012) analyse the epistemic uncertainties including the inadequate information on indigenous range of species. These uncertainties due to scarcity of evidence result in subjective interpretations. Correct identification of the source population of an invasive species is a prerequisite for testing hypotheses concerning the factors responsible for biological invasions. Although genetic analyses (e.g., Lombaert et al., 2011) may

tell, to what degree species are evolutionarily related across regions, their true origins are hard to be identified as ranges shift over geological times. The native and non-native ranges of species are, therefore, dependent upon a spatial and temporal framework based upon our present knowledge.

1.2. How and why do species invade?

In plant invasion ecology, there are more than 29 working hypotheses that may describe or explain an invasion (Catford et al., 2009). Most of them are common to aquatic invasions as well. Yet they are context-dependent and thus, can not be generalized, or refuted. Some theories are based on classical interaction theories, bio-physical and bio-chemical characteristics, genetic, evolutionary, ecological niche, and stochastic theories. Some have proposed unifying theories and models (Barney, 2008; Blackburn et al., 2011; Gurevitch et al., 2011; Whitlow, 2008). However, the crux of the problem seems that no theory or model, as Shrader-Frechette (2001) argues, is comprehensive or is a “predictive theory of invasibility.”

Ecological niche models (ENM) are generally accepted and used often in invasion ecology (Jiménez-Valverde et al., 2011). Their predictions are based upon the set of environmental variables (here onwards, we call the environmental set) of the native range, which is matched with the potentially invisable range. However, in general, there is no mechanistic basis for these models as yet. They are phenomenological or top-down statistical approaches. Thus, for example, the ENM do not usually incorporate how species functionally respond to temporal variability of the environmental set other than the tolerance of the species to extreme and constant environments. Thus, when the temporal variations of the environmental set of a novel range deviates from that of the native range, it is often hard to predict the invasibility of the novel range using ENM. Above all, ENM fails to differentiate a potential invasive from a non-invasive other than being able to calibrate the environmental set that any species can tolerate. This

weakness in ENM falls short of predicting which species are potentially invasive than others, or be the next invader in the context of invasion ecology.

1.3. Propagule pressure

The invasion process starts with a species being introduced to a novel habitat, where the species had not been found before or was non-native to, via a vector, in line with the definition of an invasive. The species first gets established and then may reproduce largely, either further spreading or expanding its population, and in some instances highly dominating or impacting the structure and functions of the novel range (Catford et al., 2009). The measurable quality or quantity of propagules (eggs or any other stage that can propagate) introduced to a novel habitat (per area over time) is known as the *propagule pressure* (Simberloff, 2009). Simberloff (2009) states that “increasing propagule size enhances the establishment probability primarily by lessening the effects of demographic stochasticity, whereas propagule number acts primarily by diminishing the impacts of the environmental stochasticity.”

The human-mediated propagule pressure, for example, via ship ballast-water discharge, is fundamental to most marine invasions (Cordell et al., 2009; Lawrence and Cordell, 2010; Seebens et al., 2013). Propagule pressure has escalated in recent times due to increased ship-trafficking catering to the demand of transportation across the seas and the oceans. Ships take up ballast water from one port to balance their weight, and discharge the water at another port. Through this process they carry the propagules that can survive the journey from one port to another over long periods (Klein et al., 2010). Propagule pressure is a main driver of invasions (Lockwood et al., 2005; 2009). It has been suggested that propagule pressure may be considered as a null model for all invasions (Colautti et al., 2006).

Recently, new regulations have been implemented to control invasions through ballast-water discharge. These include, chemical and temperature treatment of ballast-water tanks, and mid-oceanic exchange of ballast-water

(Tsolaki and Diamadopoulos, 2010; Simard et al., 2011). However, there is no guarantee that these mechanisms can reduce the invasion risk levels to a bare minimum, although they involve large costs. Besides, the quality and the quantity of propagules discharged from ships vary largely from ship to ship (Villac and Kaczmarek, 2011), and also depending on where the ballast-water tanks are filled (Lawrence and Cordell, 2010). We do not yet know how stochasticity in propagule pressure, together with environmental and demographic stochasticity, impacts the risk of population establishment, and thus, which control mechanisms optimize the effects (benefits) over costs.

To study aquatic species invasions and propagule pressure via ship ballast-water discharge, the Canadian Government has funded the Canadian Aquatic Species Network (CAISN, n.d.) project, networking scientists and the industry across Canada. We do not know the potential impact of the next invader, or which population will thrive in a novel environment and become a nuisance. We may not worry if a new species is benevolent to the existing ecological system, and provides positive trickle-down effects, but this obviously depends on our value judgement. However, the case is that nuisance species are often hard to manage (Connelly et al., 2007). Homans and Smith (2013) evaluate the management options for aquatic invasive species, and Hyytiäinen et al. (2013) address optimized frameworks for management.

1.4. Ecological impact of marine invasives (copepods and tunicates)

Non-native species can change the composition of the resident species and impact the natural resource based industries; fisheries, agriculture; infrastructure; docks, piers, dams; water supply, power plants, shipping, and recreation (Ruiz et al., 2011). In marine and estuarine waters of North America, Ruiz et al. (2011) indicates that the impacts are most frequent with introduced barnacles (75% of species), copepods (57%), and decapods (33%). Slightly over 10% of species are reported to have competition, 5% of species are reported to have effects as a result of predation (including herbivory) providing a food/prey resource, or altering

habitats. Effects on host populations by parasitism is reported for 3% of species, while the effects on threatened or endangered species are reported for 3% of species.

In further detail, Ruiz et al. (2011) indicates that in the fresh and brackish delta regions of the San Francisco Bay estuary, five non-native species of planktonic copepods, including *Pseudodiaptomus marinus* and *P. forbesi*, became abundant and dominant over the course of seven years (Cohen and Carlton, 1995; Modlin and Orsi, 1997; Orsi and Ohtsuka, 1999; Orsi and Walter, 1991). Within two years of its first detection, *P. forbesi* became the most abundant calanoid in fresh and oligohaline regions of the delta, while *Eurytemora affinis*, which was an early introduction to the estuary (Lee, 2000; Orsi, 2001), and had been a dominant mesozooplankter (Ambler et al., 1985), declined. *Pseudodiaptomus forbesi* partly replaced a previous invader, *P. inopinus*, in the Columbia River estuary (Cordell et al., 2008; Sytsma et al., 2004). At Lake Faro (Messina, Italy), *P. marinus* was the third dominant species with respect to abundance (Sabia et al., 2012). Ruiz et al. (2011) suggests that “crustaceans not only contribute to the overall spatial patterns of species distribution, but also provide an important barometer for invasion dynamics.”

Invasive tunicates are introduced to novel environments as fouling organisms on the hulls of ships. They may be introduced also as larvae through ship ballast-water discharge. Some species in Europe and Americas, thought to be indigenous, are, in fact, invaders immigrated centuries or even millennia ago (for example, European periwinkle, *Littorina littorea* (del Mundo, 2009)). In some areas, tunicates are a major threat to aquaculture operations (USGS, 2013).

It has been estimated that invasive aquatic species costs billions of dollars to the US economy over a calendar year (Lovell et al., 2011; Pyšek and Richardson, 2010). It is an ongoing debate as to whether invasives are a major cause of native species extinction and biodiversity loss (Clavero et al., 2005; Didham et al., 2005; Gurevitch and Padilla, 2004; Molnar et al., 2008; Roberts et al., 2013). However, more studies are needed to investigate whether the costs of

invasions outweigh the benefits (McLaughlan et al., 2013) at least from an anthropocentric perspective.

The major model-species considered in this thesis is the invasive marine calanoid copepod *Pseudodiaptomus marinus*. The temperature dependencies of taxa, Copepoda (in general), Calanoida Copepoda, and Tunicata, and also marine invasive species in general, are also investigated. Details of their life-histories are introduced when they are modeled. However, further details are given in Appendix 1.1.

1.5. Fluctuating environments and persistence of small populations

Fluctuations in an environment can have trended, periodic (seasonal), and stochastic effects. The study of stochastic effects in an environment on populations is commonly done using two methods: (i) top-down approach that accounts for the “environmental stochasticity” (or the temporal fluctuations in the *probability* of mortality and reproduction of all individuals of the population in the same or similar fashion (Lande et al., 2003)). This is also interpreted as the random variation in the expected fitness (the finite growth rate), which is independent of the population density (Lande et al., 2003)); (ii) bottom-up approach that directly accounts for how much stochasticity in the external environment (e.g., temperature, salinity) is functionally transformed to the stochasticity in the population. The former is commonly modeled using Ito stochastic differential equation (SDE) formulation in ecology (as in population viability analysis (PVA): Morris and Doak, 2002), and the latter, which accounts for how much stochasticity in the forced external environmental factor is reflected in the stochasticity in the population dynamics, is modeled using Ito SDE with Ito lemma (for parallels, see Alexandridis and Zaprani, 2013; Neftci, 2000). Ito lemma is the stochastic calculus counterpart of the chain rule, when one stochastic process is a function of one or more other stochastic processes.

If the noise in the SDE formulation is an approximation to continuously fluctuating noise in the environment, then the appropriate representation of the system dynamics may be the Stratonovich SDE (Ricciardi, 1986). However, the noise in the SDE formulation is an approximation to discrete pulses with finite separation to which the system responds, or the SDE is a continuous approximation to a discrete system, then Ito representation may be more appropriate (Ricciardi, 1986). Although there are different representations of the same thing (see for example, Braumann, 2007; 2008), the controversy over which SDE formula to be used has not been resolved fully. The Stratonovich and Ito SDE are, however, mathematically related (Gardiner, 2004).

The SDE population models can also take the demographic stochasticity into account. The demographic stochasticity is due to chance events of individual mortality and reproduction, which are considered to be independent among individuals. In other words, random variation in individual fitness produces the demographic stochasticity (Lande et al., 2003).

The SDE models are commonly used to predict persistence and extinction probability of populations based on the models calibrated by the past population fluctuation data for a given environment (for e.g., in PVA). Therefore, they are difficult to be calibrated before a population is introduced to a novel environment, unless the causality of the stochasticity in the population is directly weighted and calibrated in relation to the stochasticity in the external forcing variables. Therefore, in the context of invasion ecology, the SDE models remain theoretical tools yielding qualitative predictions of the effects of fluctuating environments on introduced populations, and providing management scenario analysis using simulations and analytical methods.

To quantify how seasonal or periodic fluctuations of environmental factors affect the population dynamics, or the life-history parameters (traits), we can mathematically express the population persistence metrics as functions of the environmental variables. For example, we can construct mechanistic population models describing the temperature dependencies of life-history parameters on

population persistence metrics. When the fluctuations are periodic, and the system is stage-based, the methods based on Floquet theory can be used to derive their stability conditions (Klausmeier, 2008).

Two common metrics that determine population persistence in a given environment are, the intrinsic growth rate (λ), and the net reproductive rate (R_0). The intrinsic growth rate, which is a life-history trait and a physiological fitness parameter, is defined for a population in a constant environment, or with respect to a constant external environmental forcing factor (as in Amarasekare and Savage (2012); shown with respect to temperature). It is also considered that intrinsic growth rate is sensitive to short-term transient states of the environment. The net reproductive rate is the average number of offspring produced by a female over her lifetime, which reflects the rate of population growth at a longer time-scale in a constant environment. However, the threshold conditions of the two metrics are related: λ goes through zero as R_0 goes through one; and a non-linear relationship exists between the two metrics derived for non-staged populations (Wallinga and Lipsitch, 2007).

The demographic Allee effect is defined as the negative per capita growth rate of a population at low densities (Taylor and Hastings, 2005), or a virtual absorption of the population. The Allee effect is also categorized as component Allee effects, which are the positive relationships between any measurable components of individual fitness and the population density (Courchamp et al., 2008). The degree of Allee effect is the key to persistence of small populations (Taylor and Hastings, 2005) in addition to demographic stochasticity (Lande et al., 2003). The demographic Allee effect may be dependent on the population density more than the population size, whereas, the demographic stochasticity may be dependent on the population size more than the population density. The demographic Allee effect is categorized as weak, moderate and strong (Taylor and Hastings, 2005). Furthermore, the growth of a population is also limited by density-dependence bounded by an upper population ceiling, which can be ignored when evaluating persistence of introduced small populations. These

concepts are used in the thesis when developing models for persistence of small populations in fluctuating environments.

1.6. Species response to ambient temperature

Metabolism is the underlying process that governs most biological rates (Brown et al., 2004). Temperature is fundamental to metabolism (Allen et al., 2001; Goolley et al., 2002), thereby affecting life-history traits; maturation, growth, mortality, reproductive rates of populations, and eventually reflecting on the population dynamics (Amarasekare and Savage, 2012; Savage et al., 2004; Strasser et al., 2011). Much of the variation in species diversity is also attributed to the kinetics of biochemical reactions, thus, the temperature. Hence, “the warmer the environment, the faster the evolutionary dynamics resulting higher rates of speciation and higher standing stocks of species (Brown et al., 2004).”

Based on numerous studies of species cross taxa; invertebrates, fish, and lizards; Amarasekare and Savage (2011) indicate that per capita fecundity (averaged over the reproductive life span) of a population exhibits a symmetric unimodal relationship with temperature. Similar relationships are also shown for the fecundity of ectothermic marine species (Brugnano et al., 2009; Halsband-Lenk et al., 2002; Holste and Peck, 2005; Saiz et al., 1999; Sullivan and McManus, 1986; Uye, 1981; Uye and Shibuno, 1992). Per capita mortality rate of ectothermic species is also related to temperature, increasing with increasing temperature; the relationship that can be described by the Boltzmann-Arrhenius function (Amarasekare and Savage, 2004).

Global syntheses on temperature dependencies of maturation, mortality, and fecundity rates have been shown for many species, including the copepods (Hirst and Kiørboe, 2002; Huntley and Lopez, 1992; Kiørboe and Hirst, 2008; Kiørboe and Sabatini, 1995). For tunicates, the response of generation time to temperature has been generalized (Deibel and Lowen, 2012), and it follows a pattern similar to that of the copepods (Huntley and Lopez, 1992). These relationships are similar to what is predicted by Gillooly et al. (2001; 2002)

followed by Savage et al. (2004). These suggest that the generalized models proposed by Amarasekare and Savage (2012) and Savage et al. (2004) should also hold true for marine species in general. These indicate that the distribution of marine species may be regulated and limited by habitat temperatures.

Moving to a focal study organism of the thesis, Uye et al. (1983) indicate that at Fukuyama harbour and Tomo, the growth rate of marine invasive calanoid copepod *P. marinus* is not regulated by the food concentration, but depends on the varying habitat temperature. Indeed, the geographical distribution of *P. marinus* shows that it may not thrive neither in much colder nor much warmer waters (Brylinski et al. (2012)). The distribution of *Pseudodiaptomus* genus, as a whole, also seems limited by the cold ocean temperatures (Brylinski et al., 2012). These suggest that response of *P. marinus* to temperature may be optimal at a certain range of habitat temperatures similar to what is shown by Amarasekare and Savage (2012) for ectothermic species in general.

In marine ecological studies, especially of copepods, ambient temperature is typically given by the sea surface temperature (SST). The exact meaning of *surface*, however, varies according to the measurement method being used, but it is commonly between 1 mm and 10m below the sea surface (GHRSSST, n.d.). The daily fluctuations of the upper surface layers vary on average 0.3-0.5⁰C (Guemas et al., 2011). In temperate ecoregions, the mixed layer, where the temperature is approximately homogeneous, typically has depths of 150 to 250m by end of winter (e.g., Kara et al., 2003). In tropics, the thermocline is large (Ratsimandresy et al., 2001), whereas in polar region it is the lowest and less seasonal (SIO, n.d.). However, in near-shore and shallow-water zones, the water is mixed up due to turbulence from wind driven waves, currents, tides and upwelling destabilizing the thermocline. Huntley and Lopez (1992) suggest that the vertical spatial scale appropriate for temperature related surveys on marine copepods is probably in the order of 10-100m, the upper mixed layer, where the bulk of planktonic biomass resides in, and encompasses most species at all stages of their life-history (Huntley et al., 1987; Williams and Conway 1988a; 1988b; Williams and Lindley, 1980; Williams et al., 1987). Hence, the SST may be a

reasonable proxy for a comparative study of the effect of ambient temperatures of the species in the neritic zone (shallow-water depths <200m) across regions. The neritic zone comprises of the *marine ecoregions*: the coastal regions categorized based on the similarities in geo-morphological features, currents, temperatures and ecological characteristics (Spalding et al. 2007).

The greatest variability in temperature would be expected in the near-shore temperate zones (Huntley and Lopez, 1992). The annual temperature cycles in some regions in the northern temperate ecoregions (NTE) show amplitudes exceeding 14⁰C (NOAA-ESRL, n.d.). These fluctuations are due to mixing up of cold and warm water currents (Wyrski, 1965), and also large seasonal differences in air-to-surface heat transfer occurring in the temperate ecoregions. These monthly average temperature data are commonly fit to smooth sinusoidal curves (for e.g. see Benyahya et al., 2007; Caissie et al., 1998).

Marine species, especially copepods, get acclimatized to change in temperature quickly enough that their responses to temperature are reflected in their intra-annual, seasonal, monthly and even weekly abundance variations (see Bollens et al., 2012; Jang et al., 2013; Liang and Uye, 1997a; Sullivan and McManus, 1986; Sun et al., 2011; Usov et al., 2013; Uye et al., 1983). Although the exact time-scale of population responses to change in temperature is unknown, it is said that generation time, which is in the range of days to months, is a reasonable scale for copepod temperature related experiments in a variable temperature environment (Huntley and Lopez, 1992; Landry, 1975). This has also been a rule of thumb for acclimatization of copepods before laboratory experiments.

The diversity (taxonomic richness) of copepods (Rombouts et al., 2009) and other marine species (Tittensor et al., 2010) is high in the tropics and low in the polar regions forming a latitudinal gradient, which is slightly non-linear and concave (Record et al., 2012). Mean latitudinal temperatures also form a gradient similar to the diversity gradient. The metabolic theory of ecology suggests that the latitudinal distribution of diversity and the temperature are causally positively related (Allen et al., 2002; Rombouts et al., 2009; 2011), resulting in high

individual metabolic rates and high entropy, leading to high rates of speciation (Allen et al., 2006, Gillooly and Allen, 2007). These suggest that marine species diversity is also largely limited and regulated by the ocean temperatures. Hence, organisms respond to temperature at all levels reflecting on their populations and communities.

1.7. Research questions and objectives

(A) As life-history parameters of ectothermic marine species and taxa respond to temperature markedly, then the questions arise as to;

1) How the ambient temperature in novel habitats affects the persistence and the invasiveness of ectothermic marine species, and the invasibility of habitats (from a bottom up, mechanistic approach)? Model species: marine calanoid copepod *P. marinus*.

2) Does spatial variation of habitat-temperature temporal profiles (annual temperature cycles) impact geographical distribution and range-expansion of species? Model species: marine calanoid copepod *P. marinus*.

3) Does periodic fluctuation of habitat temperatures impact marine invasive species diversity (taxonomic richness) distribution and invasibility of habitats?

4) Is global marine species diversity (taxonomic richness) distribution shaped by the fluctuation of ocean temperatures? Model taxa: calanoid copepods, copepods, and tunicates

(B) How does stochastic propagule flow impacts invasive species establishment?

The objectives of this research are to determine,

- 1) where the marine invasive species are generally originated from (generators) and where they go (sinks),
- 2) what bio-physical mechanisms drive them,
- 3) whether they impact native species distributions,
- 4) clues to differentiate invasives from non-invasives,
- 5) whether we could limit invasions by stochastic controlling of the human-mediated propagule flow.

1.8. Thesis organization

This thesis contains five research chapters, which includes an extension.

In **Chapter 2**, we model the net reproductive rate of populations, R_0 , as a function of temperature-dependent life-history parameters (traits) for invasive marine calanoid copepod *Pseudodiaptomus marinus*. The model is based on stage-structured population dynamics given by a linear system of ordinary differential equations. We parameterize the model using published laboratory and field survey data. The criterion $R_0(T) > 1$ yields the range of potentially invadable habitats for *P. marinus* on a global scale based on mean habitat temperatures (T). The model predictions match the field evidence of the species' geographical distribution and range expansion.

In **Chapter 3**, we derive two simple, biologically meaningful metrics: the cross-periodic intrinsic growth rate, which is a cross-periodic fitness parameter; and a weighted net reproductive rate, which is a measure of cross-periodic growth rate, to evaluate the stability of a stage-structured population in a habitat with periodically fluctuating temperatures. We test the consistency of the metrics with complex numerical mathematical methods. We find that, accounting for periodic

fluctuation of temperature narrows down the potentially invisable habitat range for the species compared to that predicted by the mean habitat temperature alone. The native range of *P. marinus* involves high-amplitude periodic temperatures (APT). Its *optimal immigration* from high to low APT habitats increases the temperature-dependent cross-periodic fitness by many folds by releasing the temperature-dependent stress. This may help *P. marinus* to become “invasive” in novel habitats, taking the advantage of the existing large temperature-amplitude gradient across the world’s marine ecoregions. Potentially invisable range predicted by the model is supported by recent range expansion of *P. marinus* in Europe. The theoretical results suggest, implicitly, that the effect of initial quantity, time of the year, and the frequency of introductions of individuals may only be secondary in habitats where the periodic fluctuation of temperature limits the population persistence. The model also explains the proliferating reproduction strategy shown by species live in short-summer environments, and how fluctuations help populations in extreme temperature environments. Furthermore, we show how a gradual rise in global sea surface temperature impacts the species range expansion, and how a simultaneous rise in the amplitude of periodic temperature fluctuations subdues such effect.

The metabolic theory of ecology (MTE) suggests that high mean temperatures increase the rate of speciation due to high individual metabolic rates, and high entropy, resulting high biodiversity in marine, land, and freshwater environments. This is supported by strong evidence from species richness gradients along the latitudes. However, we do not know how fluctuations of temperature, some amplitudes exceeding 14⁰C, affect marine species richness in line with the MTE. By extending MTE models, we show in **Chapter 4** that high APT in annual temperature cycles should cause a drop in the cross-periodic metabolic rates decreasing the species richness due to their non-linear dependencies. We find evidence to support this decrease in species richness with respect to diversity distribution of marine taxa, calanoid copepods, copepods, and tunicates, in the northern temperate ecoregions (NTE), where the amplitude

gradient of periodic temperatures is extremely large across the region. This finding solidifies the use of MTE as a strong analytical tool in ecology.

In **Chapter 5** we investigate how stochasticity in immigration (propagule flow), which is common in the case of marine species spreading via ship ballast-water vectors, impacts the probability of population *establishment before extinction* (EBE probability), and also the first passage time, for small populations subject to environmental and demographic stochasticity. This is in order to investigate clues to reduce the impact of propagule pressure on population establishment.

Here, we use a simple population model with an Allee effect described by a stochastic differential equation (SDE), and employ the Fokker-Planck diffusion approximation to quantify the EBE probability. We find that the effect of the stochasticity in immigration on the EBE probability depends on both the intrinsic growth rate (λ) and the mean rate of propagule flow (p). In general, if λ is large and positive (e.g., where species are introduced to favourable habitats), or if p is much greater than the rate of population decline due to demographic Allee effect (e.g., when very high rate of immigration is present), then generally the stochasticity in immigration decreases the EBE probability. If λ is large and negative (e.g., where species are introduced to unfavourable habitats), or if the rate of decline due to the demographic Allee effect is much greater than p (e.g., where very low rate of immigration is present), then generally the stochasticity in immigration increases the EBE probability. However, the mean time for *establishment before extinction* (mean time for EBE) decreases with the increasing stochasticity in immigration with both positive and negative large λ . Thus, the results suggest that ecological management of populations involves tradeoffs as to whether to increase or decrease the stochasticity in immigration in order to optimize the desired outcome. Moreover, the management of invasive species spread through stochastic control methods, for e.g., by stochastic monitoring and treatment of vectors such as ship ballast-water, may be appropriate and cost-effective where the environmental and demographic stochasticity are also present at introductions.

Chapter 6 gives a summary, conclusions and a further extension. Based on a preliminary analysis (Appendix 6.1), we show how marine invasive species, in general, are distributed around the world ecoregions similar to *P. marinus*, with respect to means and amplitudes of annual temperature cycles of the ecoregions. We find that the amplitudes of annual periodic fluctuations of temperature of the northern temperate ecoregions (NTE), within a 10-24⁰C mean ecoregion temperature range, are inversely related to invasibility of the ecoregions, which can be measured by the taxonomic richness of invasives. There is a possibility that marine invasive species in general follow the pattern of temperature-dependent fitness similar to *P. marinus* or the generalized pattern shown for ectothermic species by Amarasekare and Savage (2012). This may suggest that marine invasives that originated from extremely high APT NTE, in general, may gain a cross-periodic fitness by optimal immigration along the temperature-amplitude gradient to low APT ecoregions across the world ecoregions similar to the case of *P. marinus*. Theoretically, this process should help marine species to become “invasive” in low APT ecoregions, in general. This may question whether the invasives are originated from extremely high APT ecoregions in the NTE (invasive generators), and immigrating to low APT ecoregions (invasive sinks), in general, suggesting an existence of a *conveyor-belt* of marine invasive species generation. There is piecemeal evidence to support such theory based on documented native ranges of non-indigenous and invasive marine species distributions. If that is the case, then existence of extremely large APT gradients across the world’s ecoregions may also suggest that we should be cautious about high-degree invasions in the future, even at the level of biotic mixing of oceans and seas at the present level of human-mediated propagule pressure.

1.9. References

Alexandridis, A.K., Zapranis, A.D., 2013. Weather Derivatives: Modeling and Pricing Weather-Related Risk. Springer, NY, p. 300.

Allen, A.P., Brown, J.H., Gillooly, J.F., 2002. Global biodiversity, biochemical kinetics, and the energetic-equivalence rule. *Science* 297(5586), 1545-1548.

- Allen, A.P., Gillooly, J.F., Savage, V.M., Brown, J.H., 2006. Kinetic effects of temperature on rates of genetic divergence and speciation. *Proceedings of the National Academy of Sciences* 103(24), 9130-9135.
- Almeda, R., Calbet, A., Alcaraz, M., Yebra, L., Saiz, E., 2010. Effects of temperature and food concentration on the survival, development and growth rates of naupliar stages of *Oithona davisae* (Copepoda, Cyclopoida). *Marine Ecology Progress Series* 410, 97-109.
- Amarasekare, P., Savage, V., 2012. A framework for elucidating the temperature dependence of fitness. *American Naturalist* 179(2), 178-191.
- Ambler, J.W., Cloern, J.E., Hutchinson, A., 1985. Seasonal cycles of zooplankton from San Francisco Bay. *Hydrobiologia* 129:177-197.
- Andersen, V., Devey, C., Gubanova, A., Picheral, M., Melnikov, V., Tsarin, S., Prieur, L., 2004. Vertical distributions of zooplankton across the Almeria-Oran frontal zone (Mediterranean Sea). *Journal of Plankton Research* 26(3), 275-293.
- Atkinson, A., Ward, P., Williams, R., Poulet, S.A., 1992. Feeding rates and diel vertical migration of copepods near South Georgia: comparison of shelf and oceanic sites. *Marine Biology* 114(1), 49-56.
- Barney, J.N., Whitlow, T.H., 2008. A unifying framework for biological invasions: the state factor model. *Biological Invasions* 10(3), 259-272.
- Benyahya, L., Caissie, D., St-Hilaire, A., Ouarda, T.B., Bobée, B., 2007. A review of statistical water temperature models. *Canadian Water Resources Journal* 32(3), 179-192.
- Blackburn, T.M., Pyšek, P., Bacher, S., Carlton, J.T., Duncan, R.P., Jarošík, V., Richardson, D.M., 2011. A proposed unified framework for biological invasions. *Trends in Ecology and Evolution* 26(7), 333-339.
- Bollens, G.R., Landry, M.R., 2000. Biological response to iron fertilization in the eastern equatorial Pacific (Iron Ex II). II. Mesozooplankton abundance, biomass, depth distribution and grazing. *Marine Ecology Progress Series* 201(43-56).
- Bollens, S.M., Breckenridge, J.K., Cordell, J.R., Rollwagen-Bollens, G., Kalata, O., Claudi, R., Karatayev, A., 2012. Invasive copepods in the Lower Columbia River Estuary: Seasonal abundance, co-occurrence and potential competition with native copepods. In *Proceedings of the 17th International Conference on Aquatic Invasive Species*, San Diego, USA, September 2010. (7(1), 101-109). Regional Euro-Asian Biological Invasions Centre (REABIC).
- Bollens, S.M., Cordell, J.R., Avent, S., Hooff, R., 2002. Zooplankton invasions: a brief review, plus two case studies from the northeast Pacific Ocean. *Hydrobiologia* 480(1-3), 87-110.
- Boxshall, G., Jaume, D., 2013. Antennules and Antennae in the Crustacea. *Functional Morphology and Diversity* 1, 199.
- Bradford-Grieve, J.M., 2002. Colonization of the pelagic realm by calanoid copepods. *Hydrobiologia* 485(1-3), 223-244.

- Braumann, C.A., 2007. Harvesting in a random environment: Itô or Stratonovich calculus? *Journal of Theoretical Biology* 244(3), 424-432.
- Braumann, C.A., 2008. Growth and extinction of populations in randomly varying environments. *Computers and Mathematics with Applications* 56(3), 631-644.
- Breteler, W.K., Schogt, N., 1994. Development of *Acartia clausi* (Copepoda, Calanoida) cultured at different conditions of temperature and food. *Hydrobiologia* 292(1), 469-479.
- Brown, J.H., Gillooly, J. F., Allen, A.P., Savage, V.M., West, G.B., 2004. Toward a metabolic theory of ecology. *Ecology* 85(7), 1771-1789.
- Brugnano, C., Guglielmo, L., Ianora, A., Zagami, G., 2009. Temperature effects on fecundity, development and survival of the benthopelagic calanoid copepod, *Pseudocyclops xiphophorus*. *Marine Biology* 156(3), 331-340.
- Brylinski, J.M., Antajan, E., Raud, T., Vincent, D., 2012. First record of the Asian copepod *Pseudodiaptomus marinus* Sato, 1913 (Copepoda: Calanoida: Pseudodiaptomidae) in the southern bight of the North Sea along the coast of France. *Aquatic Invasions* 7(4), 577-584.
- Caissie, D., El-Jabi, N., St-Hilaire, A., 1998. Stochastic modelling of water temperatures in a small stream using air to water relations. *Canadian Journal of Civil Engineering* 25(2), 250-260.
- Carlton, J.T., 1996. Biological invasions and cryptogenic species. *Ecology* 77(6), 1653-1655.
- Catford, J. A., Jansson, R., Nilsson, C., 2009. Reducing redundancy in invasion ecology by integrating hypotheses into a single theoretical framework. *Diversity and Distributions* 15(1), 22-40.
- Clavero, M., Garcia-Berthou, E., 2005. Invasive species are a leading cause of animal extinctions. *Trends in Ecology and Evolution* 20(3), 110-110.
- Cohen, A.N., Carlton, J.T., 1995. Nonindigenous aquatic species in a United States estuary: a case study of the biological invasions of the San Francisco Bay and Delta. US Fish and Wildlife Service and National Sea Grant College Program (Connecticut Sea Grant), Washington, p. 213.
- Colautti, R.I., Grigorovich, I.A., MacIsaac, H.J., 2006. Propagule pressure: a null model for biological invasions. *Biological Invasions* 8(5), 1023-1037.
- Collin., S.B., Edwards, P.K., Leung, B., Johnson, L.E., 2013. Optimizing early detection of non-indigenous species: Estimating the scale of dispersal of a nascent population of the invasive tunicate. *Marine Pollution Bulletin* 73(1), 64-69.
- Connelly, N.A., O'Neill Jr, C.R., Knuth, B.A., Brown, T.L., 2007. Economic impacts of zebra mussels on drinking water treatment and electric power generation facilities. *Environmental Management* 40(1), 105-112.
- Cordell, J.R., Bollens, S.M., Draheim, R., Sytsma, M., 2008. Asian copepods on the move: recent invasions in the Columbia–Snake River system, USA. *ICES Journal of Marine Science* 65(5), 753-758.

- Cordell, J.R., Lawrence, D.J., Ferm, N.C., Tear, L.M., Smith, S.S., Herwig, R.P., 2009. Factors influencing densities of non-indigenous species in the ballast water of ships arriving at ports in Puget Sound, Washington, United States. *Aquatic Conservation: Marine and Freshwater Ecosystems* 19(3), 322-343.
- Cordell, J.R., Morgan, C.A., Simenstad, C.A., 1992. Occurrence of the Asian calanoid copepod *Pseudodiaptomus inopinus* in the zooplankton of the Columbia River estuary. *Journal of Crustacean Biology* 12(2), 260-269.
- Cordell, J.R., Morrison, S.M., 1996. The invasive Asian copepod *Pseudodiaptomus inopinus* in Oregon, Washington, and British Columbia Estuaries. *Estuaries* 19(3), 629-638.
- Cordell, J.R., Rasmussen, M., Bollens, S.M., 2007. Biology of the introduced copepod *Pseudodiaptomus inopinus* in a northeast Pacific estuary. *Marine Ecology Progress Series* 333, 213.
- Courchamp, F., Berec, L., Gascoigne, J., 2008. Allee effects in ecology and conservation. *Environmental Conservation* 36, 80-85.
- Davis, M. A., Chew, M. K., Hobbs, R. J., Lugo, A. E., Ewel, J. J., Vermeij, G. J., ... Briggs, J. C., 2011. Don't judge species on their origins. *Nature* 474(7350), 153-154.
- Deibel, D., Lowen, B., 2012. A review of the life cycles and life-history adaptations of pelagic tunicates to environmental conditions. *ICES Journal of Marine Science* 69(3), 358-369.
- del Mundo, G.M., 2009. Phylogenetic and phylogeographic study of the New Zealand endemic sea tunicate *Cnemidocarpa nisiotis*. (Thesis Dissertation), University of Canterbury, p. 236.
- Delpy, F., Pagano, M., Blanchot, J., Carlotti, F., Thibault-Botha, D., 2012. Man-induced hydrological changes, metazooplankton communities and invasive species in the Berre Lagoon (Mediterranean Sea, France). *Marine Pollution Bulletin* 64(9), 1921-1932.
- Didham, R.K., Tylianakis, J.M., Hutchison, M.A., Ewers, R.M., Gemmill, N.J. 2005. Are invasive species the drivers of ecological change? *Trends in Ecology and Evolution* 20(9), 470-474.
- Emerson, J.E., Bollens, S.M., Counihan, T.D., 2012. Zooplankton in Columbia-Snake River System Reservoirs with Special Emphasis on the Invasive Copepod *Pseudodiaptomus Forbesi* (Doctoral dissertation, Washington State University).
- Fancett, M.S., Kimmerer, W.J., 1985. Vertical migration of the demersal copepod *Pseudodiaptomus* as a means of predator avoidance. *Journal of Experimental Marine Biology and Ecology* 88(1), 31-43.
- Fleminger, A., Kramer, S.H., 1988. Recent introduction of an Asian estuarine copepod, *Pseudodiaptomus marinus* (Copepoda: Calanoida), into southern California embayments. *Marine Biology* 98(4), 535-541.
- Gardiner, C.W., 2004. *Handbook of Stochastic Methods: for Physics, Chemistry and the Natural Sciences*. Springer-Verlag, NY, pp. 80-143.

- GHRSSST. (n.d). Group for High Resolution Sea Surface Temperature. Retrieved from <https://www.ghrsst.org/>.
- Gillooly, J.F., 2000. Effect of body size and temperature on generation time in zooplankton. *Journal of Plankton Research* 22(2), 241-251.
- Gillooly, J.F., Allen, A.P., 2007. Linking global patterns in biodiversity to evolutionary dynamics using metabolic theory. *Ecology* 88(8), 1890-1894.
- Gillooly, J.F., Brown, J.H., West, G.B., Savage, V.M., Charnov, E.L., 2001. Effects of size and temperature on metabolic rate. *Science* 293(5538), 2248-2251.
- Gillooly, J.F., Charnov, E.L., West, G.B., Savage, V.M., Brown, J.H., 2002. Effects of size and temperature on developmental time. *Nature* 417(6884), 70-73.
- Grindley, J.R., Grice, G.D., 1969. A redescription of *Pseudodiaptomus marinus* Sato (Copepoda, Calanoida) and its occurrence at the Island of Mauritius. *Crustaceana* 125-134.
- Gurevitch, J., Fox, G.A., Wardle, G.M., Taub, D., 2011. Emergent insights from the synthesis of conceptual frameworks for biological invasions. *Ecology Letters* 14(4), 407-418.
- Gurevitch, J., Padilla, D.K., 2004. Are invasive species a major cause of extinctions? *Trends in Ecology and Evolution* 19(9), 470-474.
- Halsband-Lenk, C., Hirche, H., Carlotti, F., 2002. Temperature impact on reproduction and development of congener copepod populations, *Journal of Experimental Marine Biology and Ecology* 271, 121–153.
- Hays, G.C., Kennedy, H., Frost, B.W., 2001. Individual variability in diel vertical migration of a marine copepod: why some individuals remain at depth when others migrate. *Limnology and Oceanography* 2050-2054.
- Heger, T., Saul, W.C., Trepl, L., 2013. What biological invasions ‘are’ is a matter of perspective. *Journal for Nature Conservation* 21(2), 93-96
- Herman, A.W., 1983. Vertical distribution patterns of copepods, chlorophyll, and production in northeastern Baffin Bay. *Limnology and Oceanography* 28(4), 709-719.
- Hirche, H.J., 1996. Diapause in the marine copepod, *Calanus finmarchicus*—a review. *Ophelia* 44(1-3), 129-143.
- Hirst, A.G., Kiørboe, T., 2002. Mortality of marine planktonic copepods: global rates and patterns. *Marine Ecology Progress Series* 230, 195-209.
- Holste, L., Peck, M.A., 2005. The effects of temperature and salinity on egg production and hatching success of Baltic *Acartia tonsa* (Copepoda: Calanoida): a laboratory investigation, *Marine Biology* 148(5), 1061-1070.
- Homans, F.R., Smith, D.J., 2013. Evaluating management options for aquatic invasive species: concepts and methods. *Biological Invasions* 15(1), 7-16.

- Houghton, R.A., 2007. Balancing the global carbon budget. *Annual Review of Earth and Planetary Sciences* 35, 313-347.
- Huntley, M.E., Lopez, M.D., 1992. Temperature-dependent production of marine copepods: a global synthesis. *American Naturalist* 140(2), 201-242.
- Huntley, M.E., Marin, V., Escritor, F., 1987. Zooplankton grazers as transformers of ocean optics: a dynamic model. *Journal of Marine Research* 45, 911-945.
- Hyytiäinen, K., Lehtiniemi, M., Niemi, J.K., Tikka, K., 2013. An optimization framework for addressing aquatic invasive species. *Ecological Economics* 91, 69-79.
- Jang, M.C., Shin, K., Hyun, B., Lee, T., Choi, K.H., 2013. Temperature-regulated egg production rate, and seasonal and interannual variations in *Paracalanus parvus*. *Journal of Plankton Research* Doi: 10.1093/plankt/fbt050.
- Jha, U., Jetter, A., Lindley, J.A., Postel, L., Wootton, M., 2013. Extension of distribution of *Pseudodiaptomus marinus*, an introduced copepod, in the North Sea. *Marine Biodiversity Records*, 6, e53, Doi: <http://dx.doi.org/10.1017/S1755267213000286>
- Jiménez-Pérez, L.C., Castro-Longoria, E., 2006. Range extension and establishment of a breeding population of the Asiatic copepod, *Pseudodiaptomus marinus* Sato, 1913 (Calanoida, Pseudodiaptomidae) in Todos Santos Bay, Baja California, Mexico. *Crustaceana* 79(2), 227-234.
- Jiménez-Valverde, A., Peterson, A.T., Soberón, J., Overton, J.M., Aragón, P., Lobo, J.M., 2011. Use of niche models in invasive species risk assessments. *Biological Invasions* 13(12), 2785-2797.
- Jones, E.C., 1966. A New Record of *Pseudodiaptomus marinus* Sato (Copepoda, Calanoida) from Brackish Waters of Hawaii. *Crustaceana* 10(3), 316-317.
- Kara, A.B., Wallcraft, A.J., Hurlburt, H.E., 2003. Climatological SST and MLD Predictions from a Global Layered Ocean Model with an Embedded Mixed Layer. *Journal of Atmospheric and Oceanic Technology* 20(11), 1616-1632.
- Kjørboe, T., Hirst, A.G., 2008. Optimal development time in pelagic copepods. *Marine Ecology Progress Series* 367, 15-22.
- Kjørboe, T., Sabatini, M., 1994. Reproductive and life cycle strategies in egg-carrying cyclopoid and free-spawning calanoid copepods. *Journal of Plankton Research* 16(10), 1353-1366.
- Kjørboe, T., Sabatini, M., 1995. Scaling of fecundity, growth and development in marine planktonic copepods. *Marine Ecology Progress Series* 120(1-3), 285-298.
- Klausmeier, C.A., 2008. Floquet theory: a useful tool for understanding nonequilibrium dynamics. *Theoretical Ecology* 1(3), 153-161.
- Klein, G., MacIntosh, K., Kaczmarek, I., Ehrman, J.M., 2010. Diatom survivorship in ballast water during trans-Pacific crossings. *Biological Invasions* 12(5), 1031-1044.

- Klein-Breteler, W.C.M., Gonzalez, S.R., Schogt, N., 1995. Development of *Pseudocalanus elongatus* (Copepoda, Calanoida) cultured at different temperature and food conditions. *Marine Ecology Progress Series* 119, 99-99.
- Knapp, S., Kühn, I., 2012. Origin matters: widely distributed native and non-native species benefit from different functional traits. *Ecology Letters* 15(7), 696-703.
- Lande, R., Engen, S., Sæther, B.E., 2003. *Stochastic population dynamics in ecology and conservation*. Oxford University Press, GB, p. 209.
- Landry, M.R., 1975. Seasonal temperature effects and predicting development rates of marine copepod eggs. *Limnology and Oceanography* 20, 434-440.
- Lawrence, D.J., Cordell, J.R., 2010. Relative contributions of domestic and foreign sourced ballast water to propagule pressure in Puget Sound, Washington, USA. *Biological Conservation* 143(3), 700-709.
- Lee, C.E., 2000. Global phylogeography of a cryptic copepod species complex and reproductive isolation between genetically proximate populations. *Evolution* 54, 2014–2027.
- Lee, R.F., Hagen, W., Kattner, G., 2006. Lipid storage in marine zooplankton. *Marine Ecology Progress Series* 307, 273-306.
- Liang, D., Uye, S., 1997a. Population dynamics and production of the planktonic copepods in a eutrophic inlet of the Inland Sea of Japan. IV. *Pseudodiaptomus marinus*, the egg-carrying calanoid. *Marine Biology* 128(3), 415-421.
- Liang, D., Uye, S., 1997b. Seasonal reproductive biology of the egg-carrying calanoid copepod *Pseudodiaptomus marinus* in a eutrophic inlet of the Inland Sea of Japan. *Marine Biology* 128(3), 409-414.
- Liang, D., Uye, S., Onbé, T., 1996. Population dynamics and production of the planktonic copepods in a eutrophic inlet of the Inland Sea of Japan. I. *Centropages abdominalis*. *Marine Biology* 124(4), 527-536.
- Lockwood, J.L., Cassey, P., Blackburn, T., 2005. The role of propagule pressure in explaining species invasions. *Trends in Ecology and Evolution* 20(5), 223-228.
- Lockwood, J.L., Hoopes, M., Marchetti, M., 2009. *Invasion ecology*. Wiley-Blackwell, p. 456.
- Lombaert, E., Guillemaud, T., Thomas, C.E., Lawson, L.J., Li, J., Wang, S., Estoup, A., 2011. Inferring the origin of populations introduced from a genetically structured native range by approximate Bayesian computation: case study of the invasive ladybird *Harmonia axyridis*. *Molecular Ecology* 20(22), 4654-4670.
- Lovell, S.J., Stone, S.F., Fernandez, L., 2011. The economic impacts of aquatic invasive species: a review of the literature. *Agricultural and Resource Economics Review* 35(1), 195.
- Mackas, D.L., Sefton, H., Miller, C.B., Raich, A., 1993. Vertical habitat partitioning by large calanoid copepods in the oceanic subarctic Pacific during spring. *Progress in Oceanography* 32(1), 259-294.

- Mauchline, J., 1998. Introduction. In: The Biology of Calanoid Copepods. Advances in Marine Biology 33. Elsevier, p. 1–15.
- Medeiros, G.F., Medeiros, L.S., Henriques, D.M., Carlos, M.T., Faustino, G.V.B.D.S., Lopes, R.M., 2006. Current distribution of the exotic copepod *Pseudodiaptomus trihamatus* Wright, 1937 along the northeastern coast of Brazil. Brazilian Journal of Oceanography 54(4), 241-245.
- McGeoch, M.A., Spear, D., Kleynhans, E.J., Marais, E., 2012. Uncertainty in invasive alien species listing. Ecological Applications 22(3), 959-971.
- McLaughlan, C., Gallardo, B., Aldridge, D.C., 2013. How complete is our knowledge of the ecosystem services impacts of Europe's top 10 invasive species?. Acta Oecologica Doi: <http://dx.doi.org/10.1016/j.actao.2013.03.005>.
- Modlin, R.F., Orsi, J.J., 1997. *Acanthomysis bowmani*, a new species, and *A. asperali*, Mysidacea newly reported from the Sacramento-San Joaquin Estuary, California (Crustacea: Mysidae). Proceedings of the Biological Society Washington 110, 439–446.
- Molnar, J.L., Gamboa, R.L., Revenga, C., Spalding, M.D., 2008. Assessing the global threat of invasive species to marine biodiversity. Frontiers in Ecology and the Environment 6(9), 485-492.
- Morris, W.F., Doak, D.F., 2002. Quantitative conservation biology: theory and practice of population viability analysis. Sunderland, Massachusetts, USA: Sinauer Associates, p. 480.
- Neftci, S.N., 2000. An Introduction to the Mathematics of Financial Derivatives. Academic Press, p. 480.
- NOAA-ESRL., n.d. Physical Sciences Division, Boulder Colorado, USA. Retrieved from <http://www.esrl.noaa.gov/psd/data/gridded/data.noaa.oisst.v2.html>.
- Olazabal, A., Tirelli, V., 2011. First record of the egg-carrying calanoid copepod *Pseudodiaptomus marinus* in the Adriatic Sea. Marine Biodiversity Records 4(1), e85.
- Orsi, J.J., 2001. Eurytemora affinis is introduced. Inter Agency Ecol Program Newslett 14, 12.
- Orsi, J.J., Ohtsuka, S., 1999. Introduction of the Asian copepods *Acartiella sinensis*, *Tortanus dextrilobatus* (Copepoda: Calanoida), and *Limnoithona tetraspina* (Copepoda: Cyclopoida) to the San Francisco Estuary, California, USA. Plankton Biology and Ecology 46:128–131.
- Orsi, J.J., Walter, T.C., 1991. *Pseudodiaptomus forbesi* and *P. marinus* (Copepoda: Calanoida), the latest copepod immigrants to California's Sacramento-San Joaquin Estuary. Bull Plankton Soc Jap 20:553–562.
- Pillai, P.P., 1976. A review of the calanoid copepod family Pseudodiaptomidae with remarks on the taxonomy and distribution of the species from the Indian Ocean. Journal of the Marine Biological Association of India 18(2), 242-265.
- Pyšek, P., 2003. How reliable are data on alien species in Flora Europaea? Flora 198(6), 499-507.

- Pyšek, P., Richardson, D.M., 2010. Invasive species, environmental change and management, and health. *Annual Review of Environment and Resources* 35, 25-55.
- Ratsimandresy, A.W., Pelegrí, J.L., Marrero-Díaz, A., Hernández-Guerra, A., Martínez, A., 2001. Seasonal variability of the upper warmwatersphere in the Canary Basin. *Scientia Marina* 65(S1), 251-258.
- Razouls C., de Bovée F., Kouwenberg J. Desreumaux N., 2013. Diversity and Geographic Distribution of Marine Planktonic Copepods. Retrieved from: <http://copepodes.obs-banyuls.fr/en>.
- Record, N.R., Pershing, A.J., Maps, F., 2012. First principles of copepod development help explain global marine diversity patterns. *Oecologia* 170(2), 289-295.
- Ricciardi, A., 2013. Invasive Species. In *Ecological Systems*, Springer NY, p. 161-178.
- Ricciardi, A., Hoopes, M.F., Marchetti, M., Lockwood, J.L., 2013. Progress toward understanding the ecological impacts of non-native species. *Ecological Monographs* 83, 263–282.
- Ricciardi, L.M., 1986. Stochastic population theory: diffusion processes. In *Mathematical Ecology* (pp. 191-238). Springer Berlin Heidelberg.
- Richardson, D.M., Pyšek, P., Rejmánek, M., Barbour, M.G., Panetta, F.D., West, C.J., 2000. Naturalization and invasion of alien plants: concepts and definitions. *Diversity and Distributions* 6(2), 93-107.
- Roberts, P.D., Diaz-Soltero, H., Hemming, D.J., Parr, M.J., Wakefield, N.H., Wright, H.J., 2013. What is the evidence that invasive species are a significant contributor to the decline or loss of threatened species? A systematic review map. *Environmental Evidence* 2(1), 5.
- Rombouts, I., Beaugrand, G., Ibañez, F., Chiba, S., Legendre, L., 2011. Marine copepod diversity patterns and the metabolic theory of ecology. *Oecologia* 166(2), 349-355.
- Rombouts, I., Beaugrand, G., Ibañez, F., Gasparini, S., Chiba, S., Legendre, L., 2009. Global latitudinal variations in marine copepod diversity and environmental factors. *Proceedings of the Royal Society B: Biological Sciences* 276(1670), 3053-3062.
- Ruiz, G., Fofonoff, P., Steves, B., Dahlstrom, A., 2011. Marine crustacean invasions in North America: A synthesis of historical records and documented impacts. In *In the Wrong Place-Alien Marine Crustaceans: Distribution, Biology and Impacts* (pp. 215-250). Springer Netherlands.
- Sabia, L., Uttieri, M., Pansera, M., Souissi, S., Schmitt, F.G., 2012. First observations on the swimming behaviour of *Pseudodiaptomus marinus* from lake Faro. *Biol. Mar. Mediterr* 19(1), 240-241.
- Saiz, E., Calbet, A., Irigoien, X., Alcaraz, M., 1999. Copepod egg production in the western Mediterranean: response to food availability in oligotrophic environments, *Marine Ecology Progress Series* 187, 179-189.

- Sampei, M., Sasaki, H., Forest, A., Fortier, L., 2012. A substantial export flux of particulate organic carbon linked to sinking dead copepods during winter 2007-2008 in the Amundsen Gulf (southeastern Beaufort Sea, Arctic Ocean). *Limnology and Oceanography* 57(1), 90.
- Sato, T., 1913. Pelagic Copepoda, 1. Rep. Fish. Invest. Hokkaido Fish. Exp. Sta. 1: 1-79.
- Savage, V.M., Gillooly, J.F., Brown, J.H., West, G.B., Charnov, E.L., 2004. Effects of body size and temperature on population growth. *American Naturalist* 163(3), 429-441.
- Seebens, H., Gastner, M.T., Blasius, B., 2013. The risk of marine bioinvasion caused by global shipping. *Ecology Letters* 16(6), 782-790.
- Shrader-Frechette, K., 2001. Non-indigenous species and ecological explanation. *Biology and Philosophy* 16(4), 507-519.
- Simard, N., Plourde, S., Gilbert, M., Gollasch, S., 2011. Net efficacy of open ocean ballast water exchange on plankton communities. *Journal of Plankton Research* 33(9), 1378-1395.
- Simberloff, D., 2009. The role of propagule pressure in biological invasions. *Annual Review of Ecology, Evolution, and Systematics* 40, 81-102.
- SIO., n.d. Scripps Institution of Oceanography, Earthguide Retrieved from: <http://earthguide.ucsd.edu/>.
- Spalding, M.D., Fox, H.E., Allen, G.R., Davidson, N., Ferdaña, Z.A., Finlayson, M.A.X., Robertson, J., 2007. Marine ecoregions of the world: a bioregionalization of coastal and shelf areas. *BioScience* 57(7), 573-583.
- Stefaniak, L., Zhang, H., Gittenberger, A., Smith, K., Holsinger, K., Lin, S., Whitlatch, R.B., 2012. Determining the native region of the putatively invasive ascidian *Didemnum vexillum* Kott, 2002. *Journal of Experimental Marine Biology and Ecology* 422, 64-71.
- Sullivan, B.K., McManus, L.T., 1986. Factors controlling seasonal succession of the copepods *Acartia hudsonica* and *A. tonsa* in Narragansett Bay, Rhode Island: temperature and resting egg production, *Marine Ecology Progress Series* 28: 121-128.
- Sun, X.H., Sun, S., Li, C.L., Zhang, G.T., 2011. Seasonal and spatial variability in egg production, abundance and production of small copepods in and near Jiaozhou Bay, China. *Journal of Plankton Research* 33(5), 741-750.
- Sytsma, M., Cordell, J.R., Chapman, J.W., Waldeck, R.D., 2004. Lower Columbia River aquatic nonindigenous species survey 2001–2004: Final Technical Report. Center for lakes and reservoirs. Portland State University, Portland, p. 35.
- Taylor, C.M., Hastings, A., 2005. Allee effects in biological invasions. *Ecology Letters* 8(8), 895-908.
- Tittensor, D.P., Mora, C., Jetz, W., Lotze, H.K., Ricard, D., Berghe, E.V., Worm, B., 2010. Global patterns and predictors of marine biodiversity across taxa. *Nature* 466(7310), 1098-1101.

Tsolaki, E., Diamadopoulos, E., 2010. Technologies for ballast water treatment: a review. *Journal of Chemical Technology and Biotechnology* 85(1), 19-32.

USGS., n.d. Woods Hole Science Center. Retrieved from: <http://woodshole.er.usgs.gov/project-pages/stellwagen/didemnum/>.

Usov, N., Kutcheva, I., Primakov, I., Martynova, D., 2013. Every species is good in its season: Do the shifts in the annual temperature dynamics affect the phenology of the zooplankton species in the White Sea? *Hydrobiologia* 706(1), 11-33.

Uye, S.I., 1981. Fecundity studies of neritic calanoid copepods *Acartia clausi* Giesbrecht and *A. Steuerei* Smirnov: A simple empirical model of daily egg production. *Journal of Experimental Marine Biology and Ecology* 50(2), 255-271.

Uye, S., Iwai, Y., Kasahara, S., 1982. Reproductive biology of *Pseudodiaptomus marinus* (Copepoda: Calanoids) in the Inland Sea of Japan. *Bulletin of Plankton Society of Japan* 29.

Uye, S.I., Iwai, Y., Kasahara, S., 1983. Growth and production of the inshore marine copepod *Pseudodiaptomus marinus* in the central part of the Inland Sea of Japan. *Marine Biology* 73(1), 91-98.

Uye, S.I., Kasahara, S., 1983. Grazing of Various Developmental Stages of *Pseudodiaptomus marinus* (Copepoda: Calanoida) on Naturally Occurring Particles. *Bulletin of Plankton Society of Japan* 30(2), 147-158.

Uye, S.I., Shibuno, N., 1992. Reproductive biology of the planktonic copepod *Paracalanus* sp. in the Inland Sea of Japan. *Journal of Plankton Research* 14(3), 343-358.

Villac, M.C., Kaczmarska, I., 2011. Estimating propagule pressure and viability of diatoms detected in ballast tank sediments of ships arriving at Canadian ports. *Marine Ecological Progress. Series* 425, 47-61.

Wallinga, J., Lipsitch, M., 2007. How generation intervals shape the relationship between growth rates and reproductive numbers. *Proceeding of Royal Society Biological Sciences* 274(1609), 599-604.

Walter, C.T., 1986. New and poorly known Indo-Pacific species of *Pseudodiaptomus* (Copepoda: Calanoida), with a key to the species groups. *Journal of Plankton Research* 8(1), 129-168.

Walter, C.T., 1987. Review of the taxonomy and distribution of the demersal copepod genus *Pseudodiaptomus* (Calanoida: Pseudodiaptomidae) from southern Indo-West Pacific waters. *Marine and Freshwater Research* 38(3), 363-396.

Walter, C.T., 1989. Review of the new world species of *Pseudodiaptomus* (Copepoda: Calanoida), with a key to the species. *Bulletin of Marine Science* 45(3), 590-628.

Walter, C.T., Ohtsuka, S., Castillo, L.V., 2006. A new species of *Pseudodiaptomus* (Crustacea: Copepoda: Calanoida) from the Philippines, with a key to pseudodiaptomidids from the Philippines and comments on the status of the genus *Schmackeria*. *Proceedings of the Biological Society of Washington* 119(2), 202-221

Williams, R., Conway, D.V.P., 1980. Vertical distributions of *Calanus finmarchicus* and *C. helgolandicus* (Crustacea: Copepoda). *Marine Biology* 60, 57-61.

Williams, R., Conway, D.V.P., 1988. Vertical distribution and seasonal numerical abundance of the Calanidae in oceanic waters to the south-west of the British Isles. *Hydrobiologia* 167-168, 259-266.

Williams, R., Lindley, J.A., 1980. Plankton of the Fladen Ground during FLEX 76. III. Vertical distribution, population dynamics and production of *Calanus finmarchicus* (Crustacea: Copepoda). *Marine Biology* 60:47-56.

Wyrki, K., 1965. The annual and semiannual variation of sea surface temperature in the North Pacific Ocean. *Limnology and Oceanography* 307-313.

CHAPTER 2

¹Identifying potentially invisable habitats for marine copepods using temperature-dependent R_0

2.1. Introduction

Assessment of habitat invasibility often relies on statistical matching of environmental variables between native and potentially novel ranges of species via methods such as ecological niche modeling (ENM) (Jeschke and Strayer, 2008; Mercado-Silva et al., 2006). However, it is often the case that invasive species can tolerate environmental conditions that are outside of their native range (Broennimann et al., 2007; Elith and Leathwick, 2009). This indicates that the absence of a species in a particular environment may not necessarily mean that the environment is unsuitable for the species. Thus, matching up environmental variables may not be much reliable in predicting potentially invisable range.

As an alternative to ENM, the response of life-history parameters (traits for example, fecundity, maturation, and mortality rates) of a population to specific environmental variables can be measured under controlled laboratory experiments. However, these measures must be translated to a metric to determine if a population can persist and grow under a given set of environmental conditions. Here, we use the net reproductive rate R_0 of a population, modeled as a function of environmental variables, as a metric for evaluating population persistence. The R_0 is the average number of offspring produced by a female over its lifetime, which is a measure of the reproductive success of a population (Ackleha and de-Leenheerb, 2008). It is also used in evolutionary invasion analysis to predict long term evolutionary outcomes (Hurford et al., 2010). When

¹ A version of this chapter has been published. Rajakaruna, H., Strasser, C., Lewis, M., 2012. Identifying non-invasible habitats for marine copepods using temperature-dependent R_0 . *Biological Invasions* 14(3),633-647.

$R_0 > 1$, a population grows, and $R_0 < 1$, a population tends to decrease to extinction (Boldin, 2006). Therefore, we can decide whether a species can persist in a habitat by evaluating R_0 for given range of values of environmental variables.

The R_0 can be derived from a stage-structured population model described by a system of ordinary differential equations (ODE) (de-Camino-Beck et al., 2007) incorporating the life-history parameters. These life-history parameters can be modeled, in turn, as functions of the environmental variables. The ODE transmission models in epidemiology literature are commonly evaluated using R_0 , although it is less common in stage-structured life-history dynamics of populations.

The model-species *Pseudodiaptomus marinus* is a perennial egg-carrying marine calanoid copepod, reproducing year-round, and having multiple overlapping generations (Liang and Uye, 1997a; Uye et al., 1983). It is native to North West Pacific region and introduced to North East Pacific region, Southern Chile and many other locations around the world via ship ballast-water (Fleminger and Kramer, 1998; Cordell et al., 2008). Recent studies show that *P. marinus* is further expanding its range (Brylinski et al., 2012; Jiménez-Pérez and Castro-Longoria, 2006). Despite high propagule pressure (Cordell et al., 2009), *P. marinus* has not been reported in Oregon and Vancouver Harbour, BC (Piercey et al., 2000) indicating that it may be a successful invader only in selected habitats. Whether environmental factors limit its geographical distribution is unknown.

The life-history parameters such as fecundity, mortality and maturation rates of *P. marinus* are functions of temperature (Liang and Uye, 1997a; Uye et al., 1983). Hence, $R_0(T)$ of *P. marinus*, derived as a function life-history parameters, is invariably a function of temperature (T). Thus, $R_0(T)$ can be parameterized using data from experiments and surveys in published literature (e.g., Liang and Uye, 1997a; Uye et al., 1983).

In this study, we assume environmental conditions other than temperature are optimal for the populations. Liang and Uye (1997a) specifically state that the

trends in the growth of the populations they studied, where we get the data from, were temperature-dependent, but not regulated by the food concentration.

The $R_0(T)$ allows us to predict the range of temperatures that are suitable for the population persistence, and thereby, to predict the range of potentially invisable habitats for the species given the temperatures. This method can be applied to model R_0 for copepod species in general showing similar life-history dynamics.

2.2. Model and Methods

Life-history stages of *P. marinus* consist of eggs, six naupliar stages, five copepodid stages, and one adult stage. We exclude the naupliar stage 1 from the model as the data corresponding to this stage are unavailable. This is because it lasts only few minutes, and thus taking measurements is hard (Uye et al., 1983). This results in 12 effective life-history stages for our model.

We denote $\mathbf{n}(t)$ to be a vector representing the stage-composition of the population at time t , and $\mathbf{A}(T)$ to be a matrix of parameter space of maturation $\gamma_i(T)$, and mortality $\mu_i(T)$ rates that depend on the ambient temperature (T) at stage i for $i=1..12$. Here, $\beta(T)$ corresponds to the fecundity rate of the adult stage. Thus, we write the rate of change of stage composition as follows:

$$\frac{d\mathbf{n}}{dt} = \mathbf{A}(T)\mathbf{n} \quad (2.1)$$

Where, $\mathbf{n} = [n_1(t), n_2(t), \dots, n_{12}(t)]^T$

$$\mathbf{A}(T) = \begin{pmatrix} -\mu_1(T) - \gamma_1(T) & 0 & : & 0 & q\beta(T) \\ \gamma_1(T) & -\mu_2(T) - \gamma_2(T) & : & 0 & 0 \\ 0 & \gamma_2(T) & : & : & : \\ : & : & : & -\mu_{11}(T) - \gamma_{11}(T) & 0 \\ 0 & 0 & : & \gamma_{11}(T) & -\mu_{12}(T) \end{pmatrix}$$

Here, n_1 represents the number of eggs, $n_2...n_6$ represent the number of individuals in the five naupliar stages (excluding stage 1), and $n_7...n_{12}$ represent the number of individuals in the five copepodid stages and the adult stage 12. The constant q is the average proportion of ovigerous females in the adult population, which is approximately 0.61 for *P. marinus* (Liang and Uye, 1997b).

2.2.1. R_0 as a function of temperature

We follow the methods in van den Driessche and Watmough (2002) to derive the net reproductive rate R_0 based on stage-structured population dynamics described by first order linear ODE model Eq. (2.1) for *P. marinus*. First, we write the matrix \mathbf{A} partitioned as $\mathbf{A}=\mathbf{F}-\mathbf{V}$, where \mathbf{F} is the matrix of fecundity coefficients (non-negative and non-zero), and \mathbf{V} is the matrix of transition coefficients (i.e., maturation and mortality rates). Thus, R_0 can be written as $R_0 = \rho[\mathbf{FV}^{-1}]$, where ρ is the spectral radius of the matrix $[\mathbf{FV}^{-1}]$ (van den Driessche and Watmough, 2002). That is, $\rho[\mathbf{FV}^{-1}] = \max_{1 \leq i \leq n} |R_{0i}|$, where $R_{01}, R_{02}...R_{0n}$ are the eigenvalues of the square matrix $[\mathbf{FV}^{-1}]$. (Note that the intrinsic growth rate λ , defined as the maximum real eigenvalue of the square matrix \mathbf{A} , has a non-linear relationship with the net reproductive rate R_0 (Wallinga and Lipsitch, 2007), and $\lambda > 0$ if and only if $R_0 > 1$.)

We express R_0 as a function of temperature, such that, $R_0(T) = \rho[\mathbf{F}(T)\mathbf{V}(T)^{-1}]$. Using the graph reduction method (de-Camino-Beck et al., 2009) (see derivation in Appendix 2.1), we can write R_0 as

$$R_0(T) = \frac{\overbrace{q\beta(T)}^{\text{rate of production of offspring by females}}}{\underbrace{\mu_s(T)}_{\text{mortality rate at stage } s}} \prod_{i=1}^{s-1} \left(\frac{\gamma_i(T)}{\underbrace{\mu_i(T) + \gamma_i(T)}_{\text{prob. of maturing into stage } s}} \right) \quad (2.2)$$

Here, s is the last stage (stage 12) for *P. marinus*. In order to compute R_0 , we model $\beta(T)$, $\gamma_i(T)$, and $\mu_i(T)$ separately.

2.2.2. Modeling fecundity rates $\beta(T)$

Fecundity rate $\beta(T)$ can be written as $\beta(T) = f(T)/\Delta t$, where $f(T)$ is the number of eggs produced by an adult female over time Δt at average temperature T . Uye et al. (1983) fitted a linear model for $f(T)$ to parameterize $\beta(T)$. It takes the form $\beta(T) = 0.77T - 4.48$, with $R^2 = 0.84$. Residual analysis of Uye's data shows a non-random distribution of residuals along the fitted curve indicating a possible non-linear relationship. We also note a depression in fecundity rates at low temperatures. Therefore, we fit a sigmoidal model to the data assuming log normally distributed errors, and bounded fecundity at large temperatures. These may be biologically more valid assumptions compared to that of the linear model. We incorporate a lag parameter b to relax the assumption that the curve must otherwise intercept the y-axis at the origin. Although, it may be more appropriate to assume that fecundity rate is a bell-shaped curve with respect to temperature (as in Amarasekare and Savage, 2012), we did not have the data to estimate such curve where $\beta(T)$ begins to decline at high temperatures.

We write the fecundity rate as

$$\beta(T) = f_m f_l e^{w(T-b)} / [f_m + f_l (e^{w(T-b)} - 1)] \quad (2.3)$$

where, f_m is the maximum rate of fecundity, f_l is fecundity rate at the lowest temperature, and w is a shape parameter that accounts for the depression in

fecundity at lower temperatures. We compare the regression of the linear model in Uye et al. (1983) with the sigmoidal model using residual sum of squares.

2.2.3. Modeling maturation rates $\gamma_i(T)$

2.2.3.1 General solution for $n_a(t)$

We solve the system of ODE's represented by Eq. (2.1) analytically corresponding to a single individual in stage 1, $n_1(0)=1$, and $n_i(0)=0$ for $i=2,\dots,12$, starting at $t=0$. This allows us to follow a single cohort over time with no additional individuals being added to the system, and obtain the general solution for $n_a(t)$, the proportion of individuals in a given stage a at time t from Eq. (2.1) as

$$\begin{aligned} n_1(t) &= e^{-\sigma_1 t} \gamma_1 && \text{for } a=1; \\ n_a(t) &= \left(\prod_{i=1}^{a-1} \gamma_i \right) (\underline{b}_a \cdot \underline{v}_a) && \text{for } a>1; \end{aligned} \quad (2.4)$$

where, $\sigma_i = (\gamma_i + \mu_i)$, $\gamma_i > 0$ and $\mu_i > 0$ for any stage i , and $\sigma_{ij} = (\sigma_i - \sigma_j)$. Here, \underline{b}_a is a row vector of dimension $1 \times (a-1)$ of the form $\underline{b}_a = \prod_{j=1}^a \mathbf{B}_j$ for $j=1,\dots,a$, and, \mathbf{B}_j are non-square matrices such that,

$$\begin{aligned} \mathbf{B}_1 &= 1, \quad \mathbf{B}_2 = \sigma_{21}^{-1}, \quad \mathbf{B}_3 = [\sigma_{31}^{-1} - \sigma_{32}^{-1}], \quad \mathbf{B}_4 = \begin{bmatrix} \sigma_{41}^{-1} & 0 & -\sigma_{43}^{-1} \\ 0 & -\sigma_{42}^{-1} & -\sigma_{43}^{-1} \end{bmatrix} \\ \mathbf{B}_5 &= \begin{bmatrix} \sigma_{51}^{-1} & 0 & 0 & \sigma_{54}^{-1} \\ 0 & \sigma_{52}^{-1} & 0 & \sigma_{54}^{-1} \\ 0 & 0 & \sigma_{53}^{-1} & \sigma_{54}^{-1} \end{bmatrix}, \text{ and so on.} \end{aligned}$$

The general formula for \mathbf{B}_j ($j \geq 3$) can be written as

$$\mathbf{B}_j = \begin{bmatrix} \sigma_{j1}^{-1} & 0 & : & 0 & 0 & \sigma_{jj-1}^{-1} \\ 0 & \sigma_{j2}^{-1} & : & 0 & 0 & \sigma_{jj-1}^{-1} \\ : & : & : & : & : & : \\ 0 & 0 & : & \sigma_{jj-3}^{-1} & 0 & \sigma_{jj-1}^{-1} \\ 0 & 0 & : & 0 & \sigma_{jj-2}^{-1} & \sigma_{jj-1}^{-1} \end{bmatrix}_{(j-2) \times (j-1)} .$$

Note that due to the varying dimensions of the \mathbf{B}_j matrices, the product $\underline{b}_a = \prod_{j=1}^a \mathbf{B}_j$ is a row vector. The \underline{v}_a is a column vector given by

$$\underline{v}_a = \begin{bmatrix} e^{-\sigma_1 t} - e^{-\sigma_a t} \\ e^{-\sigma_2 t} - e^{-\sigma_a t} \\ e^{-\sigma_3 t} - e^{-\sigma_a t} \\ : \\ e^{-\sigma_{a-1} t} - e^{-\sigma_a t} \end{bmatrix}_{(a-1) \times 1} .$$

2.2.3.2 Analysis of the case with constant mortality among stages

In experimental studies, the maturation rates are commonly calculated using median development times, or the time it takes for 50% of the cohort to mature from eggs past a given stage (e.g., Breteler et al., 1994; Lee et al., 2003; Uye et al., 1983). An assumption underlying such conventional calculation using the ‘proportions not yet past a given stage’ is that, daily mortality rates are the same across all stages of a cohort. It excludes the mortality rate parameter from the proportions. We make the same assumption here in the calculation of maturation rates of our model as *P. marinus* data are also available only as proportions of a cohort remaining in each stage over time.

To do that, we normalize $n_a(t)$ for each time step t dividing it by the total remaining population of the cohort at the time step to yield the proportion at each stage $z_a(t)$. Thus, this assumption makes the proportion at each stage $z_a(t)$ to be independent of the mortality rates.

To see that, consider the case where each μ_i is a constant μ in the solution $n_a(t)$. We note that, σ_{ij} s become independent of μ , and as a result \underline{b}_a also becomes independent of μ . Furthermore, $(e^{-\sigma_i t} - e^{-\sigma_a t})$ term in \underline{v}_a can be written as $e^{-\mu t} (e^{-\gamma_i t} - e^{-\gamma_a t})$ for each element i . Thus, in the dot product $(\underline{b}_a \cdot \underline{v}_a)$ in the Eq. (2.4), the term $e^{-\mu t}$ is separated out as a multiplier, and yields, $n_a(t) = e^{-\mu t} \left(\prod_{i=1}^{a-1} \gamma_i \right) (\bar{\underline{b}}_a \cdot \bar{\underline{v}}_a)$, such that, the term $\left(\prod_{i=1}^{a-1} \gamma_i \right) (\bar{\underline{b}}_a \cdot \bar{\underline{v}}_a)$ becomes independent of μ , denoting, $\bar{\underline{b}}_a = \underline{b}_a$ and $\bar{\underline{v}}_a = \underline{v}_a$ for $\mu_i = 0$ for all stages i . Now, we write the proportion of each stage a at time t , $z_a(t)$, with respect to the total population at t as

$$z_a(t) = n_a(t) / \sum_{i=1}^s n_i(t) = \left(\prod_{i=1}^{a-1} \gamma_i \right) (\bar{\underline{b}}_a \cdot \bar{\underline{v}}_a) / \sum_{j=1}^s \left(\prod_{i=1}^{j-1} \gamma_i \right) (\bar{\underline{b}}_j \cdot \bar{\underline{v}}_j)$$

where, s is the total number of stages. We note that this equation is independent of μ as the term $e^{-\mu t}$ is cancelled out. We also note that the denominator of this equation is 1 as the population starts with 1 and remains with 1 at any time t in the solution. This is because the term μ is not present in the solution, $z_a(t)$. Hence, the $z_a(t)$ is simplified to

$$z_a(t) = \left(\prod_{i=1}^{a-1} \gamma_i \right) \bar{\underline{b}}_a \cdot \bar{\underline{v}}_a \quad (2.5)$$

which is equivalent to $z_a(t) = n_a(t)$ when $\mu_i = 0$ for all stages i at any t . Therefore, $z_a(t)$ can be equated with the stage sizes normalized at each time step t in the experimental data found in the literature, which makes the standard assumption in experimental data analyses that $\mu_i = \mu$ for all $i=1$ to s .

2.2.3.3 A simple model for maturation rates $\gamma_i(T)$

Using Eq. (2.5) we can write the proportion of individuals not yet past stage a , that is $\sum_{i=1}^a z_i(t)$, as

$$\sum_{i=1}^a z_i(t) = 1 - \sum_{i=1}^a \left[\prod_{\substack{j=1 \\ j \neq i}}^a \frac{\gamma_j}{\gamma_j - \gamma_i} (1 - e^{-\gamma_j t}) \right]. \quad (2.6)$$

As shown by Cox (1967), this equation can also be derived from assuming that the time that an individual stays in a stage (stage duration time) as an exponentially distributed random variable, d_a , such that, the probability density function of d_a is $\gamma_a e^{-\gamma_a t}$, and the cumulative density function of d_a is $(1 - e^{-\gamma_a t})$, where γ_a is the maturation rate at stage a , with the assumption that $\mu_a = 0$ for all stages a . The mean time taken to exit stage a , i.e. stage development time, D_a , becomes a random variable defined as $D_a = \sum_{i=1}^a d_i$ of which the cumulative density function is $(1 - \sum_{i=1}^a z_i(t))$. The quantity $\sum_{i=1}^a z_i(t)$, thus, yields the proportion of individuals not yet past stage a .

We fit stage-proportion data from Uye et al. (1983) to Eq. (2.6) using non-linear least squares regression to estimate γ_a . The data used were collected for *P. marinus* at 20°C. The mean stage duration time d_a is given by $\bar{d}_a = \frac{1}{\gamma_a}$ from the exponentially distributed d_a , and this is for the population at constant temperature 20°C. We then use d_a evaluated at 20°C to estimate the relationship between D_a and temperature (T). We assume the relationship given by the Belehradek's function for mean stage development times, $\bar{D}_a = \alpha_a (T - 1)^{-1.8}$ (as used by Uye et al. (1983) for *P. marinus*), where T is the ambient temperature in centigrade, and α_a is a temperature-independent constant that varies with stage a . We quantify α_a

's from the Belehradek's function substituting the estimated $\gamma_a(T)$ for the data given at 20⁰C using the relationships $\bar{d}_a = \frac{1}{\gamma_a}$ and $D_a = \sum_{i=1}^a d_i$. Thus, by rearranging the Belehradek's function, substituting the above two relationships, yields $\gamma_a(T)$ for any stage a for any temperature T for known α_a as

$$\gamma_a(T) = (T-1)^{1.8} / (\alpha_a - \alpha_{a-1}). \quad (2.7)$$

Here, $\alpha_0 = 0$.

2.2.3.4 An advanced model for maturation rates $\gamma_i(T)$

As an advancement to the model, we modify Eq. (2.1) assuming that stage duration times are Gamma distributed (Breteler et al., 1994; Lee et al., 2003), which replaces the earlier assumption of exponentially distributed stage duration times. That is, probability density function of d_a now becomes $\frac{\gamma^k}{\Gamma(k)} t^{k-1} e^{-\gamma t}$

where, $\Gamma(k) = (k-1)!$, $\gamma_a > 0$ and $k > 0$. Mathematically this can be achieved by assuming that there exists virtual sub-stages k within each stage a in Eq. (2.1), given that stage duration times of sub-stages are exponentially distributed. This follows from the linear chain trick in ODE (see MacDonald (1978) for the full description). Thus, the number of sub-stages k is equivalent to assuming the shape parameter k in the Gamma distributed stage duration times (as in Breteler et al., 1994; Lee et al., 2003).

The method of fitting model Eq. (2.6) with multiple sub-stages is outlined in Appendix 2.2. Now, the mean stage duration times d_a become $\bar{d}_a = \frac{k}{\gamma_a}$ for the advanced model for the Gamma distributed d_a . It yields

$$\gamma_a(T) = k(T-1)^{1.8} / (\alpha_a - \alpha_{a-1}) \quad (2.8)$$

Where, $\alpha_0 = 0$. Note that the advanced model reduces to the simpler model when $k=1$ (and also $\varepsilon=0$ in the estimation model in Appendix 2.2). We compare the model-fits for $k=1$, and $k=2, 3$ using AIC and chi-squares test to determine which model assumption is the best to estimate $\gamma_a(T)$. We also use the estimated stage-duration times to calculate mortality rates as shown in the next section.

2.2.4 Modeling mortality rates $\mu(T)$

Liang and Uye (1997a) estimated the percentage survival of nine generations of a *P. marinus* population in the West coast of Japan under different mean temperatures. We use these data to estimate the survival curves at different temperatures. Because of their estimation procedure, Liang and Uye (1997a) reported percent survival $>100\%$ in some cases; these values were reduced to 100%.

We fit the function $S_v = \exp(-\phi\alpha^\chi)$ for the proportion surviving from eggs to stage a , where ϕ is a scale parameter and χ is a shape parameter. We estimate ϕ and χ using non-linear least squares regression. We refer to S_v as a modified Weibull function because $(1 - S_v)$ is the cumulative density function of the Weibull (1951) distribution. We calculate the proportion of individuals that died in each stage with respect to the proportion of individuals that matured into the current stage from the previous stage using the estimated S_v .

To calculate the mortality rates $\mu_a(T)$ for each stage a , we divide the proportions that died in each stage by the stage duration time given by $d_a = \frac{1}{\gamma_a}$ on the assumption of exponentially distributions stage maturation times (simple model), and $d_a = \frac{k}{\gamma_a}$ on the assumption of Gamma distributed stage maturation times (advanced model) at the same temperatures.

We pool the mortality rates across stages so as to be consistent with our earlier assumption. Thus, we fit a quadratic function

$$\mu(T) = \kappa_2 T^2 + \kappa_1 T + \kappa_0 \quad (2.9)$$

for the pooled data using non-linear least squares regression. We do not use the survey measurement data at 27.4⁰C in Uye et al. (1983) for above calculations as it yields near zero daily mortality rates at such comparatively high temperature, which results in a biologically unexplainable pattern that contradicts the general trend, suggesting that those data may be outliers.

To test the validity behind the assumption of pooling the mortality rate data that, the mortality rates are the same across all stages for a given temperature (as in Breteler et al., 1994; Uye et al., 1983), we use the method of positioning means within confidence intervals (Venables and Ripley, 2002).

2.2.5. R_0 as a function of temperature given k sub-stages within a stage (an advanced model)

Now we have $\beta(T)$, $\gamma_a(T)$ and $\mu(T)$ modeled exclusively as functions of temperature, and the models parameterized using published data, to finally fit into $R_0(T)$ in Eq. (2.2). Here, we derive (see derivation in Appendix 2.1), $R_0(T)$ also for a population with any given k number of virtual sub-stages within a stage, or where stage duration times are Gamma distributed. It yields

$$R_0(T) = \frac{q\beta(T)}{\mu_s(T)} \prod_{i=1}^{s-1} \left(\frac{\gamma_i(T)}{\mu_i(T) + \gamma_i(T)} \right)^k. \quad (2.10)$$

2.2.6. Application and validation

We use the parameterized model $R_o(T)$ in Eq. (2.2) and Eq. (2.10) to predict the range of habitats that are potentially invisable to *P. marinus* on a global scale based on mean sea surface temperature data with optimum interpolation from NOAA-ESRL (n.d.) at $1^0 \times 1^0$ degree latitudinal and longitudinal resolution. The range of habitats, where $R_o(T) < 1$ is considered to be uninvasible for *P. marinus*, whereas that for $R_o(T) > 1$ is considered to be potentially invisable. We compare the model predictions with the observed distribution of *P. marinus* based on the literature.

2.3. Results

2.3.1. Life-history parameters $\beta(T)$, $\gamma_i(T)$ and $\mu(T)$

We found that the sigmoidal model for fecundity rates fits the data better than the linear model (Figure 2-1). The residual sum of squares (RSS) for the sigmoidal model was 97.37 compared to 126.08 for the linear model. Parameter estimates for the sigmoidal model were $f_m = 13.89$, $f_1 = 0.61$, $w = 0.35$, $b = 6.01^{\circ}C$. The fecundity rates reached a maximum at temperatures above $25^{\circ}C$.

The proportion of individuals not yet past a given stage for stage duration times estimated from Eq. (2.6) using the advanced model (Appendix 2-2) for the data from Uye et al. (1983) for a population in $20^{\circ}C$ is given in Figure 2-2 The model with $k=3$ yields the lowest AIC (Table 2-1). Note that p -values for the chi-square goodness-of-fit test for $k=1$ and $k=2$ with respect to $k=3$ was < 0.001 . This suggests that model with $k=3$ is a better predictor, which is significantly different from the models with $k=1$ and $k=2$. Table 2-2 gives the resulting temperature-independent α_a values computed based on the above estimates.

The parameters ϕ and χ of the modified Weibull model estimated for different generations at different temperature regimes are given in Table 2-3 and

Figure 2-3. The mortality rate model Eq. (2.9) estimated based on the pooled mortality rates data computed based on the above at different temperature regimes are given in Figure 2-4. The estimates of the coefficients were $\kappa_2=0.0022$ /day, $\kappa_1=-0.0563/^\circ\text{C}$ day, $\kappa_0=0.4211/^\circ\text{C}^2$ day. The estimates of the coefficients for stage specific mortality rates modeled with respect to temperature fell within the 95% confidence intervals of the estimates of one another. Hence, the notion that stage based mortality rates are the same across all stages is a valid assumption for *P. marinus*.

2.3.2. Net reproductive rate $R_0(T)$

The $R_0(T)$, evaluated for a range of temperature T by incorporating the parameterized sub-models $\beta(T)$, $\gamma_a(T)$ and $\mu(T)$, shows a concave function with respect to mean habitat temperatures (Figure 2-5). The $R_0(T)$ decreases at higher temperatures due to increasing mortality rates (Figure 2-4) that suppress the positive effect given by the simultaneous increase in the fecundity rates (Figure 2-1). We plotted $R_0(T)$ for the cases where $k=1$ and $k=3$ (Figure 2-5). Relatively lower values of $R_0(T)$ for higher k suggest that the fitness of the population is reduced when k is high regardless of the temperature. The $R_0(T)$ model that fits the data best was the one with $k=3$.

The uncertainty associated with the estimates of $R_0(T)$ cannot be calculated because the confidence intervals were not given for the estimates taken from the literature (Liang and Uye, 1997a; Uye et al., 1983). The potentially invisable range of habitats, that is where $R_0(T) > 1$, are those within 11°C to 23°C mean temperatures. Habitats whose mean temperatures are less than 11°C or greater than 23°C are uninvisible. This indicates that the species is more cold-adapted. Field sampling evidence depicted in Figure 2-6 suggests that the predictability of the model is reasonable. Note that the standard errors of the predictions are not given.

2.4. Discussion

In this paper, we proposed a novel methodology to model the net reproductive rate R_0 , which is a metric that evaluates population persistence, as a function of mean habitat temperature (T) for invasive marine copepod *P. marinus*. We showed how to parameterize the model based on published data from experiments and surveys. This approach may be applied to model R_0 for any marine copepod having a similar life-history stages (for example, species in Bonnet et al., 2009; Chen et al., 2006). Marine copepods, in general, have the same stage-structure. Habitats with mean temperatures forcing $R_0(T) > 1$ indicate those that are potentially invasible, given the other factors are also favourable to the species. Similarly, habitats with mean temperatures forcing $R_0(T) < 1$ indicate those that are uninvasible to the species regardless of the status of the other ecological factors (whether fixed or not). Thus, our approach conservatively predicts the habitats that are uninvasible, and thereby, potentially invasible to the species.

Habitats that are potentially invasible to *P. marinus*, as predicted by our model, matched well with field evidence of species occurrences on a global scale. In particular, we note that from Figure 2-6, Elliot Bay, Puget Sound is on the border of uninvasible range limiting $R_0(T) = 1$. *Pseudodiaptomus marinus* has been sampled at Puget Sound by Cohen (2004) according to the U.S Geological Surveys (USGS, n.d.). However, there has been no indication as yet, as to whether it has established in that location. Further northwards, Piercey et al. (2000) found that there was a large propagule pressure of *P. marinus* on Vancouver harbour: *P. marinus* were found in 25.4% ships sampled occurring in densities $2 \sim 54 \text{m}^{-3}$. Vancouver harbour is also located on the border limiting $R_0(T) = 1$. We also note that temperatures around Vancouver harbour and Puget Sound fluctuate at large amplitudes seasonally (DFO, n.d.). To predict invasibility of habitats, where the temperature is unsteady, we may need a model that accounts for the effect of seasonal fluctuation of temperature.

If we incorporated the survival data at 27 °C, as we mentioned before, then the upper bound of $R_0(T)=1$ would have shifted towards higher habitat temperatures shifting the potentially invisable range more towards the tropics. We did not incorporate those survival data because they were inconsistent with the general trend in the mortality rates with respect to increasing temperatures. Yet the field observations may fit better if we did so.

The methodological basis that we adopted, the bottom up mechanistic approach, in determining potentially invisable habitats, is contrasting to that of ENM. The ENM predicts habitat suitability based on a snapshot of environmental conditions and species occurrences (Herborg et al., 2007a; Peterson et al., 2003; 2007) by matching the set of environmental variables between native and potentially invisable ranges (Jeschke and Strayer, 2008; Mercado-Silva et al., 2006). For e.g. the Genetic Algorithm for Rule-set Prediction (GARP) (Stockwell and Peters, 1999) in ENM has been commonly used to predict habitat suitability for both terrestrial and aquatic invasive species (e.g., Herborg et al., 2007a; 2007b; Peterson, 2003; Peterson et al., 2007). This methodology implicitly assumes that a species may survive and reproduce only in habitats having similar ranges of environmental sets. Often, species tolerate environmental sets beyond what is found in their native range (Lockwood et al., 2006). For example, a species distribution may be confined to a certain native range due to natural barriers rather than environmental parameters (Lonhart, 2009) suggesting that absence is not necessarily indicative of a habitat's unsuitability. In such case, ENM may not be able to fully capture the potential environmental set that a species can tolerate. For this reason, ENM can overlook habitats where a species can potentially survive and reproduce, especially in cases where human-mediated transport can facilitate jump dispersals (e.g., Broennimann et al., 2007). Our approach avoids this particular limitation of ENM.

The model we propose here is designed to quantify R_0 for small introduced populations. Hence, we did not explicitly account for the density-dependence of the population at high population densities. Furthermore, we disregarded the Allee

effect (Courchamp et al., 2008; Kramer et al., 2008; Taylor and Hasting, 2005). It may be a factor that works against species establishment at low population densities (Lockwood et al., 2006; Whitmann et al., 2011). A different approach would be needed to analyze populations with Allee effects. Inclusion of Allee effect may remove another subset of uninhabitable habitats from the potentially inhabitable range. Thus, our predictions made without the inclusion of Allee effect may be conservative.

Sea surface temperature (SST) has been rising over the last few decades (Cane et al., 1997). Our model can be used as a tool to determine the effect of the rise in SST on species range expansion. The concave functional shape of $R_0(T)$ with respect to T , with bounds limiting $R_0(T)$ at warm and cold temperatures, suggests that the potentially inhabitable habitat range for *P. marinus* may shift towards the poles, or the colder waters, rather than a *range expansion* per se, with an increase in T or a rise in SST. However, the effect of climate change on seasonal changes, for example, the effect on the amplitude of SST, may also be critical in determining the long term effects. We note that, for example, the temperature data from Race Rocks, BC, spanning from 1921-2008, indicate that annual low temperatures have not increased as much as the annual high temperatures along with the general rise in the mean SST. The impact of such non-linear increases in temperature may have non-linear effects on R_0 . Hence, we may not be able to compute the expected shift in $R_0(T)$ by simply adding the expected increment in mean SST to the mean T of habitats in forecasting the effect (for e.g., in Moller et al., 2012). Although the change in mean habitat temperature due to rise in SST may be very small, we note that the scale at which the shift in inhabitable geographical range would be large.

A proxy for using mean temperature to characterize a habitat is appropriate in cases where the year-round temperatures force R_0 to be less than 1, or all greater than 1 through all seasons, in general. However, in habitats where the temperature fluctuates seasonally forcing $R_0(T) > 1$ in one season, and $R_0(T) < 1$ in another, the predictions made by $R_0(T)$ may not be reliable. Developing a new

metric that accounts for seasonal variation (see methods in Bacaer, 2009; Bacaer and Ouifki, 2007; Wesley and Allen, 2009 in epidemiology) may be more suitable for predicting potentially invisable habitats under such scenario.

An extension to our model would be to incorporate the effect of other environmental forcing factors, such as salinity, on life-history parameters in a multivariate model, and also the effect of the fluctuations of those factors. It may inflate the uninvisible habitat range for a species. Recent work towards modeling the combined effect of temperature and salinity on population persistence is found in Strasser et al. (2011).

Table 2-1 Model comparisons for cases $k=1, 2$ and 3 in Eq. (2.6) with advanced model (Appendix 2.2).

Model	RSS	LL	(LL/LLmax)	χ^2	Deg	AIC	Δ AIC	p -of χ^2
k=3	0.57	120.56	0.00	0.00	14	-213.12	0.00	
k=2	1.04	108.83	-11.73	23.45	13	-191.67	21.45	1.28E-06
k=1	1.88	97.29	-23.27	46.54	12	-170.58	42.54	7.83E-11

**LL-Log likelihood, LLmax-Maximum Log likelihood, AIC-Akaike information criteria

Table 2-2 The temperature-independent coefficients α_a yielded by the Belehradek's function given for stage development times at 20°C calculated based on stage maturation rates estimated by Eq. (2.6).

Stage	$\gamma_a(20^0C)$	Stage duration time $\bar{d}_a(20^0C)$ (days)	Stage development time $\bar{D}_a(20^0C)$ (days)	α_a
e	3.64	0.27	-	55.01
n2	2.53	0.40	0.67	134.21
n3	1.05	0.96	1.63	325.81
n4	0.87	1.16	2.78	557.40
n5	0.65	1.53	4.31	864.01
n6	0.81	1.23	5.54	1110.77
c1	0.54	1.84	7.39	1479.68
c2	0.58	1.73	9.12	1827.22
c3	0.60	1.66	10.78	2159.64
c4	0.40	2.48	13.26	2656.81
c5	0.29	3.48	16.74	3353.02
c6	-	4.84	21.57	4321.76

Table 2-3 Estimation of ϕ and χ in $S_v = \exp(-\phi\alpha^\chi)$ at different temperatures.

Temp ($^{\circ}\text{C}$)	10.60	14.30	16.70	20.20	21.50	22.30	25.60	27.40
ϕ	0.02	0.01	0.00	0.00	0.13	0.53	0.00	0.10
χ	2.69	2.26	7.87	2.93	1.43	0.94	29.24	1.56
RSS	0.05	0.11	0.09	0.02	0.06	0.01	0.09	0.03

**RSS-Residual sum of squares

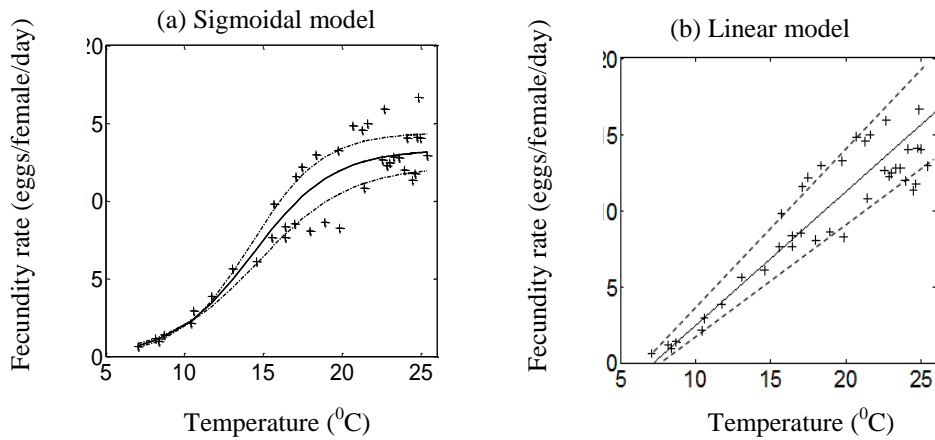


Figure 2-1 Fecundity rates of adult females at different temperatures, comparing the sigmoidal model Eq. (2.3) with the linear model in Uye et al. (1983). Dashed lines indicate the 95% confidence intervals.

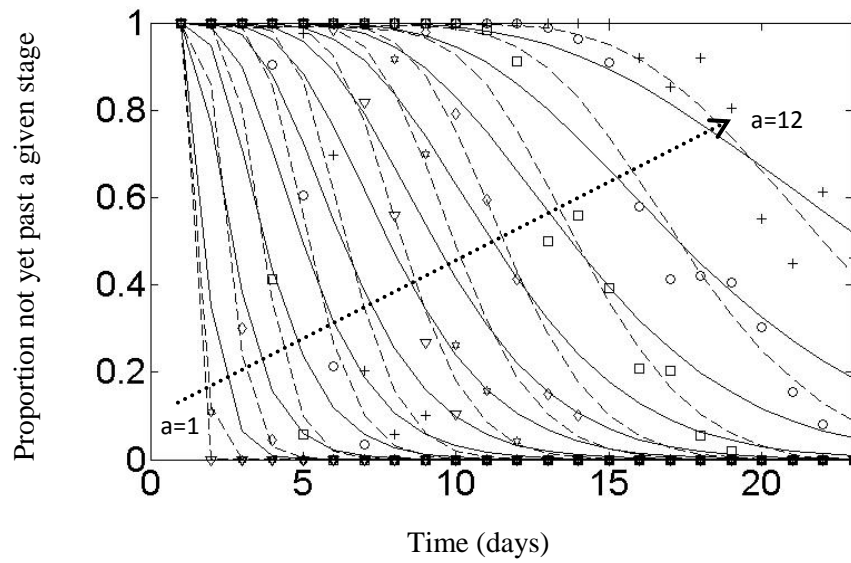


Figure 2-2 Proportion of individuals in the population not yet past a given stage a , for $a=1..12$, obtained by fitting Eq. (2.6) and its advanced model (in Appendix 2.2) to data from Uye et al. (1983). Solid lines are the fits for $k=1$, dashed lines are the fits for $k=3$.

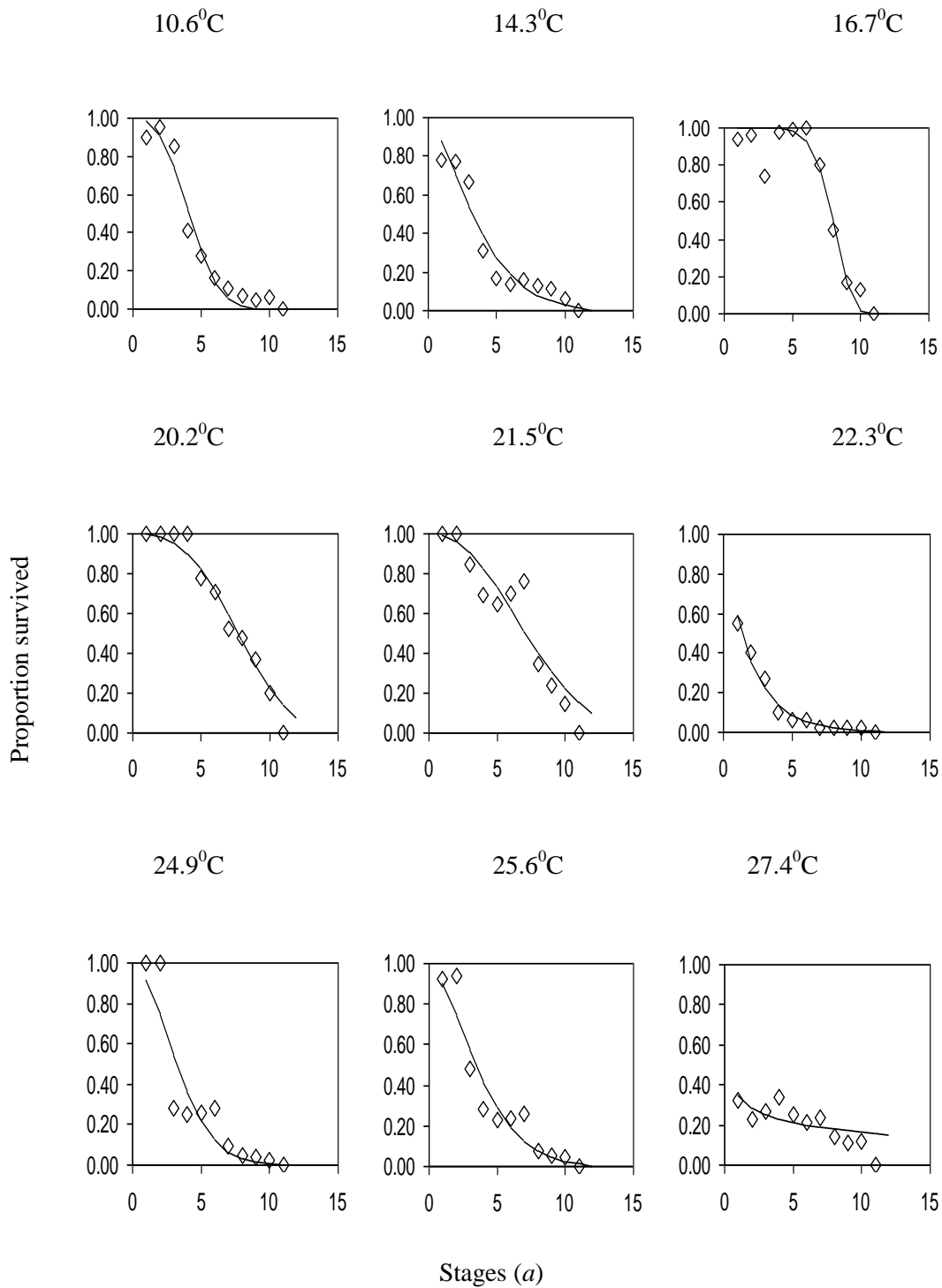


Figure 2-3 Proportion survived at the end of each stage in different temperature regimes estimated by $S_v = \exp(-\phi a^\lambda)$ based on the data from Liang and Uye (1997a).

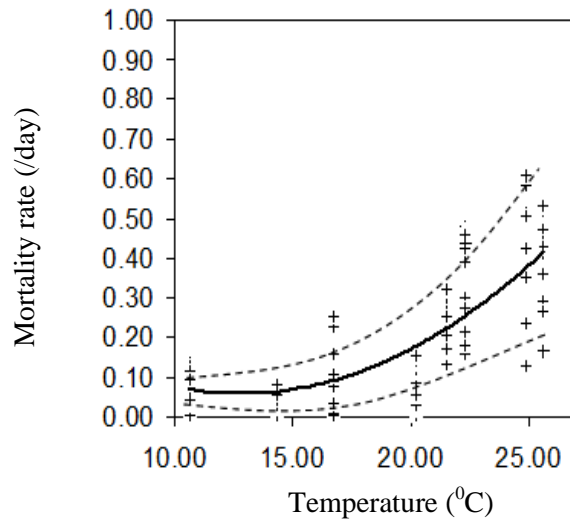


Figure 2-4 Quadratic model of daily mortality rates as a function of temperature, estimated from pooled stage-based data. Parameter estimates for mortality rate model are $\kappa_2=0.0022$ /day, $\kappa_1=-0.0563$ / $^{\circ}\text{C}$ day, $\kappa_0=0.4211$ / $^{\circ}\text{C}^2$ day. Dashed lines are 95% confidence intervals.

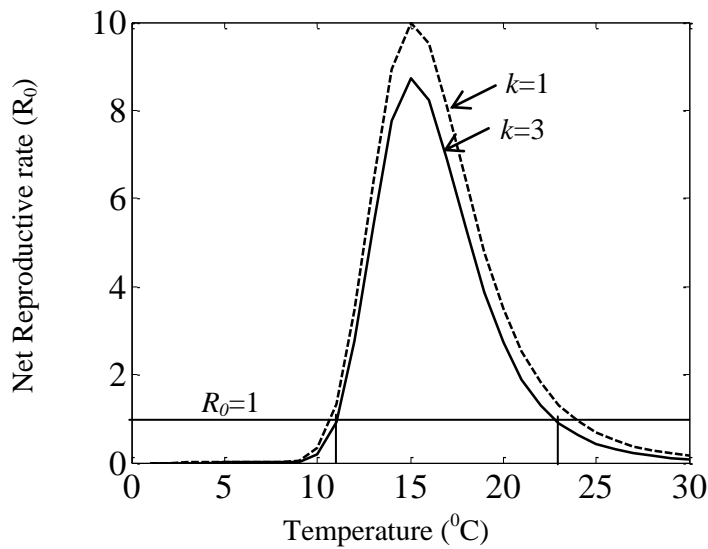


Figure 2-5 Net reproductive rate R_0 plotted as a function of temperature (T) for the cases where $k=1$ (exponentially distributed stage duration times) and $k=3$ (Gamma distributed stage duration times).

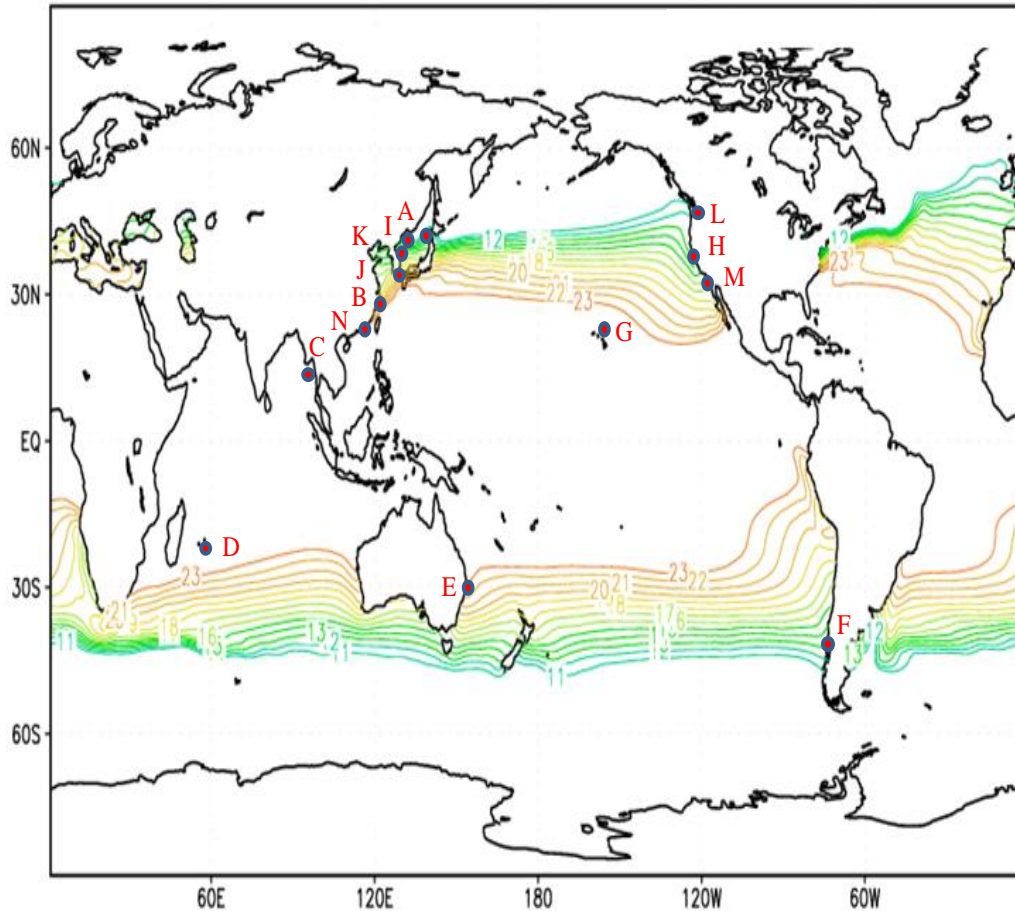


Figure 2-6 Range of potentially invivable habitats for *P. marinus*: 11^oC to 23^oC, as predicted by the model Eq. (2.10) based on $R_0(T) > 1$ for sea surface temperature (T) data averaged from year 1971-2000 through NOAA interactive database. Dots are the habitats where *P. marinus* was detected or established.

[References are from Fleminger and Kramer (1988) except *: (A) West coast of Hokkaido, Japan, Sato (1913), Walter (1986); (B) Qing-Chao and Shu-Zhen (1965); (C) Andaman Islands (Pillai 1976); (D) Mauritius (Grindley and Grice 1969); (E) Moreton Bay, Queensland (Greenwood 1977); (F)* Patagonian Waters, Southern Chile (Jones, 1966; Grindley and Grice, 1969) from Hirakawa (1986); (G) Oahu, Hawaii (Jones 1966) (Carlton 1985)*; (H)* San Francisco Bay, California (Ruiz et al. 2000); (I) Peter the Great Bay (Brodsky 1948, 1950); (J) Chiba (1956), Tanaka (1966), Tanaka and Huee (1966), Walter (1986); (K) Brodsky (1948, 1950); (L)* Elliot Bay, Puget Sound, Washington (Cohen 2004), USGS; (M) USGS; (N) Shen and Lee (1963)]

2.5. References

- Ackleha, A.S., de Leenheerb, P., 2008. Discrete three-stage population model: persistence and global stability results. *Journal of Biological Dynamics* 2(4), 415-427.
- Amarasekare, P., Savage, V., 2012. A framework for elucidating the temperature dependence of fitness. *American Naturalist* 179(2), 178-191.
- Bacaer, N., 2009. Periodic matrix population models: growth rate, basic reproductive number, and entropy. *Bulletin of Mathematical Biology* 71, 1781-1792.
- Bacaer, N., Ouifki, R., 2007. Growth rate and basic reproduction number for population models with a simple periodic factor. *Mathematical Biosciences* 210, 647-658.
- Boldin, B., 2006. Introducing a population into a steady community: the critical case, the centre manifold and the direction of bifurcation. *SIAM Journal on Applied Mathematics* 66 (A), 1424-1453.
- Bonnet, D., Harris, R.P., Yebra, L., Guilhaumon, F., Conway, D.V.P., Hirst, A.G., 2009. Temperature effects on *Calanus helgolandicus* (copepoda: calanoida) development time and egg production. *Journal of Plankton Research* 31(1), 31-44.
- Breteler, W.C.M.K., Schogt, N., van der Meer, J., 1994. The duration of copepod life stages estimated from stage-frequency data. *Journal of Plankton Research* 16(8), 1039-1057.
- Brodsky, K.A., 1948. Free-living Copepoda of the Sea of Japan. *Isv. tikhookean. nauko-issled. Inst. ryb.* Oceanography 26, 3-130.
- Brodsky, K.A., 1950. Copepods (Calanoida) of the far-eastern seas of the USSR and the polar basin. Zoological Institute of the Academy of Sciences of the USSR, Leningrad, 97-133.
- Broennimann, O., Treier, U.A., Muller-Scharer, H., Thuiller, W., Peterson, A.T., Guisan, A., 2007. Evidence of climatic niche shift during biological invasion. *Ecology Letters* 10, 701-709.
- Brylinski, J.M., Antajan, E., Raud, T., Vincent, D., 2012. First record of the Asian copepod *Pseudodiaptomus marinus* Sato, 1913 (Copepoda: Calanoida: Pseudodiaptomidae) in the southern bight of the North Sea along the coast of France. *Aquatic Invasions* 7(4), 577-584.
- Cane, M.A., Clement, A.C., Kaplan, A., Kushnir, Y., Pozdnyakov, D., Seager, R., Zebiak, S.E., Murtugudde, R., 1997. Twentieth-Century Sea Surface Temperature Trends. *Science* 275(5302), 957-960.
- Carlton, J.T., 1985. Trans-Oceanic and Interoceanic Dispersal of Coastal Marine Organisms - the Biology of Ballast Water. *Oceanography and Marine Biology* 23, 313-371.

- Chen, Q., Sheng, J., Lin, Q., Gao, Y., Lv, J., 2006. Effect of salinity on reproduction and survival of the copepod. *Pseudodiaptomus annandalei* Sewell, 1919. *Aquaculture* 258, 575–582.
- Chiba, T., 1956. Studies on the development and the systematics of Copepoda. *J. Shimonoseki Coll. Fish* 6(1), 1-90.
- Cohen, A.N., 2004. An exotic species detection program for Puget Sound. pp 52 (In *United States Geological Surveys*. Retrieved from: <http://nas.er.usgs.gov/queries/SpecimenViewer.aspx?SpecimenID=161281>).
- Cordell, J.R., Bollens, S.M., Draheim, R., Sytsma, M., 2008. Asian copepods on the move: recent invasions in the Columbia-Snake River system. *ICES Journal of Marine Science* 65(5), 753-758.
- Cordell, J.R., Lawrence, D.J., Ferm, N.C., Tear, L.M., Smith, S.S., Herwig, R.P., 2009. Factors influencing densities of non-indigenous species in the ballast water of ships arriving at ports in Puget Sound, Washington, United States. *Aquatic Conservation: Marine and Freshwater Ecosystems* 19(3), 322-343.
- Courchamp, F., Berec, L., Gascoigne, J., 2008. *Allee effects in ecology and conservation*. Oxford University Press, GB, pp 220.
- Cox, D.R., 1967. *Renewal Theory*. Science Paperbacks and Methuen & Co. Ltd., GB, pp 142.
- de-Camino-Beck, T., Lewis, M.A., van den Driessche, P., 2009. A graph-theoretic method for the basic reproduction number in continuous time epidemiological models. *Journal of Mathematical Biology* 59(4), 503-516.
- DFO., n.d. BC lighthouse sea surface temperature data. Retrieved from: , <http://www.pac.dfo-mpo.gc.ca/science/oceans/data-donnees/lighthouses-phares/index-eng.htm>.
- Elith, J., Leathwick, J.R., 2009. Species distribution models: ecological explanation and prediction across space and time. *Annual Review of Ecology, Evolution, and Systematics* 40, 677-97.
- Fleminger, A., Kramer, S.H., 1988. Recent introduction of an Asian estuarine copepod, *Pseudodiaptomus marinus* (Copepods: Calanoida), into southern California River Estuary. *Journal of Crustacean Biology* 12, 260-541.
- Greenwood, J.G., 1977. Calanoid copepods of Moreton Bay (Queensland) II. Families Calocalanidae to Centropagidae. *Proceeding of the Royal Society B* 88, 49-67.
- Grindley, J.R., Grice, G.D., 1969. A redescription of *Pseudodiaptomus marinus* Sato (Copepoda, Calanoida) and its occurrence at the Island of Mauritius. *Crustaceana* 125-134.
- Herborg, L., Jerde, C.L., Lodge, D.M., Ruiz, G.M., MacIsaac, H.J. 2007a. Predicting invasion risk using measures of introduction effort and environmental niche models. *Ecological Applications* 17(3), 663–674.

- Herborg, L., Mandrak, N., Cudmore, B., MacIsaac, H., 2007b. Comparative distribution and invasion risk of snakehead (*Channidae*) and Asian carp (*Cyprinidae*) species in North America. *Canadian Journal of Fisheries and Aquatic Sciences* 64, 1723-1735.
- Hirakawa, K., 1986. New record of the planktonic copepod *Centropages abdominalis* (copepoda, calanoida) from patagonian waters, southern chile, *Crustaceana* 51 (3), 296-299.
- Hurford, A., Cownden, D., Day, T., 2010. Next-generation tools for evolutionary invasion analyses. *Journal of the Royal Society Interface* 561–571.
- Jeschke, J.M., Strayer, D.L. 2008. Usefulness of bioclimatic models for studying climate change and invasive species. *Annals of the New York Academy of Sciences* 1134, 1–24.
- Jiménez-Pérez, J.L., Castro-Longoria, E., 2006. Range extension and establishment of a breeding population of the asiatic copepod, *Pseudodiaptomus marinus* Sato, 1913 (calanoida, Pseudodiaptomidae) in Todos Santos bay, Baja California, Mexico. *Crustaceana* 79(2), 227-234.
- Jones E.C., 1966 A New Record of *Pseudodiaptomus marinus* Sato (Copepoda, Calanoida) from Brackish Waters of Hawaii. *Crustaceana* 10(3), 316-317.
- Kramer, A.M., Sarnelle, O., Knapp, R.A., 2008. Allee effect limits colonization success of sexually reproducing zooplankton. *Ecology* 89(10), 2760–2769.
- Lee, H.W., Ban, S., Ikeda, T., Matsuishi, T. 2003. Effect of temperature on development, growth and reproduction in the marine copepod *Pseudocalanus newmani* at satiating food condition. *Journal of Plankton Research* 25(3), 261-271.
- Liang, D., Uye, S., 1997a. Population dynamics and production of the planktonic copepods in a eutrophic inlet of the island Sea of Japan. IV. *Pseudodiaptomus marinus*, the egg-carrying calanoid. *Marine Biology* 128, 415-421.
- Liang, D., Uye, S., 1997b. Seasonal reproductive biology of the egg-carrying calanoid copepod *Pseudodiaptomus marinus* in a eutrophic inlet of the island of Japan. *Marine Biology* 128, 409-414.
- Lockwood, J., Hoopes, M., Marchetti, M., 2006. *Invasion Ecology*, Wiley Blackwell, p. 312.
- Lonhart, S.I., 2009. Natural and climate change mediated invasions. In *Biological Invasions in Marine Ecosystems* (p. 57-69). Springer Berlin Heidelberg.
- MacDonald, N., 1978. *Time Lags in Biological Models*, Springer-Verlag Berlin Heidelberg, NY, p. 112.
- Mercado-Silva, N., Olden, J.D., Maxted, J.T., Hrabik, T.R., Vander Zanden, M.J., 2006. Forecasting the spread of invasive rainbow smelt in the Laurentian Great Lakes region of North America. *Conservation Biology* 20(6), 1740–1749.
- Møller, E.F., Maar, M., Jónasdóttir, S.H., Nielsen, T.G., Tönnesson, K., 2012. The effect of changes in temperature and food on the development of *Calanus finmarchicus* and *Calanus helgolandicus* populations. *Limnology and Oceanography* 57(1), 211-220.

- NOAA-ESRL., n.d. Physical Sciences Division, Boulder Colorado, USA. Retrieved from <http://www.esrl.noaa.gov/psd/data/gridded/data.noaa.oisst.v2.html>.
- Peterson, A.T., 2003. Predicting the geography of species' invasions via ecological niche modeling. *Quarterly Review of Biology* 78(4), 419-433.
- Peterson, A.T., Williams, R., Chen, G., 2007. Modeled global invasive potential of Asian gypsy moths, *Lymantria dispar*. *Entomologia Experimentalis et Applicata* 125(1), 39-44.
- Piercey, G.E., Levings, C.D., Elfert, M., Galbraith, M., Waters, R., 2000. Invertebrate fauna in ballast water collected in vessels arriving in BC ports, especially those from Western North, Pacific. *Canadian Data Report of Fisheries and Aquatic Sciences* 1060, 50.
- Pillai, P.P., 1976. A review of the calanoid copepod family Pseudodiaptomidae with remarks on the taxonomy and distribution of the species from the Indian Ocean. *Journal of the Marine Biological Association of India* 18(2), 242-265.
- Qing-Chao, C., Shu-Zhen, Z., 1965. The planktonic copepods of the Yellow sea and the east China sea. 1. *Calanoida Studia Mar Sin* 7: 20-131.
- Ruiz, G.M., Fofonoff, P., Carlton, J.T., Wonham, M.J., Hines, A.H., 2000. Invasion of coastal marine communities in North America: apparent patterns, processes, and biases. *Annual Review in Ecology and Systematics* 2000, 481-531.
- Sato, T., 1913. Pelagic Copepoda, 1. *Rep. Fish. Invest. Hokkaido Fish. Exp. Stn.*, 1: 1-79.
- Shen, C.J., Lee, F. S., 1963. The estuarine Copepoda of Chiekong and Zaikong Rivers, Kwangtung Province, China. *Acta Zoologica Sinica* 15(4), 571-596.
- Stockwell, D.R.B., Peters, D.P., 1999. The GARP modelling system: problems and solutions to automated spatial prediction. *International Journal of Geographical Information Systems* 13, 143-158.
- Strasser, C.A., Lewis, M.A., DiBacco, C. 2012. A mechanistic model for understanding invasions using the environment as a predictor of population success. *Diversity and Distributions* 17(6), 1210-1224.
- Tanaka, O., 1966. Neritic Copepoda Calanoida from the north-west coast of Kyushu. *Proc. Symp. Crustacea, Marine Biological Association of India* 1, 38-50.
- Tanaka, O., Hue, J.S., 1966. Preliminary report on the copepods found in the tide pool along the north-west coast of Kyushu. *Proceedings of the Symposium on Crustacea* 1, 34-56.
- Taylor, C.M., Hasting, A., 2005. Allee effect in biological invasions. *Ecological Letters* 8, 895-908.
- USGS., n.d. Retrieved from: <http://nas.er.usgs.gov/queries/SpecimenViewer.aspx?SpecimenID=161281>.

- Uye, S., Iwai, Y., Kasahara, S., 1983, Growth and production of the inshore marine copepod *Pseudodiaptomus marinus* in the central part of the inland Sea of Japan. *Marine Biology* 73, 91-98.
- van den Driessche, P., Watmough, J., 2002. Reproduction numbers and sub-threshold endemic equilibria for compartmental models of disease transmission. *Mathematical Biosciences* 180, 29–48.
- Venables, W.N., Ripley, B.D. 2002. *Modern applied statistics with S*. 4th Edn. Springer, p. 495.
- Wallinga, J., Lipsitch, M., 2007. How generation intervals shape the relationship between growth rates and reproductive numbers. *Proceeding of Royal Society B* 274(1609), 599–604.
- Walter, T.C., 1986. The zoogeography of genus *Pseudodiaptomus* (Calanoida: Pseudodiaptomidae). *Syllogeus* 58, 502-508.
- Weibull, W., 1951. A statistical distribution function of wide applicability, *Journal of Applied Mechanics Transactions* 18(3), 293–297.
- Wesley, C.L., Allen, L.J.S., 2009. The basic reproductive number in epidemic models with periodic demographics. *Journal of Biological Dynamics* 3(2-3), 116-129.
- Wittmann, M.J., Lewis, M.A., Young, J.D., Yan, N.D., 2011. Temperature-dependent Allee effects in a stage-structured model for *Bythotrephes* establishment, *Biological Invasions* 13(11), 2477-2497.

CHAPTER 3

Are invasive copepods generated in habitats in high-amplitude periodic temperatures? The case specific to *Pseudodiaptomous marinus*

3.1. Introduction

Copepods are a major link between primary and tertiary producers in large marine food-webs, in which, humans are the end-receivers (Kiorboe, 2008). Everyday, a large number of non-native copepod species are introduced to novel habitats across the globe through ship ballast-water discharge (e.g., Boltovskoy et al., 2011; Cordell et al., 2009). There is uncertainty as to which environmental conditions will allow them to persist (Bollens et al., 2012; Byrnes et al., 2007; Ruiz et al., 2011). Thus, capturing critical environmental thresholds that govern the stability of these species in introduced habitats has become a major research focus (Fowler et al., 2011; Pineda et al., 2012).

A wealth of knowledge and data are available on the effect of temperature on key life-history parameters of copepods (e.g., Almeda et al., 2010; Devreker et al., 2009; Lee et al., 2003; Strasser et al., 2011). Amalgamation of this knowledge in a global synthesis suggests that their fecundity, mortality, and stage maturation (transition) rate parameters are functions of ambient temperature, showing a general pattern across all species of copepods (Bunker and Hirst, 2004; Hirst and Kiørboe, 2002; Huntley and Lopwz, 1992). These rate parameters can be used to model that yields the net reproductive rate R_0 , the average number of offspring produced by a female over its lifetime, and also the intrinsic growth rate λ of a population. Using this approach, Rajakaruna et al. (2012) have modeled the $R_0(T)$ pertaining to marine calanoid copepod *Pseudodiaptomous marinus* as a function of temperature (T), and determined the habitats that are potentially invisable to the species given the mean habitat temperatures (Figure 3-1). Similarly, Amarasekare

and Savage (2012), and Strasser et al. (2011) have modeled the intrinsic growth rate $\lambda(T)$ of species as a function of the mean habitat temperature.

Global predictions made by the Rajakaruna et al. (2012) model were supported by three recent sampling studies by Brylinski et al. (2012) at Southern Bight of the North Sea along the coast of France, Olazabal and Tirelli (2011) at Adriatic Sea in northern Italy, and Sabia et al. (2012) at Lake Faro (Messina, Italy). However, this model suffices only if the habitat temperature is uniform year-round, and is not subject to fluctuations. Yet the field data from sub-tropical and temperate marine and estuary habitats indicate that temperatures fluctuate periodically with amplitudes as high as 14°C , particularly in the northern hemisphere (NOAA-ESRL, n.d.; Masson and Cummins, 2007). Under this scenario, $R_0(T)$ modeled by Rajakaruna et al., (2012) may not be a reliable predictor of population persistence when T is taken to be the average temperature. Similarly, the case of using intrinsic growth rates based on mean habitat temperatures as modeled by Amarasekare and Savage (2012) and Strasser et al. (2011) also may not be reliable.

The copepod *P. marinus* is native to the seas of Japan and China (North West Pacific coast) (Cordell et al., 2008), where the periodic fluctuation of temperature is large compared to most other marine ecoregions (NOAA-ESRL, n.d.). *Pseudodiaptomous marinus* has been introduced to the West coast of North America via ship-ballast water discharge (Cordell et al., 2008; Fleminger and Kramer, 1988), and has established in localities such as San Francisco bay (Ruiz et al., 2011) and San Diego Bay (USGS, n.d.). It has been detected also at Elliot Bay, Puget Sound, Washington (Cohen, 2004) and Todos Santos Bay (Jiménez-Pérez and Castro-Longoria, 2006). *Pseudodiaptomous marinus* continues to be sampled in large quantities in ballast-water of ships entering Puget Sound (Cordell et al., 2008; Lorenze and Cordell, 2010) and Vancouver harbour (Barry and Levings 2002; Levings et al., 2004), but has not yet established in those locations.

In this paper, we derive two simplified approximate metrics for population persistence, modeled specifically for *P. marinus* in periodically fluctuating habitat

temperatures, but broadly applicable to marine copepods in general. The metrics, based on the population dynamics described by a system of linear ordinary differential equations (ODEs), are the cross-periodic intrinsic growth rate Λ_p , and a weighted net reproductive rate R_p , which is a measure of the cross-periodic reproductive rate. Using Jensen's inequality (Jensen, 1906) we demonstrate that the temperature-dependent Λ_p and R_p are reduced when periodic fluctuations of temperature are taken into account.

To calibrate the model, we incorporate life-history parameters (fecundity, mortality, and maturation rates) estimated from the published data assuming that food conditions are at saturation as in Rajakaruna et al. (2012). This complies with Uye et al., (1983), where the data come from, indicating that the dynamics of these populations were temperature-dependent, but not regulated by the food concentration. Therefore, the persistence metrics we develop represent estimates under conditions that are ideal, except for the temperature. In other words, they are conditioned only by the temperature as they isolate the species' physiological tolerance to habitat temperature.

We test the validity and the reliability of our persistence metrics by comparing them to solutions given by numerically complex methods that determine the stability condition in periodic systems. We use them to determine the invasibility of specific localities to *P. marinus* on the West coast of North America, where there is a high *P. marinus* propagule pressure at present from ship ballast-water discharge (Cordell et al., 2009). Our analysis shows how the mean and the amplitude of yearly temperature cycles impact the invasibility of habitats to *P. marinus*. We investigate the potential range expansion of *P. marinus* on a global scale. Finally we focus on the case specific to Race Rocks in the Strait of Georgia, BC, and investigate the change in the invasibility of the habitat with respect to long term rise in the mean sea surface temperatures (SST). This gives insights into how a long term change in an environmental factor changes the habitat condition becoming favourable to an invasion of a species.

In this study, we do not incorporate density dependence and Allee effects that can suppress population growth at both high and low extreme densities. However, the addition of density dependence and the Allee effect could further reduce the chance of population establishment, decreasing an invasibility range already limited by the temperature.

Our method of analysis can be applied to other species with similar characteristics, such as marine copepods in general, or can be tailor-made to species depending on their life-history dynamics. This methodology may be used to investigate the causal mechanisms behind the general trends in marine species spread on a global scale. It will compliment the environmental niche modeling (Peterson, 2003) and contribute to management decision support systems, but use a mechanistic approach to determine the impacts of temperature fluctuations on the invasibility.

3.2. Model

The general form of a linear, stage-structured, continuous time model that depends on periodic ambient temperature T , can be written as

$$\frac{d\mathbf{n}}{dt} = \mathbf{A}[T(t)]\mathbf{n} \quad (3.1)$$

where \mathbf{n} is a vector of the stage-composition of the population, and $\mathbf{A}(T(t))$ is the transition matrix with time-periodic coefficients with period t_p . Although Eq. (3.1) is a linear system of dimension \mathbf{n} , the temperature T is assumed to be a non-linear function of time t , and the entries of the transition matrix \mathbf{A} are also non-linear functions of the temperature T . The system is called *invasible* if the $\mathbf{n}=\mathbf{0}$ equilibrium solution is unstable, and hence the ecological invasibility condition translates into a mathematical stability condition for the system in Eq. (3.1).

Rajakaruna et al. (2012) considered a model in the form of Eq. (3.1) for *P. marinus*, where $T(t)$ is replaced by the averaged habitat temperature \bar{T} . They

calculated the net reproductive rate $R_0(\bar{T})$, and used it to determine potentially invisable habitats based on the average temperature \bar{T} , and the condition $R_0(\bar{T}) > 1$. However, this approach makes no allowance for the magnitude of temperature fluctuations: high-amplitude temperature fluctuations are treated the same way as low-amplitude temperature fluctuations, or indeed, constant temperatures, as long as they possess the same mean temperature \bar{T} .

An alternative approach to averaging replaces the transition matrix \mathbf{A} by its seasonal average $\bar{\mathbf{A}}$ or the autonomous system obtained by replacing the time-varying entries in \mathbf{A} with their time-averaged values (Ma and Ma, 2006). When the entries of the transition matrix \mathbf{A} in the system are non-linear functions of T , it is generally true that $\mathbf{A}(\bar{T}) \neq \bar{\mathbf{A}}(T)$, suggesting that the stability condition evaluated based on the mean habitat temperature may deviate from that evaluated from the time-averaging method. Hence, we expect the magnitude of the fluctuations of temperature to play a role in determining the instability of the system, or the invasibility of habitats by a species.

The linear system of Eq. (3.1) cannot be solved explicitly for many forms of $\mathbf{A}(T(t))$, including the one given in Rajakaruna et al. (2012). Although there is much theory on the qualitative behaviour of periodically forced linear systems, the explicit solution to the system cannot be derived easily. Some refer to this as the “great matrix exponential tragedy.” Moler and Loan (2003) give a summary of the various complex methods available for solving the matrix exponential problem and calculating the stability conditions.

When the coefficient matrix $\mathbf{A}(T(t))$ is periodic in time with period t_p , Floquet theory (Barone and Narcowich, 1977; Lamour et al., 1998) can be used to show that a unique solution to the initial value problem exists with period t_p . This solution has an associated fundamental matrix (also referred to as the monodromy matrix), which is unique and constant, and whose exponents can be used to determine the stability of the system. Thus, a model such as Eq. (3.1) can be understood numerically by computing the monodromy matrix (Wang and Hale,

2001). Floquet theory in application to periodically driven systems in biology is found in Malik and Smith (2008), and Charron et al. (2011), and in application to ecology in Hsu and Zhao (2012), and Klausmeier (2008). The use of Floquet theory is becoming increasingly popular in ecology.

Alternative approaches of analyses include computing piecewise growth rate parameters by assuming a periodically switching system (Gokcek, 2004), using analytic approximations (Butcher et al., 2009; Casas et al., 2001; Moler and Loan, 2003), and analysing time-averaged coefficients of the system-matrix (Ma Ma, 2006; see also Wesley and Allen, 2009). In essence, all these methods and solutions agree with Floquet theory, and are efforts to transform the non-autonomous system, that is, a system with a time-dependent matrix $\mathbf{A}(T(t))$, into an autonomous system, that is, a system with a constant matrix independent of time.

Although time-averaging and the other methods can be used to determine the stability of our system given by Eq. (3.1), they provide little information as to what temperature-dependent biological mechanisms drive stability. Besides, we wish to have a metric written in an explicit functional form to evaluate the cross-periodic intrinsic growth rate, or the cross-periodic fitness of the population, giving biological insights, so that, we can predict the degree of invasibility of habitats with fluctuating temperatures. Further, we wish to simplify the metric as a function of easily measurable quantities. Hence, the biologically meaningful metrics, we develop, will evaluate both the system stability and the invasibility potential. In our method, we allow $T(t)$ to vary with time, and focus on a case where $T(t)$ is piecewise constant; with low constant-temperature seasons followed by high constant-temperature seasons within a year, which is again followed by the low constant-temperature seasons, and so on.

$$R_0(T) = \frac{q\beta_s(T)}{\mu_s(T)} \prod_{i=1}^{s-1} \left(\frac{\gamma_i(T)}{\gamma_i(T) + \mu_i(T)} \right)^k. \quad (3.2)$$

(see Rajakaruna et al., 2012). The system Eq. (3.1) is unstable, or invisable to the species, if $R_0(T) > 1$ in Eq. (3.2) for the habitats at constant temperatures T . Alternatively, if $R_0(T) < 1$, then the system is stable, or the given habitat at constant temperature T is uninvasible by the species. Hence, the R_0 in Eq. (3.2) suffices to predict the persistence of copepods if the habitat temperatures remain uniform throughout the year without any seasonal or long-term fluctuations. When the temperature is in periodic fluctuation, then we need to take a further step and investigate the stability of the system by considering the matrix $\mathbf{A}(T(t))$, and incorporating coefficients that are periodic in time.

3.2.2. Explicit functional relationship between R_0 and intrinsic growth rate λ

As mentioned before, the system is *invasible* if the $\mathbf{n}=\mathbf{0}$ equilibrium solution is unstable, and *uninvasible* if the $\mathbf{n}=\mathbf{0}$ equilibrium solution is stable. Hence the ecological invasibility condition translates into a mathematical stability condition for the system in Eq. (3.1). Thus, an alternative approach to determine the invasibility of a habitat in a temporally constant environment for a species involves the spectral bound of $\mathbf{A}=\mathbf{F}-\mathbf{V}$. The *invasibility* occurs when the real part of any one of the eigenvalues of \mathbf{A} is positive, and *uninvasibility* occurs when all the eigenvalues of \mathbf{A} have real parts that are negative. Thus, by evaluating the sign of the largest real part of the eigenvalues of \mathbf{A} , one can simply determine the stability of the system: if positive, the system is *invasible*, and if negative, the system is *uninvasible*.

The dominant eigenvalue, which is the intrinsic growth rate in ecology, can be derived for the system Eq. (3.1) in constant temperatures by deriving a Lotka-Euler type equation solving the condition, $\det[(\mathbf{F}-\mathbf{V})-\mathbf{I}\lambda]=0$, where \mathbf{I} is the identity matrix, and λ are the eigenvalues of the matrix $\mathbf{F}-\mathbf{V}$. This can be done

in a variety of ways. One way is to transform $\mathbf{F-V}$ into a triangular matrix using Gaussian elimination method, and take the product of all the diagonal elements. It yields the following characteristic polynomial for λ

$$1 = \frac{q\beta_s}{(\mu_s + \lambda)} \prod_{i=1}^{s-1} \left(\frac{\gamma_i}{\gamma_i + \mu_i + \lambda} \right)^k. \quad (3.3)$$

Here, we have dropped the explicit dependence of parameters on T for notational simplicity.

However, the Eq. (3.3) cannot be solved analytically to give the general stability condition as it yields a polynomial of degree $l=(s-1)k+1$. Only numerical approximation methods can be used to solve it for λ . These, in turn, require the parameter values to be given. Hence, the dependence of λ on model parameters cannot be given explicitly, but requires methods such as numerical sensitivity analysis.

By way of contrast, $R_0(T) < 1$ in Eq. (3.2) also gives an explicit stability condition in a constant temperature environment, and the dependence of $R_0(T)$ on model parameters is clearly given in Eq. (3.2). Yet, the dynamics of populations in fluctuating temperature environments can be better understood with λ than with R_0 . Hence, we are motivated to first derive the relationship between R_0 and λ , and then employ this relationship to derive an explicit invasibility condition in terms of R_0 for fluctuating environments.

Because matrix \mathbf{A} has a Lefkovich form, we know that the spectral bound of \mathbf{A} is the dominant eigenvalue (that is the one with the largest spectral radius), and therefore, it is a real eigenvalue. This dominant eigenvalue is one of the l solutions to Eq. (3.3). However, this is the only one of our interest from an invasibility perspective. Thus, for notational simplicity, we use λ to denote the dominant eigenvalue, which is also the intrinsic growth rate in ecology.

Dividing Eq. (3.2) by Eq. (3.3) and some manipulations yield a non-linear relationship between the net reproductive rate R_0 and the dominant eigenvalue λ ,

as $R_0 = \left(\frac{\mu_s + \lambda}{\mu_s} \right) \prod_{i=1}^{s-1} \left(\frac{\gamma_i + \mu_i + \lambda}{\gamma_i + \mu_i} \right)^k$. Recalling that $\sigma_i = \gamma_i + \mu_i$ is the overall transition rate in sub-stages in stage i , and $\sigma_s = \mu_s$ is the transition rate in the last sub-stage k of the stage $i=s$, we simplify the above equation as $R_0 = (1 + g_s \lambda) \prod_{i=1}^{s-1} (1 + g_i \lambda)^k$. Here, $g_i = 1/\sigma_i$ is the mean sub-stage maturation time in stage i after the maturation and the mortality rates are combined together.

For *P. marinus* it is reasonable to assume that identical sub-stage maturation times based on near-isochronical development (as in Uye et al., 1983, and for many other copepods at food saturation condition as in Breteler et al. 1994), that is ($g_i=g$ for $i=1..s$). This gives, $R_0 = (1 + g\lambda)^l$, where, $l = k(s-1)+1$. If the sub-stage maturation times are similar but distinct, a perturbation analysis can be employed.

Choosing $g = \frac{1}{l} \left(g_s + k \sum_{i=1}^{s-1} g_i \right)$ to be the mean sub-stage maturation time, and $d_i = g_i - g$ to be the deviations from the mean, such that, $d_s + k \sum_{i=1}^{s-1} d_i = 0$, yields $R_0 = \left((1 + g\lambda) + d_s \lambda \right) \prod_{i=1}^{s-1} \left((1 + g\lambda) + d_i \lambda \right)^k$, and hence,

$$R_0 = (1 + g\lambda)^l \xi(d). \quad (3.4)$$

Here, $\xi(d)$ is the error correction term given by

$$\xi(d) = \left(1 + \frac{d_s \lambda}{(1 + g\lambda)} \right) \prod_{i=1}^{s-1} \left(1 + \frac{d_i \lambda}{(1 + g\lambda)} \right)^k.$$

Taking the log transformation and expanding by Taylor series yields

$$\log \xi(d) = \left(\frac{\lambda}{(1 + g\lambda)} \right) \left(d_s + k \sum_{i=1}^{s-1} d_i \right) + \theta(d_i d_j) \text{ for } 1 \leq i, j \leq s.$$

As $(d_s + k \sum_{i=1}^{s-1} d_i) = 0$, this gives $\xi(d) \approx 1$ to the leading order in d_i .

Using the approximation $\xi(d) \approx 1$, Eq. (3.4) can be written as

$$R_0 = (1 + g\lambda)^l. \quad (3.5)$$

Eq. (3.5) can be written as

$$\lambda = \frac{1}{g} \left(R_0^{\left(\frac{1}{l}\right)} - 1 \right). \quad (3.6)$$

This simple approximate relationship between the intrinsic growth rate λ and net reproductive rate R_0 is valid for constant habitat temperatures T with no fluctuations.

There are several other simplifications that can be made to Eq. (3.5). As k is equivalent to the shape parameter of the Gamma distributed stage maturation times, an exponentially distributed stage-maturation times gives $k=1$, and yields $R_0 = (1 + g\lambda)^s$. The same scenario for a non-staged system ($s=1$) gives $R_0 = (1 + g\lambda)$. Considering only the last sub-stage of the last stage is reproducing, derivation of the same beginning from the fundamental equations yields $R_0 = (1 + g\lambda)^{ks}$. Finally, a non-staged ($s=1$) with Gamma distributed stage maturation times gives $R_0 = (1 + g\lambda)^k$, which can be found also in Wallinga and Lipsitch (2007).

3.2.3. Approximate condition for persistence in habitats with periodically fluctuating temperatures

In this section, we derive an approximate condition for population persistence in habitats with periodically fluctuating temperatures. The first step is to assume a piecewise constant approximation for $\mathbf{A}(t)$ (in Eq. (3.1)) with respect to time. The next step is to assume that each time-interval (t_{j-1}, t_j) , for $j=1..m$, over

which $\mathbf{A}(t)$ is approximated by constant \mathbf{A}_j is sufficiently long so as to allow the population to achieve a stable stage distribution as characterized by the eigenfunction associated with the dominant eigenvalue of \mathbf{A}_j . The end result is an approximate formula for the growth rate of the population over a period (single year). If this quantity is positive, then the habitat will be invasible, and if negative, then the habitat will be uninvasible.

We denote the initial distribution in stages as $\mathbf{n}(t_0)$. Then we can write the population at the end of the year of period t_p as,

$$\mathbf{n}(t_p + t_0) = \mathbf{n}(t_m) = \left(\prod_{j=1}^m \exp((t_j - t_{j-1})\mathbf{A}_j) \right) \mathbf{n}(t_0), \quad (3.7)$$

where \exp denotes the matrix exponentiation. Here, $t_p = \sum_{j=1}^m (t_{ij} - t_{j-1}) = t_m - t_0$. The Lefkovitch matrix \mathbf{A} has a complete set of eigenvectors and a dominant eigenvalue with a corresponding eigenvector that has non-negative entries (Lefkovitch, 1965). If the t_j 's are spaced sufficiently apart, so that, many generations can be produced during the time period $(t_j - t_{j-1})$, then it is reasonable to assume that

$$\mathbf{n}(t_j) = \exp((t_j - t_{j-1})\mathbf{A}_j) \mathbf{n}(t_{j-1}) \approx (\mathbf{n}(t_{j-1}), \mathbf{v}_j) \exp(\lambda_j(t_j - t_{j-1})) \mathbf{v}_j,$$

where (\mathbf{a}, \mathbf{b}) denotes the dot product of vectors \mathbf{a} and \mathbf{b} , and $(\lambda_j, \mathbf{v}_j)$ is the dominant eigenpair of \mathbf{A}_j for $j=1..m$, and each eigenvector is normalized so that $(\mathbf{v}_j, \mathbf{v}_j)=1$. Applying this recursively from t_0 to t_m , yields

$$\mathbf{n}(t_m) = N_0 (\mathbf{v}_0, \mathbf{v}_1) \dots (\mathbf{v}_{m-1}, \mathbf{v}_m) \mathbf{v}_m \exp \sum_{j=1}^m \lambda_j (t_j - t_{j-1}) = N_m \mathbf{v}_m. \quad (3.8)$$

Here, \mathbf{v}_0 describes the initial composition of the populations, so that, $\mathbf{n}(t_0) = N_0 \mathbf{v}_0$, where $N_0 = \|\mathbf{n}(t_0)\|$. Here, $N_m = \|\mathbf{n}(t_m)\|$, and $\mathbf{n}(t_m) = N_m \mathbf{v}_m$. Taking the inner product of Eq. (3.8) with \mathbf{v}_m yields $N_m = N_0 (\mathbf{v}_0, \mathbf{v}_1) \dots (\mathbf{v}_{m-1}, \mathbf{v}_m) \exp \sum_{j=1}^m \lambda_j (t_j - t_{j-1})$, where $N_m = (\mathbf{n}(t_m), \mathbf{v}_m)$, and $N_0 = (\mathbf{n}(t_0), \mathbf{v}_0)$. Hence, we define the average growth rate over a period as

$$\begin{aligned}\Lambda_p &= \frac{1}{t_p} \log\left(\frac{N_m}{N_0}\right) = \frac{1}{t_p} \sum_{j=1}^m \lambda_j(t_j - t_{j-1}) + \frac{1}{t_p} \sum_{j=1}^m \log(\mathbf{v}_{j-1}, \mathbf{v}_j), \text{ or} \\ &= \bar{\lambda} + V,\end{aligned}\tag{3.9}$$

where $\bar{\lambda} = \frac{1}{t_p} \sum_{j=1}^m \lambda_j(t_j - t_{j-1})$ is the time-average of the piecewise intrinsic growth rates, and $V = \frac{1}{t_p} \sum_{j=1}^m \log(\mathbf{v}_{j-1}, \mathbf{v}_j) \leq 0$ is a measure of the time-averaged variation in the stage-structure throughout the year.

Therefore, in general, we can write an approximate condition for population persistence in a periodic system as $\Lambda_p > 0$. Note that Λ_p can be interpreted as the approximate *cross-periodic intrinsic growth rate* of the population, or a *cross-periodic fitness* parameter of the population in a periodically fluctuating environment, which replaces the intrinsic growth rate λ of the population in a constant environment.

We also note that piecewise growth rates geometrically averaged from $j=1$ to m over a period is given by

$$\Psi = e^{\Lambda_p},$$

where $\left(\frac{N_m}{N_0}\right) = \Psi^{t_p} = \left(\prod_{j=1}^m \psi_j^{(t_j - t_{j-1})}\right)$, and ψ_j is defined as $\psi_j = (\mathbf{v}_{j-1}, \mathbf{v}_j) e^{\lambda_j}$ for all $j=1..m$. Note that we can write the condition for population persistence also as $\Psi > 1$. The quantity Ψ can be interpreted as a *cross-periodic geometric growth rate* of the population in a periodically fluctuating environment.

If the eigenvectors \mathbf{v}_{j-1} and \mathbf{v}_j are identical, then the time-averaged variation in stage structure V equals zero in Eq. (3.9). However, $0 < (\mathbf{v}_{j-1}, \mathbf{v}_j) < 1$, in general, resulting V to be negative, thereby decreasing the cross-periodic intrinsic growth rate Λ_p . The case with $V=0$ gives an upper bound on Λ_p so that $\Lambda_p \leq \bar{\lambda}$.

3.2.4. The persistence condition as a function of net reproductive rate and generation times of populations in periodically fluctuating temperatures

In this section, we derive a metric R_p as a piecewise function of $R_0(T)$ and $g(T)$ to determine the persistence of a population introduced to a habitat in periodically fluctuating temperature as an alternative to Λ_p . We start by defining $R_{0,j}$ and g_j to be the net reproductive rate, and the mean sub-stage maturation time, respectively, for the time-interval (t_j, t_{j-1}) associated with matrix \mathbf{A}_j .

By substituting $R_{0,j}$ and g_j in Eq. (3.6), and then using Eq. (3.9) for discretized states j in piece-wise constant habitat temperatures T_j yields

$$\Lambda_p = \frac{1}{t_p} \sum_{j=1}^m \left(R_{0,j} \binom{1}{i} - 1 \right) \left(\frac{t_j - t_{j-1}}{g_j} \right) + V.$$

Let, $P_i = \frac{\left(\frac{t_j - t_{j-1}}{g_j} \right)}{\sum_{j=1}^m \left(\frac{t_j - t_{j-1}}{g_j} \right)}$ be the proportion of the number of generations within

the interval (t_j, t_{j-1}) at temperature T_j to the total number of generations G within

the period, that is, $G = \sum_{j=1}^m \left(\frac{t_j - t_{j-1}}{g_j} \right)$. This gives

$$\Lambda_p = \frac{G}{t_p} \left(\sum_{j=1}^m P_j R_{0,j} \binom{1}{i} - 1 \right) + V.$$

Here, note that t_p / G is the average generation time of the population within the period, which we denote by g_p . This yields

$$\Lambda_p = \frac{1}{g_p} \left(\sum_{j=1}^m P_j R_{0,j} \binom{1}{i} - 1 \right) + V. \quad (3.10)$$

Note that Eq. (3.6) is a special case of Eq. (3.10) for the case with constant temperature ($m=1$). Thus, we define a *weighted net reproductive rate*,

$$R_p = \left(\sum_{j=1}^m P_j R_{0,j} \left(\frac{1}{l} \right) + g_p V \right)^l,$$

such that,

$$\Lambda_p = \frac{1}{g_p} \left(R_p^{\frac{1}{l}} - 1 \right). \quad (3.11)$$

The persistence condition is now given by $R_p > 1$, following $\Lambda_p > 0$. Also, note that, R_0 , which is defined for a constant-temperature environment (Eq. (3.6)) is replaced by R_p , which is defined for a period in a fluctuating-temperature environment (Eq. (3.11)), while, g is replaced by g_p and similarly, λ is replaced by Λ_p . Hence, R_p can be interpreted as an approximate measure of *cross-periodic reproductive rate* of the population.

In general, there is no computational advantage of calculating R_p over evaluating Λ_p , because it still requires evaluating V by solving Eq. (3.1) for Λ_p . However, there is an advantage when $V = 0$, which, we found out, is the case for the Lefkovitch matrix suitable for *P. marinus*, where the transition states of the system between discretized states does not affect the final outcome of the system. This results in $\Lambda_p = \bar{\lambda}$ in Eq. (3.9), which we define as λ_p , the cross periodic intrinsic growth rate in the case of $V=0$. This yields

$$\lambda_p = \frac{1}{g_p} \left(R_p^{\frac{1}{l}} - 1 \right), \quad (3.12)$$

where, the persistence is given by the condition

$$R_p \approx \left(\sum_{j=1}^m P_j R_{0,j}^{\left(\frac{1}{T}\right)} \right)^l > 1. \quad (3.13)$$

This suggests that the weighted cumulative effect of $R_{0,j}^{\left(\frac{1}{T}\right)}$ of the discretized states becomes a good approximation to the final outcome of the system.

As R_0 and λ relationship (Eq. 3.6) is nested within R_p and λ_p relationship (Eq. 3.12), we would expect λ_p to be left skewed compared to R_p for fixed amplitudes of temperature. This is because $1/g_p$ is a positive exponential function of temperature similar to $1/g$ while R_p is generally a concave function of temperature similar to R_0 . The R_0 and the λ peak at different temperatures, former being always on the left of the latter. This has been observed in empirical data of many taxa by Huey and Berrigan (2001).

With minor modification to the form in Eq. (3.12), we write the persistence condition, for example, for a two state seasonal switching system

(m=2) as $R_p^{\frac{1}{l}} = P_1 R_{0,1}^{\left(\frac{1}{T}\right)} + P_2 R_{0,2}^{\left(\frac{1}{T}\right)} > 1$, where, $P_2 = 1 - P_1$. Supposing that the

season $j=1$ is favourable at mean temperature T_1 , that is $R_{0,1}^{\left(\frac{1}{T}\right)} > 1$, and season $j=2$ is

unfavourable at mean temperature T_2 , that is $R_{0,2}^{\left(\frac{1}{T}\right)} < 1$, then we write the condition

for persistence as $P_1 \left(R_{0,1}^{\left(\frac{1}{T}\right)} - 1 \right) + P_2 \left(R_{0,2}^{\left(\frac{1}{T}\right)} - 1 \right) > 0$, or alternatively,

$$\frac{\left(R_{0,1}^{\left(\frac{1}{T}\right)} - 1 \right)}{\left(1 - R_{0,2}^{\left(\frac{1}{T}\right)} \right)} > \frac{h_2}{h_1}, \quad (3.14)$$

where, h_j is the number of generations found in season j , that is $h_j = \left(\frac{t_j - t_{j-1}}{g_j} \right)$,

for $j=1,2$. Note that, $\left(R_{0,1}^{\left(\frac{1}{l}\right)} - 1 \right) > 0$, and $\left(1 - R_{0,2}^{\left(\frac{1}{l}\right)} \right) > 0$ by definition.

This suggests that for the persistence of a population in a two season period, the species must have either a large reproductive rate and/or many generations in the good season compared to the bad season. A proliferating reproduction strategy, with high fecundity and short generation times in high temperature seasons, falls in line with this theory. Such strategy is shown by copepod populations in temperate waters (Bollens et al., 2012; Yamahira and Conover, 2002). It is clear that populations take the maximum advantage of the good season of the year to sustain their populations as an evolutionary optimal strategy, where the number of generations is commonly lesser in low temperatures, some generations even leading to resting eggs and other resting stages. As the effect of temperature on the development is the key that determines the number of generations per period, the mechanistic representation of temperature's effect on the development is the key to obtaining accurate predictions on temperature-dependent fitness.

3.3. Methods

We obtained monthly averaged sea surface temperature (SST) data of marine habitats on the west coast of North America: West Vancouver –Strait of Georgia (1979-93), and Race Rocks from DFO Canada (1940-2011), Puget Sound, Fort Point -San Francisco Bay, Ocean Side -San Diego Bay, and Hawaii Island Hilo from NODC-NOAA (averaged over the years), and Todos Santos Bay, Baja California from Surf-Forecast (1984-2012).

We fitted periodic sinusoidal functions of time of the form, $T(t) = \bar{T} + \alpha \sin(\omega t + \varphi)$, which is commonly used by many for modeling yearly

temperature cycles in aquatic environments (e.g., Benyahya et al., 2007, Caissie et al., 1998), to monthly mean SST data of the above localities. Here, \bar{T} is the average habitat temperature of the period, α -amplitude, $\omega = 2\pi/t_p$, and φ - phase, for $t=1..(T_0/\text{time step})$, with period t_p (year). We used non-linear least squares regression (using the optimization scheme *fminsearch* in Matlab–MathWorks minimizing the mean squared error). We used the parameterized models of $T(t)$ to compute the matrices \mathbf{A}_j for time-interval $j=1..6$, considering $T(t)$ as piecewise constants.

The parameter values specific to models $\mu(T)$, $\beta(T)$ and $\gamma(T)$ used to compute \mathbf{A}_j from Rajakaruna et al. (2012) are given in Table 3-1. Note that the parameters κ are slightly different from that of Rajakaruna et al. (2012) as we incorporated all temperature-dependent mortality data from Uye et al. (1983) including those at 27°C . We used Matlab function `eig(Ai)` to compute $(\lambda_j, \mathbf{v}_j)$ in Eq. (3.9) for each time-interval $j=1..6$ in order to calculate λ_p and V , yielding Λ_p . We also used \mathbf{A}_i to compute $R_{0,j}$ (based on Eq. (3.2)) and g_j for each discretized time-interval $j=1..6$ in order to compute P_j , R_p and g_p in Eq. (3.12) and Eq. (3.13), thereby, to evaluate λ_p . Additionally, we used a periodic step-function, constructed from the algebraic summation of square-wave functions (built-in Matlab) based on Fourier series approximation, each with different phase-shifts and amplitudes, to model the SST data from the Race Rocks.

We tested the reliability of outcomes predicted by Λ_p and λ_p (for $V=0$), computed based on R_p and g_p , against the solutions given by the standard numerical methods by (i) computing the monodromy matrix for the system with Runge-Kutta 2 scheme by Wang and Hale (2001) (suggested by Bacaer (2007) specific to solving periodic epidemiological systems), (ii) assuming a piecewise-constant switching system in Gokcek (2004), and (iii) time-averaging matrix coefficients in Ma and Ma (2006) and Wesley and Allen (2009), and (iv) Λ_p

computed directly from $(\lambda_j, \mathbf{v}_j)$ of each \mathbf{A}_j and using Eq. (3.9). We further computed $\xi(d)$ in Eq. (3.4) to evaluate whether our approximation $\xi(d) \approx 1$ was reasonable.

We define CMT-F as the critical mean temperature-fluctuations (or the mean temperature at the stability threshold $\lambda_p = 0$ in the non-autonomous case of fluctuating temperatures). Similarly, we defined CMT-S as the critical mean of temperature-steady (or the temperature at the stability threshold $\lambda = 0$ in the autonomous case of steady temperatures). We used the cross-periodic growth rate λ_p , R_p (for $V=0$), CMT-S and CMT-F, to evaluate the invasibility of the coastal marine habitats of the North America for *P. marinus*.

We plotted λ_p and R_p on a spectrum of mean habitat temperatures and with different temperature-amplitudes. We showed the habitats that *P. marinus* has invaded and is native to, based on published literature, on the same graph. Furthermore, we mapped out λ_p with respect to mean and amplitude of annual temperature cycles of SST at $1^0 \times 1^0$ resolution of longitudes and latitudes on a global scale (data from NOAA-ESRL (n.d.)) indicating the geographic range potentially invasible to *P. marinus*, and also locating the native and the invaded habitats.

We demonstrated graphically the effect of temperature-amplitude on λ_p with a theoretical description based on Jensen's inequality (Jensen, 1906). Furthermore, we showed how the population growth progresses after an introduction of a single fertilized female to a habitat with a fluctuating temperature profile, parallel with piecewise leading eigenvalue of the system in transition. We also investigated how an increased fluctuation of periodic temperature, keeping the yearly maximum or minimum temperature the same, changes the potential invasibility of a habitat. Furthermore, we demonstrated the impact of long term change in profiles of annual temperature cycles impact the invasibility of habitats using a case study pertaining to Race Rocks, BC.

3.4. Results

For the range of mean SST values of the global habitats (-4°C to 35°C), the error correction term yields $\xi(d) \approx 1$, with the deviation from the true value being in the order of 10^{-4} . If $\xi(d) < 1$, then assuming $\xi(d) = 1$ will result in R_p being overestimated. This means that the persistence condition decisions made by R_p , if $\xi(d) < 1$, are overstated, but only slightly. This also means that the true potential of the population to grow across-periods (or the cross-periodic growth rate) is also overestimated slightly. However, in our case, assuming $\xi(d) \approx 1$ was reasonable. In other words, the assumption based for this; the isochronal stage maturation times (Uye et al., 1983), is a good approximation to the system of *P. marinus*. Many other copepods at food-saturation show similar development strategy (see Breteler et al., 1994),

Furthermore, we noted that $V = 0$ for the given Lefkovich matrix of *P. marinus* in all the profiles of the global SST fluctuations that we tested. Therefore, we used the condition $\lambda_p > 0$ from Eq. (3.12), calculated based on R_p from Eq. (3.13), and alternatively $R_p > 1$ (for $V = 0$) to evaluate the population persistence. The fact that $V = 0$, in our case, may be due to a property of the Lefkovich matrix or the range of the parameter values pertaining to *P. marinus*. Also, we noted that the dominant stage class was the reproducing adults at all times, so that, there was not any abrupt switching of $(\mathbf{v}_j, \mathbf{v}_{j-1})$ to 0 at any instance, which otherwise collapses the system violating the assumptions in the model derivation.

Supposing if $R_p < 1$ for a case wrongly assuming $V = 0$, still the true R_p remains less than 1 because $V \leq 0$ always. This means that the persistence conditions made by R_p without the term V are conservative when $V \neq 0$. This also means that the true potential for the population to grow across-periods (or the cross-periodic growth rate) is overestimated. Similarly, supposing if $R_p > 1$ for a case wrongly assuming $V = 0$, then there is a possibility that true R_p to be less than

1 because $V \leq 0$ always. Hence, $V=0$ is a conservative approximation from a perspective of invasive species management, because it may predict the invasibility of a habitat even if the true potential can be marginally less.

The cross periodic growth rate λ_p (simplified Eq. (3.12) for $V = 0$) for the system of *P. marinus* for temperature profiles given for North East Pacific coastal habitats (the west coast for North America) (Table 3-2) yielded close values (differences in the order of 10^{-2}) to those given by the monodromy matrix computation, the piecewise constant computation, and the matrix averaging methods.

Table 3-2 and Figure 3-2 indicate that the higher the amplitude, the higher the critical mean habitat temperature (CMT-F) on the colder water front (lower temperature bound at $R_p=1$), and the lower the CMT-F on the warmer water front (upper temperature bound at $R_p=1$). That is, with the incorporation of the effect of temperature fluctuations, the CMT-F moves to a higher temperature level relative to the CMT-S on the higher latitudinal border, whereas the CMT-F moves to a lower temperature level relative to the CMT-S on the lower latitudinal border. Thus, the invincible mean temperature range given by the non-autonomous solutions (CMT-F) incorporating periodic fluctuations is narrower than the invincible mean temperature ranges given by the autonomous solutions (CMT-S assuming steady temperatures). Table 3-2 further indicates that the model predictions on population persistence support the field evidence. Habitats in BC coast of Canada, in particular, are on the edge of invincible mean habitat temperatures to *P. marinus*, given the amplitudes.

Figure 3-2 indicates that increased amplitudes of temperature profiles decrease λ_p and R_p of *P. marinus*. Furthermore, Figure 3-2 and Figure 3-3 show that the direction of *P. marinus* spread on a global scale are pointed towards the low-amplitude temperature, low-stress novel habitats from high-amplitude temperature, high-stress native habitats.

The graphical demonstration in Figure 3-4 indicates the theoretical underpinning of the effect of temperature-amplitude on λ_p . The basis of depression that occurs due to increased amplitude is explained by Jensen's inequality (Jensen, 1906). That is, the concavity of the intrinsic growth rate $\lambda(T)$ with respect to mean habitat temperature T results in lowering of the cross-periodic fitness λ_p with an increase in the amplitude of the periodic temperature. This effect is universal if λ_p is a concave function of mean temperatures, which is true for the case of *P. marinus*. However, Amarasekara and Savage (2012) show that λ_p can also be a bell-shaped curve with respect to temperature for some ectothermic species. Under such scenarios, the amplitude can increase the cross-periodic growth rate of the species around the convex part of the curve depending on the convexity of λ_p and the amplitude of the temperature.

Furthermore, Figure 3-5 shows how the population size progresses with an introduction of a single fertilized female to a habitat with fluctuating temperature profiles. The piecewise leading eigenvalues $\lambda(T)$ fluctuate in synchrony with the fluctuation of temperature, taking positive and negative values, forcing the populations to fluctuate with an exponential average growth with an increasing amplitude. For linear models, there are no solutions exist with limit cycles. The final outcome; the population establishment or the extinction; depends on $R_p > 1$ ($\lambda_p > 0$), or $R_p < 1$ ($\lambda_p < 0$).

Figure 3-6 depicts the scenario showing how increased seasonal fluctuations of temperature, keeping the yearly maximum or minimum temperature the same, increase the potential for population persistence. This suggests that the lowest or the highest habitat temperatures alone cannot be used as reliable predictors of habitat invasibility if the temperature of the habitat fluctuates seasonally largely. This scenario is clearly different from the effect of increased temperature amplitudes, keeping the same mean habitat temperature, on R_p and λ_p .

Under the modeling section (3.2.4) we showed also that for persistence of a population in a two season period, the species must have either a large reproductive rate and/or many generations in the good season compared to the bad season. A proliferating reproduction strategy, with high fecundity and short generation times in high-temperature seasons, falls in line with this theory. The temperatures lethal for the organisms may crash the system unless the species produce resting stages under such harsh conditions, given that the condition changes to favourable from unfavourable seasonally.

Furthermore, Figure 3-7 indicates that at Race Rocks, the mean SST is on the rise over the years, shifting from the data averaged from years 1941-80, to that from 1981-2006 (boundaries were decided arbitrarily). Our results show that, with a rise in the mean temperature about another 1°C , the habitat will become, on average, invisable to *P. marinus* if the trend persists. Yet, it also shows, by the difference in CMT-S and CMT-F, that the amplitude of the periodic temperature fluctuations has suppressed the effect of the rise in the mean SST on the habitat invasibility. This is indicated by lower positioning of the CMT-S compared to CMT-F. A phase-shift, that was apparent during those years, has no effect on the R_p , as can be expected from the theoretical assumption behind the model derivation.

The system given for *P. marinus* is independent of initial-time, quantity, and frequency of species introductions. This was fundamental to the mathematical methods we used for model derivation.

3.5. Discussion

The habitat invasibility metric introduced in this chapter, Λ_p , and alternatively, R_p determine the persistence potential of marine invasive copepod *P. marinus* introduced to habitats in periodically fluctuating temperatures depending on whether $\Lambda_p > 0$, $R_p > 1$. The metric Λ_p (λ_p when $V=0$) can be

interpreted as an approximate cross-periodic intrinsic growth rate (a cross-periodic fitness parameter) of a population in periodically fluctuating habitat temperatures, and replaces the intrinsic growth rate λ defined for populations in constant-temperature environments. Similarly, the metric R_p redefines R_0 when an autonomous system (e.g., one with steady temperatures) turns into a non-autonomous system (e.g., one with periodically fluctuating temperatures). Therefore, R_p can be interpreted as a weighted net reproductive rate, which is a measure of the cross-periodic reproductive rate of a population.

Here, Λ_p and R_p were derived as functions of temperature-dependent net reproductive rate $R_0(T)$ and maturation times $g(T)$ at periodic piecewise constant temperatures T , based on the explicit functional relationship we derived between $R_0(T)$ and the intrinsic growth rate $\lambda(T)$ of the population, of which, Wallinga and Lipsitch (2007) relationship is a special case. The simplified versions of Λ_p (which is λ_p) and R_p that we derived assuming sum of the log dot products of the eigenvectors in transition matrices between discretized intervals are approximately zero (that is, $V=0$), are reliable indicators of the stability and the growth of the system for *P. marinus*. Quantifying R_p , and thereby λ_p , using $R_0(T)$ and $g(T)$ is a convenient approach compared to solving the full system using advanced numerical methods. This is also because, $R_0(T)$ and $g(T)$ can be calibrated easily using laboratory experiments, and also are readily available in the literature based on statistical (phenomenological) calibrations (for e.g., R_0 : Carriere and Boivin, 1997; Dannon et al., 2010; Dreyer and Baumgartner, 1996; Hou and Weng, 2010; Jandricic et al., 2010, Morgan et al., 2001; and, g : Huntley and Lopez, 1992). As marine copepods, in general, have life-history stages similar to *P. marinus*, the assumption based for simplification of these models may be generalized for marine copepods at large.

The persistence condition based on R_p can be interpreted in many other ways. In essence, R_p is a weighted net reproductive rate, which is a measure of cross-periodic reproductive rate of a population subject to a periodic forcing

cycle. Bacaer (2012) defined a net reproductive rate in a variable environment as the asymptotic ratio of the total births in two successive generations of the family tree. Ma and Ma (2006) and Wesley and Allen (2009), yet, showed that R_0 calculated based on the time-averaged population matrix over a period is sufficient to evaluate the cross-periodic persistence, which holds true in our case also. However, our metric R_p determines the system stability, and also the growth in a biologically meaningful way, capturing the system functionality and transitions at the level of sub-stages of a population by geometrically averaging the weighted $R_0(T)$'s at piecewise T 's over an entire period. Our metric simply suggests that the average number of female offspring at the end of a period, produced by generations of females of the family tree, starting from a single fertilized female at the beginning of the period, must to be greater than 1 for the persistence of a population.

The critical mean habitat temperature (CMT) at system stability thresholds, and also the cross-periodic growth rates λ_p for the given temperature profiles closely matched the solutions given by the complex computer intensive numerical schemes such as monodromy matrix computation (Bacaer, 2007; Wang and Hale, 2006.), piecewise continuous system solutions (Gokcek, 2004), and matrix averaging by Wesley and Allen (2009) that determine the system stability thresholds in periodic systems. These methods are in consistent with Floquet theory (Yakubovich and Starzhinskii, 1975). The advantage of using our approach is that it requires only simple calculations, and is expressed in biologically meaningful terms that give insights into the underlying processes governing the stability and also the growth of the system. The methodology proposed here can be used to model invasibility metric for ectothermic species in general by deriving λ_p , for e.g., for the generalized cases by Amarasekare and Savage (2012), or the case specific to *E. affinis* by Strasser et al. (2011).

The seas of Japan and China, where *P. marinus* is native to, the temperature fluctuates, on average, at amplitudes 12⁰C yearly compared to 2.5⁰C in the west coast of North America, 5⁰C in the North Sea and the Adriatic Seas

(NOAA-ESRL, n.d.), where *P. marinus* has recently established: Brylinski et al. (2012) have recently sampled *P. marinus* at Southern Bight of the North Sea along the coast of France, Olazabal and Tirelli (2011) at Adriatic Sea in northern Italy, and Sabia et al. (2012) at Lake Faro (Messina, Italy). Our results showed that the direction of spread of *P. marinus* was along an amplitude-gradient of SST from high to low-amplitude periodic temperature (APT) regions. The cross-periodic growth rate or the cross-periodic fitness of the species increases by many folds when they migrate from high to low-amplitude temperature habitats, thus causing a multi-fold increase in their invasiveness.

This leads to a question whether aquatic invasive species, in general, are a product of habitats, where the environmental forcing factors such as temperature, fluctuate periodically largely causing high-stress for the species. Does the adaptation of species to high-stressed environments invariably make them reproductively effective in low-stressed environments that result in an increased cross-periodic fitness?

Supporting this general proposition, evidence suggests that eight invasive copepod species native to the coast of Japan, where the temperature fluctuates periodically largely, have invaded the San Francisco Bay and the adjacent west coast of North America (Cordell et al., 2008), where the temperature fluctuates less, in addition to the pattern observed for *P. marinus*. These species include two of the same genus, namely, *P. inopinus* and *P. forbesi*. In contrast, there are no reports to date on the establishment of invasive copepods native to the west coast of North America in the Sea of Japan or adjacent seas. Later, *P. inopinus* has become the dominant species at Columbia River estuary (Cordell et al., 1992), whilst *P. forbesi* has replaced some of the natives (Bollens et al., 2012).

Furthermore, Ruiz et al. (2011) have shown that temperate West coast of North America, where the temperature fluctuates less, harbours a larger number of marine invasive and non-indigenous crustaceans than that on the East coast, where the temperature fluctuates largely. This observation is consistent with our proposition. DiBacco et al. (2011) have attributed a similar difference in marine

non-indigenous species between the East and the West coast of Canada to the apparent correlated difference in the propagule pressure by ship ballast-water discharge. However, the theory of differential propagule pressure falls short of explaining the observation as to why not many non-indigenous or invasive marine copepods (also marine species, in general) native to temperate southern hemisphere have spread into the northern hemisphere (see Doi et al., 2011; Gouletquer et al., 2002; Hanfling et al., 2011; IUCN, n.d.; Ruiz et al., 2011), while species immigrated to southern hemisphere from northern hemisphere is much (Ahyong and Wilens, 2011; Griffith et al., 2011; Olenin et al., 2011; Orensanz et al., 2002; Ruiz et al. 2011). Our proposition may explain these trends well as the periodic fluctuations of temperature are high in the northern hemisphere compared to the southern hemisphere, which decreases the fitness of the species moving from the southern to the northern hemisphere, especially to northern temperate ecoregions where the temperature amplitudes are extremely high.

Metabolic theory of ecology (MTE) suggests that species taxonomic richness should be large in environments with high annual mean temperatures resulting from the capacity of high temperatures to generate high metabolic rates, high entropy, leading to high rates of speciation (Allen et al., 2002; Gillooly and Allen, 2007). Recently, Rombouts et al. (2009) have shown that marine copepod diversity is correlated to mean habitat temperatures, an explanation for which has been theorized by Record et al. (2012) and Rombouts et al. (2011) based on the MTE. However, in some marine regions, peak-to-peak SST fluctuations exceed 28⁰C within a year. Thus, based on our result, we speculate that species' metabolic responses to periodic temperatures may also affect the species richness, and the MTE may require a revisiting, incorporating the effect of fluctuating temperatures on biodiversity generation. Some of our preliminary results show that copepod diversity data fits better, functionally, to habitat temperatures when the effect of fluctuating temperature is incorporated.

When populations, adapted to native habitats in extremely high-fluctuating temperatures, are introduced to novel habitats surrounding the same mean but low-amplitude temperatures, their across-periodic fitness increases by many folds compared to when they are in the native habitat. We speculate, as we observed in our preliminary analyses, that the higher the pointedness of $R_0(T)$ of a population, the greater is their potential to increase fitness in low fluctuating temperatures. This suggests that the degree of concavity of $R_0(T)$ may distinguish the degree of invasiveness of a species, and separate them from non-invasive colonizers. We need more theoretical and applied research to test this hypothesis in greater detail before a generalization.

This study and Rajakaruna et al. (2012) showed how life-history parameters in this model, that are functionally related to temperature, can be parameterized from the data from laboratory and field experiments, and predict potentially habitable range of a species limited by the year-round variable temperatures. This methodology can be extended to test the effect of salinity and other environmental forcing factors. Our approach is bottom-up and mechanistic in contrast to methods such as ecological niche modeling (ENM) methods (Elith and Leathwick, 2009; Peterson, 2003). Recent literature advocates mechanistic approaches to improve ENM as well (Kearney and Portor, 2009).

Some studies show that, time for acclimatization for copepods takes few hours to days. For example, Hansen et al. (2010) show that *Acartia tonsa* takes few hours to a week for acclimatization and to reach the maximum hatching success for the given temperature; faster acclimatization in higher temperatures. Huntley and Lopez (1992) suggest that generation time is a reasonable scale for oceanic surveys in changing ocean temperatures. In laboratory studies of copepods, acclimatization is commonly done for one generation before specific treatments (e.g., Devreker et al., 2007). In our study we used time-intervals as large as 60 days when incorporating the effect of the changes in temperature on population life-history parameters (Note that the average generation time is approximately 23 days, and the average stage maturation time is approximately 2

days at 20⁰C for *P. marinus*). To answer what is biologically optimal time-interval to follow the change in parameter values in response to change in temperature, and if the temperature-time curves are more complex than a simple sinusoidal form, we may need further laboratory experimentations. However, we did not encounter complex monthly average temperature-time curves in field samples.

In habitats on the edge of the suitable mean temperature range, large periodically fluctuating temperatures can limit the population persistence. This was shown by the relative shift of CMT-F from CMT-S. This result is consistent with the broad theory that increased environmental fluctuations increase the extinction probability of local populations in general (Lande et al., 2003). In other words, our results suggest that, on a given longitude, the range of habitats that are tolerable to a species tends to narrow down when the periodic fluctuation of temperatures are taken into account compared to that predicted by the mean habitat temperatures alone (as in Rajakaruna et al., 2012). This effect may be greater towards the thresholds of colder waters, as it is apparent from the data that temperature fluctuations are larger in the temperate marine ecoregions than the tropical and the subtropical marine ecoregions, in general.

Some studies suggest that the cessation of reproduction at lower temperatures is a critical driver of population growth rate, for example, in small fish (Raimondo, 2012). In copepods, dormancy occurs at various times of the year, prevailing in higher and temperate latitudes, when the temperature becomes harsh (Dahms, 1995). It is expressed as resting eggs and as arrested development, and is seen as an energy saving trait allowing the individual to bridge periods of environmental harshness. This suggests that the duration and the degree of adverse environmental condition, that dormancy depends upon, for example, the lower or the higher critical temperatures, may determine the species persistence. Partly contrastingly, and partly complementarily, our results show that the duration and the degree of the favourable temperatures that compensates the effect of the adverse temperatures determine the persistence of a copepod population, rather than the effect of the adverse temperature alone, if not lethal.

Furthermore, if the amplitudes of seasonal SST fluctuations increase along with the gradual sea surface warming (see Masson and Cummins, 2007) as was slightly evident from the Race Rocks data then we may expect increased temperature fluctuations to suppress the effect of increased mean habitat temperatures on range expansion of the species. Furthermore, the Race Rocks data show a phase-shift in annual cycles of SST over the years similar to that in land temperatures (see Stine et al., 2009). Yet the mathematical principles, that are based for the stability solutions in our study, do not allow a phase-shift to impact population stability. Studying the change in the whole temperature profile at a spatial scale that applies to species populations may be crucial when calibrating the effect of global warming on species range expansion or contraction. This is because the locality specific temperature profiles at different spatial scales may create differential effects on the population stability by counteracting the forcing by the general rise in the mean SST.

Our results also showed that in West Vancouver, higher fluctuations lowered the invasibility potential of the habitat for *P. marinus*. Evidently, *P. marinus* has not been detected in West Vancouver area, although it has been heavily sampled in ballast water discharge (Barry and Levings, 2002; Levings et al., 2004). In Puget Sound (Lawrence and Cordell, 2010) and Hawaii Islands (Carlton, 1985; Jones, 1966), *P. marinus* has been detected, yet our metric indicates that those localities are only marginally uninvasible.

The type of parameters and the method of analyses we introduced here may be useful for investigating the effect of other seasonal environmental (external forcing) factors that limit population establishment or extinction of populations. In future work, we could also incorporate density-dependence and the Allee effect that suppress populations at high and low extreme densities. Further investigations could also include the effect of variable salinity that may affect population fitness. The hypotheses generated from this work could also be tested on the spread of invasive freshwater copepods and other species across lake systems and rivers.

Table 3-1 The parameter values specific to models $\mu(T)$, $\beta(T)$ and $\gamma(T)$ used to compute $A(T(t))$ (from Rajakaruna et al., 2012). Temperature is measured in $^{\circ}\text{C}$.

Model	Parameter values
$\beta(T) = f_m f_l e^{w(T-b)} / [f_m + f_l (e^{w(T-b)} - 1)]$	$f_m = 13.89$, $f_l = 0.61$, $w = 0.35$, $b = 6.01^{\circ}\text{C}$
$\gamma_a(T) = k(T-1)^{1.8} / (\alpha_a - \alpha_{a-1})$	$k = 3$, α_a for each sub-stage within stages $a = 1..12$, where, $\alpha_0 = 0$ [55.01, 134.21, 325.81, 557.4, 864.01, 1110.77, 1479.68, 1827.22, 2159.64, 2159.64, 2656.81, 3353.02, 4321.76]
$g_a = k / \gamma_a(T)$	$k = 3$
$\mu(T) = \kappa_2 T^2 + \kappa_1 T + \kappa_0$	$\kappa_2 = 0.0017/\text{day}$, $\kappa_1 = -0.0426 / ^{\circ}\text{C day}$, $\kappa_0 = 0.32 / ^{\circ}\text{C}^2$

Table 3-2 Critical mean habitat temperatures (CMT-S and CMT-F) and λ_p (cross-periodic intrinsic growth rate) of *P. marinus* at localities where it is introduced at large densities through ship ballast-water discharge. (S-steady temperatures, F-fluctuating temperatures). CMT-S are the mean habitat temperatures (T) where $R_0(T)=1$, and similarly, CMT-F where $R_p = 1$. Thus, both CMT-S and CMT-F have Upper and Lower Bounds (UB, LB). If a mean habitat temperature is within LB and UB for the given degree of amplitude, then the habitat is potentially invasible. The (LB, UP) range of CMT-F is narrower than that of CMT-S.

	Lower critical temperature threshold CMT-S				Upper critical temperature threshold CMT-S		
	Race Rocks –the Strait of Georgia	West Vancouver	Puget Sound	Fort Point -San Francisco Bay	Ocean Side -San Diego Bay	Todos Santos Bay, Baja California	Hawaii Island Hilo
Temp							
Mean	9.24	10.92	10.56	13.40	16.62	24.25	22.92
Amplitude	1.77	5.24	2.81	1.79	2.99	3.75	1.04

Phase	0.61	0.82	0.48	0.36	0.57	0.36	0.34
CMT-S	10.52 (LB)	10.52 (LB)	10.52 (LB)	10.52 (LB)	24.81 (UB)	24.81 (UB)	24.81 (UB)
CMT-F	10.82 (LB)	12.22 (LB)	10.94 (LB)	10.84 (LB)	24.32 (UB)	24.16 (UB)	24.70 (UB)
λ_p	-0.021<0	-0.007<0	-0.004<0	0.046>0	0.071>0	0.056>0	0.047>0
Invasibility	No	No/Marginal	No/Marginal	Yes	Yes	Yes	Yes
Present Status	No information (propagules are discharged to the Strait of Georgia, BC)	Detected in propagules discharged (Barry and Levings, 2002; Levings et al., 2004)	Detected (Cohen, 2004); High propagule pressure (Lawrence and Cordell, 2010, et al., 2009)	Established (Ruiz et al., 2000)	Established (USGS, 2004)	Detected (Jiménez-Pérez and Castro-Longoria, 2006)	Detected (Carlton, 1985; Jones, 1966)

**CMT-F solutions are the same from all methods: 1) Monodromy matrix solution (Bacaer, 2007; Wang and Hale, 2001); 2) Piecewise solution (Goeck, 2004); 3) Matrix Averaging solution (Ma and Ma, 2006; Wesely and Allen, 2002); 4) Λ_p ($\xi(d) \neq 1$ and $V \neq 0$); 5) λ_p ($\xi(d) = 1$ and $V = 0$) (the basis of R_p); and λ_p solutions are the same to the rounded second decimal place from all methods.

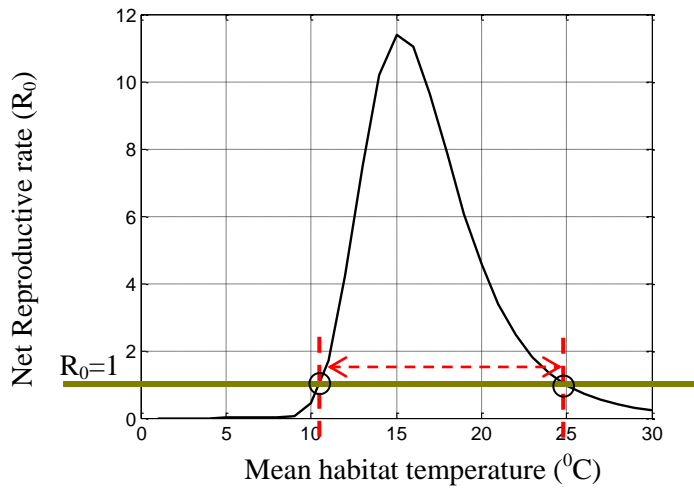


Figure 3-1 Net reproductive rate R_0 as a function of mean habitat temperature (T) considering autonomous (non-fluctuating) system dynamics (reconstructed following methods in Rajakaruna et al. (2012) after incorporating all the temperature-dependent mortality data from Uye et al. (1983), including the ones at 27°C).

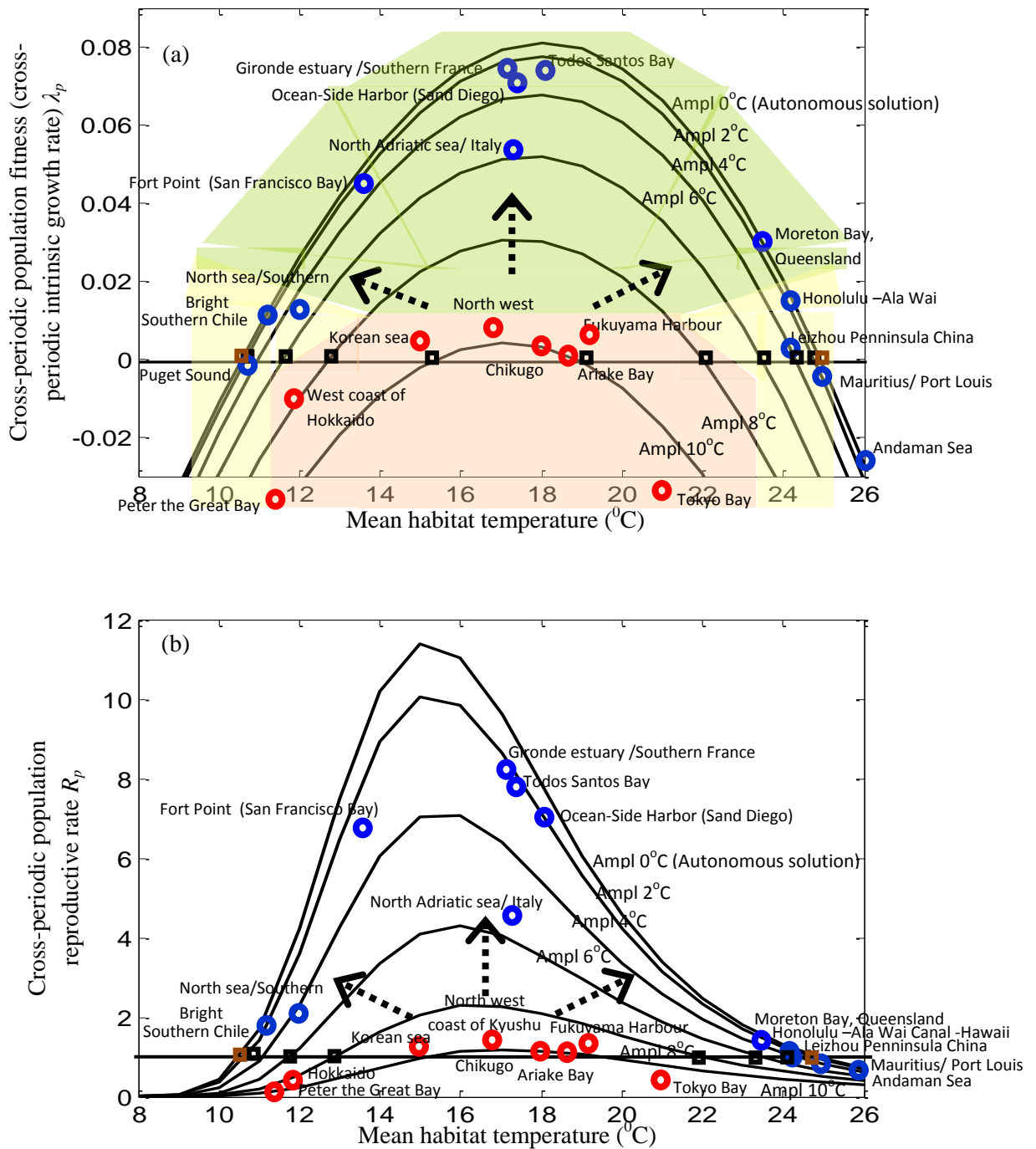


Figure 3-2 Cross-periodic fitness (λ_p) and reproductive rate (R_p) with respect to mean habitat temperatures with different amplitudes. An increase in the amplitude of the periodic temperature decreases λ_p and R_p , narrowing down the range of mean habitat temperatures that the species can persist (that is, the potentially invisable range bounded by the lower and the upper CMT-F). Amplitudes tending towards zero, converges the

solution asymptotically to the autonomous solution (the solution assuming steady year-round temperatures). Red circles are the native habitat range of *P. marinus* (Walter, 1986); the blue circles are the established or the detected habitat range (Brylinski et al., 2012) based on field samples. Black arrows show the direction of the invasion, which is from high to low-amplitude habitat temperatures. Note that λ_p is slightly left-skewed due to the multiplicative terms of R_0 and inverse exponential stage duration times with respect to temperature (Eq. 3.11). Thus, their peaks are shifted. The records of Andaman Island, Peter the Great Bay, and Tokyo Bay, which are deviated from the predicted range of the model, could be explained if we incorporated the standard errors of the R_p estimates. Light pink, green and yellow shades indicate native, invasive, and colonizing ranges from a conceptual standpoint. Here, habitats where $\lambda_p > 0$ and $R_p > 1$ are the potentially invisable range. Small black boxes: CMT-F. Small brown boxes: CMT-S.

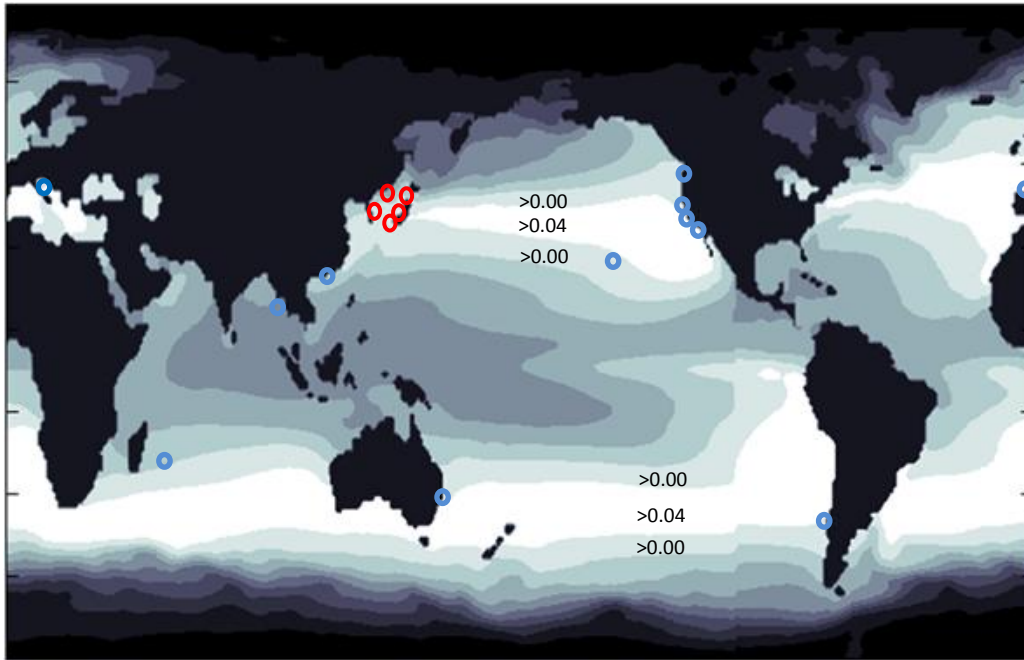


Figure 3-3 Invasible costal habitat range given by the cross-periodic intrinsic growth rate λ_p . Habitats within the white band are the ones where *P. marinus* has the highest λ_p (>0.04) given the periodic habitat temperatures. The adjacent lighter blue band is the next highest ($0 < \lambda_p < 0.04$). Red circles show where *P. marinus* is native to (Walter, 1986), and originally spreading from. Blue circles show the areas where *P. marinus* has established or detected. Data: SST data from NOAA-ESRL Physical Sciences Division, Data of localities from Rajakaruna et al., (2012). Latest reporting at Southern Bight of the North Sea along the coast of France (Brylinski et al., 2012), and the other at Adriatic Sea in northern Italy (Olazabal and Tirelli, 2011) are also marked. Longitudinal and latitudinal resolution: $1^0 \times 1^0$.

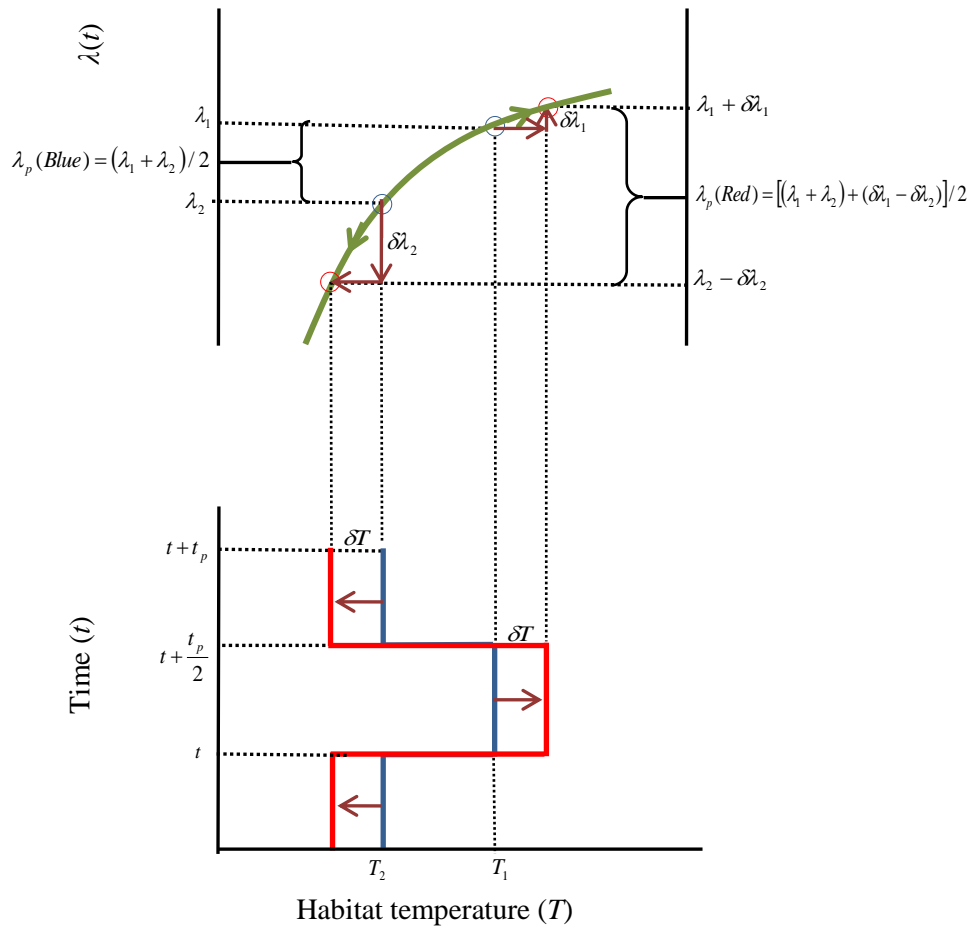


Figure 3-4 The effect of increased amplitude of temperature on cross-periodic fitness λ_p . Supposing a sinusoidal temperature curve can be approximated by a square wave (blue) with piecewise constant two seasonal temperatures T_1 and T_2 within time period t_p , and the amplitude of the wave is increased by δT (red) while having the same mean temperature. Green curve indicates $\lambda(T)$, the intrinsic population growth rate, with respect to habitat temperatures (T): λ_1 and λ_2 corresponds to temperature T_1 , T_2 , respectively. Arrows indicate the direction of the change of λ following the change of T after the amplitude of temperature is increased. As a result of the concavity in λ with respect to T (which follows from the function $R_0(T)$ from Figure 3-1 and Figure 3-2a), we show that the cross periodic growth λ_p decreases with increased amplitude of the

periodic temperature. The blue temperature profile gives $\lambda_p(\text{blue}) = \frac{1}{2}(\lambda_1 + \lambda_2)$. The higher amplitude red temperature profile gives

$$\lambda_p(\text{red}) = \frac{1}{2}(\lambda_1 + \delta\lambda_1 + \lambda_2 + -\delta\lambda_2) = \lambda_p(\text{blue}) + \frac{(\delta\lambda_1 - \delta\lambda_2)}{2} < \lambda_p(\text{blue}),$$

because $\delta\lambda_2 > \delta\lambda_1$. Thus, fluctuations give rise to lower values of λ_p . The higher the fluctuations, the lower the value of λ_p . That is, a population in high-amplitude temperatures becomes less likely to persist compared to that in low-amplitude temperatures, given that their mean temperatures are the same. This result remains the same for habitats surrounding the higher bounds of T , warmer waters, meaning that in general, high-amplitude temperatures decrease the persistence potential of a population. This is a result of Jensen's inequality. Note that these effects can be opposite in the ranges of temperature where λ can be a convex function of temperature. This can happen for some other species.

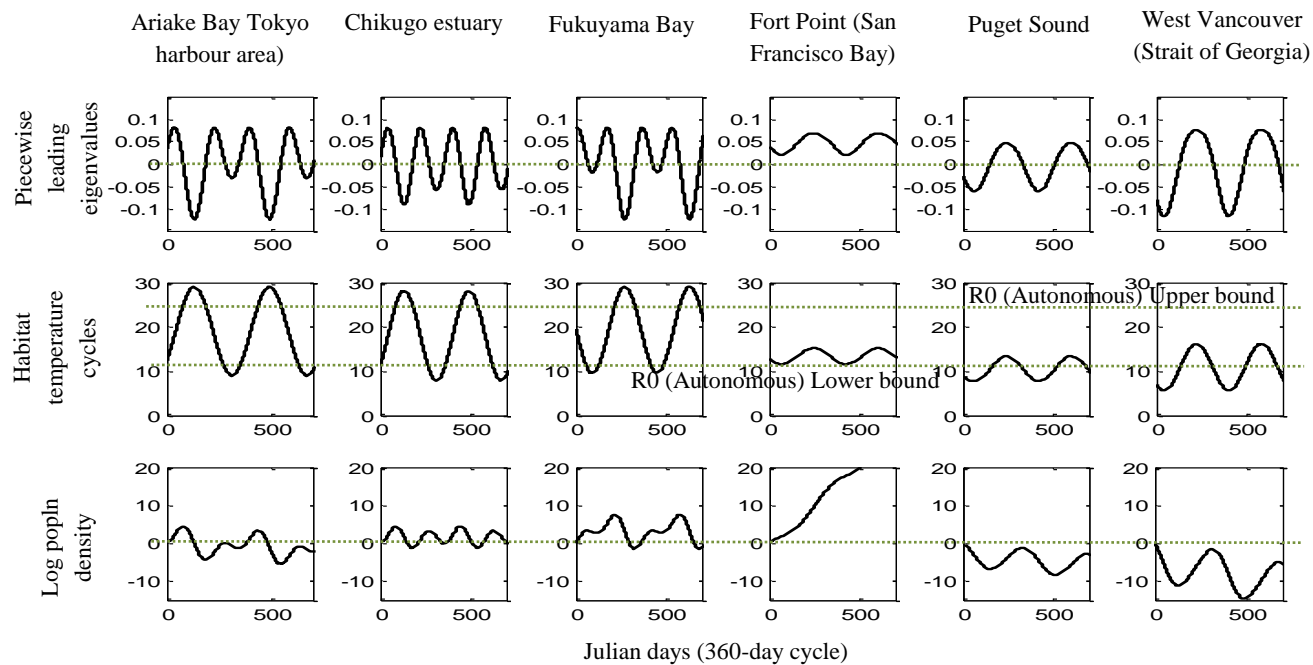


Figure 3-5 Piecewise temperatures, leading eigenvalues, and population density over time. This shows how a population progresses after an introduction of one fertilized female to a habitat with the given temperature profiles. Depending on temperature fluctuations, and the following leading eigenvalue cutting across the zero bounds becoming positive or negative, the population tends to increase or decrease accordingly. The population size has two peaks in some solutions, depending on how the profile of fluctuating temperature split the leading eigenvalue into two peaks. The *P. marinus* is native to Ariake, Chikugu, and Fukuyama Bays, and has invaded San Francisco Bay, and detected at Puget Sound, but not established, whereas, not detected in West Vancouver area as yet, although the propagule pressure of the species was large. Although we have not analyzed it in detail here, timing of these peaks seems to match the field observations, for which we may need an advanced model that can capture periodically stable systems. Temperature (mean, amplitude, phase): Ariake Bay (19, -10, 2.4); Chikugo estuary (18.0, -10.1, 2.4); Fukuyama (19.3, -9.7, -0.1); Fort Point (San.Fr. Bay) (13.4, -1.8; 0.4); West Vancouver (10.9, -5.2, 0.8); Puget Sound (10.6, -2.8, 0.5).

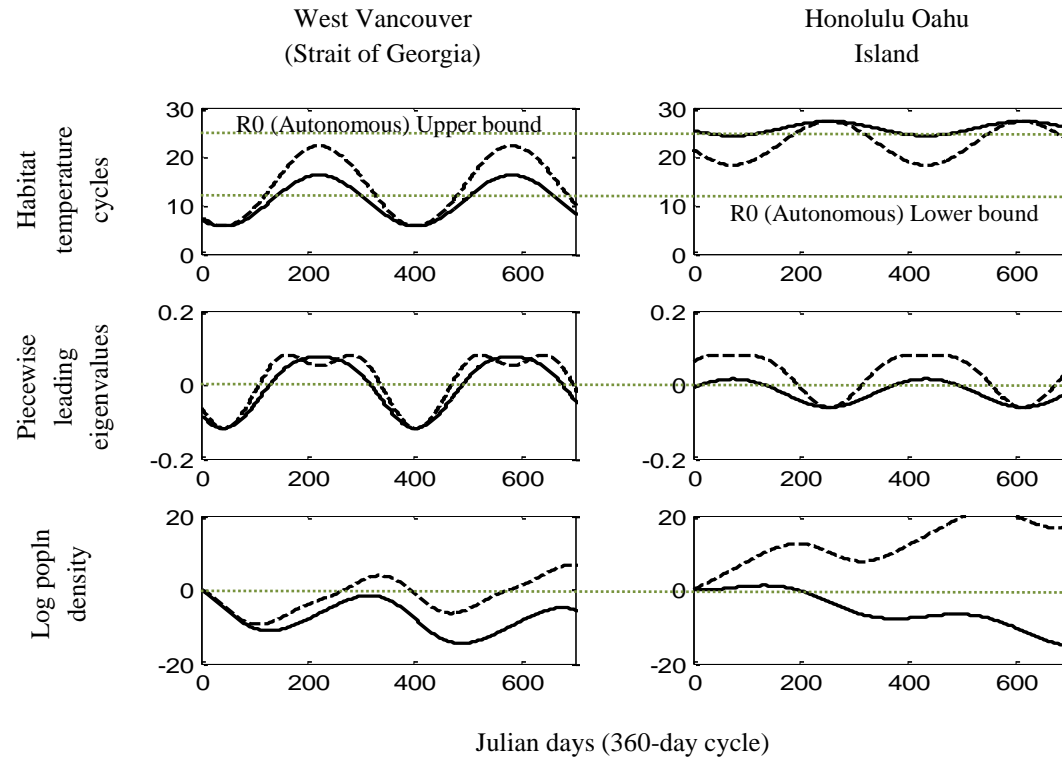


Figure 3-6 A demonstration of the effect of increased temperature amplitudes, keeping the maximum or minimum temperature the same, on the dynamics of *P. marinus* population introduced with one fertilized female, based on the temperature profiles of the two localities; one having high, and the other having low mean temperatures. The solid line indicates the true case, whereas, the dashed line indicates a simulated high-amplitude temperatures, keeping the minimum the same in the case of West Vancouver, and maximum the same in the case of Honolulu Oahu Island. With increased temperature amplitude, the populations tend to persist in both cases. Thus, this suggests that the minimum or the maximum temperature alone is not a reliable predictor of population persistence. The duration and the magnitude of habitat temperatures in favourable temperatures compensate the effect of harsh temperatures. Temperature (mean, amplitude, phase): West Vancouver [(10.9, -5.2, 0.8)~(13.9, -8.2, 0.8)] ; Honolulu Oahu Island [(25.7, 1.5, -2.8)~(22.7, 4.5, -2.8)].

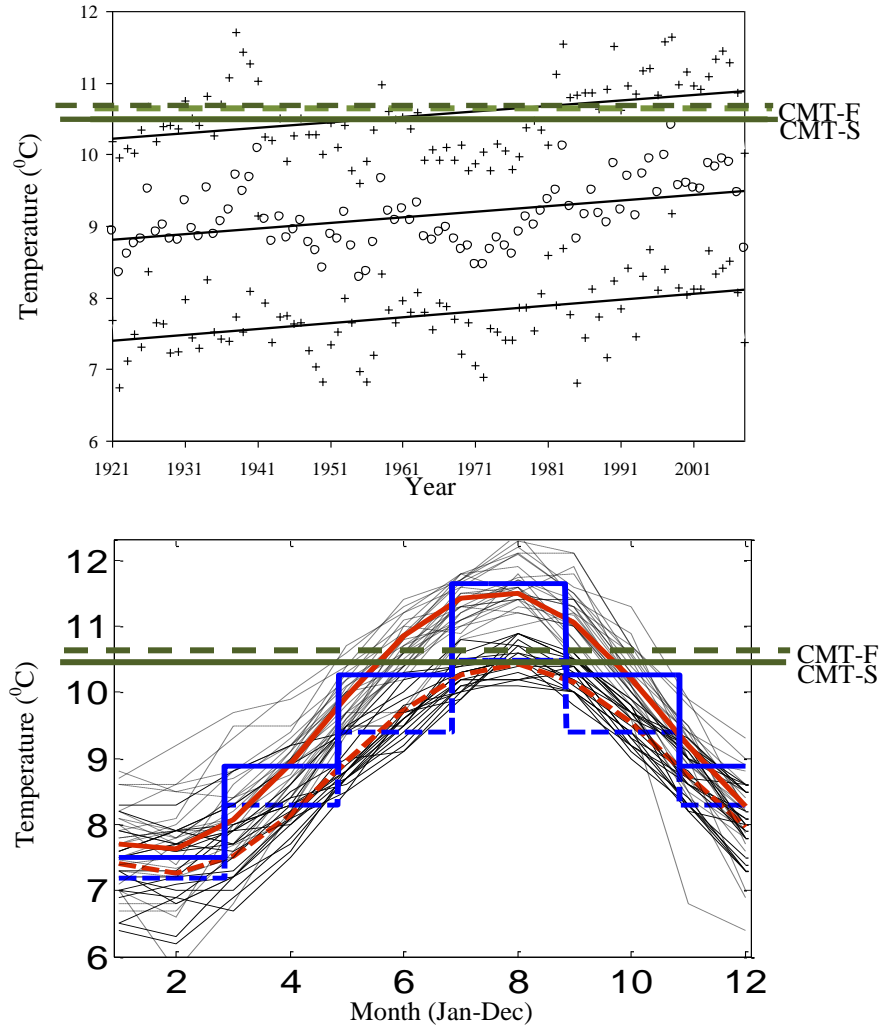


Figure 3-7a Yearly mean SST at Race Rocks, BC, indicating how mean temperature rise change the habitat invasibility. Black solid lines indicate the mean and the standard deviations of monthly variations. Mean temperatures tend towards the CMTs of *P. marinus* having the habitat pushed towards the potentially invisable threshold. **b)** Black lines show the monthly SST fluctuations at Race Rocks (solid: 1940:80, dashed: 1981:2006). Red lines indicate the best-fitted sinusoidal function (dashed-early period, solid-latter period) depicting a shift in the mean yearly temperatures over the two distinct periods. Blue lines indicate the best-fitted square wave functions for the same data. In addition to a mean shift, the graphs also indicate an increase in amplitude ($1.59 \rightarrow 1.97^{\circ}\text{C}$), and slight phase-shift towards the later years. The increase in temperature over the summer months is greater than that in the winter months of the year.

3.6. References

- Ahyong, S.T., Wilkens, S.L., 2011. Aliens in the Antipodes: Non-indigenous marine crustaceans of New Zealand and Australia. In *In the Wrong Place-Alien Marine Crustaceans: Distribution, Biology and Impacts* (p. 451-485). Springer Netherlands.
- Allen, A.P., Brown, J.H., Gillooly, J.F., 2002. Global biodiversity, biochemical kinetics, and the energetic-equivalence rule. *Science* 297(5586), 1545-1548.
- Almeda, R., Calbet, A., Alcaraz, M., Yebra, L., Saiz, E., 2010. Effects of temperature and food concentration on the survival, development and growth rates of naupliar stages of *Oithona davisae* (Copepoda, Cyclopoida). *Marine Ecology Progress Series* 410, 97-109.
- Amarasekare, P., Savage, V., 2012. A framework for elucidating the temperature dependence of fitness. *American Naturalist* 179(2), 178-191.
- Bacaër, N., 2007. Approximation of the basic reproduction number R_0 for vector-borne diseases with a periodic vector population. *Bulletin of Mathematical Biology* 69(3), 1067-1091.
- Bacaër, N., 2012. On the biological interpretation of a definition for the parameter R_0 in periodic population models. *Journal of Mathematical Biology* 65(4), 601-621.
- Barone, S.R., Narcowich, M.A., Narcowich, F.J., 1977. Floquet theory and applications. *Physical Review A* 15, 1109-1125.
- Barry, K.L., Levings, C.D., 2002. Feasibility of using the RAMAS-Metapopulation model to assess the risk of a non-idegenous copepod (*Pseudodiaptomus marinus*) establish in Vancouver Harbour from ballast water. *Canadian Technical Report of Fisheries and Aquatic Sciences* 2401(i-iv), 1-25.
- Benyahya, L., Caissie, D., St-Hilaire, A., Ouarda, T.B., Bobée, B., 2007. A review of statistical water temperature models. *Canadian Water Resources Journal* 32(3), 179-192.
- Bollens, S.M., Breckenridge, J. K., Cordell, J.R., Rollwagen-Bollens, G., Kalata, O., Claudi, R., Karatayev, A. 2012. Invasive copepods in the Lower Columbia River Estuary: Seasonal abundance, co-occurrence and potential competition with native copepods. In *Proceedings of the 17th International Conference on Aquatic Invasive Species*, San Diego, USA, September 2010. (7(1), 101-109). Regional Euro-Asian Biological Invasions Centre (REABIC).
- Boltovskoy, D., Almada, P., Correa, N. 2011. Biological invasions: assessment of threat from ballast-water discharge in Patagonian (Argentina) ports. *Environmental Science & Policy* 14(5), 578-583.
- Brylinski, J. M., Antajan, E., Raud, T., Vincent, D., 2012. First record of the Asian copepod *Pseudodiaptomus marinus* Sato, 1913 (Copepoda: Calanoida: Pseudodiaptomidae) in the southern bight of the North Sea along the coast of France. *Aquatic Invasions* 7(4), 577-584.

- Bunker, A.J., Hirst, A.G., 2004. Fecundity of marine planktonic copepods: global rates and patterns in relation to chlorophyll a, temperature and body weight. *Marine Ecology Progress Series* 279, 161-181.
- Butcher, E. A., Sari, M. E., Bueler, E., Carlson, T., 2009. Magnus' expansion for time-periodic systems: Parameter-dependent approximations. *Communications in Non-linear Science and Numerical Simulation* 14(12), 4226-4245.
- Byrnes, J.E., Reynolds, P.L., Stachowicz, J.J., 2007. Invasions and extinctions reshape coastal marine food webs. *PLoS One* 2(3), e295.
- Caissie, D., El-Jabi, N., St-Hilaire, A., 1998. Stochastic modelling of water temperatures in a small stream using air to water relations. *Canadian Journal of Civil Engineering* 25(2), 250-260.
- Carlton, J.T., 1985. Trans-Oceanic and Interoceanic Dispersal of Coastal Marine Organisms - the Biology of Ballast Water. *Oceanography and Marine Biology* 23, 313-371.
- Carrière, Y., Boivin, G., 1997. Evolution of thermal sensitivity of parasitization capacity in egg parasitoids. *Evolution* 51(6), 2028-2032.
- Casas, F., Oteo, J.A., Ros, J. 2001. Floquet theory: exponential perturbative treatment. *Journal of Physics A: Mathematical and General* 34(16), 3379.
- Charron, M.V., Seegers, H., Langlais, M., Ezanno, P., 2011. Seasonal spread and control of Bluetongue in cattle. *Journal of Theoretical Biology* 291, 1-9.
- Cohen, A.N., Olympia, W., 2004. An exotic species detection program for Puget Sound. Puget Sound Action Team. In: United States Geological Surveys, p. 52. Retrieved from: <http://nas.er.usgs.gov/queries/SpecimenViewer.aspx?SpecimenID=161281>.
- Cordell, J.R., Bollens, S.M., Draheim, R., Sytsma, M., 2008. Asian copepods on the move: recent invasions in the Columbia–Snake River system, USA. *ICES Journal of Marine Science* 65(5), 753-758.
- Cordell, J.R., Lawrence, D.J., Ferm, N.C., Tear, L.M., Smith, S.S., Herwig, R.P., 2009. Factors influencing densities of non-indigenous species in the ballast water of ships arriving at ports in Puget Sound, Washington, United States. *Aquatic Conservation: Marine and Freshwater Ecosystems* 19(3), 322-343.
- Cordell, J.R., Morgan, C.A., Simenstad, C.A., 1992. Occurrence of the Asian calanoid copepod *Pseudodiaptomus inopinus* in the zooplankton of the Columbia River estuary. *Journal of Crustacean Biology* 12(2), 260-269.
- Dahms, H.U., 1995. Dormancy in the Copepoda -an overview. *Hydrobiologia* 306(3), 199-211.
- Dannon, E.A., Tamò, M., van Huis, A., Dicke, M., 2010. Functional response and life history parameters of *Apanteles taragamae*, a larval parasitoid of *Maruca vitrata*. *BioControl* 55(3), 363-378.
- Devreker, D., Souissi, S., Forget-Leray, J., Leboulenger, F., 2007. Effects of salinity and temperature on the post-embryonic development of *Eurytemora affinis* (Copepoda;

Calanoida) from the Seine estuary: a laboratory study. *Journal of Plankton Research* 29 (1), 117-133.

Devreker, D., Souissi, S., Winkler, G., Forget-Leray, J., Le Boulenger, F., 2009. Effects of salinity, temperature and individual variability on the reproduction of *Eurytemora affinis* (Copepoda; Calanoida) from the Seine estuary: A laboratory study. *Journal of Experimental Marine Biology and Ecology* 368(2), 113-123.

DFO., n.d. BC Lighthouse website. Retrieved from: <http://www.pac.dfo-mpo.gc.ca/science/oceans/data-donnees/lighthouses-phares/index-eng.htm>.

DiBacco, C., Humphrey, D.B., Nasmith, L.E., Levings, C.D., 2012. Ballast water transport of non-indigenous zooplankton to Canadian ports. *ICES Journal of Marine Science: Journal du Conseil* 69(3), 483-491.

Doi, W., Watanabe, S., Carlton, J.T., 2011. Alien marine crustaceans of Japan: a preliminary assessment. In *In the Wrong Place-Alien Marine Crustaceans: Distribution, Biology and Impacts* (p. 419-449). Springer Netherlands.

Dreyer, H., Baumgärtner, J., 1996. Temperature influence on cohort parameters and demographic characteristics of the two cowpea coreids *Clavigralla tomentosicollis* and *C. shadabi*. *Entomologia Experimentalis et Applicata* 78(2), 201-213.

Elith, J., Leathwick, J. R., 2009. Species distribution models: ecological explanation and prediction across space and time. *Annual Review of Ecology, Evolution, and Systematics* 40, 677-697.

Fleminger, A., Kramer, S.H., 1988. Recent introduction of an Asian estuarine copepod, *Pseudodiaptomus marinus* (Copepoda: Calanoida), into southern California embayments. *Marine Biology* 98(4), 535-541.

Fowler, A.E., Gerner, N.V., Sewell, M.A., 2011. Temperature and salinity tolerances of Stage 1 zoeae predict possible range expansion of an introduced portunid crab, *Charybdis japonica*, in New Zealand. *Biological Invasions* 13(3), 691-699.

Gillooly, J.F., Allen, A.P., 2007. Linking global patterns in biodiversity to evolutionary dynamics using metabolic theory. *Ecology* 88(8), 1890-1894.

Gökçek, C., 2004. Stability analysis of periodically switched linear systems using Floquet theory. *Mathematical Problems in Engineering* 2004(1), 1-10.

Gouletquer, P., Bachelet, G., Sauriau, P. G., Noel, P., 2002. Open Atlantic coast of Europe—a century of introduced species into French waters. *Invasive aquatic species of Europe, distribution, impacts and management* (p. 276-290). Kluwer, Dordrecht.

Griffiths, C., Robinson, T., Mead, A., 2011. The alien and cryptogenic marine crustaceans of South Africa. In *In the Wrong Place-Alien Marine Crustaceans: Distribution, Biology and Impacts* (p. 269-282). Springer Netherlands .

Hänfling, B., Edwards, F., Gherardi, F., 2011. Invasive alien Crustacea: dispersal, establishment, impact and control. *BioControl* 56(4), 573-595.

- Hansen, B.W., Drillet, G., Madsen, K.V., Pedersen, M.F., Sørensen, T.F., 2010. Temperature effects on copepod egg hatching: does acclimatization matter? *Journal of Plankton Research* 32(3), 305-315.
- Hirst, A.G., Kiørboe, T., 2002. Mortality of marine planktonic copepods: global rates and patterns. *Marine Ecology-Progress Series* 230, 195-209.
- Hou, Y., Weng, Z., 2010. Temperature-dependent development and life table parameters of *Octodonta nipae* (Coleoptera: Chrysomelidae). *Environmental Entomology* 39(5), 1676-1684.
- Hsu, S.B., Zhao, X.Q., 2012. A Lotka–Volterra competition model with seasonal succession. *Journal of Mathematical Biology* 64(1-2), 109-130.
- Huntley, M. E., Lopez, M.D., 1992. Temperature-dependent production of marine copepods: a global synthesis. *American Naturalist* 201-242.
- IUCN., n.d. Retrieved from: <http://www.issg.org/database/species/search.asp?s t=100ss>.
- Jandricic, S.E., Wraight, S.P., Bennett, K.C., Sanderson, J.P., 2010. Developmental times and life table statistics of *Aulacorthum solani* (Hemiptera: Aphididae) at six constant temperatures, with recommendations on the application of temperature-dependent development models. *Environmental Entomology* 39(5), 1631-1642.
- Jensen, J.L.W.V., 1906. Sur les fonctions convexes et les inégalités entre les valeurs moyennes. *Acta Mathematica* 30(1), 175–193.
- Jiménez-Pérez, L. C., Castro-Longoria, E., 2006. Range extension and establishment of a breeding population of the Asiatic copepod, *Pseudodiaptomus marinus* Sato, 1913 (Calanoida, Pseudodiaptomidae) in Todos Santos Bay, Baja California, Mexico. *Crustaceana* 79(2), 227-234.
- Jones, E.C., 1966. A New Record of *Pseudodiatomus marinus* Sato (Copepoda, Calanoida) from Brackish Waters of Hawaii. *Crustaceana* 10(3), 316-317.
- Kearney, M., Porter, W., 2009. Mechanistic niche modelling: combining physiological and spatial data to predict species' ranges. *Ecology Letters* 12(4), 334-350.
- Kiørboe, T., 2008. A mechanistic approach to plankton ecology. Princeton University Press, NJ, p. 208.
- Klausmeier, C.A., 2008. Floquet theory: a useful tool for understanding non-equilibrium dynamics. *Theoretical Ecology* 1(3), 153-161.
- Lamour, R., März, R., Winkler, R., 1998. How Floquet theory applies to index 1 differential algebraic equations. *Journal of Mathematical Analysis and Applications* 217(2), 372-394.
- Lawrence, D.J., Cordell, J. R., 2010. Relative contributions of domestic and foreign sourced ballast water to propagule pressure in Puget Sound, Washington, USA. *Biological Conservation* 143(3), 700-709.

- Lee, H.W., Ban, S., Ikeda, T., Matsuishi, T., 2003. Effect of temperature on development, growth and reproduction in the marine copepod *Pseudocalanus newmani* at satiating food condition. *Journal of Plankton Research* 25(3), 261-271.
- Lefkovich, L.P., 1965. The study of population growth in organisms grouped by stages. *Biometrics* 1-18.
- Levings, C.D., Cordell, J.R., Ong, S., Piercey, G.E., 2004. The origin and identity of invertebrate organisms being transported to Canada's Pacific coast by ballast water. *Canadian Journal of Fisheries and Aquatic Sciences* 61(1), 1-11.
- Liang, D., Uye, S., 1997a. Population dynamics and production of the planktonic copepods in a eutrophic inlet of the Inland Sea of Japan. IV. *Pseudodiaptomus marinus*, the egg-carrying calanoid. *Marine Biology* 128(3), 415-421.
- Liang, D., Uye, S., 1997b. Seasonal reproductive biology of the egg-carrying calanoid copepod *Pseudodiaptomus marinus* in a eutrophic inlet of the Inland Sea of Japan. *Marine Biology* 128(3), 409-414.
- Ma, J., Ma, Z., 2006. Epidemic threshold conditions for seasonally forced seir models. *Mathematical Biosciences and Engineering* 3(1), 161-172.
- Malik, T., Smith, H.L., 2008. Does dormancy increase fitness of bacterial populations in time-varying environments? *Bulletin of Mathematical Biology* 70(4), 1140-1162.
- Masson, D., Cummins, P.F., 2007. Temperature trends and interannual variability in the Strait of Georgia, British Columbia. *Continental Shelf Research* 27(5), 634-649.
- MathWorks., n.d. Retrieved from <http://www.mathworks.in/help/matlab/ref/fminsearch.html>.
- Moler, C., Van Loan, C., 2003. Nineteen dubious ways to compute the exponential of a matrix, twenty-five years later. *SIAM Review* 45(1), 3-49.
- Molnar, J.L., Gamboa, R.L., Revenga, C., Spalding, M.D., 2008. Assessing the global threat of invasive species to marine biodiversity. *Frontiers in Ecology and the Environment* 6(9), 485-492.
- Morgan, D., Walters, K.F.A., Aegerter, J.N., 2001. Effect of temperature and cultivar on pea aphid, *Acyrtosiphon pisum* (Hemiptera: Aphididae) life history. *Bulletin of Entomological Research* 91(1), 47-52.
- NOAA-ESRL., n.d. Physical Sciences Division, Boulder Colorado, USA. Retrieved from <http://www.esrl.noaa.gov/psd/data/gridded/data.noaa.oisst.v2.html>.
- NODC-NOAA., n.d. Retrived from: website (<http://www.nodc.noaa.gov/dsdt/cwtg/index.html>).
- Olazabal, A., Tirelli, V., 2011. First record of the egg-carrying calanoid copepod *Pseudodiaptomus marinus* in the Adriatic Sea. *Marine Biodiversity Records* 4(1), e85.
- Olenin, S., Elliott, M., Bysveen, I., Culverhouse, P.F., Daunys, D., Dubelaar, G.B.J., Gollasch, S., Gouletquer, P., Jelmert, A., Kantor, Y., Mezeth, K.B., Minchin, D., Occhipinti-Ambrogi, A., Olenina, I., Vandekerckhove, J., 2011. Recommendations on

methods for the detection and control of biological pollution in marine coastal waters. *Marine Pollution Bulletin* 62 (12), 2598–2604.

Orensanz, J.M.L., Schwindt, E., Pastorino, G., Bortolus, A., Casas, G., Darrigran, G., ... Vallarino, E.A., 2002. No longer the pristine confines of the world ocean: a survey of exotic marine species in the southwestern Atlantic. *Biological Invasions* 4(1-2), 115-143.

Peterson, A.T., 2003. Predicting the geography of species' invasions via ecological niche modeling. *The Quarterly Review of Biology* 78(4), 419-433.

Pineda, M.C., Turon, X., López-Legentil, S., 2012. Stress levels over time in the introduced ascidian *Styela plicata*: the effects of temperature and salinity variations on hsp70 gene expression. *Cell Stress and Chaperones* 17(4), 435-444.

Raimondo, S., 2012. Incorporating temperature-driven seasonal variation in survival, growth, and reproduction into population models for small fish. *Marine Ecology Progress Series* 469, 101-112.

Rajakaruna, H., Strasser, C., Lewis, M., 2012. Identifying non-invasible habitats for marine copepods using temperature-dependent R0. *Biological Invasions* 14(3), 633-647.

Record, N.R., Pershing, A.J., Maps, F., 2012. First principles of copepod development help explain global marine diversity patterns. *Oecologia* 170(2), 289-295.

Rombouts, I., Beaugrand, G., Ibañez, F., Gasparini, S., Chiba, S., Legendre, L., 2009. Global latitudinal variations in marine copepod diversity and environmental factors. *Proceedings of the Royal Society B: Biological Sciences* 276(1670), 3053-3062.

Rombouts, I., Beaugrand, G., Ibanez, F., Gasparini, S., Chiba, S., Legendre, L., 2010. A multi-variate approach to large-scale variation in marine planktonic copepod diversity and its environmental correlates. *Limnology and Oceanography* 55(5), 2219–2229.

Ruiz, G., Fofonoff, P., Steves, B., Dahlstrom, A., 2011. Marine crustacean invasions in North America: A synthesis of historical records and documented impacts. In *In the Wrong Place-Alien Marine Crustaceans: Distribution, Biology and Impacts* (p. 215-250). Springer Netherlands.

Sabia, L., Uttieri, M., Pansera, M., Souissi, S., Schmitt, F.G., 2012. First observations on the swimming behaviour of *Pseudodiaptomus marinus* from lake Faro. *Biol. Mar. Mediterr* 19(1), 240-241.

Stine, A.R., Huybers, P., Fung, I. Y., 2009. Changes in the phase of the annual cycle of surface temperature. *Nature* 457(7228), 435-440.

Strasser, C.A., Lewis, M.A., DiBacco, C., 2011. A mechanistic model for understanding invasions: using the environment as a predictor of population success. *Diversity and Distributions* 17(6), 1210-1224.

Surf-Forecast., n.d. Retrieved from: http://www.surf-forecast.com/breaks/Palm-Beach_Todos-Santos/seatemp.

USGS., n.d. Retrieved from: <http://nas.er.usgs.gov/queries/SpecimenViewer.aspx?SpecimenID=161281>.

Uye, S., Iwai, Y., Kasahara, S., 1983. Growth and production of the inshore marine copepod *Pseudodiaptomus marinus* in the central part of the Inland Sea of Japan. *Marine Biology* 73(1), 91-98.

Wallinga, J., Lipsitch, M., 2007. How generation intervals shape the relationship between growth rates and reproductive numbers. *Proceedings of the Royal Society B* 274(1609), 599-604.

Wang, X., Hale, J.K., 2001. On monodromy matrix computation. *Computer Methods in Applied Mechanics and Engineering* 190(18), 2263-2275.

Wesley, C.L., Allen, L.J. 2009. The basic reproduction number in epidemic models with periodic demographics. *Journal of Biological Dynamics* 3(2-3), 116-129.

Yakubovich, V.A., Starzhinskiĭ, V.M., 1975. *Linear differential equations with periodic coefficients*. Wiley (New York), p.70-151.

Yamahira, K., Conover, D.O., 2002. Intra-vs. interspecific latitudinal variation in growth: adaptation to temperature or seasonality? *Ecology* 83(5), 1252-1262.

CHAPTER 4

High-amplitude periodic temperatures cause a reduction in species taxonomic richness

4.1. Introduction

The species richness gradient along the latitudes in land (Hawkins et al., 2007), marine (Rombouts et al., 2011), and freshwater (Oberdorff et al., 1995) taxa has been explained by the metabolic theory of ecology (MTE) proposed by Allen et al. (2002). This theory is based on the biochemical kinetics and the energetic-equivalence rule (Damuth, 1987), which is now well-established in the literature. One implicit assumption in MTE by Allen et al. (2002) is that habitat temperatures do not vary largely through seasons within a year. However, the optimum interpolation (OI) sea surface temperature (SST) data at resolution $1^{\circ} \times 1^{\circ}$ of latitudes and longitudes from NOAA-ESRL (n.d.) show that ocean temperatures fluctuate periodically largely, amplitudes exceeding 14°C at some northern temperate *marine ecoregions* (NTE). (*Marine ecoregions* are a biogeographic classification of coastal regions based on similarities in biota, geomorphological features, currents, and temperature, which covers all coastal and shelf waters shallower than 200 m (Spalding et al., 2007).)

If ambient temperature fluctuates periodically at this scale of magnitudes, it should affect the metabolism of populations, and thus, the assumption of constant temperature in MTE is violated. As the metabolic rate of organisms has non-linear dependencies on temperature, the computations based on yearly averaged temperatures may not be a reasonable representation of the bio-energetic mechanics of a periodic system. Thus, the question is whether the amplitude of temperature subsequently impacts the richness of species of taxa exposed to periodically fluctuating temperatures.

In this study, we extend the MTE by incorporating the effect of annual variation in temperature into the model, deriving the functional relationships in

biologically meaningful terms, and investigating the impact of amplitude of temperature on species richness. Based on our model, we test the hypothesis that high-amplitude periodic temperatures cause a reduction in species richness of ectothermic marine taxa; calanoid copepods, copepods, and tunicates. We sample diversity of species pertaining to marine ecoregions of the world (MEOW) digitally from the mega-database Ocean Bio-geographic Information Systems (OBIS, n.d.). The NTE provides a solid testing ground for our hypothesis as the amplitude of temperatures varies across this region dramatically, while their mean temperatures are confined to a narrow range. We further use our model, calibrated from the data of the NTE, to predict the copepod richness across the Atlantic Ocean by latitudes and also by mean habitat temperatures using the data reconstructed from Rombouts et al. (2009).

Our results show that high-amplitude periodic temperatures play a major role in the reduction of marine species (taxonomic) richness depending on the level of exposure of these taxa to periodically fluctuating temperatures. When the mean temperatures between ecoregions do not differ significantly, the ratio of their temperature-amplitudes, if large, determines the ratio of their species richness. For this reason, the temperature-amplitude may differentiate the species richness along the longitudes where the latitudes have the same mean temperatures. Furthermore, our extended MTE model explains the subtle variations in marine copepod diversity between the northern and the southern hemispheres.

4.2. Model

Consider an area A with species S , and population density N_j of species j per unit area, $j=1..S$. The total number of individuals across all species is $J = \sum_{j=1}^S N_j A$. Based on Allen et al. (2002), the metabolic rate B_j (Jules s^{-1}) of an average individual of species j varies with body-size M_j , and the ambient

temperature T , such that $B_j = b_0 M_j^{3/4} e^{-E/k_b(T+273.2)}$. Here, b_0 is a normalization constant independent of body size and temperature ($b_0 \sim 2.65 \times 10^{10} \text{ W g}^{-3/4}$), and the Boltzmann factor $e^{-E/k_b(T+273.2)}$ describes the temperature dependence of the metabolic rate. The quantity E is the activation energy of metabolism ($\sim 0.78 \text{ eV}$) (Allen et al., 2002), k_b is the Boltzmann constant ($8.62 \times 10^{-5} \text{ eV K}^{-1}$), and $(T + 273.2)$ is Kelvin (T –centigrade), such that, the average metabolic rate of an average individual in the community is given by

$$\bar{B} = b_0 \bar{M}^{3/4} e^{-E/k_b(T+273.2)}, \quad (4.1)$$

where \bar{M} is the average body size of an individual. Note that Eq. (4.1) is a convex increasing function of T . Based on the energetic-equivalence rule (Damuth, 1987), Allen et al. (2002) write the average energy flux of a population in the community as

$$\bar{B}_T = \bar{B} \bar{N}. \quad (4.2)$$

Here, \bar{B}_T is considered as a temperature-independent constant, and $\bar{N} = \frac{1}{S} \sum_{j=1}^S N_j$ is the density of the population averaged over the number of species. The total density of individuals across the populations, by definition (Allen et al., 2002), is given as

$$J/A = S \bar{N}. \quad (4.3)$$

Savage et al. (2004), following Gillooly et al. (2001), show that the generation time g_j of an ectothermic population j , having average body size of an individual M_j , can be written in relation to temperature as $g_j \propto M_j^{1/4} \exp^{E/k_b(T+273.2)}$. It has been shown that generation time g_j can be generalized, for example, for marine copepods (Huntley and Lopez, 1992) and tunicates (Deibel and Lowen, 2011). Therefore, by considering the individuals of the populations having average body size \bar{M} , and the average generation time per species \bar{g} , we rewrite the above proportionality (similar to Eq. (4.1)) as

$$\bar{g} = \eta \bar{M}^{1/4} \exp^{E/k_b(T+273.2)}. \quad (4.4)$$

Here, η is the proportionality constant. Note that Eq. (4.4) is a concave decreasing function of T . Thus, the higher the temperature the lower the generation times suggests that population expends metabolic energy at a faster rate. Although these models based on the Boltzmann-Arrhenius function consider maturation rates to monotonically increase with temperature, in reality, they may start to decline with increasing temperature beyond the point of enzyme inactivation.

Eq. (4.1) to Eq. (4.4) yield

$$\bar{g}S = \left(\frac{\eta b_0 \bar{M} J}{A \bar{B}_T} \right). \quad (4.5)$$

Note that the product $\bar{g}S$ is a constant that varies with the taxa. In other words, a constant average energy flux for the populations means that the taxonomic richness is inversely proportional to the generation time ($\bar{g} \propto 1/S$) once the relationship between metabolic rate Eq. (4.1) and generation time Eq. (4.4) is taken into account. Taking the log-transformation of Eq. (4.5) to the base 10, which is a standard for scaling species taxonomic richness, we write the log linear form of the model as *Model 1*:

$$\log S = -\log \bar{g} + \log(\eta b_0 \bar{M} J / A \bar{B}_T) \quad (4.6)$$

The gradient of this equation, ideally, should equal -1. The last term is a temperature-independent constant as per Allen et al. (2002) that varies with the taxa. That is, this model implicitly assumes temperature-invariance for the abundance J , and for the average derived from the body size distribution \bar{M} . Thus, *Model 1* (Eq. (4.6)) suggests that the smaller the average generation time of a population in the community, or the faster the average lifecycle, the higher the species richness. In other words, because the average energy flux through a population, \bar{B}_T in Eq. (4.2), is temperature-independent, the high temperatures result in an increase in the average individual metabolic rate \bar{B} decreasing \bar{N} . Therefore, this should result in an increase in S as we hold J per A to be constants

in Eq. (4.3). Linear model of temperature by Rombouts et al. (2011) is mathematically related to *Model 1*.

What is crucial for our investigation is that *Model 1* (Eq. (4.6)) makes an implicit assumption that temperature remains constant over time. Yet, we note that temperature fluctuates, periodically, at large amplitudes in the northern temperate ecoregions. Thus, this is a violation of a major assumption fundamental to \bar{g} in Eq. (4.6), which was derived based on the MTE model proposed by Allen et al. (2002). If temperature changes over time in synchrony with organisms' capacity to acclimatize to the changing temperature, then it should be reflected in the generation times of the populations. Therefore, we assume that the generation time varies depending on the temperatures of the seasons within a period.

To incorporate the effect of changing temperatures into the model, we assume that the periodic fluctuations of temperature (e.g., yearly) occur on a much longer timescale T_0 (year) than the generation-time timescale. This allows us to define the average generation time per species over the period T_0 as

$$G = \left(\frac{1}{T_0} \int_t^{t+T_0} \bar{g} dt \right),$$
 which is a biologically meaningful quantity. Thus,

integrating both sides of the Eq. (4.6) over a period T_0 (year) from time t to $t+T_0$, we fix Eq. (4.6) to be time-invariant, yielding

$$SG = \left(\frac{\eta b_0 \bar{M} J}{A \bar{B}_T} \right). \quad (4.7)$$

Here, note that $G \propto 1/S$, and G is independent of time but dependent on the type of the temperature profile of the habitat rather than the mean habitat temperature over the period. This model contrasts with that by Rombouts et al. (2011) following Allen et al. (2002), which is, in fact, a version of *Model 1*, that takes into account only the mean habitat temperatures over the period (year). Thus, Eq. (4.7) yields *Model 2* as

$$\log S = -\log G + \log(\eta b_0 \bar{M} J / A \bar{B}_T). \quad (4.8)$$

Note that *Model 2* (Eq. (4.8)) is a simple linear function of $\log G$, whose gradient, ideally, should equal -1 , and whose intercept is a temperature-independent constant that varies with the taxa.

In essence, here we converted the oscillating time-dependent system to a time-independent system by time-averaging the system over the period, because the variations in temperature are periodic in time, thus, capturing the species' taxonomic richness of the periodic-system that runs over centuries or millennia. As the temperature is non-linear with respect to time, and the generation time is a non-linear negative exponential function with respect to temperature, a value of \bar{g} based on the average temperature of the year, should be less than the value of G based on the time-averaging system over a year, capturing the within year variations (Figure 4-1). This effect is due to Jensen's inequality. Therefore, according to *Model 1* and *Model 2*, the richness of species having shorter generation times should be lower in high-fluctuating habitat temperatures compared that in steady habitat temperatures. This is the hypothesis we test.

In application of the models to data, we expect that the taxonomic richness of ectothermic marine calanoid copepods responds largely to seasonally variable temperatures, followed by copepods in general, and tunicates even to a lesser degree. This is because the calanoid copepods, mostly pelagic, and mostly live in the mixed layers of the ocean in the marine ecoregions, are more likely to be exposed to periodically variable temperatures in the upper ocean layers compared to copepods in general, and tunicates.

4.3. Methods

To calibrate *Model 1* and *Model 2* with the data for marine species, we reconstructed a digital map at $1^0 \times 1^0$ spatial resolution of longitudes and latitudes of the northern temperate *ecoregions* (42 in total, indexed 20-61 in Spalding et al., 2007. Also see Appendix 4.1) following MEOW (Marine Ecoregions of the World) digital maps given in OBIS (n.d.). As mentioned before, *marine ecoregions* are a bio-geographic classification of coastal regions based on

similarities in biota, geomorphological features, currents, and temperature, which covers all coastal and shelf waters shallower than 200m (Spalding et al., 2007). On this basis the environmental profiles within an ecoregion are assumed to be less deviated than across, thus, the species distributed in an ecoregion have the exposure to approximately the same spatial and temporal structure of the environmental factors (Spalding et al., 2007). Therefore, this classification assumes homogeneous temperature and ecological communities within these ecoregions than across.

The ambient temperature of marine copepods is typically given by the sea surface temperature (SST). We super-imposed the monthly averaged sea surface temperature data (SST) on the map, spanning from 1970-2001 from NOAA-ESRL (n.d.) pertaining to northern temperate ecoregions (NTE). Huntley and Lopez (1992) suggest that the vertical spatial scale appropriate for temperature related surveys on marine copepods of the globe is probably in the order of 10-100m, the upper mixed layer, where the bulk of planktonic biomass resides in, and encompasses most species at all stages of their life-history. Hence, the SST may be a reasonable proxy for a comparative study of the effect of ambient temperatures of the species, especially copepods, in *marine ecoregions*, across the region.

We modeled the time-dependent temperature by fitting a simple sinusoidal form $T = \bar{T} + \frac{\alpha}{2} \sin(\omega t + \varphi)$ to the pooled data of each $1^0 \times 1^0$ pixel in each ecoregion. The sinusoidal functional form is commonly used to model monthly mean temperature data in marine habitats (see Benyahya et al., 2007; Caissie et al., 1998). We estimated the mean (\bar{T}) and the peak-to-peak amplitude (α) of yearly ecoregion temperatures using non-linear least squares method (using the minimization procedure *fminsearch* in Matlab for mean squared errors). Here, $\omega = 2\pi/T_0$ is the frequency, φ is the phase, and $t=1..(T_0/\text{time-interval})$ with period T_0 . For example, $T_0=366$ days with the modeled time-interval given by 61 days results in 6 steps ($t=1: 6$). It is commonly said that generation time is a reasonable scale for copepod temperature related experiments in a variable

temperature environment (Huntley and Lopez, 1992; Landry, 1975). For example, the generation time for *Pseudodiaptomous marinus* in 20°C is approximately 23 days.

We sampled the species taxonomic richness data of calanoid copepods, copepods, and tunicates digitally from the online interactive digital maps of the database Ocean Bio-geographic Information Systems (OBIS, n.d.) pertaining to the NTE. Here, we ignored the ecoregion 32 (Levantine Sea in the south-eastern Mediterranean ocean), and 61 (Magdalena Transition), as they were markedly under-sampled; the former compared to its adjacent ecoregions 31, 33, 34, and the latter compared to its adjacent ecoregions 59, 60, although the inclusion of which did not change the general pattern in the data. This left with 40 ecoregions in NTE as the sample size.

We calibrated \bar{g} for marine copepods from the data reconstructed from Huntley and Lopez (1992) simplifying the model Eq. (4.4) as $\bar{g} = \bar{h}_1 \exp(-\bar{h}_2[1/(T + 273.2)])$ with an appropriate selection of parameters (Figure 4-1), $\bar{h}_1 = \eta \bar{M}^{1/4}$, $\bar{h}_2 = E/k_b$, $k_b = 8.62 \text{ eVK}^{-1}$, and using non-linear least squares regression (*lsqcurvefit* function Matlab). Similarly, we calibrated \bar{g} for tunicates from the data reconstructed from Deibel and Lowen (2012) (Figure 4-1). Ideally, we should get $1000\kappa_2 \sim 0.9\text{K}$ as the activation energy E for aquatic taxa is $\sim 0.78\text{eV}$ (Allen et al., 2002).

We used simple linear regressions for fitting *Model 1* and *Model 2* fixing the gradients at -1 as the models described. We also used the Reduced Major Axis (RMA) regression method in Sokal and Rolf (1981), software developed by Bohonak (2004). Allen et al. (2002) also used the RMA method for the regression. Note that RMA assumes both the dependent and the predictor variables are subjected to errors. We also allowed a parameter for the gradient of the models, instead of fixing the value at -1, to evaluate the deviation of the estimated gradients from the expected value (-1). The gradient estimated by RMA regression method is computed as the division of the standard deviation of y

variable by that of x variable, which, in contrast, is multiplied by the coefficient of variation in the standard regression (Holland, n.d.).

We note that, although the predictor variables in *Model 1* to *Model 2* are functionally nested, the *Model 1* and *Model 2* are not nested with respect to the estimations (as we have the x-variables; g and G , already calculated), which leads to the same number of estimated parameters (in terms of the degrees of freedom). Therefore, we used the adjusted R^2 denoted by R_{Adj}^2 for model selection, given by

$$R_{Adj}^2 = 1 - \frac{(n-1)}{(n-p)}(1 - R^2) \quad (\text{Kadane and Lazar, 2004}).$$

Here, p is the sample size, and n is the number of parameters. This is an alternative to using residual sum of squares (RSS). Based on R_{Adj}^2 of *Model 1* and *Model 2*, we evaluated whether *Model 2* performs better than *Model 1*, thus, if the amplitude of periodic (yearly) temperature has an effect on the species taxonomic richness. We also evaluated if there is a pattern in these effects due to the taxa, greatest for calanoid copepods, followed by copepods in general, and tunicates for the reasons that we have discussed in the earlier section. Furthermore, we tested if the periodic amplitude of temperature directly causes a reduction in the species taxonomic richness for all three taxa, using a simple linear regression, and also, whether the amplitudes correlate with the mean temperatures of the northern temperate ecoregions.

We also used *Model 2*, calibrated from the copepod data of the northern temperate ecoregions from OBIS (n.d.), to predict the copepod diversity of the whole Atlantic Ocean for the data reconstructed from Rombouts et al. (2009). We did these predictions with respect to the mean habitat temperatures, and also the latitudes. As Rombouts et al. (2009) data of taxonomic richness are a collection of point sampling sources from the Atlantic Ocean, whereas, our data are for the whole ecoregions in the northern temperate ecoregions, this results in a bias (our estimates being on the high side). These systematic marginal differences may be due to the species-area relationship described by Preston (1962). To reduce the bias caused by the difference in the units of sampling, we added a scaling

parameter $\log(w)$ to the mean estimates. The rescaled *Model 2* is then given by *Model 3* as

$$\log S = -\log G + \log(\eta b_0 \overline{MJ} / \overline{AB}_T) + \log w. \quad (4.9)$$

Except for parameter $\log(w)$, all the other parameters were estimates from the data from the northern temperate ecoregions, which results in a constant shift of the model predictions along the y-axis ($\log S$), not by shape along the x-axis ($\log G_T$).

We estimated the latitudinal averages and standard deviations of the means and the amplitudes of temperature profiles at $1^0 \times 1^0$ (longitudes and latitudes) spatial resolutions. We fitted *Model 3* (already calibrated from NTE without the error term $\log(w)$) to Rombouts et al. (2009) taxonomic richness data given with respect to latitudes for estimating the bias, $\log(w)$, using the latitudinal averages of the means and the amplitudes of temperatures we computed. We also plotted the calibrated *Model 3* by adding and subtracting two standard deviations of the means and the amplitudes of the latitudinal temperatures, and 90% CI of the *Model 2* calibrated from the NTE yielding two other curves. (Note that Rombouts et al. (2009) data do not provide temperature-amplitudes of the sampled habitats.)

We also fitted the calibrated *Model 3* to Rombouts et al. (2009) data of marine copepods given with respect to mean habitat temperatures by plugging in the expected amplitudes corresponding to the means of the ecoregion temperatures. We also plotted the deviations using the earlier method.

4.4. Results and Discussion

Based on standard regression, Figure 4-2 indicates that temperature-amplitude of ecoregions by itself is not a good predictor of species taxonomic richness unless it is accounted mechanistically into *Model 2*. Based on RMA, temperature-amplitudes show a significant negative correlations with log species taxonomic richness, p -values for the model (for null hypothesis: gradient=0)

<0.001 for all taxa; calanoid copepods, copepods, and tunicates suggesting strong relationships. However, R^2 for the models are low yielding 0.05, 0.02 and 0.07, respectively showing weak model fits. Based on R_{Adj}^2 , Table 4-1 suggests that *Model 2*, which accounts for the effect of the amplitude of periodic temperature on bio-mechanics, performs better than the *Model 1*, which is a linear relationship with respect to mean ecoregion temperatures (a modified version of the model by Rombouts et al. (2011) based on Allen et al., (2002)) for all three taxa. The improvement of R_{Adj}^2 , going from *Model 1* to *Model 2*, suggests that *Model 2* is a more reliable predictor. As both models have the same number of parameters, difference in R_{Adj}^2 between the two models is a sufficient criterion to evaluate which model performs better.

The mean and the amplitude of periodic temperatures of the ecoregions did not show a significant correlation at alpha-level 0.05 ($F=53.53$, $df=39$, $p=0.56$). This may suggest that any improvement to the models yielded by incorporating the temperature-amplitudes is independent of the effect of the mean ecoregion temperatures.

Both *Model 1* and *Model 2* are statistically significant yielding extremely low p -values ($<10^{-04}$ for all three taxa) rejecting the null hypothesis that gradient=0 for the case we assigned a parameter for the gradient. The lowest p -value is yielded for calanoid copepods, followed by copepods, and tunicates. The gradients estimated for *Model 1* yielded -0.71,-0.70, and -2.18 for calanoid copepods, copepods, and tunicates, respectively (Table 4-2). The gradients we estimated for *Model 2* yielded -0.71,-0.70, and -1.94, respectively. Figure 4-2 shows the degree of deviation of these gradients from -1, graphically. However, the gradients are not significantly different from -1 based on Monte Carlo resampling tests (p -value ≈ 0.52 for all three taxa). For *Model 1*, where the gradients were fixed at -1, R_{Adj}^2 are 0.43, 0.41, and -1.90 for calanoid copepods, copepods, and tunicates respectively, while for *Model 2* R_{Adj}^2 are 0.46, 0.42, and -1.70, respectively. The values of R^2 , which suggests how well the model fits to the

data, decrease from calanoid copepods, copepods, to tunicates indicating that calanoid copepods are the most affected by the periodic fluctuations of temperature followed by copepods and tunicates.

The above results are in conformity with the ecology of the three taxa. For example, calanoid copepods have colonized the pelagic part of the water column, in contrast to copepods in general (Bradford-Grieve, 2002). Some copepods (both individuals and some species) in pelagic environment show diurnal vertical migration: increase metabolism while active in the upper layers within the mixed layer (average 50m: e.g., Hays et al., 2001), where the temperature is close to homogeneous (for example, Andersen et al., 2004; Atkinson et al., 1992; Herman, 1983;), and rest during the day at deeper layers around the edge of the mixed layer (average 150m: e.g., Hays et al., 2001) (Andersen et al., 2004; Kiørboe and Sabatini, 1994) in NTE. Some pelagic copepod species does not show diurnal migration, and maintain vertical zonation within the mixed layer and down to the thermocline (e.g., Bollens and Landry, 2000; Mackas et al., 1993). In contrast most tunicates are benthic. Therefore, the calanoid copepod species may be more exposed to seasonally fluctuating temperatures occurring largely in the mixed ocean layers. Because we tested these relationships for species within the coastal *marine ecoregions* (neritic: <200m depth) where large depths are subject to mixing and periodically fluctuating temperatures, the observed effects of all taxa seem substantial. Thus, it is apparent from our results that temperature-amplitude plays a role in species richness, where the species are exposed to seasonally fluctuating temperatures.

Figure 4-3 indicates that the ratio of mean temperatures can be used as a predictor of the ratio of copepod taxonomic richness between two ecoregions, especially when the ratio of the amplitudes is large, and the mean temperatures of these regions are within a narrow range. Thus, if the mean temperatures are the same between two ecoregions, then we may look to the ratio of amplitudes between the ecoregions as a predictor of the ratio of their species richness.

Figures 4-4a and 4-4b show our model predictions of the marine copepod richness in the Atlantic Ocean for data reconstructed from Rombouts et al. (2009). The effect of the amplitude and the mean temperatures on species richness explains the pattern in the data well. The predictions given by the mechanistic *Model 3* is in contrast to that given by models in Rombouts et al. (2011; 2009) and Record et al. (2012). Our model explains the differences in the humps in copepod richness near the tropics, and faster rates of drop towards the northern latitudes compared to southern latitudes. The difference in the shape of the species richness curves between the two hemispheres seems to have been caused by the double-negative effect of the apparent faster drop in the mean temperatures (Figure 4-4c) and the higher amplitudes (Figure 4-4d) in the northern hemisphere compared to the southern hemisphere. We further note that the pattern in the data also match well with the predicted confidence intervals.

There is an unresolved issue regarding the scaling of body mass with respect to metabolic rates of organisms. Some argue that body mass is proportional to metabolic rate to the power $3/4$, while some argue that it is $2/3$ (see West and Brown, 2005), which is still under controversy. However this exponent may not change the qualitative aspect of our result, while it may affect the degree of impact of amplitude of temperature on species richness slightly. Furthermore, Record et al. (2012) investigate the case if the body mass varies with temperature, which yields a model that gives a non-linear fit to copepod richness data with respect to temperature, which may be a better fit than the linear fit by Rombouts et al. (2009). This suggests that the assumptions based for MTE may need further empirical investigation. Our model also gives a non-linear fit (see Figure 4-4a), which describes the variation in copepod richness data strongly. This is a result of spatial variations in periodic fluctuations of temperature that we incorporated into our model in addition to mean habitat temperatures. The fact remains that marine copepods and tunicates, having short generation times, show sensitivity, although subtle, to fluctuation of temperature regardless of the metabolic theoretical backing (see Figure 4-2). It makes sense therefore to describe this effect using MTE models that fits to data better than the case of phenomenological relations,

while having an advantage of describing the underlying dynamics of these processes mechanistically.

4.5. Conclusion

The amplitude of periodic temperature has a non-linear effect on the bio-energetic, thus, the global marine copepod species taxonomic richness in particular, and also tunicates to a certain degree. Although the mean of temperature cycles alone is a good predictor of marine species richness, incorporating the amplitude into the model improves the predictability of species richness depending on the exposure of the taxa to such temperature variations. The amplitude differences along the longitudes may explain the longitudinal variation in species diversity as the temperature remains the same along the longitudes. The evidence we show here, that supports the theoretical advancement we propose to MTE, capturing the effect of subtle year-round variations in temperature on the bio-mechanics, may solidify the use of MTE in thermotical ecology.

In light of this, we may predict that an increase in the amplitude of periodic temperature could counteract the effect of the global warming, possibly balancing off its net effect on the change of species richness of those species that are affected by the amplitude of temperature. Our theoretical result may also be valid for diversity relations with temperature shown for the other marine species (Tittensor et al., 2010) and also terrestrial species (Allen et al., 2002; Hawkins, et al. 2007). Our hypothesis provides new insight into the understanding of the global species richness distribution. Thus, this is a novel improvement to the MTE.

For further validation of these theories, we may need to investigate the changing diversity patterns over geological times from a paleoecological perspective (Louys et al., 2012), for example, cases such as “hopping hotspots” of

marine biodiversity (Renema et al., 2008), and historical biodiversity tracking of the earth's temperature (Mayhew et al., 2012).

Table 4-1 Regression results of *Model 1* and *Model 2* based on the RMA regression (fixed gradient =-1).

Taxa	Model	No. para	RSS df=39	R^2_{Adj}	Model Rank Based on R^2_{Adj}
Calanoid copepods	<i>Model-1</i>	1	3.75	0.43	2
	<i>Model-2</i>	1	3.65	0.46	1
Copepods	<i>Model-1</i>	1	3.87	0.41	2
	<i>Model-2</i>	1	3.85	0.42	1
Tunicates	<i>Model-1</i>	1	8.45	-1.9	2
	<i>Model-2</i>	1	8.25	-1.7	1

Table 4-2 Regression results of *Model 1* and *Model 2* based on RMA regression estimating an additional gradient for the linear models without fixing it at -1. This is to evaluate the deviations of gradients from -1.

Taxa	Model	No. para	Estimated gradient (should be -1 ideally)	p-value (Null: gradient=0)	R^2_{Adj}	Model Rank Based on R^2_{Adj}
Calanoid copepods	<i>Model-1</i>	2	-0.71	1.7E-06	0.43	2
	<i>Model-2</i>	2	-0.71	9.3E-07	0.45	1
Copepods	<i>Model-1</i>	2	-0.70	3.3E-06	0.41	2
	<i>Model-2</i>	2	-0.70	2.6E-06	0.42	1
Tunicates	<i>Model-1</i>	2	-2.13	0.006	0.15	2
	<i>Model-2</i>	2	-1.94	0.004	0.17	1

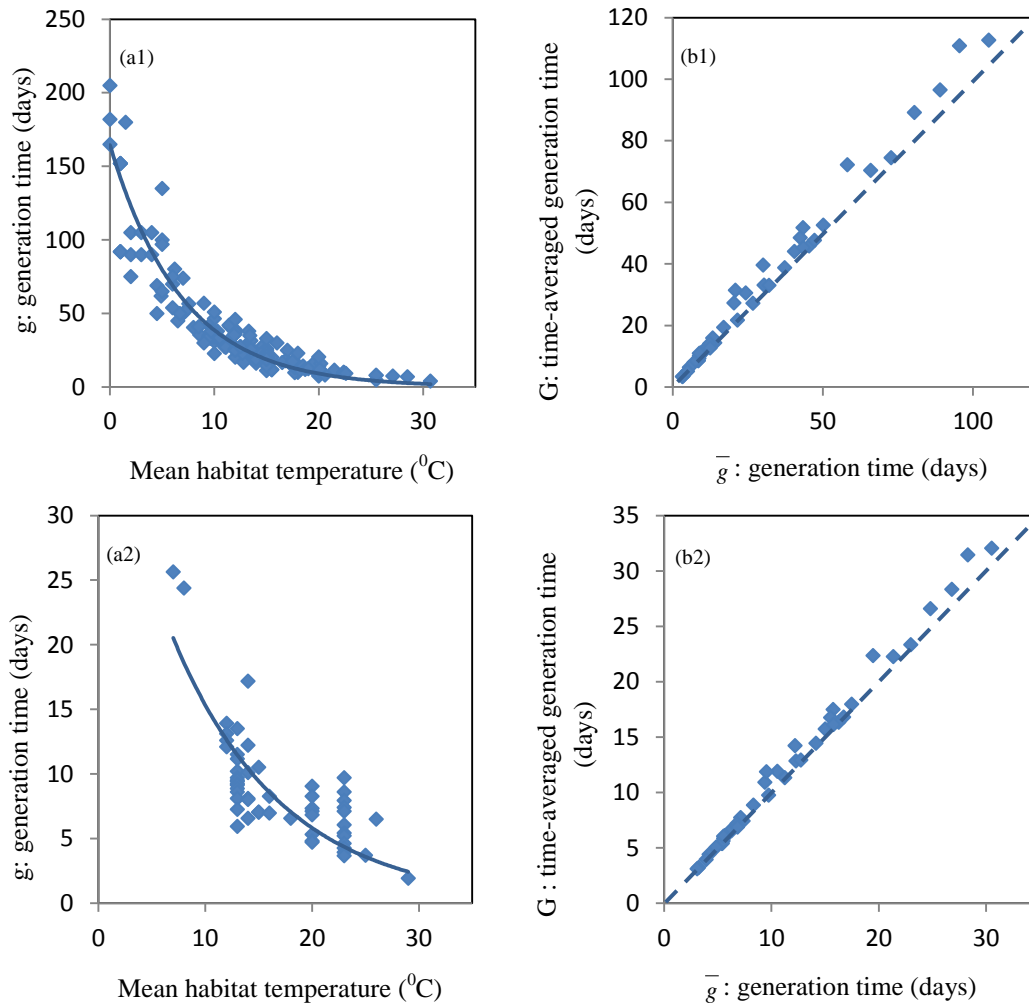


Figure 4-1 (a1) Generation times of copepods modelled with respect to mean ambient temperature: Estimated by Eq. (4.6) (\bar{g} in *Model 1*): $\bar{g} = 7.97 \times 10^{-16} \exp\{10871.59 [1/(T+273.2)]\}$, where $E/1000k_b = -1.26$. $R^2 = 0.88$. The data reconstructed from Huntley and Lopez (1992). (b1) The time-averaged generation times (G in *Model 2*) of the northern temperate marine ecoregions (time discretized at 60 day intervals) plotted against the generation times of the same based on average ambient temperature (\bar{g} in *Model 1*). Similarly, (a2) \bar{g} estimated by Eq. (4.6) for tunicates: $\bar{g} = 6.68 \times 10^{-12} \exp\{8069.83 [1/(T+273.2)]\}$, where $E/1000k_b = 0.94$. $R^2 = 0.65$. The data reconstructed from Deibel and Lowen (2012). (b2) G with respect to \bar{g} estimated for tunicates following the same method as above.

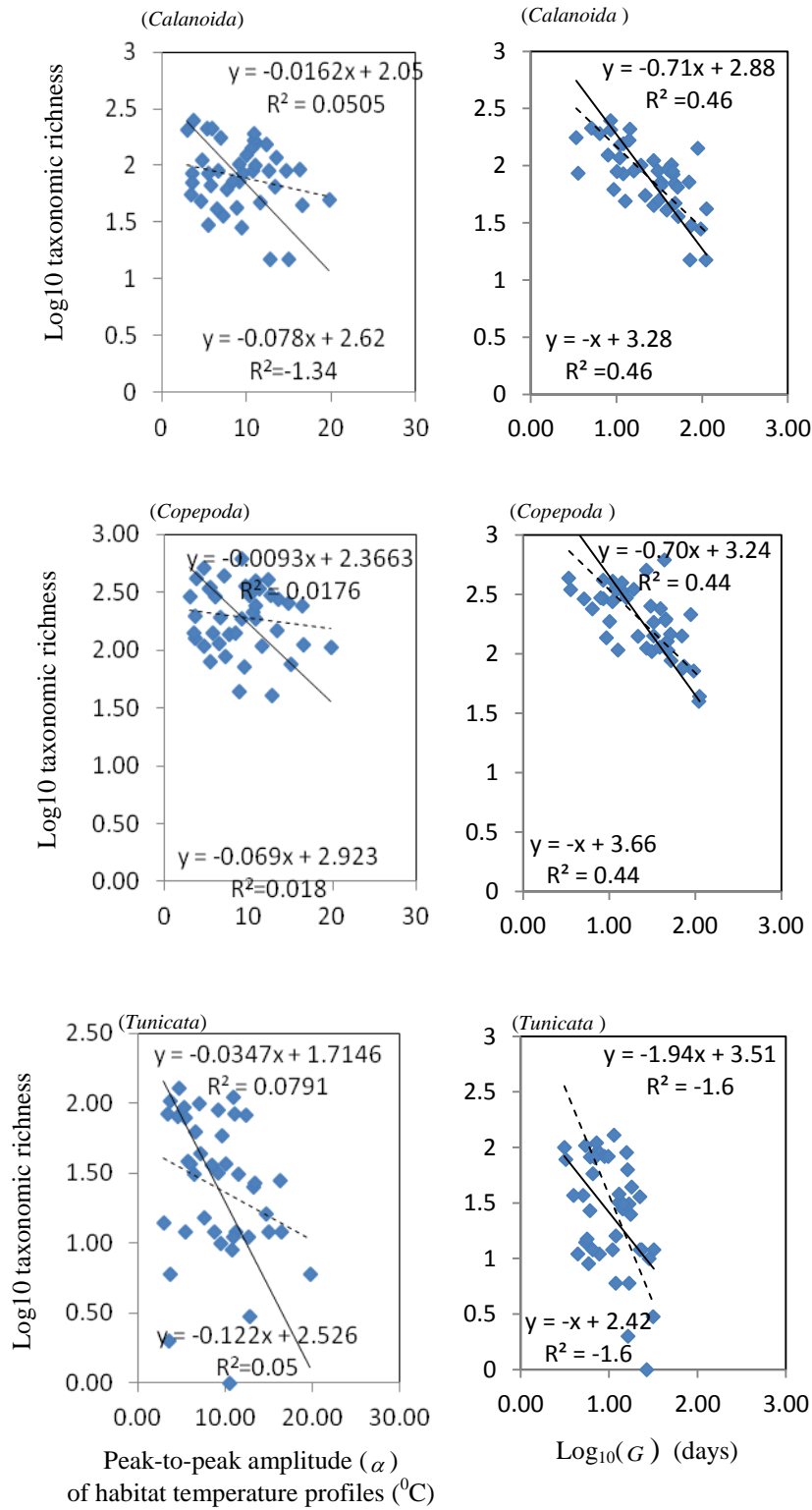


Figure 4-2 Species taxonomic richness (log₁₀) of calanoid copepods, copepods, and tunicates for the data pertaining to the northern temperate marine eco-regions (index 20-

61 by Saplding et al., 2007) modeled against (a) Peak-to-peak amplitude (α) of habitat temperature; (b) $\text{Log}_{10}(G)$ (*Model 2*). Solid regression lines in left panels are from the RMA regression, and dotted lines are from the conventional regression. Note that RMA method gives more acute gradients for the model-fits ($p < 0.001$), yet with lower R^2 . Solid regression lines in right panels are for model-fits fixing gradient at -1, and dotted lines are for model-fits estimating an additional parameter for the gradient (both using RMA method). In all three taxa, the gradients are not significantly different from -1 based on Monte Carlo resampling tests ($p\text{-value} \approx 0.52$).

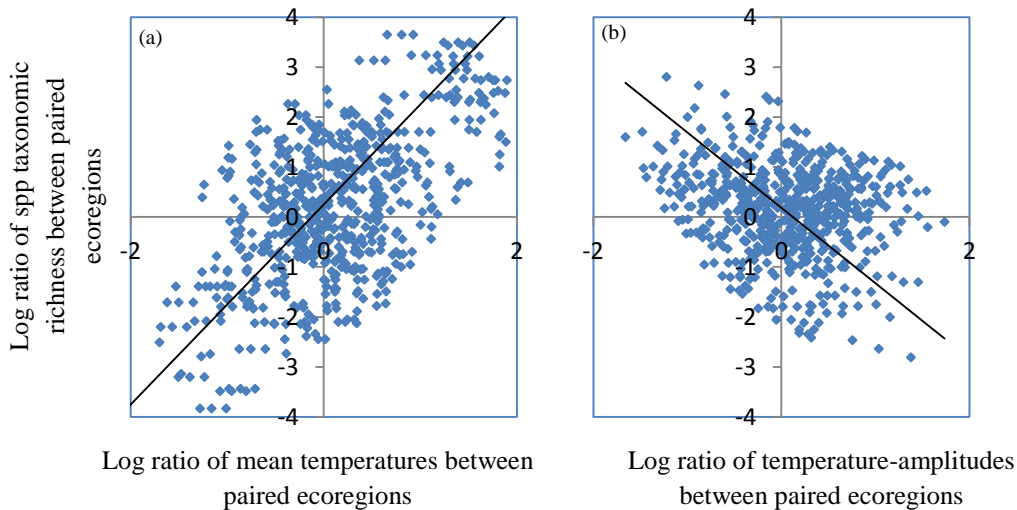


Figure 4-3 Log ratio of copepod species richness between paired ecoregions with respect to log ratio of their (a) mean ($p < 0.001$, $R^2 = 0.34$), and (b) amplitude ($p < 0.001$, $R^2 = 0.05$) of temperatures. Regression lines are by RMA method. The ratios of means, and also amplitudes, if large, are good predictors of the ratios of species richness between ecoregions. Therefore, where the mean temperatures are the same between two ecoregions, the amplitude difference, if large, will indicate the richness ratios.

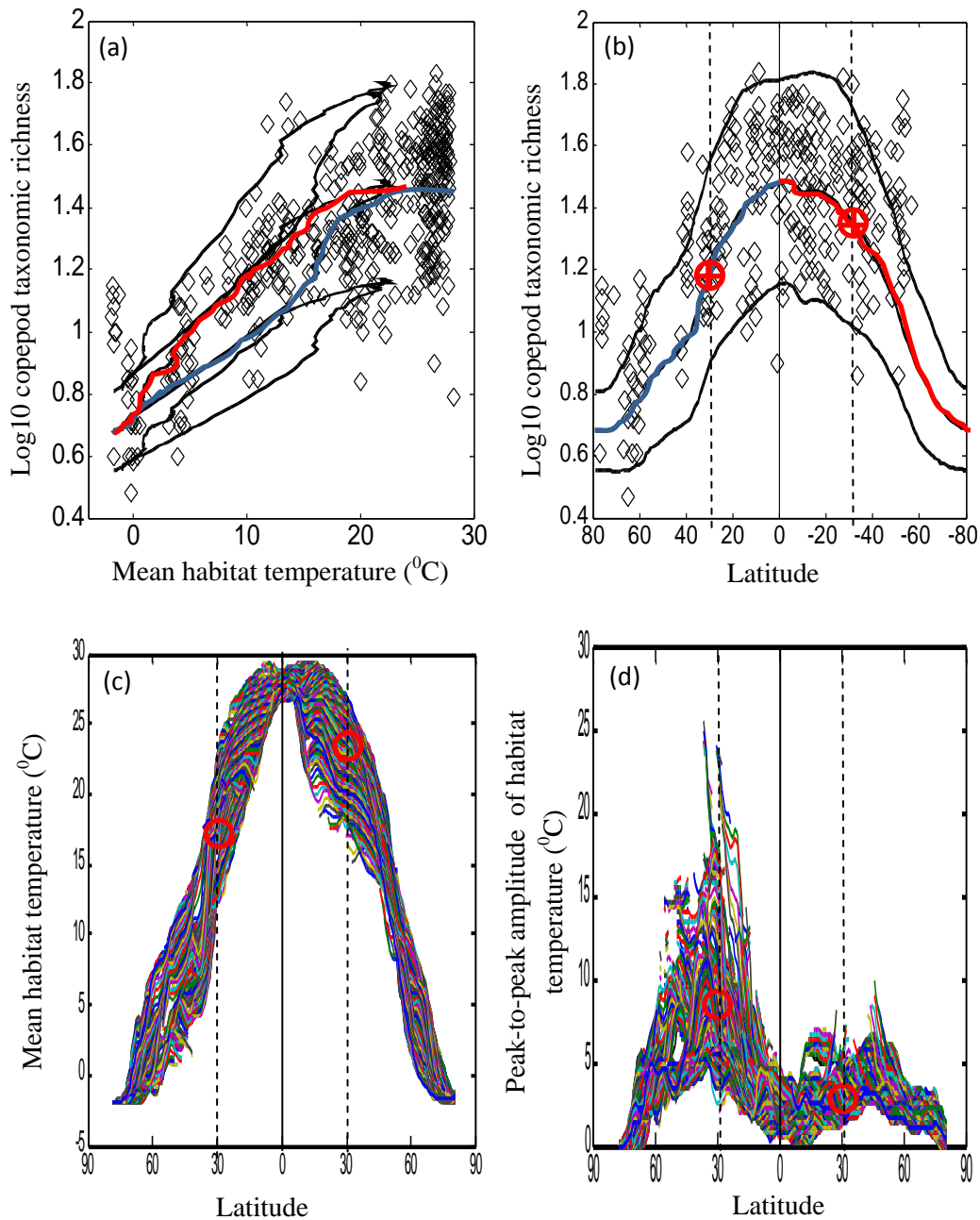


Figure 4-4 Copepod taxonomic richness (data reconstructed from Rombouts et al., 2009) in the Atlantic Ocean, predicted (a) by mean habitat temperatures, (b) by latitude, using *Model 3* (which is *Model 2* parameterized from OBIS data of the NTE, and then estimating a scaling parameter $\log(w)$ from Rombouts et al. (2009) data, yielding $w=5.62$). The scaling constant shifts the curve along the y-axis, but should not change its shape. Black dashed lines are the predictions made by adding (top curve) and subtracting (bottom curve) (i) 90% CI of the of the estimates of *Model 2*, and (ii) copepod taxonomic

richness given by two standard deviations of the monthly mean and amplitudes of temperatures averaged by latitude. (c) Yearly mean SST by latitudes, and (d) yearly amplitudes of SST by latitudes (as per the scale $1^0 \times 1^0$ spatial resolution of latitudes and longitudes based on NOAA-ESRL SST data from 1971-2001). Here, x-axis (left 90-0): Northern hemisphere. x-axis [right 0-90]: Southern hemisphere. Red circles are the points where the mean values of the variables in y-axis crosses the latitudes $\pm 30^0$. In line with our theory, the double-negative effect of high amplitudes and low mean temperatures seems to have lowered the diversity distribution in the northern hemisphere (blue line) compared to that in the southern hemisphere (red line).

4.6. References

- Allen, A.P., Brown, J.H., Gillooly, J.F., 2002. Global biodiversity, biochemical kinetics, and the energetic-equivalence rule. *Science* 297(5586), 1545-1548.
- Andersen, V., Devey, C., Gubanova, A., Picheral, M., Melnikov, V., Tsarin, S., Prieur, L., 2004. Vertical distributions of zooplankton across the Almeria–Oran frontal zone (Mediterranean Sea). *Journal of Plankton Research* 26(3), 275-293.
- Atkinson, A., Ward, P., Williams, R., Poulet, S.A., 1992. Feeding rates and diel vertical migration of copepods near South Georgia: comparison of shelf and oceanic sites. *Marine Biology* 114(1), 49-56.
- Benyahya, L., Caissie, D., St-Hilaire, A., Ouarda, T.B., Bobée, B., 2007. A review of statistical water temperature models. *Canadian Water Resources Journal* 32(3), 179-192.
- Bohonak, A.J., 2004. Software for Reduced Major Axis Regression, San Diego State University, USA, Retrieved from: <http://www.bio.sdsu.edu/pub/andy/RMAmanual.pdf>.
- Bollens, G.R., Landry, M.R., 2000. Biological response to iron fertilization in the eastern equatorial Pacific (Iron Ex II). II. Mesozooplankton abundance, biomass, depth distribution and grazing. *Marine Ecology Progress Series* 201(43-56).
- Bradford-Grieve, J.M., 2002. Colonization of the pelagic realm by calanoid copepods. *Hydrobiologia* 485(1-3), 223-244.
- Caissie, D., El-Jabi, N., St-Hilaire, A., 1998. Stochastic modelling of water temperatures in a small stream using air to water relations. *Canadian Journal of Civil Engineering* 25(2), 250-260.
- Damuth, J., 1987. Interspecific allometry of population density in mammals and other animals: the independence of body mass and population energy-use. *Biological Journal of the Linnean Society* 31(3), 193-246.

Deibel, D., Lowen, B., 2012. A review of the life cycles and life-history adaptations of pelagic tunicates to environmental conditions. *ICES Journal of Marine Science: Journal du Conseil* 69(3), 358-369.

GHRSSST., n.d. Retrieved from: <https://www.ghrsst.org/ghrsst-science/sst-definitions/>.

Gillooly, J.F., Brown, J.H., West, G.B., Savage, V.M., Charnov, E.L., 2001. Effects of size and temperature on metabolic rate. *Science* 293(5538), 2248-2251.

Hawkins, B.A., Albuquerque, F.S., Araujo, M.B., Beck, J., Bini, L.M., Cabrero-Sanudo, F.J., Williams, P., 2007. A global evaluation of metabolic theory as an explanation for terrestrial species richness gradients. *Ecology* 88(8), 1877-1888.

Hays, G.C., Kennedy, H., Frost, B.W., 2001. Individual variability in diel vertical migration of a marine copepod: why some individuals remain at depth when others migrate. *Limnology and Oceanography* 2050-2054.

Herman, A.W., 1983. Vertical distribution patterns of copepods, chlorophyll, and production in northeastern Baffin Bay. *Limnology and Oceanography* 28(4), 709-719.

Holland, S., n.d. Retrieved from <http://strata.uga.edu/6370/lecturenotes/regression.html>.

Huntley, M.E., Lopez, M.D., 1992. Temperature-dependent production of marine copepods: a global synthesis. *American Naturalist* 201-242.

Kadane, J.B., Lazar, N.A., 2004. Methods and criteria for model selection. *Journal of the American Statistical Association* 99(465), 279-290.

Kara, A.B., Wallcraft, A.J., Hurlburt, H.E., 2003. Climatological SST and MLD Predictions from a Global Layered Ocean Model with an Embedded Mixed Layer. *Journal of Atmospheric and Oceanic Technology* 20(11), 1616-1632.

Kjørboe, T., Sabatini, M., 1994. Reproductive and life cycle strategies in egg-carrying cyclopoid and free-spawning calanoid copepods. *Journal of Plankton Research* 16(10), 1353-1366.

Lande, R., Engen, S., Sæther, B.E., 2003. *Stochastic population dynamics in ecology and conservation*. Oxford University Press, GB, p. 209.

Louys, J., Wilkinson, D.M., Bishop, L.C., 2012. Ecology needs a paleontological perspective. In: *Paleontology in Ecology and Conservation* Springer Berlin Heidelberg, p. 23-38.

Mackas, D.L., Sefton, H., Miller, C.B., Raich, A., 1993. Vertical habitat partitioning by large calanoid copepods in the oceanic subarctic Pacific during spring. *Progress in Oceanography* 32(1), 259-294.

Mayhew, P.J., Bell, M.A., Benton, T.G., McGowan, A.J., 2012. Biodiversity tracks temperature over time. *Proceedings of the National Academy of Sciences* 109(38), 15141-15145.

NOAA-ESRL., n.d. Physical Sciences Division, Boulder Colorado, USA. Retrieved from <http://www.esrl.noaa.gov/psd/data/gridded/data.noaa.oisst.v2.html>.

Oberdorff, T., Guégan, J.F., Hugueny, B., 1995. Global scale patterns of fish species richness in rivers. *Ecography* 18(4), 345-352.

OBIS., n.d. Ocean Bio-geographic Information Systems. Retrieved from: <http://www.iobis.org/>.

Powell, M.G., Beresford, V.P., Colaianne, B.A., 2012. The latitudinal position of peak marine diversity in living and fossil biotas. *Journal of Biogeography* 39(9), 1687-1694.

Preston, F.W., 1962. The canonical distribution of commonness and rarity: Part I. *Ecology* 43, 185-215.

Record, N.R., Pershing, A.J., Maps, F., 2012. First principles of copepod development help explain global marine diversity patterns. *Oecologia* 170(2), 289-295.

Renema, W., Bellwood, D.R., Braga, J.C., Bromfield, K., Hall, R., Johnson, K.G., Pandolfi, J.M., 2008. Hopping hotspots: global shifts in marine biodiversity. *Science* 321(5889), 654-657.

Rombouts, I., Beaugrand, G., Ibañez, F., Chiba, S., Legendre, L., 2011. Marine copepod diversity patterns and the metabolic theory of ecology. *Oecologia* 166(2), 349-355.

Rombouts, I., Beaugrand, G., Ibañez, F., Gasparini, S., Chiba, S., Legendre, L., 2009. Global latitudinal variations in marine copepod diversity and environmental factors. *Proceedings of the Royal Society B: Biological Sciences* 276(1670), 3053-3062.

Savage, V.M., Gillooly, J.F., Brown, J.H., West, G.B., Charnov, E.L., 2004. Effects of body size and temperature on population growth. *The American Naturalist* 163(3), 429-441.

Sokal, R.R., Rohlf, F.J., 1981. *Comparison of regression lines*. *Biometry*. 2nd edition. New York, NY: Freeman and Co, p 499-509.

Spalding, M.D., Fox, H.E., Allen, G.R., Davidson, N., Ferdaña, Z.A., Finlayson, M.A.X., Robertson, J., 2007. Marine ecoregions of the world: a bioregionalization of coastal and shelf areas. *BioScience* 57(7), 573-583.

Tittensor, D.P., Mora, C., Jetz, W., Lotze, H.K., Ricard, D., Berghe, E.V., Worm, B. 2010. Global patterns and predictors of marine biodiversity across taxa. *Nature* 466(7310), 1098-1101.

West, G.B., Brown, J.H., 2005. The origin of allometric scaling laws in biology from genomes to ecosystems: towards a quantitative unifying theory of biological structure and organization. *Journal of Experimental Biology* 208(9), 1575-1592.

CHAPTER 5

²On controlling stochastic immigration of colonizing and declining populations

5.1. Introduction

Species colonization and extirpation have been known since the birth of ecology. These can occur through natural processes, but their rates have been accelerated recently due to human activities (Simberloff, 2009). Some colonizing species become invasive (Colautti and MacIsaac, 2004; Valery et al., 2008). Invasive species keep expanding range (Sorte et al., 2010), some threatening indigenous species (Sanderson et al., 2009), and becoming a major threat to biological diversity (Lockwood et al., 2005), imposing trickledown effects detrimental or beneficial to the habitat dependents (Keller et al., 2007). They are a cause of the endangerment of 48% of the species listed under the US Endangered Species Act (ESA) (Czech and Krausman, 1997; Wilcove et al., 1998), and are estimated to cost the US economy more than \$120 billions a year (Pimentel, 2009). Although one can argue that humans are not in a position to morally judge their impact on the ecology of the systems, we can all agree that some invasive species have become nuisance (Lovell et al., 2006), whereas the extinction of a species may come with a price (Wilson et al., 2011). Indeed, the next invader and its effects are largely unknown. Similarly, we do not know the effect of the next species going extinct.

Thus, if we are to control the colonization of non-indigenous species that are rapidly propagated through human-mediated vectors and become invasive in novel habitats (Lovell et al., 2006; Simberloff, 2009), then we need to know how the immigration dynamics affect the colonization success. Similarly, if we are to

² A version of this chapter has been published. Rajakaruna, H., Potapov, A., Lewis, M., 2013. Impact of stochasticity in immigration and reintroductions on colonizing and declining populations. *Theoretical Population Biology*, 85, 38-48.

stock declining indigenous populations preventing them from going extinct, or if we are to reintroduce extirpated indigenous populations (IUCN, 2010; Snyder et al., 1996) that are subject to stochastic factors, then we need to know how the immigration dynamics affects their re-colonization success. In this paper, we address the aspect of how *stochasticity in immigration* (propagule flow) affects the population dynamics and their outcomes. In an empirical sense, it is the randomness in the fluctuation of propagules being discharged or immigrated to novel habitats.

Propagule pressure is a main driver of colonization (Colautti et al., 2006; Simberloff, 2009). For example, non-indigenous marine species such as diaptomid copepods, *Pseudodiaptomus inopinus*, *P. marinus*, and *P. forbesi* have been invading the west coast of North America from their native range in the North West Pacific coast through human-mediated vectors such as ship ballast-water discharge (Cordell et al., 2008). The Canadian Aquatic Invasive Species Network (CAISN, n.d.) has developed a research program to study propagule pressure and assess risks associated with aquatic invasive species establishment. To control unwanted colonization, efforts are made to reduce human-mediated immigration (Olenin et al., 2011).

On reinforcement of populations against going extinct, science-based relocation (Sheean et al., 2011), translocation (Weeks et al., 2011), and assisted colonization programs (Seddon, 2010) are becoming increasingly popular. For example, indigenous species from the Superfamily Diaptomidae, *Hesperodiaptomus shoshone*, have been extirpated from their native habitats in alpine lakes after fish-stocking (Sarnelle and Knapp, 2004). Kramer et al. (2008) have carried out re-colonization experiments to investigate the constraining factors of *H. shoshone*'s population recovery. To sustain such endangered, threatened or declining species, efforts are made to artificially replenish populations by captive breeding and stocking (Paragamian and Hansen, 2011; Thomas et al., 2010), and to recover extirpated populations, efforts are made to reintroduce (IUCN, 2010; Lorenzen et al., 2010).

In the contexts of both the spreading of colonizing populations through natural or human-mediated propagule pressure, and stocking or reintroduction of declining populations, we observe that the dynamics of a population where the propagules are flowing into a habitat as *immigration* in general. Armstrong and Seddon (2007) have proposed that the knowledge gained from colonization dynamics of invasive species can be used to improve the success of stocking and reintroduction programs of declining or extirpating populations.

Cordell et al. (2009) have sampled large densities of non-indigenous species in ballast-water from ships entering Puget Sound. However, most species found in the ballast-water discharge have not colonized yet. Numerous control methods such as mid oceanic exchange of ballast water (NOAA, 2007; Simard et al., 2011), chemical treatments (Nanayakkara et al., 2011) and temperature treatments of ballast-water tanks (Quilez-Badia et al., 2008) are deployed to control immigration (Olenin et al., 2011), and thus to minimize colonization risks. Yet, not all ships carry the same densities of species at all times. They are subject to variation (see data in Cordell et al., 2009). Moreover, there is no guarantee that such control methods can reduce risks to zero. Hence, deploying costly methods uniformly or arbitrarily to reduce immigration may not be economically optimal when the immigration is variable and environmental and demographic stochasticity are present. If we know how stochasticity in immigration impacts the chances of colonization in the presence of other stochastic factors, then we can calibrate the manner in which these treatments should be deployed to make them more effective in reducing the invasion risks to acceptable levels. The optimal control methods to decrease the spread have been investigated from the economic standpoint by Finnoff et al. (2010).

Declining populations are commonly associated with negative intrinsic growth rates given unfavourable environments, and some of these populations are stressed by stochastic factors (Morris and Doak, 2002). Few efforts of stocking and reintroductions have been successful in sustaining declining and endangered populations (Noël et al., 2011; Rasmussen et al., 2009; Schooley and Marsh,

2007; Wada et al., 2010). Noël et al. (2011) have indicated that failures of close to 50% were evident in the reintroduction of 50 populations of 7 wetland species. Godefroid et al. (2011) have shown that the causes for 34% of the failures in reintroductions were not known, while 8% were due to known unexpected changes in the habitats. Some failures have been attributed to the environmental stochasticity (Vincenzi et al., 2012). Schaub et al. (2009) has suggested incorporating demographic stochasticity in making decisions when to end release programs so as to guarantee success.

Often there is unaccounted stochasticity apparent in the population densities and in the timing of stocking and reintroductions (e.g., see data in Shute et al., 2005). However, in the presence of environmental and demographic variations, we do not yet know how the variation in stocking or reintroduction rates will impact the subsequent colonization or re-colonization success. If we were to know this, then we could strategize stocking and reintroduction schemes to optimize their positive effects. To our knowledge, there have been no analyses to date on the effects of variability in stocking, translocations, or reintroductions in determining establishment success of declining populations.

The probabilities associated with colonization and extirpation of populations are commonly quantified using stochastic differential equations (SDE) and diffusion approximations through Fokker-Planck equations (FPE) (Dennis, 2002; Morris and Doak, 2002; Ovaskainen and Meerson, 2010). Dennis (2002) has used the Fokker-Planck diffusion method (as in Gardiner, 2004) to quantify the probability of a population size *first hitting one arbitrary threshold before another*. Drake and Lodge (2006) have used the same mathematical method of first passage probability to quantify the probability of a population *first becoming a nuisance species before going extinct* using a model that accounts for continuous immigration, and shown that an increase in the rate of immigration increases the probability under stochastic demographic conditions. We call this probability the *EBE probability*, or the probability of population *establishment*

before extinction. However, the impact of *stochasticity in immigration* on the EBE probability has not yet received enough attention.

Here, the *extinction threshold* is defined on the assumption that the species go functionally extinct below a lower population density. Assumption of the existence of such quasi-extinction threshold is standard in population viability analyses (Dennis, 2002; Morris and Doak, 2002). However, when the immigration is continuous and indefinite in time, we note that any population realization that hits even a zero density level (or go extinct) can later replenish from extirpation. Of course, the imposition of ecologically meaningful population thresholds on a model is only an approximation to the more complex full system. It is certainly possible that a population that drops below the extinction threshold can recover through stochastic effects alone.

Taylor and Hasting (2005) have described how a *strong demographic Allee effect* (Courchamp et al., 2008) will force the per capita population growth rate to become negative below a low population size threshold. This threshold, defined as the Allee threshold, also can be used as an extinction threshold for quantifying the EBE probability when the immigration is continued indefinitely. This is because, we note that the negative growth rate caused by the demographic Allee effect due to individuals being unable to replace themselves, can counteract the rate of immigration at low population levels and creates a functional extinction threshold. There is empirical evidence to support the assertion that populations introduced at a level below a demographic Allee threshold tend to go extinct (e.g. Kramer et al., 2008). Kramer et al. (2009) have found substantial evidence for Allee effects in animal populations; 69% of 91 studies. There was conclusive evidence for a component Allee effect, the demographic Allee effect, or both. Twenty two studies showed the presence of the demographic Allee effect, in which, seven showed a critical density below which the population growth rate was negative, that is, the presence of the strong demographic Allee effect. Yet, Gregory et al. (2010) have concluded that there was relatively high potential for

the demographic Allee effects in populations they studied, but only few cases were observed across many taxa.

In the case of declining and extirpated populations, where often the stocking is carried out only until a population either gets established or is gone extinct, we can investigate the impact of stochasticity in stocking on the EBE probability similar to invasive species. Thus, here we define *immigration* broadly as natural and human-mediated introductions through vectors, translocations, relocations, and artificial replenishment of populations through captive breeding and release to habitats.

In the context of invasive species (assuming populations of high fitness, or having large positive intrinsic growth rates given the environment), we investigate how stochasticity in immigration continues to impact the EBE probability of an initial population impulse that exceeded the extinction threshold. In the context of declining populations (assuming populations of low fitness, or having large negative intrinsic growth rates given the environment), we investigate how the stochasticity in stocking or reintroduction continues to impact the EBE probability of an existing population. To make our model realistic we allow for the demographic Allee effect, demographic stochasticity and environmental stochasticity in the population dynamics (see Lande et al., 2004 for details) although our main focus is the impact of stochasticity in immigration.

5.2. Model

First, we analyze a deterministic exponential Allee model for the case where stochasticity is not present in the immigration. Next, we incorporate environmental, demographic, and immigration stochasticity into the model, heuristically, and solve the corresponding Fokker-Planck diffusion equation for the EBE probabilities for the cases with and without stochasticity in immigration under two scenarios: species moving into (A) favourable habitats (i.e., where the intrinsic growth rate is large and positive), for example, colonizing high fitness

populations as in the case of invasive species, and, (B) unfavourable habitats (i.e., where the intrinsic growth rate is large and negative), for example, stocking low fitness populations as in the case of endangered, threatened, or declining populations, or even colonizing low fitness populations.

We solve the Fokker-Planck equation (FPE) for the cases incorporating (i) all three types of stochasticity (environmental, demographic and immigration) using a finite-difference numerical method (Grasselli and Pelinovsky, 2008), and the cases specific to (ii) demographic and immigration stochasticity, and (iii) immigration stochasticity, analytically. We also derive the equation that yields the moments of first passage times for the population first hitting the establishment threshold before the extinction threshold, or the time for EBE, which is not found in the literature, and analyze the impact of stochasticity in immigration on mean time for EBE.

Deriving SDE heuristically from their counterpart deterministic models has been a major concern in theoretical ecology literature. The suitability of the SDE formulations, whether to use Ito (Mao, 1997) or Stratonovich (1963), has been thoroughly discussed by Turelli (1977) followed by Ricciardi (1986), and more recently by Braumann (2007; 2008). Ricciardi (1986) following up on Turelli (1977) has shown that if the system is intrinsically a continuous growth process in a random environment, then it is more appropriate to model it using the Stratonovich formulation followed by appropriate calculus. Goel and Richer-Dyn (2004) have used this approach to investigate stochastic models in biology in the case when the underlying processes are continuous in time. If a process is discrete in time, then the Ito SDE formulation may be more appropriate (Ricciardi, 1986). Population viability analysis models commonly use the Ito formulation (Dennis, 2002; Morris and Doak, 2002), so as the invasive species study by Drake and Lodge (2006). We also used the Ito one. For generality, the results are mathematically comparable regardless of which method is used, so that the specific method may only be relevant when fitting the model to real data to calibrate parameters (Braumann, 2007).

5.2.1. Deterministic population model

We write the growth rate of a population having density x as $dx/dt=f(x)+p$, where $f(x)$ is the average rate of population growth, and p is the mean rate of immigration into the population. Function $f(x)$ can take various linear (e.g., density-independent) and non-linear (e.g., density-dependent) forms.

Here, we do not intend to investigate the case at $x=0$, or at large values limited by the population density. Our modeling focus is to investigate the dynamics of a population far below the level of density dependent regulation. Thus, we take the linearized form of the model near the low population equilibrium (the Allee threshold), where $dx/dt=0$ (Figure 5-1). Thus, the model reduces to a simple Malthusian form, such that, $f(x) = \lambda x - a$, and thus we write $dx/dt = \lambda x - a + p$. Here, λ is the intrinsic growth rate of the population that depends on the individuals' responses to environmental parameters, which was defined as r_m in Fagan et al. (2010). The parameter a is the virtual rate of population loss due to individuals that cannot, on average, replace themselves resulting from the demographic Allee effect (the simplest Allee form described in Gregory, 2010). Depending on whether $\lambda > 0$ (scenario A) demonstrating a high fitness, or $\lambda < 0$ (scenario B) demonstrating a low fitness, we consider that the habitats the species are introduced to, or living in, are either *favourable* or *unfavourable* to the population on average (Sibly and Hone, 2002). Thus, we assume that invading species commonly show $\lambda > 0$, and endangered or declining populations commonly show $\lambda < 0$. We define the net inflow rate to be $j = p - a$. Thus, note that a reduces the per capita growth rate to be negative at low population densities, and p can counteract a as an opposing force to raise the per capita growth rate to be positive (Figure 5-1).

Figure 5-2a illustrates the situation when habitats are favourable ($\lambda > 0$, scenario A). If the demographic Allee effect is strong ($a > p$, scenario A1), then the per capita growth rate becomes negative for populations below the Allee threshold ($x < j/\lambda$), an unstable equilibrium below which the population eventually tends to

zero. For initial values of $x > j/\lambda$, the population tends to any high arbitrary level. We note that when $a < p$ the Allee threshold is removed (scenario A2). Therefore, for the scenario $\lambda > 0$, the Allee threshold exists only if $a > p$.

Figure 5-2b illustrates the situation when habitats are unfavourable ($\lambda < 0$, scenario B). If the Allee effect is weak ($a < p$, scenario B2), then the per capita growth rate becomes positive for small $x < j/\lambda$, and negative for $x > j/\lambda$, with $x = j/\lambda$ be a stable equilibrium. In scenario B1 ($a > p$), the per capita growth rate remains negative as x is varied. Thus, when $\lambda < 0$ (scenario B), the population may persist in a low equilibrium density or tend to zero depending on whether $a < p$ (scenario B2) or $a > p$ (scenario B1), respectively. The low equilibrium density occurs solely due to the forcing by propagules continuously flowing into the system and exceeding the negative growth rate caused by the demographic Allee effect.

The two scenarios above, $\lambda > 0$, and $\lambda < 0$, suggest that if $a > p$ (scenario A1 and B1), we may define a functional extinction threshold that is forced by a strong demographic Allee effect, because the negative net per capita growth rate of a population near zero drives the population to extinction. By way of contrast, scenarios A2 and B2 have positive net per capita growth rates at small population levels. Hence, the idea of a functional extinction threshold does not make sense for scenarios A2 and B2 when the propagule flow is continuous and indefinite. However, in practical situations (such as the stocking of declining populations), assuming the existence of an extinction boundary may make sense for all scenarios, including A2 and B2, as human intervention can halt propagule flow wherever the population hits any arbitrary lower threshold.

Hence, in the context of colonizing populations ($\lambda > 0$), the probability of population *establishing before going extinct* (EBE probability) may have biological relevance limited to scenarios A1. In the context of endangered populations ($\lambda < 0$), if stocking, translocation, or reintroduction is carried out only *until* the population hits either an establishment or a functional extinction

threshold, then EBE probability has a practical relevance in scenarios B1 and B2. However, all the scenarios are worth investigating if our interest is quantifying the probability of a population size *first hitting an arbitrary upper threshold before first hitting an arbitrary lower threshold* (as in Gardiner, 2004).

5.2.2. Stochastic population model

Based on the deterministic counterpart, we modeled the corresponding SDE heuristically, incorporating environmental, demographic and immigration stochasticity. Thus, we write the growth process characterized by the stochastic dynamical equation satisfied by the population x as

$$dx = \alpha(x)dt + \beta(x)dW \quad (5.1)$$

(as in Dennis, 2002). Here, we have the infinitesimal mean of the process, $\alpha(x) = \lambda x + j$, and, $\beta(x) = \sqrt{\sigma_e^2 x^2 + \sigma_d^2 x + \sigma_p^2}$, where $\sigma_e^2 x^2$, $\sigma_d^2 x$ and σ_p^2 are the infinitesimal variances in the population fluctuations corresponding to the environment (see Ricciardi, 1986), demography (see Feller, 1951), and immigration. Here, $dW \sim N(0, dt)$, or is zero correlated Gaussian noise (Dennis, 2002). The differential of the diffusion process of x is formulated in terms of Ito stochastic integral as in Dennis (2002) and Drake and Lodge (2006). Tire and Hanson (1981) studied the case where demographic and environmental stochasticity are incorporated together into a SDE population model, which was later used by Drake and Lodge (2006) to investigate invasive species populations. Here, we further extend the idea to incorporate the immigration stochasticity.

We note that the processes involving propagules flowing into a system, either natural or human-mediated, can be Poisson (e.g., Drury et al., 2007, Jerde and Lewis, 2007). In our paper, we assume this processes to be Gaussian allowing the immigration to be overdispersed. We assume the same properties of stochasticity in immigration in the event of replenishment of declining populations by stocking, translocation or reintroduction. Such assumptions also

simplify the formulation of the SDE into a form that satisfies the FPE, and can be solved analytically for EBE probabilities.

5.2.3. Diffusion approximation for EBE probabilities

We note that the transition probability density $P(x_0, t)$ for a population at *initial* position (x_0) and time $(-t)$, given that the final position and time are *fixed*, for Eq. (5.1), satisfies the backward FPE. Solving the backward FPE, we can calculate the probability of a population remaining between, or exiting two fixed population levels, such as establishment and extinction thresholds. Thus, we can write the backward FPE that satisfies the SDE in Eq. (5.1) as

$$\partial_t P(x_0, -t) = A(x) \partial_x P(x_0, -t) + \frac{1}{2} B(x) \partial_{xx} P(x_0, -t), \quad (5.2)$$

where the diffusion coefficient is $B(x) = 2(\beta_e x^2 + \beta_d x + \beta_p)$, and $2\beta_e = \sigma_e^2$, $2\beta_d = \sigma_d^2$ and $2\beta_p = \sigma_p^2$ are the spectral densities of the zero average Gaussian processes corresponding to environmental, demographic, and immigration stochasticity, and the drift coefficient is $A(x) = \alpha(x)$.

We define $G(x_0)$ broadly as the *probability of the population first hitting an arbitrary upper threshold (x_d) before first hitting an arbitrary lower threshold (x_e)* assuming initial position $x_d > x_0 > x_e$. Here, x_d and x_e can be interpreted as the establishment and the extinction thresholds in the ecological context, and thus, $G(x_0)$ can be defined as the EBE probability. The $G(x_0)$ satisfies the time-homogeneous version of Eq. (5.2). That is,

$$A(x_0) \partial_{x_0} G(x_0) + \frac{1}{2} B(x_0) \partial_{x_0 x_0} G(x_0) = 0 \quad (5.3)$$

with boundary conditions $G(x_d) = 1$, and $G(x_e) = 0$ (Gardiner, 2004). We solve the general case above using a finite-difference numerical method (Grasselli and Pelinovsky, 2008).

The analytical solution for the special case of the FPE in Eq. (5.3), with demographic and immigration stochasticity, yields the EBE probability

$$G(x_0) = \frac{E(x_0) - E(x_e)}{E(x_d) - E(x_e)} \quad (5.4)$$

with initial population size at x_0 . Here, $E(x_i) = (bx_i + c)^k {}_1F_1\left(k, k+1; \frac{-\lambda}{b^2}(bx_i + c)\right)$,

$b \equiv \sigma_d^2/2$, $c \equiv \sigma_p^2/2$, $k = \left(\frac{\lambda c}{b^2} - \frac{j}{b}\right) + 1$, and x_i denotes x_0 , x_e , and x_d . Here, ${}_1F_1$ is

the Kummer confluent hypergeometric function of the first kind (Slater, 1960)

given by ${}_1F_1(a, b, z) = 1 + \frac{az}{b} + \frac{(a)_2 z^2}{(b)_2 2!} + \dots + \frac{(a)_n z^n}{(b)_n n!}$ s.t., $a_n = a(a+1)(a+2)\dots(a+n)$

(see Appendix 5.1 for derivation). An analytical solution for the special case of Eq. 5.3, with immigration stochasticity alone, yields the EBE probability by Eq.

5.4 with $E(x_i) = \text{Erf}_z\left(\frac{j + \lambda x_i}{\sigma_p \sqrt{\lambda}}\right)$ for initial population size at x_0 (see Appendix 5.1

for derivation). Here, Erf_z is the error function (Abramowitz and Stegun, 1972), and x_i takes subscript values $i=0, e, d$.

5.2.4. The point of changing the direction of impact of immigration stochasticity on EBE probability

The point at which the direction of impact of stochasticity in immigration

on the EBE probability switches, satisfies the condition $\frac{\partial G(x_0)}{\partial \sigma_p} = 0$. Thus for the

case where immigration stochasticity alone is present (Eq. 5.4), the equation to be satisfied by the parametric combination is given by

$$\left(\frac{(j + \lambda x_0)e^{k_0} - (j + \lambda x_e)e^{k_e}}{(j + \lambda x_d)e^{k_d} - (j + \lambda x_e)e^{k_e}}\right) - \left(\frac{E(x_0) - E(x_e)}{E(x_d) - E(x_e)}\right) = 0. \quad (5.5)$$

Here, $k_i = \frac{(j + \lambda x_i)^2}{\lambda \sigma_p^2}$, and $E(x_i) = \text{Erf}_z \left(\frac{j + \lambda x_i}{\sigma_p \sqrt{\lambda}} \right)$, with subscript values $i=0, e, d$.

Here, Erf_z is the error function (Abramowitz and Stegun, 1972), and x_i takes subscript values $i=0, e, d$.

5.2.5. First passage time

We define $T_n(x_d, x_0)$ as the n^{th} moment of the first passage time, given that the population size first hits an arbitrary upper threshold, x_d , before an arbitrary lower threshold, x_e . As before, x_d and x_e can be interpreted as establishment and extinction boundaries in ecology, thus $T_n(x_d, x_0)$ can be defined as the n^{th} moment of first passage time for EBE assuming the initial position of the population size is at $x_d > x_0 > x_e$.

Thus, the function $T_n(x_d, x_0)$ satisfies

$$A(x_0) \partial_{x_0} G(x_0) T_n(x_d, x_0) + \frac{1}{2} B(x_0) \partial_{x_0 x_0} G(x_0) T_n(x_d, x_0) = -n G(x_0) T_{n-1}(x_d, x_0) \quad (5.6)$$

(see Appendix 5.2 for the derivation). The boundary condition at $x_0 = x_d$ is determined by $G(x_d) = 1$, $T_n(x_d, x_d) = 0$, and hence giving $G(x_d) T_n(x_d, x_d) = 0$. The boundary condition at $x_0 = x_e$ is determined by $G(x_e) = 0$, and hence giving $G(x_e) T_n(x_d, x_e) = 0$. The cases $n=1,2$ yield the mean and the second moment of first passage times, respectively. Thus, the above equation for the special case $n=1$ yields the mean time for EBE, which is given in Gardiner (2004). However, the general equation given in Eq. (5.6) with the boundary conditions is not found in the literature.

We solve the mean time for EBE iteratively using a finite-difference numerical method (Grasselli and Pelinovsky, 2008) by incorporating the solutions given in Eq. (5.4) for $G(x_0)$ in Eq. (5.6).

5.3. Results

Solutions to the time-homogeneous Eq. (5.3), based on the range of parameter values given, show that increased stochasticity in immigration decreases the EBE probability for populations of high fitness, or populations introduced to favourable habitats ($\lambda > 0$) (e.g. invasive populations) (Figure 5-3). Increased stochasticity in immigration increases the EBE probability of populations in low fitness, or in unfavourable habitats ($\lambda < 0$) (e.g. declining populations) further amplifying the effect caused by the environmental and demographic stochasticity on the EBE probability. The effect is generally higher at low-moderate environmental and demographic stochasticity, and greater when the initial population size is nearing the extinction threshold for $\lambda > 0$, and greater when the initial population size is nearing the establishment threshold for $\lambda < 0$ (Figure 5-4).

Figure 5-5a shows that the stochasticity in immigration, based on the range of parameter values given, decreases the EBE probability for scenario B2 ($\lambda < 0, j > 0$) when j is large and positive (for e.g., resulting from large p compared to demographic Allee effect a), given that stocking is ceased when the population hits a threshold. Stochasticity in immigration increases the EBE probability when j is large and negative (for e.g., resulting from large a compared to p).

However, Figure 5-5b shows that the point at which the direction of the impact of stochasticity in immigration on EBE probability changes sign is shifting towards negative λ given that j is positive and large, and shifting towards positive λ given that j is negative and large. This suggests that the direction of the impact of stochasticity in immigration on EBE probability cannot be determined by the

sign of the intrinsic growth rate or the net propagule flow j alone when their signs are opposite.

Figure 5-6, drawn based on the cases satisfying Eq. (5.5), indicates that the stochasticity in immigration decreases the EBE probability when $\lambda > 0$ and $j > 0$ (scenario A2), or, when j is positive and large enough compared to negative λ , or λ is positive and large enough compared to negative j . That is, in general, when the net population growth rate remains positive. The stochasticity in immigration increases the EBE probability when $\lambda < 0$ and $j < 0$, or when λ is negative and large enough compared to positive j , or j is negative and large enough compared to positive λ . That is, in general, when the net population growth rate remains negative. Thus, we note that when λ and j have opposite signs, we cannot predict the direction of the impact of immigration stochasticity on the EBE probability by examining their signs alone unless we calculated the critical point at which the switching occurs.

It follows that, in general, when the EBE probability becomes large, either due to comparatively large and positive intrinsic growth rate, or large and positive mean immigration rate, the stochasticity in immigration tends to decrease the EBE probability. When the EBE probability becomes small due to comparatively large and negative intrinsic growth rate or low immigration rates with large Allee effect, then the stochasticity in immigration tends to increase the EBE probability.

Figure 5-7, drawn based on Eq. (5.6), indicates that the log mean time for EBE decreases when the immigration is stochastic, regardless of whether the population is introduced to, or existing in a favourable ($\lambda > 0$) or an unfavourable ($\lambda < 0$) habitat. This effect, simulated for the case with environmental stochasticity, is qualitatively the same had we incorporated the demographic stochasticity.

5.4. Discussion

Our results show that, in general, the *stochasticity* in high immigration rates, exceeding the demographic Allee effect, decreases the *establishment before*

extinction (EBE) probability of populations that are of high fitness, or introduced to favourable habitats, or having high positive intrinsic growth rates ($\lambda > 0$), such as the colonizing invasive populations. Thus, it counteracts the increased EBE probability due to high mean immigration rates shown by Drake and Lodge (2006). This decreased EBE probability is further decreased by the environmental and the demographic stochasticity. The decrement is larger when the population is moderately closer to the extinction threshold. However, the impact of *stochasticity* in low immigration rates, if lower than the demographic Allee effect, on the EBE probability depends on how favourable is the habitat to the population, or how large is the positive λ .

In declining populations, where $\lambda < 0$, the *stochasticity* in low immigration rates increases the EBE probability. Gonzales and Holt (2002) have shown a similar effect of immigration stochasticity at low immigration rates on reinforcing populations in ecological sinks. However, if the immigration rate is large, exceeding the demographic Allee effect, then the impact of the stochasticity in immigration depends on how unfavourable is the habitat to the population, or how large is the negative λ .

However, we indicated that the EBE probability can be defined ecologically meaningfully when the demographic Allee effect (if exists) exceeds the immigration rate allowing a functional extinction threshold to exist, or otherwise, if the immigration can be stopped by an intervention after the population reached a lower threshold below which the extinction is the most likely scenario. If the immigration rate exceeds the demographic Allee effect removing the existence of a functional extinction threshold, continuation of immigration then results in the population to replenish from any lower threshold driving the population to become colonized eventually. As we have little control over the invasive species propagating into new habitats, especially in the cases such as propagules of marine invasive copepods discharged to ecologically favourable habitats through ship ballast water (Cordell et al., 2008; 2009), the above scenario of inevitable-colonization can often be a reality. Under such

scenario, what remains to be of any interest is the mean time for the population to establish (Potapov and Rajakaruna, 2013).

The impact of stochasticity in immigration on the EBE probability is qualitatively and quantitatively the same as the probability of a population *first hitting an arbitrary upper threshold before an arbitrary lower threshold* regardless of the knowledge of the ecological nature of the boundaries. Thus, the results of the EBE probabilities are the same as the first passage probabilities. It follows that if the immigration of invasive species is made to fluctuate by human-mediation, while keeping the average immigration rate be the same, then we expect the chance that the population first reaching a high population level (and get established) before a low level (and go extinct) would be less than the case had the flow of propagules been steady (or uniform, or without stochasticity). However, if a functional extinction threshold did not exist (at the given rate of immigration and the demographic Allee effect), then the population eventually gets colonized inevitably regardless of the fluctuations we would create in the flow of propagules or in the immigration. Therefore, an advantage for an invasive species management will be the case if an extinction threshold does exist without our knowledge. Thus, implementing strategies to fluctuate the expected propagule flow (as opposed to keeping it steady or uniform) regardless of the knowledge of the existence of an extinction threshold seems benevolent to the management as it creates a chance to reduce the probability of invasive population hitting high thresholds creating windows for establishment.

Hence, the impact of stochasticity in immigration on colonization may be incorporated into the decision-making formula for stochastic controlling of invasions. For example, invasive marine species propagated through ship ballast-water can be managed optimally through stochastic monitoring and stochastic treatment efforts: mid oceanic exchange of ship ballast-water (NOAA, 2007; Simard et al., 2011), chemical treatments (Nanayakkara et al., 2011) and temperature treatments of ballast-water tanks (Quilez-Badia et al., 2008). Although, the policies can be designed and implemented to lower the mean

discharge rate of propagules, as an alternative, the same result can be theoretically obtained by increasing the stochasticity in the propagule flow rate while keeping the mean discharge rate the same. This stochastic control strategy can produce high benefits (effects) over costs ratio by deploying the same resources, incurring the same costs, while increasing the effect, as an alternative to reducing the mean discharge rate.

The idea of stochastic monitoring and treatment suggests random checking and treatment of ship-ballast water discharged by the ships with variable intensity. While monitoring and treatment reduce the propagule flow rate, random monitoring and treatment enhances the stochastic effect of propagule flow rate, thereby decrease the EBE probability of invasives compared to the case where monitoring and treatment is uniform. Therefore, if we keep the cost of the resources deployed for random checking and treatment as same as the case of uniform checking and treatment, then the random approach should be more cost effective. This is a hypothesis we could test based on the model prediction.

Programs are implemented to stock or reintroduce declining populations through captive breeding and release, and artificially replenish populations before they go extinct (Bell et al., 2008; Fraser, 2007; Seddon et al., 2007). Our results indicate that increased stochasticity in stocking (or translocations, or reintroductions) increases the EBE probability in declining populations under stochastic environments and demographic conditions compared to the case when stocking is steady (or uniform), given that either the intrinsic growth rate is large and negative, or the stocking rate lower than the demographic Allee effect. This effect is stronger when the population is nearing the establishment threshold.

However, when the mean stocking rate becomes large resulting in a high EBE probability, then the stochasticity, in turn, can decrease the EBE probability. This suggests that the direction of the impact of stochasticity in stocking on the EBE probability depends on the mean rate of stocking in relation to the demographic Allee effect and the intrinsic growth rate of the population. Thus, if we are to make a decision as to whether to amplify or de-amplify the stochasticity

in stocking in order to increase the EBE probability under practical circumstances, then we will need to assess the critical point at which the direction of the impact on EBE switches as we have shown under the results section. However, it may be more effective to begin reintroductions with regulated stochasticity, and later turn it into a steady flow with subsequent increase in population densities. Under the right conditions, increasing the stochasticity at a low average stocking rate may be a low cost strategy compared to increasing the average stocking rate, as both may yield the same result.

Studies that quantified the effect of stochasticity in reintroductions, translocations, or stocking on population establishment success have not been found in the literature. Apparently, some data in reintroduction and stocking studies (e.g., Verspoo and Leaniz, 1997; Shute et al., 2005) show unplanned variations in the release of propagules. Shute et al. (2005) indicated reintroduction success of 4 species of fishes in Abrams Creek, Tennessee, apparently indicating high variations in stocking. Similarly, Verspoo and Leaniz (1997) indicated stocking success of Scottish Atlantic salmon in two Spanish rivers. Yet, their data do not seem to have enough information to be able to test the effect of stochasticity in immigration on the establishment success. A well-designed experiment can be implemented to test our hypothesis more concretely.

We have also found that the stochasticity in immigration decreases the mean time for a population to *establish before going extinct* (mean time for EBE) for both high and low fitness populations. Potapov and Rajakaruna (2013) show a scenario where populations *tunnel* to establishment through otherwise impossible strong Allee effect by means of stochasticity in low immigration rates. If not for the stochasticity in immigration, environmental or demographic, they show that populations having strong Allee effect can never colonize at small rates of immigration. Stochasticity can mask the Allee effect in the measurements manifesting in the populations without the Allee effects.

Thus, the management of invasive species has an interesting theoretical trade-off as to whether to lower the EBE probability, and thus risks, by increasing the immigration stochasticity, or to increase the mean time for the population to

establish by decreasing the immigration stochasticity after a population is detected in a novel habitat. In the case of stocking declining populations, we have observed that an increase in stochasticity in stocking decreases the mean time for the population to establish. Thus, such strategy is also complementing the increase in probability of the population *establishing before going extinct* when the mean stocking rate is low. However, care must be taken because the risks of these decisions are high as the mean stocking rate can become large without our knowledge far exceeding the demographic Allee effect, thus causing the stochasticity in stocking to eventually suppress the EBE probability. The knowledge of the critical point at which the impact on the EBE probability switches direction is crucial in making those decisions. However, we need to test our hypotheses using empirical studies before application.

In a nutshell, the study suggests that stochasticity in immigration, together with environmental and the demographic stochasticity, suppresses the colonization success of invading populations, yet increases the reestablishment success of declining populations in general. Either way, it seems to serve the interests of the ecological management, and helps producing low cost strategies.

Further developments may include improving the model to reflect periodic variation in environmental forcing factors with stochasticity in immigration, which may be a scenario much evident in marine habitats. It may enable us to analyze the stochastic impacts on the cases with time-dependent introductions.

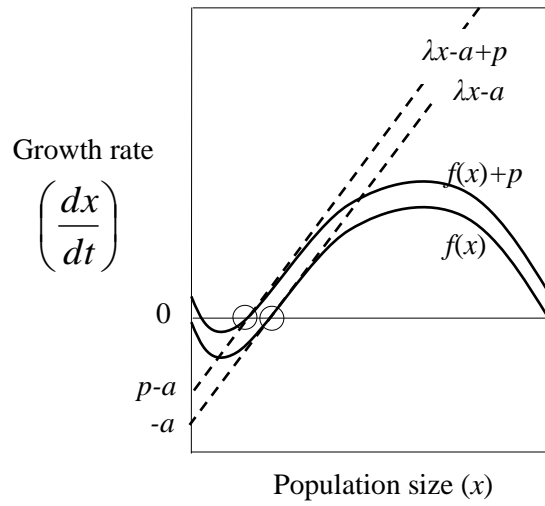
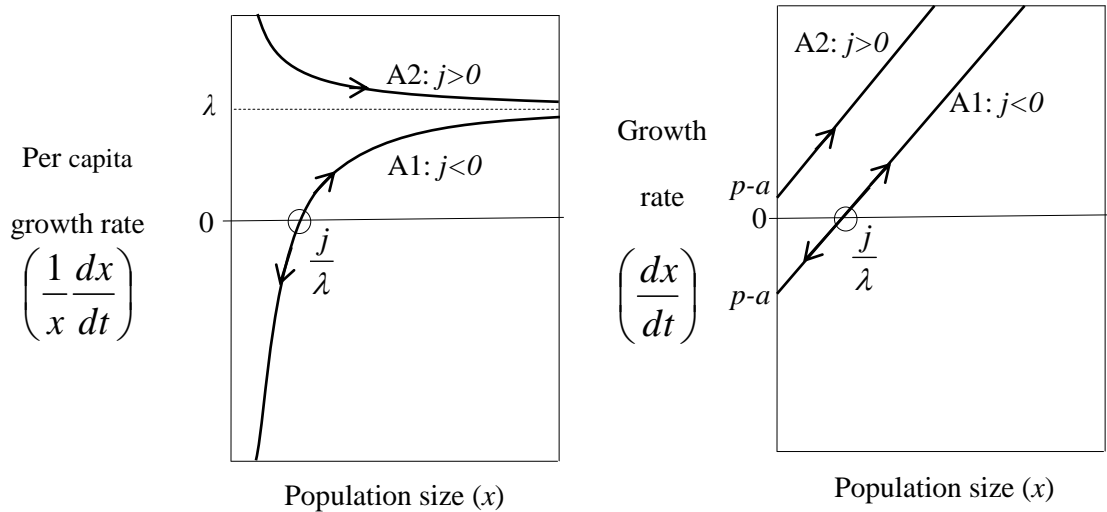
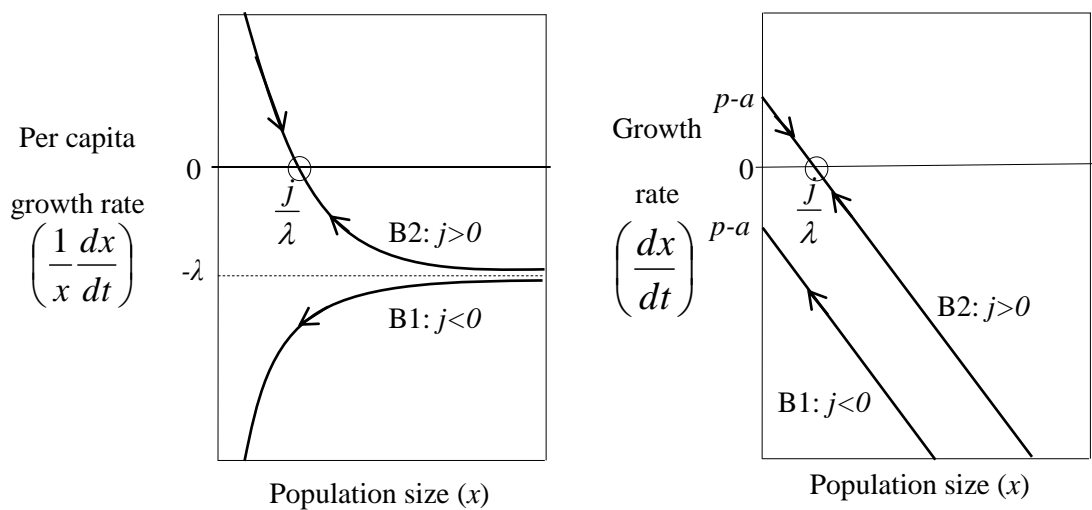


Figure 5-1 Population models $\frac{dx}{dt} = f(x)$, and, $\frac{dx}{dt} = f(x) + p$, with dashed lines for the cases linearized at $\frac{dx}{dt} = 0$.



a) Scenario A (favourable habitats where $\lambda > 0$)



b) Scenario B (unfavourable habitats where $\lambda < 0$)

Figure 5-2 Dynamics of deterministic population model $\frac{1}{x} \frac{dx}{dt} = \lambda + \frac{j}{x}$ when net-flow rates (j) and intrinsic growth rates (λ) are positive and negative. Here, $j=p-a$.

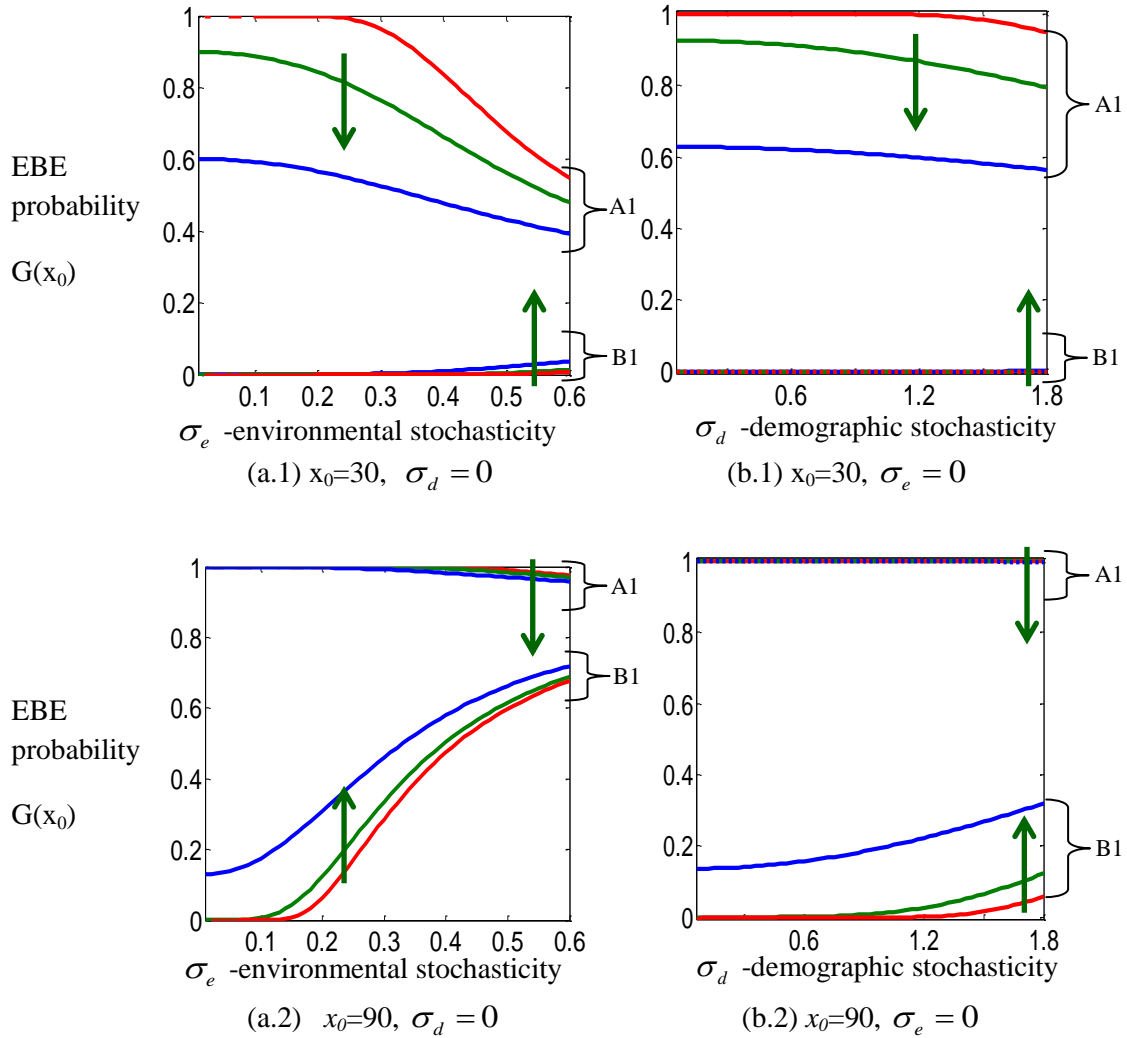


Figure 5-3 Probability of population *establishment before extinction*, $G(x_0)$, with respect to increasing (a) environmental stochasticity, and (b) demographic stochasticity. Initial population size is at x_0 . Net propagule flow rate $j=-4$ (such that $p < a$). (A1) favourable habitats ($\lambda=0.4$); (B1) unfavourable habitats ($\lambda=-0.4$). Red: propagule flow, $\sigma_p = 0$ (that is, without propagule flow stochasticity); green: $\sigma_p = 10$; blue: $\sigma_p = 20$. Other parameters are: extinction threshold $x_e=10$, establishment threshold $x_d=100$. Arrows show the direction of the impact of stochasticity in propagule flow on the EBE probability.

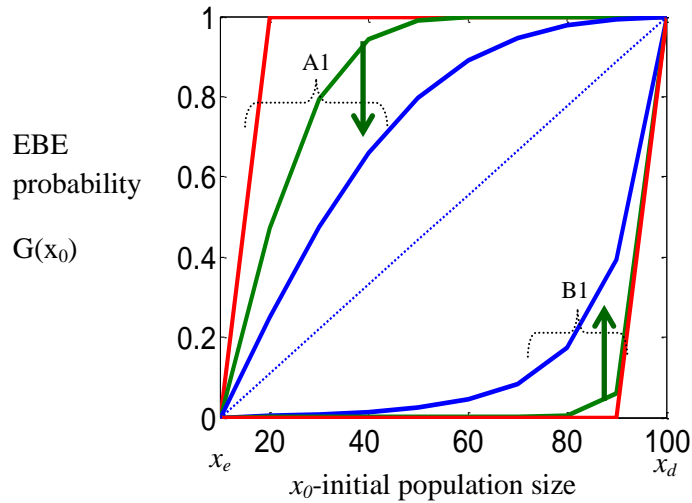


Figure 5-4 Probability of population *establishment before extinction*, $G(x_0)$, with respect to increasing initial population size at x_0 . (A1) favourable habitats ($\lambda=0.4$), (B1) unfavourable habitats ($\lambda=-0.4$). Net propagule flow rate $j=-4$ (such that $p < a$). Red: propagule flow, $\sigma_p = 0$ (that is, without propagule flow stochasticity); green: $\sigma_p = 10$; blue: $\sigma_p = 20$. Other parameters are: environmental stochasticity, $\sigma_e = 0$, demographic stochasticity $\sigma_d = 0$, extinction threshold $x_e=10$, establishment threshold $x_d = 100$. Probability converges to the diagonal dotted line for higher σ_p . Note that for the case of propagule flow stochasticity alone is present, $G(x_0) \rightarrow \left(\frac{x_0 - x_e}{x_d - x_e} \right)$, which is the diagonal line, for $\sigma_p \rightarrow \infty$ (Appendix 5.1). Arrows show the direction of the impact of stochasticity in propagule flow on the EBE probability.

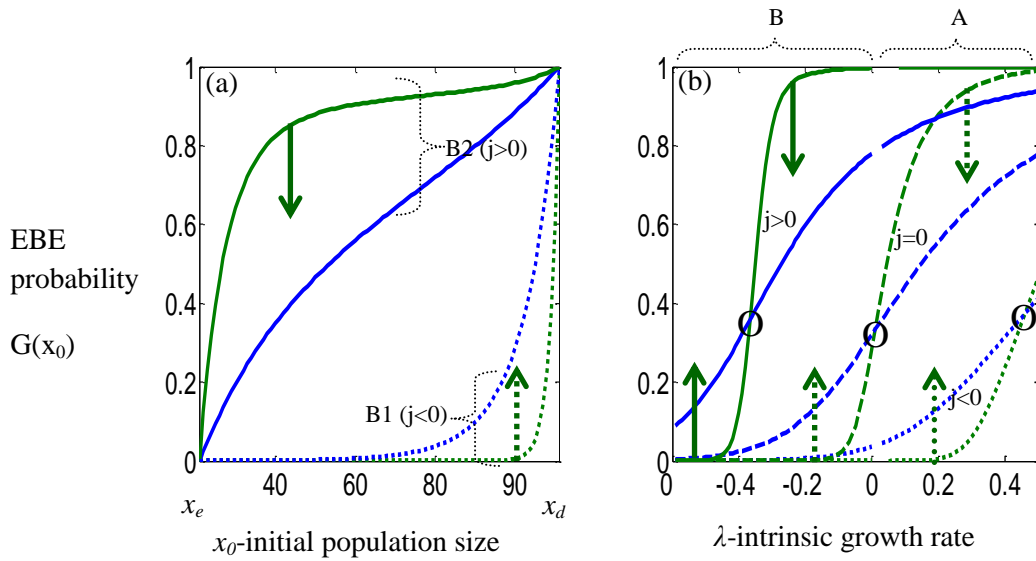


Figure 5-5 (a) Probability of population *establishment before extinction*, $G(x_0)$, with respect to increasing initial population size. Here, $j=-20$ (dotted lines, such that $p<a$: scenario 1), and $j=20$ (solid lines, such that $p>a$: scenario 2), $\lambda=-0.3$. green: $\sigma_p = 10$; blue: $\sigma_p = 20$. This shows the effect of stochasticity in propagule flow on the EBE probability when j is turning to positive ($p>a$) from negative ($p<a$), that is when p is increased from a small value given that the demographic Allee effect, a , is fixed. (b) $G(x_0)$ with respect to intrinsic growth rate for the same scenarios as above, with $x_0=40$. Dashed lines depict the case for $j=0$ (that is, $p=a$). Circled are the points at which the direction of the impact of propagule flow stochasticity on the EBE probability changes sign. For both illustrations above, the other parameters are: environmental stochasticity, $\sigma_e = 0$, demographic stochasticity $\sigma_d = 0$, extinction threshold $x_e=10$, establishment threshold $x_d=100$. Arrows show the direction of the impact of stochasticity in propagule flow on the EBE probability.

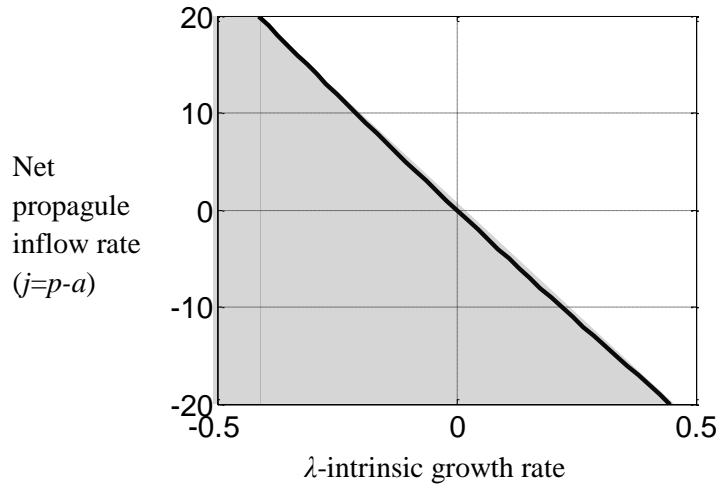


Figure 5-6 The solid line (which is slightly non-linear) depicts the parametric combination of intrinsic growth rate (λ) and net propagule flow rate (j) at which the direction of the impact of stochasticity in propagule flow on EBE probability changes sign satisfying Eq. (5.5). Shaded area depicts the combinations where the stochasticity in propagule flow increases the EBE probability, non-shaded area depicts where it decreases the EBE probability. When λ and j take opposite signs, whether the EBE probability increases or decreases depends on their specific values. The other parameters are: environmental stochasticity, $\sigma_e = 0$, demographic stochasticity, $\sigma_d = 0$, propagule flow stochasticity, $\sigma_p = 5$, extinction threshold $x_e=10$, establishment threshold $x_d=100$.

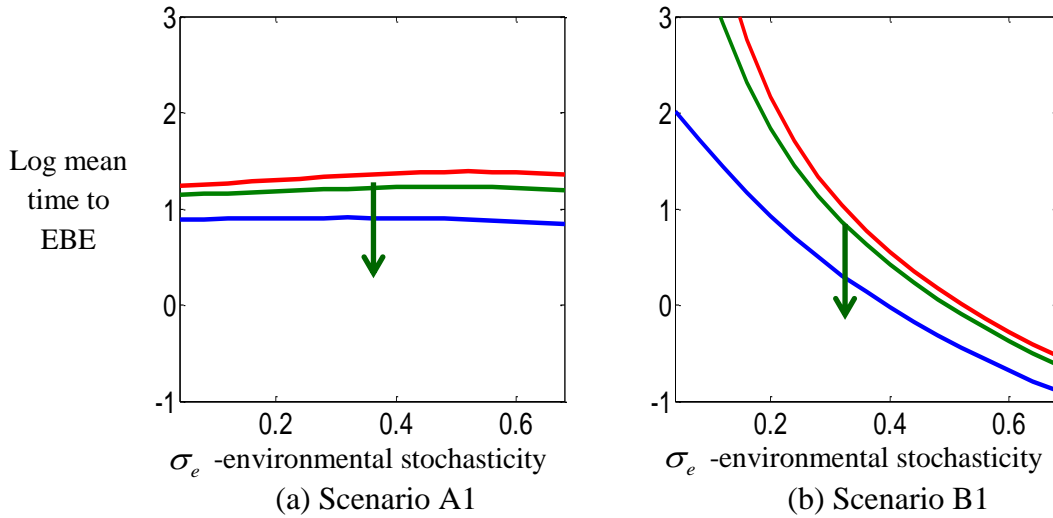


Figure 5-7 Mean time for population *establishment before extinction*, $T_n(x_d, x_0)$, with respect to increasing environmental stochasticity. (a) In favourable habitats ($\lambda=0.4$, $x_0=30$). (b) In unfavourable habitat ($\lambda=-0.4$, $x_0=90$). Red: propagule flow stochasticity, $\sigma_p = 5$; blue: $\sigma_p = 10$; green: $\sigma_p = 20$. Other parameters are: extinction threshold $x_e=10$, establishment threshold $x_d=100$, and net propagule flow rate $j=-4$. Arrows show the direction of the impact of stochasticity in propagule flow on log mean time to EBE.

5.5. References

Abramowitz, M., and Stegun, I.A., 1972. Handbook of Mathematical Functions with Formulas, Graphs, and Mathematical Tables. Dover, New York, p. 260.

Armstrong, D.P., Seddon, P.J., 2007. Directions in reintroduction biology. *TRENDS in Ecology and Evolution* 23(1), 20-25.

Bell, J., Leber, K.M., Blankenship, H.L., Loneragan, N.R., Masuda, R. 2008. A new era for restocking, stock enhancement and sea ranching of coastal fisheries resources. *Reviews in Fisheries Science* 16(1-3), 1-9.

Braumann, C.A., 2007. Ito versus Stratonovich calculus in random population growth. *Mathematical Biosciences* 206, 81-107.

Braumann, C.A., 2008. Growth and extinction of populations in randomly varying environments. *Computers and Mathematics with Applications* 56(3), 631-644.

- CAISN, 2011. Canadian Aquatic Species Network, Retrieved from: <http://www.caissn.ca/en/research-overview.php>.
- Colautti, R.I., MacIsaac, H.J., 2004. A neutral terminology to define 'invasive' species. *Diversity and Distributions* 10, 135–141.
- Colautti, R.I., Grigorovich, I.A., MacIsaac, H.J., 2006. Propagule pressure: a null model for biological invasions. *Biological Invasions* 8(5), 1023-1037.
- Cordell, J.R., Bollens, S.M., Draheim, R., Sytsma, M. 2008. Asian copepods on the move: recent invasions in the Columbia-Snake River system. *ICES Journal of Marine Science* 65(5), 753-758.
- Cordell, J.R., Lawrence, D.J., Ferm, N.C., Tear, L.M., Smith, S.S., Herwig, R.P., 2009. Factors influencing densities of non-indigenous species in the ballast water of ships arriving at ports in Puget Sound, Washington, United States. *Aquatic Conservation: Marine and Freshwater Ecosystems* 19, 322–343.
- Courchamp, F., Berec, L., Gascoigne, J., 2008. *Allee Effect in Ecology and Conservation*. Oxford University Press, p. 272.
- Czech, B., Krausman, P., 1997. Distribution and causation of species endangerment in the United States. *Science* 277, 22.
- Dennis, B., 2002. Allee effect in stochastic populations, *Oikos* 96, 389-401.
- Drake, J.M., Lodge, D.M., 2006. Allee effect, propagule-flow and the probability of establishment: risk analysis for biological invasions, *Biological Invasions* 8, 365-375.
- Drury, K.L.S., Drake, J.M., Lodge, D.M., Dwyer, G., 2007. Immigration events dispersed in space and time: Factors affecting invasion success, *Ecological Modeling* 206(1-2), 63-78.
- Fagan, W.F., Lynch, H.J., Noon, B.R., 2010. Pitfalls and challenges of estimating population growth rate from empirical data: consequences for allometric scaling relations. *Oikos* 119, 455–464.
- Feller, W., 1951. Diffusion process in genetics. *Proceedings of Second Berkeley Symposium on Mathematics, Statistics and Probability*, p. 227-246.
- Finnoff, D., Potapov, A., Lewis, M.A., 2010. Control and the management of a spreading invader. *Resource and Energy Economics* 32, 534–550.
- Fraser, D.J., 2007. How well can captive breeding programs conserve biodiversity? A review of salmonids. *Evolutionary Applications* 1(4), 535-586.
- Gardiner, C.W., 2004. *Handbook of Stochastic Methods: for Physics, Chemistry and the Natural Sciences*. Springer-Verlag, NY, p. 80-143.
- Godefroid, S., Piazza, C., Rossi, G., Buord, S., Stevens, A.D., Aguraiuja, R., Cowell, C., Weekley, C.W., Vogg, G., Iriondo, J.M., Johnson, I., Dixon, B., Gordon, D., Magnanon, S., Valentin, B., Bjureke, K., Koopman, R., Vicens, M., Virevaire, M.,

- Goel, N.S., Richter-Dyn, N., 2004. *Stochastic Models in Biology*. Academic Press, NY, p.73-99.
- Gonzalez, A., Holt, R.D., 2002. The inflationary effects of environmental fluctuations in source–sink system, *Proceedings of the National Academy of Sciences* 99(23), 14872-14877.
- Grasselli, M., Pelinovsky, D., 2008. *Numerical Mathematics*. Johnes and Bartlett Publishers, Toronto, p. 511-574.
- Gregory, S.D., Bradshaw, C.J.A., Brook, B.W., Courchamp, F., 2010. Limited evidence for the demographic Allee effect from numerous species across taxa. *Ecology* 91(7), 2151–2161.
- IUCN, 2010. *Global Re-introduction Perspectives: Additional case-studies from around the globe*, IUCN/SSC Re-introduction Specialist Group & Environment Agency-ABU DHABI, p. 349.
- Jerde, C.L., Lewis, M.A., 2007. Waiting for Invasions: A Framework for the Arrival of Nonindigenous Species. *American Naturalist* 170(1), 1-9.
- Keller, R.P., Lodge, D.M., Finnoff, D.C., 2007. Risk assessment for invasive species produces net bioeconomic benefits. *PNAS* 104(1), 203-207.
- Kramer, A., Sarnelle, O., Knapp, R.A., 2008. Allee effect limits colonization success of sexually reproducing zooplankton. *Ecology* 89, 2760–2769.
- Kramer, A.M., Dennis, B., Liebhold, A.M., Drake, J.M., 2009. The evidence for Allee effects. *Population Ecology* 51, 341–354.
- Lande, R., Engen, S., Saether, B.H., 2004. *Stochastic Population Dynamics in Ecology and Conservation*. Oxford University Press, Oxford, p. 220.
- Lockwood, J.L., Cassey, P., Blackburn, T., 2005. The role of propagule flow in explaining species invasions, *Trends in Ecology and Evolution* 20, 223-228.
- Lorenzen, K., Leber, K.M., Blankenship, H.L. 2010. Responsible approach to marine stock enhancement: An update. *Reviews in Fisheries Science* 18(2), 189–210.
- Lovell, S.J., Stone, S.F., Fernandez, L., 2006. The economic impacts of aquatic invasive species: A review of the literature. *Agricultural and Resource Economics Review* 35(1): 195–208.
- Mao, X., 1997. *Stochastic Differential Equations and Applications*. Horwood Publishing Limited, England, p 294.
- Morris, W.F., Doak, D.F., 2002. *Quantitative Conservation Biology: Theory and Practice of Population Viability Analysis*, Sinauer Associates, Inc. Publishers, p. 480.
- Nanayakkara, K.G.N., Zheng, Y., Alam, A.K.M.K., Zou, S., Chen, J.P., 2011. Electrochemical disinfection for ballast water management: Technology development and risk assessment. *Marine Pollution Bulletin* 63, 119–123.

- NOAA, 2007. Current State of Understanding about the Effectiveness of Ballast Water Exchange (BWE) in Reducing Aquatic Nonindigenous Species (ANS) Introductions to the Great Lakes Basin and Chesapeake Bay, USA: Synthesis and Analysis of Existing Information, Technical Memorandum GLERL-142, National Oceanic and Atmospheric Administration, p. 127.
- Noël, F., Prati, D., van Kleunen, M., Gygax, A., Moser, D., Fischer, M., 2011. Establishment success of 25 rare wetland species introduced into restored habitats is best predicted by ecological distance to source habitats. *Biological Conservation* 144, 602–609.
- Olenin, S., Elliott, M., Bysveen, I., Culverhouse, P.F., Daunys, D., Dubelaar, G.B.J., Gollasch, S., Gouletquer, P., Jelmert, A., Kantor, Y., Mezeth, K.B., Minchin, D., Occhipinti-Ambrogi, A., Olenina, I., Vandekerckhove, J., 2011. Recommendations on methods for the detection and control of biological pollution in marine coastal waters. *Marine Pollution Bulletin* 62 (12), 2598–2604.
- Ovaskainen, O., Meerson, B., 2010. Stochastic models of population extinction. *Trends in Ecology and Evolution* 25(11), 643–652.
- Paragamian, V.L., Hansen, M.J., 2011. Stocking for rehabilitation of burbot in the Kootenai River, Idaho, USA and British Columbia, Canada. *Journal of Applied Ichthyology* 27 (S.1), 22–26.
- Pimentel, D., 2009. Invasive plants: Their role in species extinctions and economic losses to agriculture in the USA, In: Intergit (Ed.), *Management of Invasive weeds*. Springer, p. 1–7.
- Polyanin, A.D., Zaitsev, V.F. 2003. *Hand book of exact solutions to ordinary differential equations*. Chapman and Hall/CRC, p. 455.
- Potapov, A., Rajakaruna, H., 2013. Allee threshold and stochasticity in biological invasions: Colonization time at low propagule pressure, *Journal of Theoretical Biology*. <http://dx.doi.org/10.1016/j.jtbi.2013.07.031>.
- Quilez-Badia, G., McCollin, T., Josefsen, K.D., Vourdashas, A., Gill, M.E., Mesbahi, E., Frid, C.L.J., 2008. On board short-time high temperature heat treatment of ballast water: A field trial under operational conditions. *Marine Pollution Bulletin* 56, 127–135.
- Rasmussen, J.E., Belk, M.C., Pec, S.L., 2009. Endangered species augmentation: a case study of alternative rearing methods. *Endangered Species Resources* 8, 225–232.
- Ricciardi, L.M., 1986. Stochastic population theory: Diffusion processes, In: Hallam, T.G., Levin, S.A. (Eds.), *Mathematical Ecology: An Introduction*. Springer-Verlag, New York, p. 191–236.
- Sanderson, B.L., Barnas, K.A., Rub, A.M.W., 2009. Nonindigenous species of the Pacific Northwest: An overlooked risk to endangered salmon? *BioScience* 59, 245–256.
- Sarnelle, O., Knapp, R.A., 2004. Zooplankton recovery after fish removal: limitations of the egg bank. *Limnology and Oceanography* 49, 1382–1392.

- Schaub, M., Zink, R., Beissmann, H., Sarrazin, F., Arlettaz, R., 2009. When to end releases in reintroduction programmes: demographic rates and population viability analysis of bearded vultures in the Alps. *Journal of Applied Ecology* 46, 92–100.
- Schooley, J.D., Marsh, P.C., 2007. Stocking of endangered razorback suckers in the lower Colorado river basin over three decades: 1974-2004. *North American Journal of Fisheries Management* 27(1), 43-51.
- Seddon, P.J., 2010. From reintroduction to assisted colonization: Moving along the conservation translocation spectrum. *Restoration Ecology* 18(6), 796–802.
- Seddon, P.J., Armstrong, D.P., Maloney, R.F., 2007. Developing the science of reintroduction biology. *Conservation Biology* 21(2), 303–312.
- Sheean, V.A., Manning, A.D., Lindenmayer, D.B., 2011. An assessment of scientific approach towards species relocation in Australia, *Austral Ecology* 37, 204–215.
- Shute, J.R., Rakes, P.L., Shute, P.W., 2005. Reintroduction of Four Imperiled Fishes in Abrams Creek, Tennessee. *South Eastern Naturalist* 4(1), 93–110.
- Sibly, R.M., Hone, J., 2002. Population growth rate and its determinants: An overview. *Philosophical Transactions of Royal Society B* 357, 1153–1170.
- Simard, N., Plourde, S., Gilbert, M., Gollasc, S., 2011. Net efficacy of open ocean ballast water exchange on plankton communities. *Journal of Plankton Research* 33 (9), 1378-1395.
- Simberloff, D., 2009. The role of propagule pressure in biological invasions. *Annual Review of Ecology Evolution and Systematics* 40, 81–102.
- Slater, L.J., 1960. *Confluent Hypergeometric Functions*. Cambridge Univ. Press, p. 247.
- Snyder, N.F.R., Derrickson, S.R., Beissinger, S.R., Wiley, J.W., Smith, T.B., Toon, W.D., Miller, B., 1996. Limitations of captive breeding in endangered species recovery. *Conservation Biology* 10(2), 338-348.
- Sorte, C.J.B., Williams, S.L., Carlton, J.T., 2010. Marine range shifts and species introductions: Comparative spread rates and community impacts. *Global Ecology and Biogeography* 19, 303–316.
- Stratonovich, R.L., 1963. Topic in Theory of random Noise, Vol I. Gordon and Breach, NY, p. 610.
- Taylor, C.M., Hasting, A., 2005. Allee effect in biological invasions. *Ecological Letters* 8, 895-908.
- Thomas, G.R., Taylor, J., de Leaniz, C.G., 2010. Captive breeding of the endangered freshwater pearl mussel *Margaritifera margaritifera*. *Endang. Species. Res.* 12, 1–9.
- Tier, C., Hanson, F.B., 1981. Persistence in density dependent stochastic populations. *Mathematical Bioscience* 53, 89-117.
- Turelli, M. 1977. Random environments and stochastic calculus, *Theoretical Population Biology* 12, 140-178.

- Vale'ry L., Fritz, H., Lefeuvre, J., Simberloff, D., 2008. In search of a real definition of the biological invasion phenomenon itself. *Biological Invasions* 10, 1345–1351.
- Vanderborght, T., 2011. How successful are plant species reintroductions? *Biological Conservation* 144, 672–682.
- Verspoor, E., de Lea'niz, C.G., 1997. Stocking success of Scottish Atlantic salmon in two Spanish rivers. *Journal of Fish Biology* 51, 1265–1269.
- Vincenzi, S., Crivelli, A.J., Jesensek, D., de Leo, G.A., 2012. Translocation of stream-dwelling salmonids in headwaters: insights from a 15-year reintroduction experience. *Reviews of Fish Biology and Fisheries* 22, 437–455.
- Wada, T., Yamada, T., Shimizu, D., Aritaki, M., Sudo, H., Yamashita, Y., Tanaka, M., 2010. Successful stocking of a depleted species, spotted halibut *Verasper variegatus*, in Miyako Bay, Japan: evaluation from post-release surveys and landings, *Marine Ecological Progress Series* 407, 243-255.
- Weeks, A.R., Sgro, C.M., Young, A.G., Frankham, R., Mitchell, N.J., Miller, K.A., Byrne, M., Coates, D.J., Eldridge, M.D.B., Sunnucks, P., Breed, M.F., James, E.A., Hoffmann, A.A., 2011. Assessing the benefits and risks of translocations in changing environments: A genetic perspective. *Evolutionary Applications* 4 (6), 709–725.
- Wilcove, D.S., Rothstein, D., Dubow, J., Phillips, A., Losos, E., 1998. Quantifying threats to imperiled species in the United States. *BioScience* 48, 607-615.
- Wilson, H.B., Joseph, L.N., Moore, A.L., Possingham, H.P., 2011. When should we save the most endangered species? *Ecology Letters* 14 (9), 886–890.

CHAPTER 6

Summary, Conclusions, and further Extensions

The world's marine ecosystems are undergoing a biotic homogenization (McKinney and Lockwood, 2001) with an escalated human-mediated colonization of species (Simberloff, 2009). In this process, invasives are recognized, arguably, as one of the main causes of local extinction of populations (Gurevitch and Padilla, 2004), and also, of ecological change leading to biodiversity loss (Didham et al., 2005). However, it has also been observed that the higher the biodiversity, the higher the number of invasives (see for e.g., Altier et al., 2010). Regardless, the puzzle remains as to how species that are well-adapted to, and long persisted in native habitats expand range and dominate novel (non-native) habitats (Fridley et al., 2007) that are sometimes ecologically, physically, and chemically different from the native ranges. In this vein, more than 29 working hypotheses have been postulated (Catford et al., 2009) as to how and why an invasion occurs in the case of plant invasions, most of which are also common to aquatic invasions. Due to their context dependence, none of them have been clearly refuted nor have they provided generalized or a unified theory of invasion ecology.

In invasion ecology, the levels of analyses expand across taxa, processes, and characteristics (Hayes and Barry, 2008). Comparisons are made between niches of native and potentially invulnerable ranges based upon mainly the principles of ecological niche modeling (Jimenez-Valverde et al., 2012), which predicts the environmental range that suits a species. The role of stochasticity in factors, internal and external to the processes, for example, the demography, environment, and propagule pressure, is also under scrutiny (Potapov and Rajakauna, 2013). There is a general agreement that propagule pressure should be treated as a null model for invasion success (Colautti et al., 2006). The challenge is to predict an invasion of a new species before an invasion occurs, especially where a new

invasive would originate from, and where it would go. If we are to predict which species will be the next potential invader generated in and moving from which potential habitat, given the increasing rate of human-mediated biotic-mixing of the world's marine regions through propagule pressure, then we need to know the underlying processes that drive an invader. In this context, existing theories, models, hypotheses (Catford et al., 2009) are insufficient to give us a complete answer.

The temperature is fundamental to all biological systems and metabolic processes of ectothermic species, and reflected in their population dynamics (Amarasekare and Savage, 2012; Savage et al., 2004) and species diversity distribution (Allen et al., 2002; Brown et al., 2004; Gillooly et al., 2001). In his thesis, I investigated how spatial variation of temporal temperature profiles across the global *marine ecoregions* impact persistence, immigration, and distribution of ectothermic marine taxa (calanoid copepods, copepods, tunicates), and what potential differences they make for some species to become “invasive” than others. Intense human-mediated propagule flow across oceans and seas has provided a “mega-laboratory” for this work.

The *marine ecoregions* are a bio-geographic classification of coastal regions based on similarities in biota, geomorphological features, currents, and temperature, which covers all coastal and shelf waters shallower than 200 m (Spalding et al., 2007). On this basis the environmental profiles within an ecoregion are assumed to be less deviated than across, thus, the species distributed in an ecoregion have the exposure to approximately the same spatial and temporal structure of the environmental factors (Spalding et al., 2007). Therefore, this classification assumes homogeneous temperature and ecological communities within these ecoregions than across.

Temperatures in some northern temperate ecoregions (NTE) are subject to extremely large yearly fluctuations compared to other world regions. This may be a result of the particular geometric shapes of the oceans, seas, and land masses of the NTE that drive cold and warm ocean currents in some regions to mix up

seasonally (Wyrski, 1965), besides large seasonal variations in air-to-surface temperature transfer occurring in the temperate regions. The NTE also have regions with almost steady year-round temperatures. Therefore, the heterogeneity in temperature profiles within the NTE, in particular, provided an ideal ground to test the effect of large differences in temperature profiles across physically contiguous ecoregions on population dynamics and species distribution, given the intense biotic-mixing across the region due to propagule pressure.

The two simple biologically meaningful metrics we developed are the temperature-dependent cross-periodic intrinsic growth rate Λ_p , which is a cross-periodic fitness (CPF) parameter, and a weighted net reproductive rate R_p , which is a measure of the cross-periodic reproductive rate. These were used to evaluate species invasiveness and habitat invasibility pertaining to, first, the ectothermic marine calanoid copepod *Pseudodiaptomus marinus* in environments with steady and periodically fluctuating temperatures. Here, we assumed that factors other than temperature are ideal for the species. The results given by the new metrics are consistent with that is given by advanced numerical mathematical methods, such as, computations using the monodromy matrix (Wang and Hale, 2001), assuming piecewise continuous switching system (Gökçek, 2004), and the time-averaging method (Ma and Ma, 2006; Wesley and Allen, 2009).

The persistence criteria given by $R_0 > 1$ and $\lambda > 0$ for populations in constant environments are nested within that given by $R_p > 1$ and $\Lambda_p > 0$, respectively, for populations in fluctuating environments. The fundamental basis of relating Λ_p with R_p is given by an explicit functional relationship we derived between λ and R_0 for a stage-structured population in a constant environment. The methodology we proposed here can be used to derive metrics and evaluate the persistence of populations for any given periodically fluctuating external environmental forcing factor, such as salinity, turbidity, dissolved oxygen, food concentration and so forth, in addition to temperature.

For marine calanoid copepod *P. marinus*, high-amplitude periodic temperatures (APT) of habitats decrease the Λ_p of the species, thereby, decreasing

the cross-periodic fitness, and increasing the temperature-dependent stress. This suppression in Λ_p is due to the concavity of the functional relationship of λ with respect to the mean habitat temperatures, which can be explained by Jensen's inequality. Therefore, species emigrating from extremely high APT habitats to low APT habitats should increase Λ_p by many folds, thus increasing the CPF, and thereby, their invasiveness. In line with this theory, field evidence show that *P. marinus* is expanding its range from extremely high APT ecoregions, where it is native to, to low APT ecoregions at optimal mean temperature range around the globe increasing the CPF by many folds. Recent evidence of *P. marinus* range expansion in Adriatic Sea, Italy (Mediterranean Sea) (Olazabal and Tirelli, 2011), Southern Bight of the North Sea coast of France (Brylinski et al., 2012), North Sea, Germany (Jha et al., 2013), and Lake Faro (Messina, Italy) (Sabia et al., 2012) further substantiates the model predictions.

The potentially invisable habitats for *P. marinus* are limited to a latitudinal range given by 10.52-24.81⁰C mean habitat temperatures (considering no fluctuations in habitat temperatures). This range narrows down depending on the degree of amplitude of the annual temperature cycles of habitats on the outskirts (where the temperature bounds are at $R_p=1$). The optimal temperature condition that suits *P. marinus* is found within the temperate and the subtropical low-amplitude temperature ecoregions, for example, the West coasts of Europe, America, and Africa, and Southern Australia, New Zealand, and the Western Mediterranean Sea, which fall within the range of the mean habitat temperatures of its native range; the North West Pacific: the Seas of Japan and China (Walter, 1987). The temperature-dependent fitness may be a plausible reason as to why *P. marinus* has not established yet in Vancouver harbour and Puget Sound areas, where the temperature fluctuates periodically largely, and thereby, marginalizing the persistence potential, although the propagule pressure of *P. marinus* is large in these regions (Cordell et al., 2009).

The method of predicting the potentially invisable range of habitats based on R_p and Λ_p , modeled from a bottom-up mechanistic approach, and calibrated from

the data from laboratory experiments, is contrasting and complementary to the top-down phenomenological approach in Ecological Niche Modeling (ENM) (Jeschke and Strayer, 2008; Mercado-Silva et al., 2006). Our method may give an edge over ENM for being able to predict the potentially invisable range by taking into account the temporal variability of the temperature (or any other external environmental forcing factor for that matter), and the response of the population to temperature (or the factor) beyond what is observed in the native range.

In ideal habitat conditions, where the persistence is limited only by the periodic temperature fluctuations, the timing, quantity and frequency of introductions are secondary. The duration and the degree of favourable and unfavourable temperature of the seasons affect the population persistence. The extreme temperature of a habitat (either low or high), and the mean habitat temperatures may not single handedly determine the population persistence, unless lethal, rather the degree of seasonal variability matters. A proliferating reproduction strategy, with high fecundity and short generation times in high-temperature seasons, falls in line with this theory. Such strategy is shown by copepod populations in temperate waters (Bollens et al., 2012; Yamahira and Conover, 2002).

Furthermore, an increase in the amplitude of periodic temperature over the years can subdue the impact of the rise in the mean habitat temperatures in the light of global warming. This effect can counteract the range expansion of species (for e.g., as in Doney et al., 2012), and the potential increase in biodiversity in the long run (in line with Mayhew et al., 2012). Thus, the local level changes may need thorough investigation before generalizing the effects on a global scale.

In theory, we speculate that the temperature-dependent invasiveness of a species may differ from one species to another depending on the peakedness of their R_p with respect to mean temperature at zero amplitude. The higher the peakedness, the greater is the degree of invasiveness for a species native to high APT ecoregions, whereas, the higher the peakedness, the lesser is the degree of species invasiveness for a species native to low APT ecoregions.

The above findings pertaining to *P. marinus* may question whether invasive marine species, in general, take a similar multi-fold physiological advantage by emigrating from high to low APT ecoregions, or whether they are affected by any other fluctuating stress-dependent forcing factors. In Appendix 6.1., we present some preliminary results based on a phenomenological analysis supporting the above case for marine species (a total of 329 invasives) from Molnar et al. (2008), which include the dominant marine taxa: crustaceans (59 species), molluscs (54), algae (46), fish (38), annelids (31), plants (19), and cnidarians (17), compiled from 350 data sources, with at least one species being documented in 194/232 marine ecoregions. The invasibility of marine ecoregions is significantly suppressed by the degree of the APT. The invasibility of NTE, in particular, is inversely correlated to the APT significantly within the range of 10-24⁰C mean ecoregion temperatures, and increasing the model-fit for even narrower ranges (Figure 6-1). It can be deducible from these results that a temperature-dependent optimal immigration path may exist for marine species across the global ecoregions similar to the case of *P. marinus*.

We note that these marine invasives are mostly near-shore or coastal dwelling species belonging to the neritic zone (<200m depths). By virtue of the mechanism of their spread (via ships taking up ballast-water from upper layers of the near-shore, shallow-water ports, or via bio-fouling (Lockwood et al., 2005), or ocean currents), most these invasives may essentially have propagules or life-history stages get exposed to annual periodic fluctuations of temperature of the ocean, which is most prominent in the upper mixed layer of the oceans extending to 150-250m deep in the NTE (see Kara et al., 2003). The APT of the habitats, therefore, seems to have a significant effect on the population dynamics of these invasive species in general.

At individual level, species native to extremely high APT ecoregions may generate a potential to become “invasive” in low APT ecoregions if their temperature-dependent cross-periodic growth rates are generally concave functions of temperature similar to the case of *P. marinus*, or the generalized case for ectotherms in Amarasekare and Savage (2004). This is because it may help

them gaining a multi-fold increase in cross-periodic fitness by temperature-dependent optimal immigration. This effect is fundamentally due to Jensen's inequality. This raises the questions as to whether invasive species are generally originated from (or native to) mid-latitudinal, extremely high APT ecoregions of the world oceans, particularly in the NTE similar to *P. marinus*, thereby they increase their fitness by optimal immigration to low APT ecoregions within a range of optimal mean temperatures. Is their persistence and spread, hence, limited by extremely high and low mean temperatures of the tropical and cold water oceans? Are extremely high APT ecoregions in the NTE the temperature-dependent "invasive generators", and low APT ecoregions the "invasive sinks"? Should this be the same for marine non-indigenous species as well in general?

Several studies indicate that a large proportion of marine invasive and non-indigenous species, those traceable and recorded (for example, crustaceans, molluscs, tunicates, bryozoans, starfish, jellyfishes and sponges) are native to at least one or more of the world's extremely high APT ecoregions: temperate North West Pacific (surrounding Sea of Japan, East China Sea, Yellow sea), North West Atlantic (e.g., Gulf of Maine, St. Lawrence), and Europe seas (e.g., Ponto Caspian, Western Mediterranean, Black, and Baltic) (yellowish areas in Figure 6-2) (based on Cordell et al. (2009); Doi et al. (2011); Gouletquer et al. (2002); Hangfling et al. (2011); IUCN (2012); Noel (2011); Olenin (2005); Orensanz et.al. (2002); Ricciardi and Maclsaac (2001) (Table 6-1)). However, it is hard to track all the species down to where they were exactly originated from. Low amplitude ecoregions within the northern temperate ecoregions, where there are invasive, consist of mostly the West coasts of America, Africa, and Europe, part of Mediterranean Sea, southern Australia and New Zealand.

The apparent temperature-dependent optimal immigration path from high to low APT ecoregions may be a potential *conveyor belt* of marine invasive species generation driven by the existing large gradient of amplitudes of periodic temperatures across world's ecoregions. In a broader sense, any fluctuating, externally forcing, stress-inducing environmental variable can cause a similar effect on species invasiveness. They may include, for example, salinity in marine

environments. We could apply the same philosophical approach to calibrate such effects on invasiveness.

It can also be true that West coasts undergo upwelling bringing nutrient rich waters to the surface making the habitats favourable to species in general. Therefore, there is a possibility that the effect of upwelling may also compliment to this invasion process.

In theory, a high concentration of extremely high APT ecoregions (invasive generators) and low APT ecoregions (invasive sinks) within the NTE, and their physical proximity to each other causing large intra-propagule pressure, may explain why low APT ecoregions in the NTE has more invasives compared to other world regions in general (Appendix 6.1). This also complements the intermediate distance hypothesis (Seebens et al., 2013) but with the above condition. In contrast to NTE, the temperature-amplitude gradient within the southern temperate ecoregions (STE) is markedly low due to all-low APT ecoregions across the STE in general (Figures 6-2; 6-3). Thus in line with our theory, invasive species generation and retention in the STE should be low compared to that in the NTE. At the same time, STE is less vulnerable to invasives from the NTE (where the invasives are most likely generated), although they have the same range of mean temperatures as in the NTE. This may be due to the physical distance between the NTE and the STE, which results in a low propagule pressure in STE exerted from the NTE. Thus the generation and the retention of invasives in the NTE should be, in theory, far greater than that in the STE or any other ecoregion in the world. This is shown in the marine invasive species diversity distribution data by Molnar et al. (2008).

In theory, the NTE, where the invasive marine species are most likely generated, the net flux of invasives should be generally directed towards the low APT ecoregions on the East coasts from high APT ecoregions on the West coasts of the oceans following the temperature-amplitude gradient (Figure 6-2). The data from Molnar et al. (2008) showed a high proportion of invasives species on the West coasts compared to the East coasts of the NTE (Appendix 6.1). (Here, the

East coasts of the continent do not include the Europe seas, having comparatively large APT.)

Furthermore, in theory, the ideal habitats (sinks) with respect to habitat temperatures for marine invasives generally converge to a narrow geographical coastal range on the East coasts, but stretch widely on the West coasts of the continents due to geophysical patterns of the ocean currents. The species native to high-dynamic ecoregions on the East coasts, in terms of temperature, especially in the NTE, immigrating to comparatively steady ecoregions on the West coasts have a propensity to spread widely geographically.

In support of these propositions, Ruiz et al. (2011) showed a significantly large proportion of invasive and non-indigenous crustaceans on the West coasts compared to the East coast of North America. Furthermore, DiBacco et al. (2012) showed a similar quantitative difference in marine non-indigenous species between the West and the East coast ports in Canada, which they, however, attributed to the apparent differential propagule pressure between the ports. Furthermore, Molnar et al. (2008) showed that the distribution of Pacific Oyster in the world is mostly on the west coasts of the continents. Although, propagule pressure may be a trigger of invasions and may explain some of the variations in the invasive species diversity data, it may not explain the underlying bio-physical dynamics that suits one species over another, or what conditions suit invasive species in general. Propagule pressure hypothesis may not fully explain, for example, as to why eight invasive copepods native to high-APT, high-stress ecoregions in the seas surrounding Japan and China are found in low-APT coast of California (Cordell et al. 2008), whereas, not many native to the coast of California are found in the seas surrounding Japan, given the propagule pressure exerted between each other cannot be very much different (see in Kaluza et al., 2010). Our theory may explain these patterns of invasive species diversity data by region better. However, the high proportion of marine invasives in the South-Eastern Australia and New Zealand compared to the West Coast of South America may be explained by the difference in propagule pressure exerted from

NTE (see in Kaluza et al., 2010), because in theory, all ecoregions in the STE are temperature-dependent invasive sinks, while having no apparent invasive generators (Appendix 6.1).

In summary, we hypothesise that the likelihood of temperature-dependent invasive species generation may depend on three basic factors: (1) a large peakedness of the temperature-dependent cross-periodic fitness curve of a species at zero-amplitude; (2) a high concentration of (or physically contiguous) steady and extremely variable temperature ecoregions within a narrow range of mean habitat temperatures; and (3) biotic-mixing across ecoregions by propagule pressure. The baseline principles behind these processes may also be the same for other fluctuating external forcing factors affecting invasions.

The Metabolic Theory of Ecology (MTE) describes the latitudinal gradient of biodiversity (Allen et al., 2002; Brown et al., 2004; Rombouts et al., 2011). The extended MTE model, we proposed, that takes into account the effect of periodic fluctuations of temperature of the ecoregions, improves the predictability of marine species (calanoid copepods, copepods, and tunicates) taxonomic richness of the NTE. The effect of subtle periodic variations in temperature, recurring over millions of years, on speciation seems substantial (complementing Allen et al., 2006; Gillooly and Allen, 2007). This solidifies the use of MTE as a tool for understanding the underlying dynamics of ecological processes.

The extended MTE model explains the global diversity distribution of marine copepods on a latitudinal gradient better than any other comparative model. This includes the explanation of the difference in the diversity gradient between the Northern and the Southern Hemispheres, with a hump off the tropics. The greatest improvement given by the extended MTE model is shown for the marine calanoid copepods followed by copepods (in general), and tunicates. This was expected because most calanoid copepods live in the upper mixed layer of the water column (Huntley and Lopez, 1992), where the periodic variation in temperature is much greater, followed by copepods (in general) and tunicates.

Although, MTE model fits well to the existing marine diversity distribution data, even better with the proposed extension that takes into account the temperature-amplitudes, there may be other temperature-dependent processes that contribute to the latitudinal gradient of the biodiversity of marine species. For example, we speculate that the temperature-dependent conveyor belt of invasive species generation that we proposed here may also be one such contributor driving species on temperature-dependent optimal immigration. It can generate biodiversity in optimal temperature ecoregions over millennia via natural vectors such as ocean currents (which are directed coincidentally from high to low APT ecoregions in the NTE, e.g. Gulf Stream) that can carry possibly resting stages over long distances (a conceptual framework given in Gillespie et al., 2012). There is also a possibility that optimally immigrating species may potentially be subject to allopatric speciation at novel ecoregions over millennia, or local extinction at their native high APT ecoregions (due to high stress, as can be explained by our theory, and also the stochastic theories (Lande et al., 2003), where they may have originated from. These processes can transform the non-indigenous species (and invasives) from the quadratic concave invasive species richness curve (as data from Molner et al. (2008) show) to “native” status on the less concave high-lying latitudinal marine biodiversity gradient curve (in Tittensor et al., 2010) (both drawn with respect to mean habitat temperatures) as an ongoing long-standing natural process over millions of years. There is so much epistemic uncertainty regarding the indigenous status of the species, as they are working definitions based on fuzzy spatio-temporal boundaries (McGeoch et al., 2012). Would this mean that the temperature-dependent conveyor belt of invasive species generation is a mean to marine biodiversity generation at optimal low APT ecoregions at least for the species exposed to high APT in native ecoregions? We need more investigation of these possibilities, both mathematically and empirically.

The evidence in support of, or against this proposition may come from investigations based on the connections between natural propagation paths by oceanic currents (McGeoch et al., 2012), latitudinal biodiversity peaks occurring

at off-tropics (Powell et al., 2012), hopping marine biodiversity hot-spots over millennia (Renema et al., 2008), historical biodiversity tracking of the earth's temperature (Mayhew et al., 2012), freshwater-invading estuary copepods (Lee, 1999), and diversity difference between the Southern and the Northern Hemisphere (Powell et al., 2012). Perhaps, we need more research from a paleoecological perspective (Louys et al., 2012) to determine the underlying mechanics of the processes, outcomes of invasions, and eventual diversity distribution over changing geometric shapes of the world's landmasses, oceans and seas over millennia. We may need to examine temperature-dependent cross-periodic fitness curves of more species individually, including native and non-indigenous species, and test whether a generalized model and a framework may explain the geological history of biodiversity distribution. Above all, we may also need concrete, quantifiable, mathematical definitions in invasion ecology nomenclature.

Human-mediated propagule pressure is fundamental to the present level of biotic mixing of the world's ecoregions (Simberloff, 2009). Given the existing large gradient of temperature-amplitudes across the marine ecoregions, and the resulting potential conveyor belt in operation, especially in the NTE, it is likely that there will be potential for high-degree invasions in the future at the present level of propagule pressure. In theory, the potential for high degree invasion of species from the Northern to the Southern temperate ecoregions is also large, yet not realized, possibly due to physical separation (because of the time the propagules have to survive in ballast-water tanks, or any other vector, across these regions is longer: the intermediate distance hypothesis (Seebens et al., 2013)). Fast moving vessels that are likely to replace the present ones in the future may increase biotic-mixing across Southern and Northern oceans, potentially increasing the invasives in the STE.

To control establishment of invasive populations, a thorough quantitative understanding of populations at the edge of extinction is needed. The rate of human-mediated immigration (propagule flow), such as via ship ballast-water discharge, is highly fluctuating in marine environments (Cordell et al., 2009).

Besides, species introduced to novel environments are always subject to environmental and demographic fluctuations.

We showed, in theory, that invasions can be managed cost-effectively optimally through stochastic control methods. The impact of the degree of stochasticity in propagule flow on probability of populations *establishment before extinction* (EBE probability) depends on the rate of intrinsic growth and the rate of net flow of propagules into a habitat (or population). High EBE probability due to high mean rate of propagule flow into favourable habitats (Drake and Lodge, 2006) is subdued by high stochasticity in the propagule flow (assuming that the mean flow rate is maintained at constant). This effect is greater in the presence of environmental and demographic stochasticity. When populations have negative intrinsic growth rates, the stochasticity in small immigration rates inflate the EBE probability, similar to what Gonzalez and Holt (2002) have shown in sink populations,

In general, if invasive species are introduced to extremely favourable habitats, or/and if the propagule flow rate is greater than the rate of virtual population decline due to demographic Allee effect (rate at which the individuals are unable to replace themselves), then the stochasticity in propagule flow decreases the EBE probability. If invasive species are introduced to unfavourable habitats (or the population is on the decline in a novel location), or/and if the rate of population decline due to the demographic Allee effect is much greater than the propagule inflow rate, then the stochasticity in propagule flow increases the EBE probability. However, the mean time for population establishment before extinction decreases with the increasing stochasticity in propagule flow regardless of the favorability of the habitat.

These give insights into controlling human-mediated propagule flow through stochastic means. For example, to control high-degree marine invasions, one can increase the stochasticity in propagule flow by stochastic monitoring and stochastic treatment (intensity and frequency) of ship ballast-water in contrast to constant monitoring and treatment. While both management scenarios; one with and the other without incorporating the stochasticity; reduce the mean propagule

flow rate, the former scenario should yield a greater effect in reducing the EBE probability. If the resources deployed remain the same in both scenarios (zero-sum), then the stochastic control methods should be theoretically more cost effective. However, if the propagule flow is continuous in time, then any type of control method has only limited time effect, because a population can replenish sooner or later from temporary extinction (see also, Potapov and Rajakaruna, 2013). These theoretical results give insights also into stochastic methods of eradicating the invasives already established in novel locations. However the applied quantitative measurements of the stochastic control methods may need field data and case specific investigations.

We do not know if the process that we call an “invasion” in our short and measurable time scales has existed over millennia through natural mechanisms of dispersion and colonisation following the underlying temperature-dependent or any other bio-physical stress releasing mechanisms. The mechanics of colonizing species, possibly taking the advantage of releasing stress and increasing the temperature-dependent cross-periodic fitness by optimal immigration to low-amplitude temperature habitats, may have also contributed to marine biodiversity generation around the world’s ecosystems in addition to what MTE models postulate. In addition to temperature dependence we tested, there may be other periodic and stochastic external forcing factors that may cause similar effects. However, there is a high potential for the marine colonizers to become high-degree invasives in the future, given the existing large temperature-amplitude gradients, or the temperature-dependent stress gradients, and the level of propagule pressure across the world’s ecoregions.

Table 6-1 Percentages of exotic marine and estuary species native to at least an ecoregion with high-amplitude periodic temperatures based on the published data.

Ecoregions	Source	Species type	Traceable No. of spp. in the sample	% native to high-amplitude temperate ecoregions: Temperate North West Pacific (surrounding Sea of Japan, East China Sea, Yellow sea), North West Atlantic (Gulf of Maine, St. Lawrence), & Europe Seas: Ponto Caspian, Western Mediterranean, Black, and Baltic)								
World	IUCN (n.d.)	Invasive marine and estuary crustaceans, molluscs, tunicates, bryozoans, starfish and sponges	41/62	80.49%								
				<table border="1"> <tr> <td>0.46</td> <td>Sea of Japan /China</td> </tr> <tr> <td>0.19</td> <td>Europe Seas</td> </tr> <tr> <td>0.05</td> <td>Gulf of Maine</td> </tr> <tr> <td>0.12</td> <td>Gulf of Mexico</td> </tr> </table>	0.46	Sea of Japan /China	0.19	Europe Seas	0.05	Gulf of Maine	0.12	Gulf of Mexico
0.46	Sea of Japan /China											
0.19	Europe Seas											
0.05	Gulf of Maine											
0.12	Gulf of Mexico											
World	Hangfling et al. (2011)	Invasive alien crustaceans	22/22	81.81%								
SouthWestern Atlantic	Orensanz et al. (2002)	Exotic marine species	72/72	~77.80%								
San Francisco and Columbia River estuary	Cordell. et al. (2009)	Introduced copepod species	12/12	~66.67%								
Open Atlantic coast of Europe	Gouletquer et al. (2002)	Non- indigenous marine species	101/101	~76.24%								
Baltic Sea	Olenin (2005)	Non- indigenous aquatic invertebrates	29/29	~87.93%								
				<table border="1"> <tr> <td>55.17</td> <td>Ponto Caspian N America East</td> </tr> <tr> <td>27.59</td> <td>Coast</td> </tr> <tr> <td>10.34</td> <td>NW Pacific</td> </tr> </table>	55.17	Ponto Caspian N America East	27.59	Coast	10.34	NW Pacific		
55.17	Ponto Caspian N America East											
27.59	Coast											
10.34	NW Pacific											

Chille		Non-indigenous spp	16/16	~62.50%												
Sea of Japan	Doi et al. (2011)	Alien marine crustaceans	23/23	<table border="1"> <thead> <tr> <th colspan="2">~50%</th> </tr> </thead> <tbody> <tr> <td>5.56</td> <td>NW Pacific</td> </tr> <tr> <td>22.22</td> <td>NE Pacific</td> </tr> <tr> <td>44.44</td> <td>NW Atlantic</td> </tr> <tr> <td>11.11</td> <td>NE Atlantic</td> </tr> <tr> <td>16.67</td> <td>IO/SP</td> </tr> </tbody> </table>	~50%		5.56	NW Pacific	22.22	NE Pacific	44.44	NW Atlantic	11.11	NE Atlantic	16.67	IO/SP
~50%																
5.56	NW Pacific															
22.22	NE Pacific															
44.44	NW Atlantic															
11.11	NE Atlantic															
16.67	IO/SP															
European Atlantic coast	Noel (2011)	Non-indigenous spp	42/42	~64.29%												

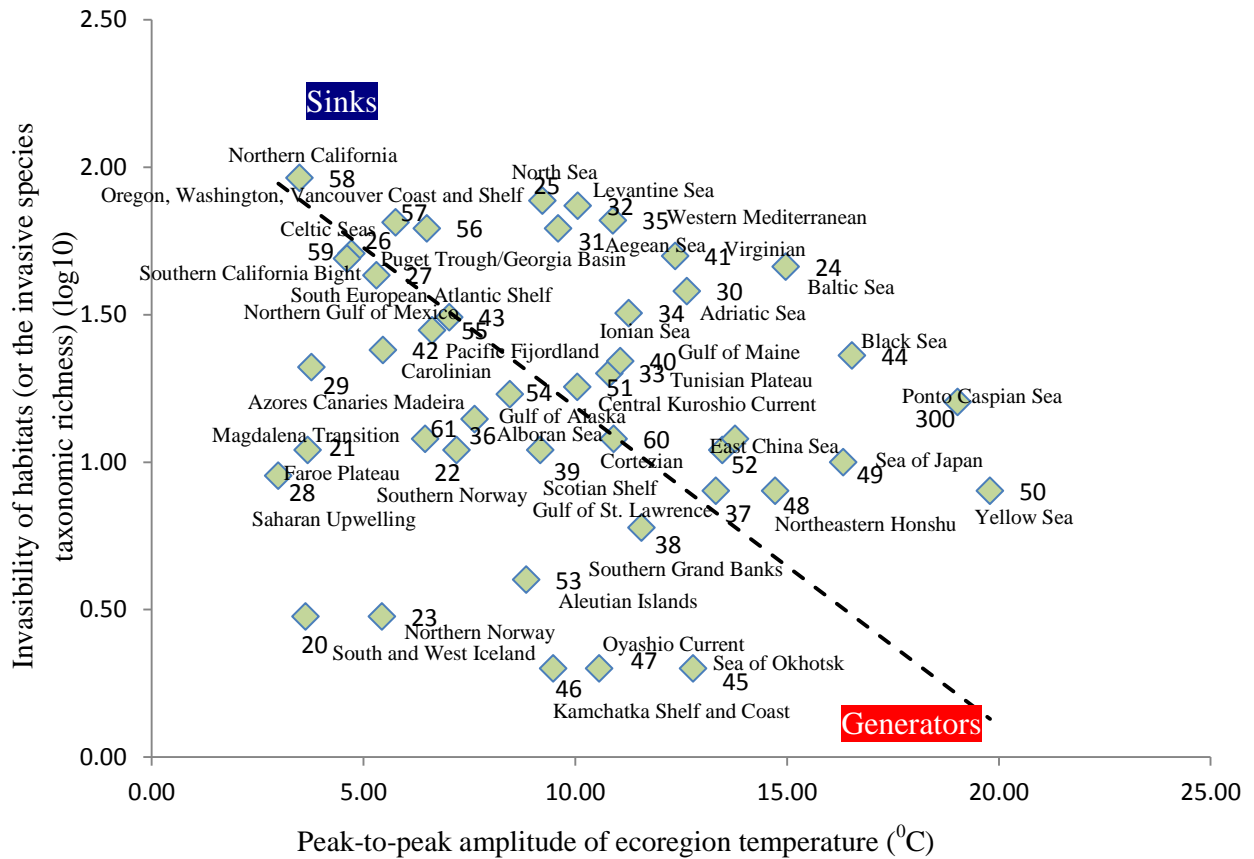


Figure 6-1 Invasive species taxonomic richness linearly regressed with respect to peak-to-peak amplitude of the northern temperate ecoregion (NTE) temperatures. The relationship is significant within the range of mean ecoregion temperatures (10-24⁰C) yielding $p=0.04$ ($F=4.66$, $df=1,25$, $R^2=0.16$) suggesting that invasibility is low in high-amplitude periodic temperature (APT) ecoregions. The theoretical expectation that these species may respond to temperature similar to *P. marinus* supposing that their temperature-dependent intrinsic growth rates follow the pattern proposed by Amarasekare and Savage (2012) generalized for ectotherms, may suggest that these species immigrating to low APT ecoregions can increase their cross-periodic fitness by many folds in line with our theory in Chapter 3. Thus, these may suggest that marine invasives are generated in extremely high APT ecoregions in the NTE. Therefore, in a conceptual framework, we suggest that the top-left may indicate the *invasive sinks*, and the bottom-right may indicate the *invasive generators* in general.

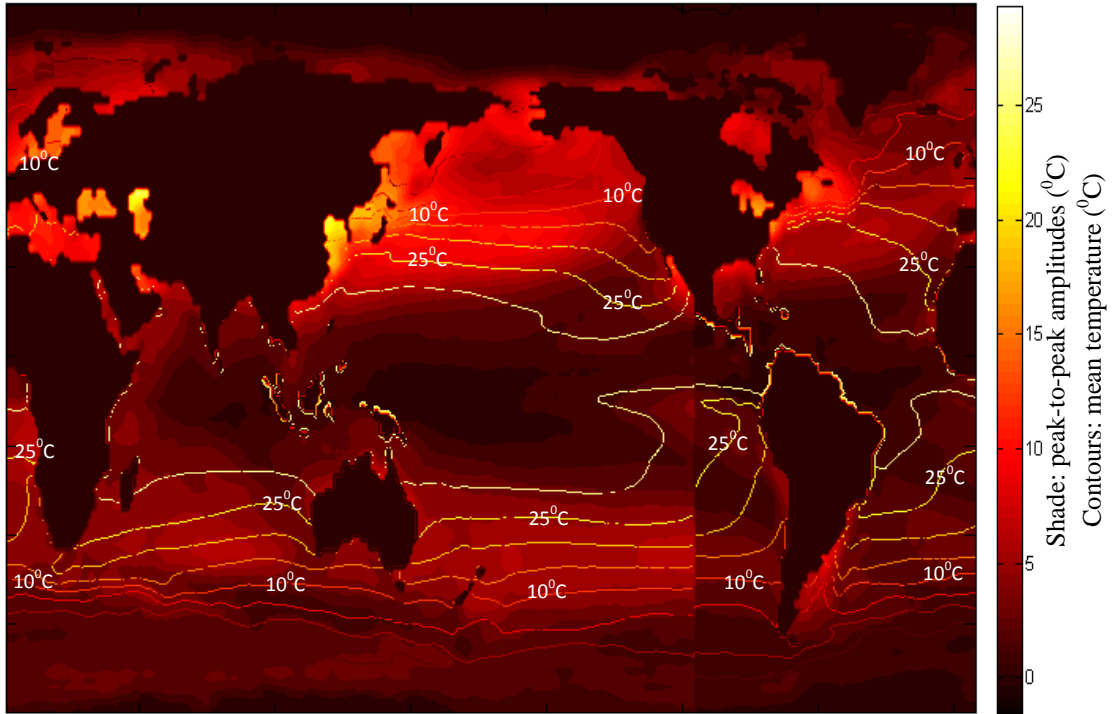


Figure 6-2 Peak-to-peak amplitude (shade) and mean (contours) of annual sea surface temperature cycles modeled using a simple sine function (methods in Chapter 3) based on the data (1971-2001) from NOAA-ESRL (n.d.) at $1^{\circ} \times 1^{\circ}$ degree resolution of latitudes and longitudes.

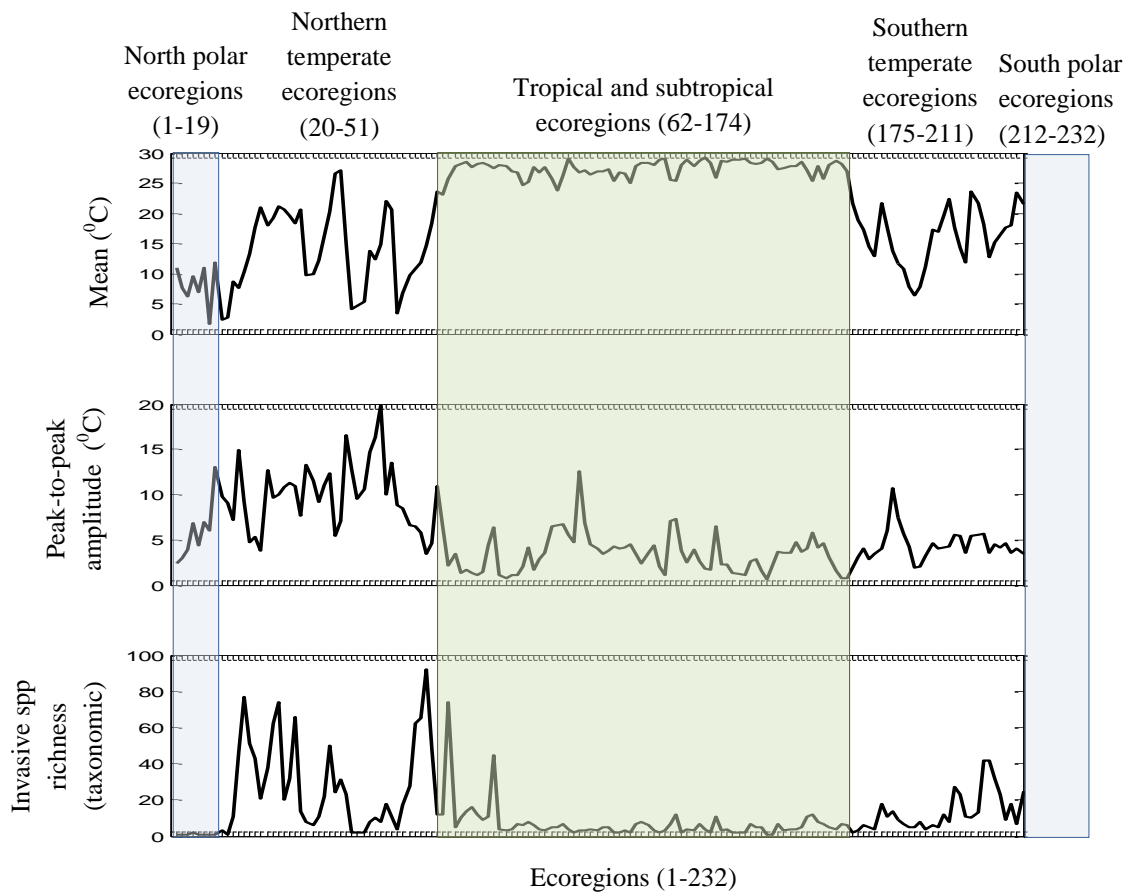


Figure 6-3 The means and the amplitudes of annual temperature cycles of marine ecoregions, and the invasive species taxonomic richness. Invasive species diversity is higher in the regions where the concentration of extremely high-amplitude (invasive generators) and low-amplitude (invasive sinks) temperature ecoregions are greater: the northern temperate ecoregions (NTE) followed by the southern temperate ecoregions (STE). The physical proximity between the potential generators and sinks, which results in high intra-propagule pressure, thereby the optimal immigration may reflect in the large diversity of invasives in the NTE.

References

- Allen, A.P., Brown, J.H., Gillooly, J.F., 2002. Global biodiversity, biochemical kinetics, and the energetic-equivalence rule. *Science* 297(5586), 1545-1548.
- Allen, A.P., Gillooly, J.F., Savage, V.M., Brown, J.H., 2006. Kinetic effects of temperature on rates of genetic divergence and speciation. *Proceedings of the National Academy of Sciences* 103(24), 9130-9135.
- Altieri, A.H., van Wesenbeeck, B.K., Bertness, M.D., Silliman, B.R., 2010. Facilitation cascade drives positive relationship between native biodiversity and invasion success. *Ecology* 91(5) 1269-1275.
- Amarasekare, P., Savage, V., 2012. A framework for elucidating the temperature dependence of fitness. *American Naturalist* 179(2), 178-191.
- Bollens, S.M., Breckenridge, J. K., Cordell, J.R., Rollwagen-Bollens, G., Kalata, O., Claudi, R., Karatayev, A. 2012. Invasive copepods in the Lower Columbia River Estuary: Seasonal abundance, co-occurrence and potential competition with native copepods. In *Proceedings of the 17th International Conference on Aquatic Invasive Species*, San Diego, USA, September 2010. (7(1), 101-109). Regional Euro-Asian Biological Invasions Centre (REABIC).
- Brown, J.H., Gillooly, J.F., Allen, A.P., Savage, V.M., West, G.B., 2004. Toward a metabolic theory of ecology. *Ecology* 85(7), 1771-1789.
- Brylinski, J.M., Antajan, E., Raud, T., Vincent, D., 2012. First record of the Asian copepod *Pseudodiaptomus marinus* Sato, 1913 (Copepoda: Calanoida: Pseudodiaptomidae) in the southern bight of the North Sea along the coast of France. *Aquatic Invasions* 7(4), 577-584.
- Catford, J. A., Jansson, R., Nilsson, C., 2009. Reducing redundancy in invasion ecology by integrating hypotheses into a single theoretical framework. *Diversity and Distributions* 15(1), 22-40.
- Colautti, R.I., Grigorovich, I.A., MacIsaac, H.J., 2006. Propagule pressure: a null model for biological invasions. *Biological Invasions* 8(5), 1023-1037.
- Cordell, J.R., Bollens, S.M., Draheim, R., Sytsma, M., 2008. Asian copepods on the move: recent invasions in the Columbia–Snake River system, USA. *ICES Journal of Marine Science: Journal du Conseil* 65(5), 753-758.
- Cordell, J.R., Lawrence, D.J., Ferm, N.C., Tear, L.M., Smith, S.S., Herwig, R.P. 2009. Factors influencing densities of non-indigenous species in the ballast water of ships arriving at ports in Puget Sound, Washington, United States. *Aquatic Conservation: Marine and Freshwater Ecosystems* 19(3), 322-343.
- DiBacco, C.,D.B. Humphrey, L.E. Nasmith, C.D. Levings, 2012. Ballast water transport of non-indigenous zooplankton to Canadian ports, *ICES Journal of Marine Science* 69(3), 483–491.

- Didham, R.K., Tylianakis, J.M., Hutchison, M.A., Ewers, R.M., Gemmill, N.J. 2005. Are invasive species the drivers of ecological change? *Trends in Ecology and Evolution* 20(9), 470-474.
- Doi, W., Watanabe, S., Carlton, J.T., 2011. Alien marine crustaceans of Japan: a preliminary assessment. In *In the Wrong Place-Alien Marine Crustaceans: Distribution, Biology and Impacts* (p. 419-449). Springer Netherlands.
- Doney, S.C., Ruckelshaus, M., Duffy, J.E., Barry, J.P., Chan, F., English, C.A., ... Talley, L.D., 2012. Climate change impacts on marine ecosystems. *Marine Science* 4, 11-37.
- Drake, J.M., Lodge, D.M., 2006. Allee effect, propagule-flow and the probability of establishment: risk analysis for biological invasions, *Biological Invasions* 8, 365-375.
- Fridley, J.D., Stachowicz, J.J., Naeem, S., Sax, D.F., Seabloom, E.W., Smith, M. D.,... Holle, B.V., 2007. The invasion paradox: reconciling pattern and process in species invasions. *Ecology* 88(1), 3-17.
- Gillespie, R.G., Baldwin, B.G., Waters, J.M., Fraser, C.I., Nikula, R., Roderick, G.K. 2012. Long-distance dispersal: a framework for hypothesis testing. *Trends in Ecology and Evolution* 27(1), 47-56.
- Gillooly, J.F., Allen, A.P., 2007. Linking global patterns in biodiversity to evolutionary dynamics using metabolic theory. *Ecology* 88(8), 1890-1894.
- Gillooly, J.F., Brown, J.H., West, G.B., Savage, V.M., Charnov, E.L., 2001. Effects of size and temperature on metabolic rate. *Science* 293(5538), 2248-2251.
- Gökçek, C., 2004. Stability analysis of periodically switched linear systems using Floquet theory. *Mathematical Problems in Engineering* 2004(1), 1-10.
- Gonzalez, A., Holt, R.D., 2002. The inflationary effects of environmental fluctuations in source-sink system, *Proceedings of the National Academy of Sciences* 99(23), 14872-14877.
- Gouletquer, P., Bachelet, G., Sauriau, P.G., Noel, P., 2002. Open Atlantic coast of Europe: a century of introduced species, in: Leppäkoski, E., Gollasch, S.; Olenin, S. (Ed.) (2002). *Invasive aquatic species of Europe: distribution, impacts and management*, Kluwer/Kluwer Academic: Dordrecht, p. 276-290
- Gurevitch, J., Padilla, D.K., 2004. Are invasive species a major cause of extinctions? *Trends in Ecology and Evolution* 19(9), 470-474.
- Hänfling, B., Edwards, F., Gherardi, F., 2011. Invasive alien Crustacea: dispersal, establishment, impact and control. *BioControl* 56(4), 573-595.
- Hayes, K.R., Barry, S.C., 2008. Are there any consistent predictors of invasion success?. *Biological Invasions* 10(4), 483-506.
- Huntley, M.E., Lopez, M.D., 1992. Temperature-dependent production of marine copepods: a global synthesis. *American Naturalist* 140(2), 201-242.

IUCN, n.d. Invasive Species Database. Retrieved from: <http://www.issg.org/database/welcome/>.

Jeschke J.M., Strayer D.L., 2008. Usefulness of bioclimatic models for studying climate change and invasive species. *Annals of the New York Academy of Sciences* 1134, 1–24.

Jha, U., Jetter, A., Lindley, J. A., Postel, L., Wootton, M., 2013. Extension of distribution of *Pseudodiaptomus marinus*, an introduced copepod, in the North Sea. *Marine Biodiversity Records* 6, e53.

Jiménez-Valverde, A., Peterson, A.T., Soberón, J., Overton, J.M., Aragón, P., Lobo, J.M., 2011. Use of niche models in invasive species risk assessments. *Biological Invasions* 13(12), 2785-2797.

Kaluza, P., Kölzsch, A., Gastner, M.T., Blasius, B., 2010. The complex network of global cargo ship movements. *Journal of Royal Society Interface* 7(48), 1093-1103.

Kara, A.B., Wallcraft, A.J., Hurlburt, H.E., 2003. Climatological SST and MLD Predictions from a Global Layered Ocean Model with an Embedded Mixed Layer. *Journal of Atmospheric and Oceanic Technology* 20(11), 1616-1632.

Lande, R., Engen, S., Sæther, B.E., 2003. *Stochastic population dynamics in ecology and conservation*. Oxford University Press, GB, p. 209.

Lee, C.E., 1999. Rapid and repeated invasions of fresh water by the copepod *Eurytemora affinis*. *Evolution* 1423-1434.

Lockwood, J.L., Cassey, P., Blackburn, T., 2005. The role of propagule pressure in explaining species invasions. *Trends in Ecology and Evolution* 20(5), 223-228.

Louys, J., Wilkinson, D.M., Bishop, L.C., 2012. Ecology needs a paleontological perspective. In: *Paleontology in Ecology and Conservation* Springer Berlin Heidelberg, p. 23-38.

Ma, J., Ma, Z., 2006. Epidemic threshold conditions for seasonally forced seir models. *Mathematical Biosciences and Engineering* 3(1), 161-172.

Mayhew, P.J., Bell, M.A., Benton, T.G., McGowan, A.J., 2012. Biodiversity tracks temperature over time. *Proceedings of the National Academy of Sciences* 109(38), 15141-15145.

McKinney, M.L., Lockwood, J.L., 2001. Biotic homogenization: a sequential and selective process. In *Biotic homogenization* (pp. 1-17). Springer US.

Mercado-Silva, N., Olden, J.D., Maxted, J.T., Hrabik, T.R., Vander Zanden, M.J., 2006. Forecasting the spread of invasive rainbow smelt in the Laurentian Great Lakes region of North America. *Conservation Biology* 20(6), 1740–1749.

McGeoch, M.A., Spear, D., Kleynhans, E.J., Marais, E., 2012. Uncertainty in invasive alien species listing. *Ecological Applications* 22(3), 959-971.

Molnar, J.L., Gamboa, R.L., Revenga, C., Spalding, M.D., 2008. Assessing the global threat of invasive species to marine biodiversity. *Frontiers in Ecology and the Environment* 6(9), 485-492.

- Noël, P. Y., 2011. Checklist of cryptogenic and alien Crustacea of the European Atlantic coast. In *In the Wrong Place-Alien Marine Crustaceans: Distribution, Biology and Impacts* (pp. 345-375). Springer Netherlands.
- NOAA-ESRL., n.d. Physical Sciences Division, Boulder Colorado, USA. Retrieved from <http://www.esrl.noaa.gov/psd/data/gridded/data.noaa.oisst.v2.html>.
- Olazabal, A., Tirelli, V., 2011. First record of the egg-carrying calanoid copepod *Pseudodiaptomus marinus* in the Adriatic Sea. *Marine Biodiversity Records* 4(1), e85.
- Olenin, S., 2005. Invasive aquatic species in the Baltic states. Klaipeda University, Coastal Research and Planning Institute, p. 42.
- Orensanz, J.M.L., Schwindt, E., Pastorino, G., Bortolus, A., Casas, G., Darrigran, G., ... Vallarino, E.A., 2002. No longer the pristine confines of the world ocean: a survey of exotic marine species in the southwestern Atlantic. *Biological Invasions* 4(1-2), 115-143.
- Potapov, A., Rajakaruna, H., 2013. Allee threshold and stochasticity in biological invasions: Colonization time at low propagule pressure, *Journal of Theoretical Biology*. <http://dx.doi.org/10.1016/j.jtbi.2013.07.031>.
- Powell, M.G., Beresford, V.P., Colaianne, B.A., 2012. The latitudinal position of peak marine diversity in living and fossil biotas. *Journal of Biogeography* 39(9), 1687-1694.
- Rajakaruna, H., Potapov, A., Lewis, M., 2013. Impact of stochasticity in immigration and reintroductions on colonizing and declining populations. *Theoretical Population Biology* 85, 38-48.
- Renema, W., Bellwood, D.R., Braga, J.C., Bromfield, K., Hall, R., Johnson, K.G., Pandolfi, J.M., 2008. Hopping hotspots: global shifts in marine biodiversity. *Science* 321(5889), 654-657.
- Ricciardi, A., H.J. MacIsaac, 2000. Recent mass invasion of the North American Great Lakes by Ponto-Caspian species, *Trends in Ecology and Evolution* 15(2), 62:65.
- Rombouts, I., Beaugrand, G., Ibañez, F., Chiba, S., Legendre, L., 2011. Marine copepod diversity patterns and the metabolic theory of ecology. *Oecologia* 166(2), 349-355.
- Rombouts, I., Beaugrand, G., Ibañez, F., Gasparini, S., Chiba, S., Legendre, L., 2009. Global latitudinal variations in marine copepod diversity and environmental factors. *Proceedings of the Royal Society B: Biological Sciences* 276(1670), 3053-3062.
- Ruiz, G., Fofonoff, P., Steves, B., Dahlstrom, A., 2011. Marine crustacean invasions in North America: A synthesis of historical records and documented impacts. In *In the Wrong Place-Alien Marine Crustaceans: Distribution, Biology and Impacts* (p. 215-250). Springer Netherlands.
- Sabia, L., Uttieri, M., Pansera, M., Souissi, S., Schmitt, F.G., Zagami, G., Zambianchi, E. 2012. Swimming behaviour of the calanoid copepod *Pseudodiaptomus marinus* from Lake Faro. *Biologia Marina Mediterranea* 19, 240-241.

- Savage, V.M., Gillooly, J.F., Brown, J.H., West, G.B., Charnov, E.L., 2004. Effects of body size and temperature on population growth. *The American Naturalist* 163(3), 429-441.
- Seebens, H., Gastner, M.T., Blasius, B., 2013). The risk of marine bioinvasion caused by global shipping. *Ecology Letters* 16(6), 782-790.
- Simberloff, D., 2009. The role of propagule pressure in biological invasions. *Annual Review of Ecology Evolution and Systematics* 40: 81–102.
- Spalding, M.D., Fox, H.E., Allen, G.R., Davidson, N., Ferdaña, Z.A., Finlayson, M.A.X., Robertson, J., 2007. Marine ecoregions of the world: a bioregionalization of coastal and shelf areas. *BioScience* 57(7), 573-583.
- Tittensor, D.P., Mora, C., Jetz, W., Lotze, H.K., Ricard, D., Berghe, E.V., Worm, B., 2010. Global patterns and predictors of marine biodiversity across taxa. *Nature* 466(7310), 1098-1101.
- Walter, T.C., 1987. Review of the taxonomy and distribution of the demersal copepod genus *Pseudodiaptomus* (Calanoida: Pseudodiaptomidae) from southern Indo-West Pacific waters. *Marine and Freshwater Research* 38(3), 363-396.
- Wang, X., Hale, J.K., 2001. On monodromy matrix computation. *Computer methods in applied mechanics and engineering* 190(18), 2263-2275.
- Wesley, C.L., Allen, L.J. 2009. The basic reproduction number in epidemic models with periodic demographics. *Journal of Biological Dynamics* 3(2-3), 116-129.
- Wyrski, K., 1965. The annual and semiannual variation of sea surface temperature in the North Pacific Ocean. *Limnology and Oceanography* 307-313.
- Yamahira, K., Conover, D.O., 2002. Intra-vs. interspecific latitudinal variation in growth: adaptation to temperature or seasonality? *Ecology* 83(5), 1252-1262.

APPENDICES

Appendix 1.1. Biology of species

1.1.1. Marine copepods (Subclass Copepoda)

Approximately, 2500 marine planktonic copepod species have been identified to date under the class Maxillopoda in Subphylum Crustacea (Razouls et al., 2013). They are typically 1 to 2 mm long. All crustaceans have an exoskeleton, and are ectothermic. Copepods link the primary production to higher trophic levels providing food for small fish, whales, seabirds and other crustaceans such as krill. They are dominant members of the zooplankton community, perhaps the largest animal biomass on earth.

Marine copepods reproduce sexually and asexually. Their female adults are free spawning or egg-sac carrying. Eggs hatch into nauplius larvae. Nauplius consists of a head with a small tail, but no thorax or true abdomen. It moults six times before turning into copepodite. Copepodite has an unsegmented abdomen, and three pairs of thoracic limbs. There is a marked metamorphosis between the last nauplius and the first copepodite stage. After five moults, the copepodite becomes an adult. The entire process from hatching to adulthood may take a week to few months mostly depending on the temperature and food concentration (e.g., Klein-Breteler et al. 1995). The temperature dependency of life cycles of copepods has been studied thoroughly during the last few decades by many authors (for e.g., Almeda et al., 2010; Breteler et al., 1994; Breteler and Schogt, 1994; Huntley and Lopez, 1992; Liang et al., 1996; Record et al., 2012), and so forth for zooplanktons also in general (for e.g., Gillooly, 2000).

Although most copepods have single median compound eye, some are eyeless, they sense predators and prey through setae, distinguishing predators from prey through mechanoreceptors (Boxshall and Jaume, 2013). Many smaller copepods directly feed on phytoplankton catching cells singly, while some larger

species predate on smaller organisms. Herbivorous copepods, particularly those in higher latitudes (polar regions) and deeper waters (benthic), store up energy from food as oil droplets to survive winters (Lee et al., 2006).

The surface layers of the oceans are the world's largest carbon sink (Houghton, 2007); the carbon absorption is equivalent to approximately one third of human carbon emission. Copepods contribute to the carbon sink largely (Sampei, 2012), perhaps reducing the impact of atmospheric carbon content on the global warming.

1.1.2. Marine calanoid copepods (Order Calanoida; Subclass Copepoda)

Calanoid copepods colonize all parts of the pelagic environments of estuaries, coastal and marine waters. They include around 43 families with about 1800 species in both marine and freshwater. Calanoid copepods are dominant in the plankton communities making up to 55–95% of plankton samples. Many commercial fish are dependent on them for diet: baleen whales such as bowhead whales, sei whales, right whales and fin whales feed on calanoid copepods.

Calanoid copepods can be distinguished from other planktonic copepods by having their first antennae at least half the length of the body, and biramous second antennae. Anatomically, their key defining feature is the joint between the fifth and sixth body segments. Calanoid copepods are primarily suspension feeders eating mainly phytoplankton and protozoan. They use their mouthparts to create water currents that bring food particles towards them, capturing small particles passively, and large particles by fling and clap movements with the surrounding water packet.

Calanoid reproduction is sexual, and sperm are transferred from male to female in a sac-like spermatophore (Mauchline, 1998). Some calanoid are free spawning, while others carry eggs in one or two masses, sacs, or strings until hatching. Females of some species may produce tens to hundreds of eggs in a life

time. Development times from egg to adult typically vary from 1 to 6 weeks, but may also take several months depending on the ambient temperature and the food availability. The lifespan of adults is from one to several months in laboratory conditions. Some calanoid copepods have resting eggs and stages that enable avoidance of harsh environmental conditions and help dispersal. Resting eggs have a thick shell, which can survive extended periods of dormancy.

Calanoid copepods have colonized the pelagic part of the water column, in contrast to copepods in general (Bradford-Grieve, 2002). Some copepods (and some species) in pelagic environment show diurnal vertical migration: increase metabolism while active in the upper layers (average 50m: e.g., Hays et al., 2001) within the mixed layer (where temperature is close to homogeneous) (e.g., Andersen et al., 2004; Atkinson et al., 1992; Herman, 1983), and rest (dormant) during the day at lower layers (average 150m: e.g., Hays et al., 2001) (Andersen et al., 2004; Kiørboe and Sabatini, 1995). Some pelagic copepod species do not show diurnal migration, and maintain vertical zonation in the mixed layer and down to thermocline (e.g., Bollens and Landry, 2000; Mackas et al., 1993). Some cold and boreal water copepods show arrested development, and reduced metabolism in late developmental stages in order to survive long periods of food shortages (Hirche, 1996).

1.1.3. Genus *Pseudodiaptomus* (Family Pseudodiaptomidae; Order Calanoida)

Pseudodiaptomidae is the family of the genre *Pseudodiaptomus* of the marine-estuary calanoid copepod *Pseudodiaptomus marinus* (Sato, 1913). *Pseudodiaptomus* occurs worldwide in tropical and temperate fresh to marine waters (Walter, 1986; Walter, 1987; Walter, 1989). To date, 77 species of *Pseudodiaptomus* have been identified (Walter et al., 2006) of which, four species are invasive: *P. inopinus* (Cordell et al., 1992; Cordell and Morrison, 1996; Biology: Cordell et al., 2007), *P. forbesi* (Bollens et al., 2002; Cordell et al., 2008;

Emerson et al., 2012), *P. marinus* (Brylinski et al., 2012; Deply et al., 2012; Fleminger and Kramer, 1988; Jha et al., 2013; Jiménez-Pérez and Castro-Longoria, 2006; Jones, 1966; Olazabal and Tirelli, 2011), and *P. trihamatus* (Medeiros et al., 2006), all native to Indo-Pacific region.

1.1.4. Marine-estuary copepod *Pseudodiaptomus marinus* (Family Pseudodiaptomidae; Order Calanoida)

Pseudodiaptomus marinus was first described near the coast of Hokkaido, Northern Japan, and subsequently considered as native to North Western Pacific Ocean (Walter, 1987). It has also been reported from Andaman Islands, West-Thailand (Pillai, 1976) and Mauritius (Grindley and Grice, 1969). It was introduced to Hawaii (Jones, 1966) and few other localities along the West coast of North America: Puget Sound, Washington (Lawrence and Cordell, 2010), Mission and San Francisco Bays, California (Fleminger and Kramer, 1988; Orsi and Walter, 1991), and Baja California (Jiménez-Pérez and Longoria, 2006). Recently, *P. marinus* has been reported from Southern Europe: in Adriatic Sea-Italy, Mediterranean Sea (Olazabal and Tirelli, 2011), Southern Bight of North Sea -coast of France (Brylinski et al., 2012), North Sea –Germany (Jha et al., 2013), and Lake Faro -Messina, Italy (Sabia et al., 2012). Cordell et al. (2009) show that *Pseudodiaptomus* species are found in large densities in ballast-water of ships entering Puget Sound in North America indicating a potentially high rate of discharge of their propagules into near-shore environments in the region.

Although *P. marinus* lives in shallow near-shore marine waters and estuaries; pelagic during the night and epibenthic during the day (Fancett and Kimmerer, 1985; Uye and Kasahara, 1983), it has recently shown an entirely planktonic behaviour at Lake Faro (Italy) (Sabia et al., 2012). *Pseudodiaptomus marinus* belongs to the Ramosus group, which is characterized by the dominance of marine forms (Walter et al., 2006). *Pseudodiaptomus marinus* has life-history characteristics shared by the *Pseudodiaptomus* species and Calanoida in general (Uye and Kasahara, 1982). Female reproduces sexually and is carrying an egg-

sac. *Pseudodiaptomous marinus* produces year-round (Liang and Uye, 1997b; Uye et al., 1983).

Life-history parameters of *P. marinus* such as fecundity, maturation, and mortality rates show strong temperature dependencies (Liang and Uye, 1997a; 1997b; Uye et al., 1983). Its growth rates at Fukuyama Harbour and Tomo were temperature-dependent, but not limited by the food concentration (Liang and Uye, 1997b). Growth rates of *Acartia omorii*, *Centropages abdominalis*, *Oithona davisae*, and *Paracalanus* sp. at Fukuyama Harbour also were largely independent of the food concentration (Liang and Uye, 1997b). *Pseudodiaptomous marinus* feeds on diatoms, flagellates, and naturally occurring non-living organic particles (Uye and Kasahara, 1983) and is predated by the ctenophores and other larger fish species (e.g., juvenile Japanese anchovy *Engraulis japonicus*). The *P. marinus* live in euhaline waters (30-35 ‰).

1.1.5. Marine tunicates (Subphylum Tunicata; Phylum Urochordata)

Tunicates are marine chordates of the Subphylum Tunicata. They have cylindrical or round bodies that are unsegmented and having a tougher outer covering. Tunicate larvae are free-swimming with a notochord. Many species such as the sea squirts and sea pork, lose the notochord as adults, and attach to rocks and other hard underwater surfaces. They often form colonies and are usually found in shallow waters. Dense tunicate swarms, hundreds of kilometres wide and many meters deep, are common in the open ocean.

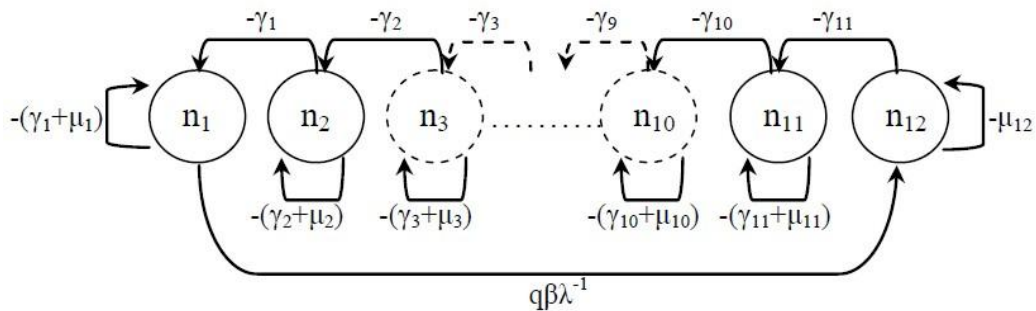
Tunicates have a life cycle that alternates between sexual (fertilization of an egg by sperm) and asexual (through budding) reproduction. They are capable of breeding year-round. The functional responses of their developmental times to temperature and food concentration are similar to that of copepods (Deibel and Lowen, 2012).

Adult stages of some tunicates such as salps, doliolids and pyrosomes are free-swimming or drifters, and living in the pelagic zone. Salps can form aggregations of millions of individuals and are among the fastest growing multicellular organisms. They release sperm into the sea, but the eggs are retained within the body and fertilised by the sperms brought in. The eggs are brooded within the body until they hatch.

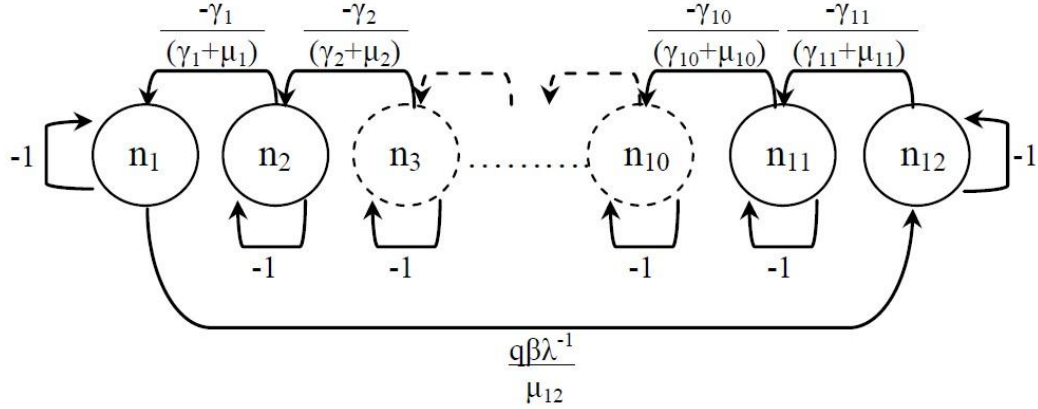
Tunicates are filter feeders of tiny planktonic organisms. They are predated by sharks, skates, and other bottom-dwelling animals including periwinkles. Many tunicates have poisonous flesh to avoid predators. Using rhythmic contraction of circular muscles, they move by jet propulsion. Some tunicates are invasive (Collin et al., 2013).

Appendix 2.1. Deriving R_0 from graph theoretic method

We follow the method given in de-Camino-Beck et al. (2009). After decomposing matrix \mathbf{A} from Eq. (2.1) into matrices \mathbf{F} , fecundity, and \mathbf{V} , transition, we have a real 12×12 matrix $(\mathbf{F}\lambda^{-1} - \mathbf{V}) = a_{ij}$. For this matrix $(\mathbf{F}\lambda^{-1} - \mathbf{V})$, there corresponds a labelled directed graph, $D(\mathbf{F}\lambda^{-1} - \mathbf{V})$, with nodes $1, 2, \dots, 12$, and a directed edge (arc) $j \rightarrow i$. The weight of this arc is a_{ij} , and $D(\mathbf{F}\lambda^{-1} - \mathbf{V})$ has a loop at node i of weight a_{ij} if $a_{ij} \neq 0$. Thus, we can draw the diagraph, $D(\mathbf{F}\lambda^{-1} - \mathbf{V})$, as follows.



We create trivial nodes using graph reduction Rule 1 in de-Camino-Beck et al. (2009) by reducing the loops $-a_{ii} < 0$ to -1 at node i 's, for every arc entering i divided by weight a_{ii} . Thus the diagraph reduces to the following.



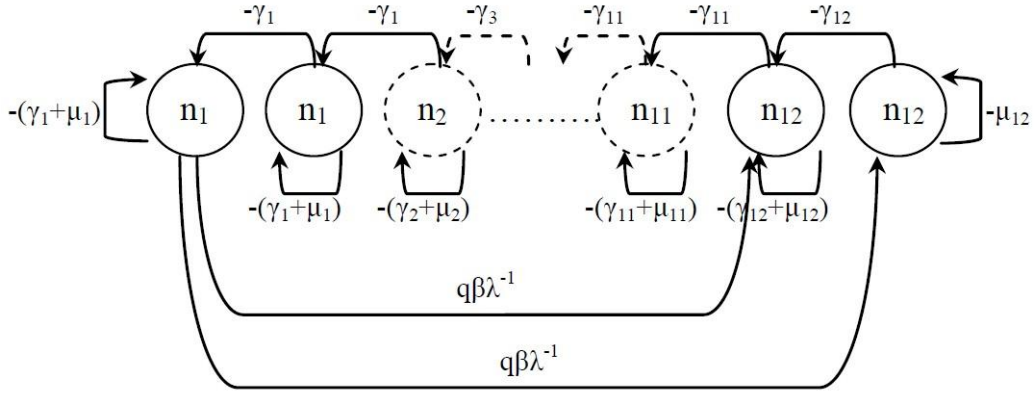
Using Rule 2 in de-Camino-Beck et al. (2009), by eliminating arcs through trivial nodes, here we replace two arcs at a time by $j \rightarrow k$ with weights equal to the product of weights on arc $j \rightarrow i$ and $i \rightarrow k$, for trivial nodes i on a path $j \rightarrow i \rightarrow k$. Thus, it finally yields the following diagraph with a single node.

$$-1 + \frac{q\beta}{\mu_{12}} \prod_{i=1}^{11} \left(\frac{\gamma_i}{\gamma_i + \mu_i} \right) \lambda^{-1} \quad \text{loop on } n_{12}$$

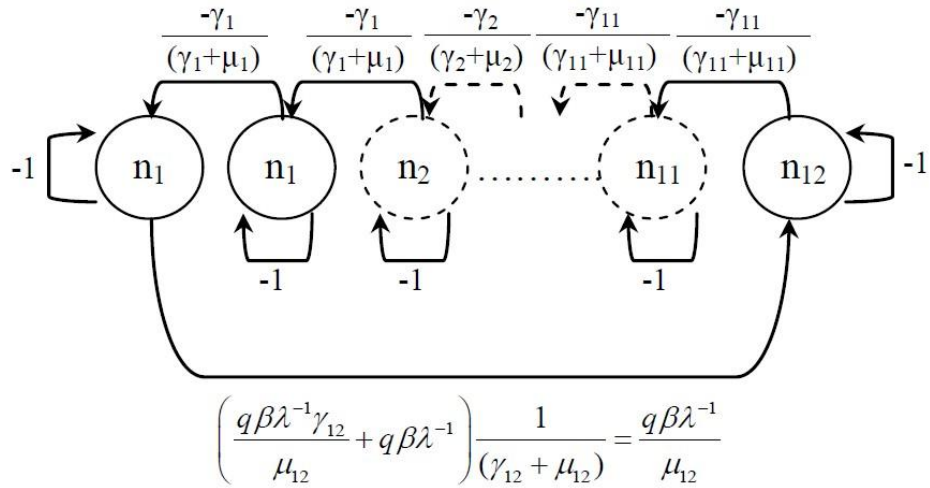
Now we set the weight of this loop to zero giving an equation for lambda. The smallest positive roots of this equation yielded R_0 .

$$R_0 = \frac{q\beta}{\mu_{12}} \prod_{i=1}^{11} \left(\frac{\gamma_i}{\gamma_i + \mu_i} \right)$$

Furthermore, when there are 2 sub-stages in each stage (that is $k=2$), the initial graph is given as follows:



Using Rule 1, this can be reduced as follows.



It finally yields

$$-1 + \frac{q\beta}{\mu_{12}} \prod_{i=1}^{11} \left(\frac{\gamma_i}{\gamma_i + \mu_i} \right)^2 \lambda^{-1} \quad \text{with a self-loop on } n_{12}$$

Thus,
$$R_0 = \frac{q\beta}{\mu_{12}} \prod_{i=1}^{11} \left(\frac{\gamma_i}{\gamma_i + \mu_i} \right)^2$$

Similarly, for any k sub-stages, this yields

$$R_0 = \frac{q\beta}{\mu_{12}} \prod_{i=1}^{11} \left(\frac{\gamma_i}{\gamma_i + \mu_i} \right)^k$$

The same result can be easily derived from $R_0 = \rho[FV^{-1}]$ also.

Appendix 2.2. Fitting Eq. (2.6) to data using multiple sub-stages

To derive the solution to the advanced model Eq. (2.1), assuming k number of virtual sub-stages within each stage, or Gamma distributed stage duration times, requires using the Laplace transformation. It yields a complicated analytical result. Also, the solution in Eq. (2.6) cannot be simply transformed into a general solution because in such case the denominator of the solution becomes zero, as $\sigma_{ij} = 0$ when i and j were redefined for sub-stages in each stage, such that $\sigma_i = \sigma_j$.

Instead, we modify Eq. (2.6) to include sub-stages within stages by assuming small differences in maturation rates among sub-stages. Thus, we implement the sub-stages for a given stage a by adding and subtracting a small constant ε to and from γ_a in Eq. (2.6) for $\varepsilon \ll \gamma_a$. For example, splitting γ_a into three sub-stages would yield maturation rates $[\gamma_a - \varepsilon, \gamma_a, \gamma_a + \varepsilon]$. This does not make $\sigma_{ij} = 0$ in Eq. (2.6) as per the original assumption. Now, we estimate γ_a by fitting the modified or the advanced Eq. (2.6) to data from Uye et al. (1983) for small values of ε .

Appendix 4.1. Marine ecoregions and the global invasive species diversity distribution

Northern temperate ecoregions (Spalding et al., 2007):

Index	Eco-region	Province
20	South and West Iceland	Northern European Seas
21	Faroe Plateau	Northern European Seas
22	Southern Norway	Northern European Seas
23	Northern Norway and Finnmark	Northern European Seas
24	Baltic Sea	Northern European Seas
25	North Sea	Northern European Seas
26	Celtic Seas	Northern European Seas
27	South European Atlantic Shelf	Lusitanian
28	Saharan Upwelling	Lusitanian
29	Azores Canaries Madeira	Lusitanian
30	Adriatic Sea	Mediterranean Sea
31	Aegean Sea	Mediterranean Sea
32	Levantine Sea	Mediterranean Sea
33	Tunisian Plateau/Gulf of Sidra	Mediterranean Sea
34	Ionian Sea	Mediterranean Sea
35	Western Mediterranean	Mediterranean Sea
36	Alboran Sea	Mediterranean Sea
37	Gulf of St. Lawrence - Eastern Scotian Shelf	Cold Temperate Northwest Atlantic
38	Southern Grand Banks - South Newfoundland	Cold Temperate Northwest Atlantic
39	Scotian Shelf	Cold Temperate Northwest Atlantic
40	Gulf of Maine/Bay of Fundy	Warm Temperate Northwest Atlantic
41	Virginian	Warm Temperate Northwest Atlantic
42	Carolinian	Warm Temperate Northwest Atlantic
43	Northern Gulf of Mexico	Warm Temperate Northwest Atlantic
44	Black Sea	Black Sea
45	Sea of Okhotsk	Cold Temperate Northwest Pacific
46	Kamchatka Shelf and Coast	Cold Temperate Northwest Pacific
47	Oyashio Current	Cold Temperate Northwest Pacific
48	Northeastern Honshu	Cold Temperate Northwest Pacific
49	Sea of Japan	Cold Temperate Northwest Pacific
50	Yellow Sea	Cold Temperate Northwest Pacific
51	Central Kuroshio Current	Warm Temperate Northwest Pacific
52	East China Sea	Warm Temperate Northwest Pacific
53	Aleutian Islands	Cold Temperate Northeast Pacific
54	Gulf of Alaska	Cold Temperate Northeast Pacific
55	North American Pacific Fjordland	Cold Temperate Northeast Pacific

56	Puget Trough/Georgia Basin Oregon, Washington, Vancouver Coast and Shelf	Cold Temperate Northeast Pacific
57	Northern California	Cold Temperate Northeast Pacific
58	Southern California Bight	Cold Temperate Northeast Pacific Warm Temperate Northeast Pacific
59	Cortezian	Warm Temperate Northeast Pacific
60	Magdalena Transition	Warm Temperate Northeast Pacific
61		

Appendix 5.1. EBE Probability

5.1.1. Special case: EBE probabilities of population in the presence of demographic and immigration stochasticity

Here, we solve Eq. (5.3) in the main text, $A(x)\partial_x G(x) + \frac{1}{2}B(x)\partial_{xx} G(x) = 0$ for the case $A(x) = \lambda x + j$, and, $B(x)/2 = (bx + c)$, where we denote $b \equiv \sigma_d^2/2$, and $c \equiv \sigma_p^2/2$. We substitute x by $z = \frac{1}{b} \ln(bx + c)$, thus, $x = \frac{1}{b} [\exp(bz) - c]$, $dx = (bx + c)dz$. Thus, we can write Eq.(5.3) as

$$\partial_{zz} G(z) + \left(\frac{\lambda}{b} e^{bz} + \left(j - \frac{\lambda c}{b} - b \right) \right) \partial_z G(z) = 0$$

as $\partial_{xx} G(x) = \frac{1}{(bx+c)^2} (\partial_{zz} G(z) - b \partial_z G(z))$, and, $\partial_x G(x) = \frac{1}{(bx+c)} \partial_z G(z)$.

Thus, it follows from Polyanin and Zaitsev (2003: 2.1.3-27) that the transformation of an equation of the above form with substitutions, $\xi = e^z$ (Polyanin and Zaitsev, 2003: 2.1.3-27) leads to the equation of the form,

$$\xi^2 \partial_{\xi\xi} G(\xi) + \left(\frac{r}{b} \xi^b + \left(j - \frac{\lambda c}{b} - b + 1 \right) \right) \xi \partial_{\xi} G(\xi) = 0, \text{ in (Polyanin and Zaitsev,}$$

2003: 2.1.2-146). Substitutions $\zeta = \xi^b$ and, $W(\zeta) = G(\xi)\xi^{-k}$, where

$$k = \frac{1}{b} \left(\frac{\lambda c}{b} - j + b \right) \text{ leads to the equation of the form}$$

$$b^2 \zeta \partial_{\zeta\zeta} W(\zeta) + \left(\lambda \zeta + b \left(\frac{\lambda c}{b} - j + b \right) + b^2 \right) \partial_{\zeta} W(\zeta) + \frac{\lambda}{b} \left(\frac{\lambda c}{b} - j + b \right) W(\zeta) = 0$$

(Polyanin and Zaitsev, 2003: 2.1.2-108). Transforming into the Kummer's equation (Polyanin and Zaitsev, 2003: 2.1.2-108), it yields the general solution following Polyanin and Zaitsev (2003: 2.1.2-70)

$$W(\zeta) = C_{11} F_1 \left(k, k+1, \frac{-\lambda}{b^2} \zeta \right) + C_2 \zeta^k {}_1F_1 \left(0, 1-k, \frac{-\lambda}{b^2} \zeta \right)$$

where $k = \frac{1}{b} \left(\frac{\lambda c}{b} - j + b \right)$, and, ${}_1F_1(a, b, z) = 1 + \frac{az}{b} + \frac{(a)_2 z^2}{(b)_2 2!} + \dots + \frac{(a)_n z^n}{(b)_n n!}$ s.t.

$a_n = a(a+1)(a+2)\dots(a+n)$, which is the confluent hypergeometric function of first kind (for more details: Slater, 1960; Abramowitz and Stegun, 1972).

Thus, we can write, $W(\zeta) = C_{11} F_1 \left(k, k+1, \frac{-\lambda}{b^2} \zeta \right) + C_2 \zeta^k$. By reverse transformation, $\zeta = \xi^b$ and, $W(\zeta) = G(\xi)\xi^{-k}$, it yields,

$$G(z) = C_1 e^{bkz} {}_1F_1 \left(k, k+1; \frac{-\lambda}{b^2} e^{bz} \right) + C_2$$

Substituting for x for z , we get

$$G(x) = C_1 (bx + c)^k {}_1F_1 \left(k, k+1; \frac{-\lambda}{b^2} (bx + c) \right) + C_2.$$

Applying boundary conditions, $G(x_d) = 1$, and $G(x_e) = 0$, it yields,

$$G(x_0) = \frac{E(x_0) - E(x_e)}{E(x_d) - E(x_e)},$$

where $E(x_i) = (bx_i + c)^k {}_1F_1\left(k, k + 1; \frac{-\lambda}{b^2}(bx_i + c)\right)$ for x_k denoting x_0 , x_e , and x_d .

Here, $k = \left(\frac{\lambda c}{b^2} - \frac{j}{b}\right) + 1$.

5.1.2. Special case: EBE probabilities of population in the presence of immigration stochasticity

Here, we solve Eq. (5.3) in the main text, $A(x)\partial_x G(x) + \frac{1}{2}B(x)\partial_{xx} G(x) = 0$

for the case $A(x) = \lambda x + j$, and, $B(x)/2 = c$, where we denote $c \equiv \sigma_p^2/2$.

Thus, equation, $A(x)\partial_x G(x) + \frac{1}{2}B(x)\partial_{xx} G(x) = 0$ has a general solution,

$$G(x) = \int_x C \exp\left(-\int_{x'} \frac{2A(x')}{B(x')} dx'\right) dx'',$$

where C is a constant. After applying boundary conditions at $x_0 = x_d$ determined by $G(x_d) = 1$, and at $x_0 = x_e$ determined by $G(x_e) = 0$, we obtain

$$G(x_0) = \frac{E(x_0) - E(x_e)}{E(x_d) - E(x_e)}$$

where, $E(x_i) = \text{Erf}_z\left(\frac{q + \lambda x_i}{\sqrt{2c\lambda}}\right)$, or can also be expressed in terms of confluent

hypergeometric function of first kind, as $E(x_i) = (q + \lambda x_i) {}_1F_1\left(\frac{1}{2}, \frac{3}{2}, -\frac{(j + \lambda x_i)^2}{2\lambda c}\right)$.

Here, x_i for subscript $i=0, e, d$, and Erf_z is the error function.

Note that, $G(x_0) \rightarrow \left(\frac{x_0 - x_e}{x_d - x_e}\right)$ for $c \rightarrow \text{inf}$.

Appendix 5.2. Moment generating function of passage times of the population first hitting an upper boundary before a lower boundary

Following the methods in Gardiner (2004), here, we derive the n^{th} moment of time for a population initially at x_0 in (x_d, x_e) to exit through an upper boundary x_d before first hitting a lower boundary x_e . We define the total probability that population initially at $(x_0, 0)$ exited through x_d at time t given by the time integral of the probability current at x_d by

$$q_{x_d}(x_0, t) = -\int_0^t dt' J(x_d, t' | x_0, 0) = \int_0^t dt' \left\{ -A(x_d)P(x_d, t' | x_0, 0) + \frac{1}{2} \partial_{x_d} [B(x_d)P(x_d, t' | x_0, 0)] \right\}$$

Here, $P(x_d, t' | x_0, 0)$ is the transition probability density function that satisfies FPE corresponding to SDE Eq. (5.1). We let the time that population leaves (x_d, x_e) be T . Thus the probability that population has exited at time t given that it exited through x_d be

$$\Pr(T_{x_d} < t) = \frac{q_{x_d}(x_0, t)}{q_{x_d}(x_0, \infty)}.$$

Here, $q_{x_d}(x_0, t)$ is the probability that population exited through x_d at time t . We note that $P(x_d, t' | x_0, 0)$ satisfies a backward Fokker-Planck equation. From here onwards, we ignore subscript zero that indicates the initial position as a variable.

Thus,

$$A(x) \partial_x q_{x_d}(x, t) + \frac{1}{2} B(x) \partial_{xx} q_{x_d}(x, t) = -\int_0^t dt' \partial_t J(x_d, t' | x_0, 0) = -J(x_d, t' | x_0, 0) = \partial_t q_{x_d}(x, t) \quad (\text{I})$$

Note that for the time-homogeneous case (letting, $t \rightarrow \infty$) the above Eq. I reduces to Eq. (5.3) in the main text, that is, $A(x) \partial_x G(x) + \frac{1}{2} B(x) \partial_{xx} G(x) = 0$, such that,

$$G(x) \equiv q_{x_d}(x, \infty) = \int_0^{\infty} dt' J(x_d, t' | x, 0), \text{ which is the probability that population}$$

establishing before going extinct (or first hitting x_d before first hitting x_e) with boundary conditions, $G(x_d) = 1$, and $G(x_e) = 0$.

We write the mean exit time, given that population exits through x_d as

$$T_1(x_d, x) = \int_0^{\infty} t \partial_t \Pr(T_{x_d} < t) dt.$$

This is because, $\Pr(T_{x_d} < t)$ is the cumulative density function that population exited before time t of the probability density function, $\partial_t \Pr(T_{x_d} < t)$, that population exited at time t given that it exited through x_d . Thus, we write the n th moment of the exit time, given that population exited through x_d as

$$T_n(x_d, x) = \int_0^{\infty} t^n \partial_t \Pr(T_{x_d} < t) dt = \int_0^{\infty} t^n \partial_t \left(\frac{q_{x_d}(x, t)}{q_{x_d}(x, \infty)} \right) dt = \frac{\int_0^{\infty} t^n \partial q_{x_d}(x, t)}{G(x)}.$$

After integration by part, $T_n(x_d, x) = \frac{\int_0^{\infty} [\partial t^n q_{x_d}(x, t) - n q_{x_d}(x, t) t^{n-1} \partial t]}{G(x)}$. Here we

find, $\int_0^{\infty} \partial t^n q_{x_d}(x, t) = 0$, thus, it yields

$$T_n(x_d, x)G(x) = -n \int_0^{\infty} q_{x_d}(x, t) t^{n-1} \partial t. \quad (\text{II})$$

Multiplying Eq. I by t^{n-1} it yields

$$A(x) \partial_x t^{n-1} q_{x_d}(x, t) + \frac{1}{2} B(x) \partial_{xx} t^{n-1} q_{x_d}(x, t) = t^{n-1} \partial_t q_{x_d}(x, t) = \partial_t t^{n-1} q_{x_d}(x, t) - (n-1) q_{x_d}(x, t) t^{n-2}.$$

Integrating w.r.t t from 0 to infinity it yields

$$A(x)\partial_x \int_0^\infty t^{n-1} q_{x_d}(x,t) \partial t + \frac{1}{2} B(x)\partial_{xx} \int_0^\infty t^{n-1} q_{x_d}(x,t) \partial t = \int_0^\infty \partial t^{n-1} q_{x_d}(x,t) - (n-1) \int_0^\infty q_{x_d}(x,t) t^{n-2} \partial t .$$

As $\int_0^\infty \partial t^{n-1} q_{x_d}(x,t) = 0$, it yields

$$A(x)\partial_x \int_0^\infty t^{n-1} q_{x_d}(x,t) \partial t + \frac{1}{2} B(x)\partial_{xx} \int_0^\infty t^{n-1} q_{x_d}(x,t) \partial t = -(n-1) \int_0^\infty q_{x_d}(x,t) t^{n-2} \partial t .$$

Substituting Eq. II on the above, and denoting $x=x_0$, finally it yields

$$A(x_0)\partial_{x_0} G(x_0)T_n(x_d, x_0) + \frac{1}{2} B(x_0)\partial_{x_0 x_0} G(x_0)T_n(x_d, x_0) = -nG(x_0)T_{n-1}(x_d, x_0). \quad (\text{III})$$

The boundary condition at $x_0 = x_d$ is determined by $G(x_d) = 1, T_n(x_d, x_d) = 0$, and hence, $G(x_d)T_n(x_d, x_d) = 0$. The boundary conditions at $x_0 = x_e$ is determined by $G(x_e) = 0$, and hence, $G(x_e)T_n(x_d, x_e) = 0$. The cases $n=1,2$ yield the mean and the second moments of first passage times respectively. By substituting $G(x_0)$ from the solution to Eq. (5.3), we solve Eq. III above numerically for $T_n(x_d, x_0)$ for the n^{th} moment of first passage time iteratively for the population first hitting an upper threshold x_d , before a lower threshold x_e .

Appendix 6.1. Marine invasive species generation driven by high-amplitude gradients of global ocean temperature cycles

Here, we present some preliminary statistical results as to how the *invasibility* of marine ecoregions, which can be measured by the invasive species taxonomic richness, is related to mean and amplitudes of annual temperature cycles of marine ecoregions. We use the same methods as in Chapter 4 to derive the data of sea surface temperatures pertaining to marine ecoregions (Indexed 1-232 based on Spalding et al., 2007). Additionally, we include Ponto Caspian Sea

(Index: 300). We obtained marine species taxonomic richness data by ecoregion from Molnar et al. (2008).

The invasibility of NTE is inversely correlated to the temperature-amplitudes strongly within a range of mean temperatures (10-24⁰C) yielding $p=0.04$ ($F=4.66$, $df=1,25$, $R^2=0.16$) (Figure 6-1). The narrower the mean temperature range within NTE (for example, 10-20⁰C), the stronger the relationship ($p=0.02$, $R^2=0.19$).

Based on Molnar et al. (2008) data, we observe that the ratio of invasives per ecoregion between the Northern Hemisphere (NH) and Southern Hemisphere (SH) is 27.57/12.68 (NA/SA: 30.24/8.42, and, NP/ SP: 23.65/15). Here, A-Atlantic, P-Pacific, N-North, S-South, E-East, W-West. Between the East coast and the West coast ecoregions of the northern temperate ecoregions, the proportions are: NWA/NEA: 21.71/33.56 and NWP/NEP: 7.2/42.13, and those in the southern temperate ecoregions are: SWP/SEP: 19.93/4.43, and SWA/SEA: 9.86/6.4.

Northern temperate ecoregions (NTE) have a high concentration of extremely high and extremely low-amplitude periodic temperature (APT) ecoregions at close physical proximity compared to other regions (Figure 6-3). High APT ecoregions, as extreme as those in the NTE, are not found anywhere else in the world's marine regions.